

CONVERGENCE OF MIXED METHODS  
IN CONTINUUM MECHANICS  
AND FINITE ELEMENT ANALYSIS

*by*

FAROOQUE AQUIL MIRZA

B.Sc., University of Karachi, 1966  
B.Eng., McGill University, 1971  
M.Eng., University of British Columbia, 1973

A THESIS SUBMITTED IN PARTIAL FULFILMENT  
OF THE REQUIREMENTS FOR THE DEGREE OF  
DOCTOR OF PHILOSOPHY

in

THE FACULTY OF GRADUATE STUDIES  
(Department of Civil Engineering)

We accept this thesis as conforming  
to the required standard

THE UNIVERSITY OF BRITISH COLUMBIA

January, 1977

© Farooque Aquil Mirza, 1977.

In presenting this thesis in partial fulfilment of the requirements for an advanced degree at the University of British Columbia, I agree that the Library shall make it freely available for reference and study.

I further agree that permission for extensive copying of this thesis for scholarly purposes may be granted by the Head of my Department or by his/her representatives. It is understood that copying or publication of this thesis for financial gain shall not be allowed without my written permission.

Department of Civil Engineering

The University of British Columbia  
Vancouver, B.C., V6T 1W5  
Canada

January, 1977

CONVERGENCE OF MIXED METHODS  
IN CONTINUUM MECHANICS  
AND FINITE ELEMENT ANALYSIS

ABSTRACT

The energy convergence of mixed methods of approximate analysis for problems involving linear self-adjoint operators is investigated. A new energy product and the associated energy norm are defined for such indefinite systems and then used in establishing the strain energy convergence and estimation of error for problems in continuum mechanics. In the process, the completeness requirements are laid out for approximate solutions. Also established is the mean convergence of the basic variables, e.g. displacements and stresses.

After accomplishing a new mathematical framework for the mixed methods in continuum, the theory is then extended to the finite element method. The completeness requirements, convergence criteria and the effect of continuity requirements on convergence are established. The flexibility offered by the mixed methods in incorporating the boundary conditions is also demonstrated. For stress singular problems, the strain energy convergence is established and an energy release method for determining the crack intensity factor  $K_I$  is presented.

A detailed eigenvalue-eigenvector analysis of the mixed finite element matrix is carried out for various combinations of interpolations for the plane stress linear elasticity and the linear part of the Navier-Stokes equations. Also discussed is its relation to the completeness requirements.

Finally, numerical results are obtained from applying the mixed finite element method to several examples. These include beam bending,

a plane stress square plate with parabolically varying end loads, a plane stress cantilever and plane strain stress concentration around a circular hole. A plane stress example of a square plate with symmetric edge cracks is also solved to study the strain energy convergence. Lastly, two rectangular plates, one with symmetric edge cracks and the other with a central crack are considered to determine the crack intensity factor  $K_I$ . In most of the examples, the strain energy convergence rates are predicted and compared with the numerical results, and excellent agreement is observed.

# TABLE OF CONTENTS

	<u>Page</u>
ABSTRACT . . . . .	ii
TABLE OF CONTENTS . . . . .	iv
LIST OF TABLES . . . . .	vii
LIST OF FIGURES . . . . .	x
NOTATION . . . . .	xiii
ACKNOWLEDGEMENTS . . . . .	xiv
CHAPTER	
1. INTRODUCTION . . . . .	1
1.1 Background . . . . .	1
1.2 Purpose and Scope . . . . .	3
1.3 Limitations . . . . .	4
2. MATHEMATICAL PRELIMINARIES . . . . .	5
2.1 Basic Concepts . . . . .	5
2.2 The Limit Process in Hilbert Spaces . . . . .	7
2.3 Orthogonality and Orthonormal Basis . . . . .	8
2.4 Subspaces and Projections . . . . .	9
2.5 Application to Linear Elasticity . . . . .	12
3. MIXED METHODS . . . . .	15
3.1 Mixed Variational Principle . . . . .	16
3.2 Projection Operators . . . . .	20
3.3 Mixed Galerkin Method . . . . .	22
3.4 Concepts and Definitions . . . . .	24
3.5 Convergence of the Mixed Method . . . . .	31
3.6 Completeness . . . . .	39

CHAPTER		Page
	3.7 Estimation of Error in the Energy Product . . . . .	39
	3.8 Extension . . . . .	41
4.	FORMULATION AND CONVERGENCE OF THE MIXED FINITE ELEMENT METHOD . . . . .	47
	4.1 Generation of a Finite Element Approximation . . .	47
	4.2 Generation of an Element Matrix . . . . .	51
	4.3 Assemblage of Element Matrices . . . . .	53
	4.4 Convergence Criteria . . . . .	55
	4.5 Completeness Criterion . . . . .	58
	4.6 Stress Singularities . . . . .	67
	4.6.A Strain Energy Convergence for Problems with Stress Singularity . . . . .	68
	4.6.B Determination of Stress Intensity Factor $K_I$ . . . . .	73
5.	APPLICATION OF BOUNDARY CONDITIONS . . . . .	78
	5.1 Homogeneous Boundary Conditions . . . . .	80
	5.2 Homogeneous Mixed Boundary Conditions . . . . .	81
	5.3 Nonhomogeneous Boundary Conditions . . . . .	83
	5.4 Boundary Residual Concept . . . . .	91
6.	EIGENVALUE ANALYSIS OF THE ELEMENT MATRIX . . . . .	93
	6.1 Linear Elasticity Problem . . . . .	93
	6.2 Linear Part of the Navier-Stokes Equations . . . . .	103
7.	APPLICATIONS OF THE MIXED FINITE ELEMENT METHOD . . . . .	118
	7.1 Beam Problem . . . . .	118
	7.1.A Two Second Order Equations . . . . .	119
	7.1.B Four First Order Equations . . . . .	125
	7.2 Plane Linear Elasticity . . . . .	128
	7.2.A Plane Stress: Square Plate with Parabolically Varying End Loads . . . . .	129

CHAPTER	<u>Page</u>
7.2.B Cantilever (Plane Stress) . . . . .	130
7.2.C Stress Concentration around a Circular Hole (Plane Strain) . . . . .	133
7.3 Stress Singularities . . . . .	134
7.3.A Strain Energy Convergence . . . . .	134
7.3.B Evaluation of the Stress Intensity Factor $K_I$ . . . . .	136
8. CONCLUSIONS . . . . .	138
BIBLIOGRAPHY . . . . .	142
APPENDIX A: CALCULATION OF THE FINITE ELEMENT MATRIX; LINEAR DISPLACEMENTS AND STRESSES OVER A TRIANGULAR ELEMENT	206
APPENDIX B: EIGENVALUE DISTRIBUTION FOR A REAL SYMMETRIC MATRIX	212
APPENDIX C: EQUIVALENCE OF ENERGY PRODUCTS FOR FOUR FIRST ORDER BEAM EQUATIONS AND PLANE LINEAR ELASTICITY EQUATIONS	219
APPENDIX D: ELASTICITY SOLUTION FOR A CANTILEVER . . . . .	223

LIST OF TABLES

<u>Table(s)</u>	<u>Page</u>
I      Eigenvalues and eigenvectors of element matrix for tri- angular elements using different combinations of interpolations for $u, v, \tau$ 's; linear elasticity plane stress . . . . .	146
II     Eigenvalues and eigenvectors of element matrix for rectangular elements using different combinations of interpolations for $u, v$ , and $\tau$ 's; linear elasticity plane stress . . . . .	147
III    Eigenvalues and eigenvectors of element matrix for tri- angular elements using different combinations of interpolations for $u, v, p$ and $\tau$ 's ( $\tau_{xx}, \tau_{yy}, \tau_{xy}$ ); two- dimensional, incompressible creeping flow (linear part of the Navier-Stokes equations) . . . . .	148
IV     Eigenvalues and eigenvectors of element matrix for rec- tangular elements using different combinations of interpolations for $u, v, p$ and $\tau$ 's ( $\tau_{xx}, \tau_{yy}, \tau_{xy}$ ); two- dimensional, incompressible creeping flow (linear part of the Navier-Stokes equations) . . . . .	149
V      Numerical results for two second order beam equations; v-linear, M-linear . . . . .	150
VI     Numerical results for two second order beam equations; v-quadratic, M-quadratic . . . . .	152
VII    Numerical results for two second order beam equations; v-cubic, M-cubic . . . . .	154

<u>Table(s)</u>	<u>Page</u>
VIII Numerical results for four first order beam equations; forced boundary conditions on $v$ and $M$ ; $v, \theta, M$ and $V$ all linear . . . . .	156
IX Strain energy estimations for four first order beam equations with forced boundary conditions on $v$ and $\theta$ ; $M, V, \theta$ , and $v$ all linear . . . . .	158
X Numerical results for four first order beam equations; forced boundary conditions on $v$ and $\theta$ ; shear strain energy term $V$ included; $M, V, \theta, v$ all linear . . . . .	158
XI Numerical results for parabolically loaded plane stress problem . . . . .	160
XII Numerical results for the cantilever (plane stress) with boundary conditions B.C.1 (Figure 19). Mixed finite element; displacements and stresses linear . . . . .	161
XIII Numerical results for the cantilever (plane stress) with boundary conditions B.C.2 (Figure 19). Mixed finite element; displacements and stresses linear . . . . .	161
XIV Comparison amongst C.S.T., L.S.T., Q.S.T., and mixed finite element. Cantilever with boundary conditions B.C.2 (Figure 19). . . . .	162
XV Numerical results for the plane stress problem of square plate with edge cracks, Figure 29 . . . . .	163
XVI Stress intensity factors from the finite element analysis of the rectangular plate with symmetric edge cracks, Figure 33(a) . . . . .	164
XVII Stress intensity factors from the finite element analysis of the rectangular plate with a central crack, Figure 33(b) . . . . .	164

Table(s)Page

XVIII	Comparison of stress intensity factors obtained from energy release rate using different elements and procedures . . . . .	165
-------	--	-----

LIST OF FIGURES

<u>Figure(s)</u>		<u>Page</u>
1	Mode I crack (opening mode) . . . . .	166
2	Typical contour for evaluation of J-integral . . . . .	166
3	Accommodation of crack extension $\Delta a$ by advancing nodes on the path $\Gamma_0$ . . . . .	167
4	Node numbers and degrees of freedom for a triangular element . . . . .	168
5	Node numbers and degrees of freedom for a rectangular element . . . . .	168
6	Mechanism for the fourth zero eigenvalue . . . . .	169
7	Forces acting on an infinitesimal beam element . . . . .	169
8	Forced boundary conditions on $v$ and $M$ for the beam problem . . . . .	170
9	Degrees of freedom for the beam element--two second order equations . . . . .	171
10	Two second order beam equations; displacement linear and moment linear . . . . .	172
11	Two second order beam equations; displacement quadratic, moment quadratic . . . . .	176
12	Two second order beam equations; displacement cubic and moment cubic . . . . .	177
13	Four first order beam equations, forced boundary conditions on $v$ and $M$ ; $v, M, \theta$ and $V$ all linear . . . . .	178
14	Four first order beam equations, forced boundary conditions on $v$ and $\theta$ ; $v, \theta, M$ and $V$ all linear . . . . .	180
15	Four first order beam equations, forced boundary conditions on $v$ and $\theta$ ; shear strain energy included . . . . .	181

<u>Figure(s)</u>	<u>Page</u>
16	Parabolically loaded plane stress problem (N=4) . . . . . 183
17	Parabolically loaded plane stress problem using mixed element; displacements and stresses linear . . . . . 184
18	Parabolically loaded plane stress problem using displace- ment element (cubic displacements), Ref. [5]. . . . . 186
19	Linear elasticity cantilever problem and forced boundary conditions used . . . . . 187
20	Convergence plots for the cantilever with boundary condi- tions B.C.1, using mixed finite element; stresses and displacements all linear . . . . . 188
21	(a): Grids used for the constant stress triangular elements . . . . . 189
	(b): Grids used for the linear stress triangles . . . . . 190
	(c): Grids used for the quadratic stress triangles . . . . . 191
22	Typical mesh used for mixed finite element (N=4) . . . . . 192
23	Plots for the cantilever with boundary conditions B.C.2 using mixed finite element; stresses and displacements all linear . . . . . 192
24	Convergence of tip deflection for C.S.T., L.S.T., Q.S.T. and mixed finite element with stresses and displace- ments linear for boundary conditions B.C.2 . . . . . 194
25	Model for infinite plate by a square plate with a circu- lar hole at centre, isotropic and orthotropic . . . . . 195
26	Finite element grid for the square plate with a circular hole in the middle. Isotropic and orthotropic cases . . . . . 196
27	Comparison of theoretical and finite element (mixed) results for infinite plate with a circular hole in the middle . . . . . 197

<u>Figure(s)</u>	<u>Page</u>
28	Comparison of theoretical and constant stress finite element, Zienkiewicz [42], results with the same material properties as used in the mixed method; $\tau_0 = -1.0$ . . . . . 197
29	Plane stress problem considered for investigation of energy convergence in the case of stress singularities 198
30	Plots of strain energy versus the mesh size for the plane stress problem with symmetric edge cracks--Figure 29 199
31	Strain energy convergence for the plane stress problem; square plate with symmetric edge cracks--Figure 29 . . 200
32	Normal stress distribution along the middle of a square plate with symmetric edge cracks--Figure 29(b), (N=12) 201
33	Rectangular plates with cracks used for determining the crack intensity factor $K_I$ . . . . . 202
34	Finite element mesh for determining the crack intensity factor $K_I$ , used for both symmetric edge and central cracks . . . . . 203
35	Normal stress distribution along the edge OA of the rectangular plates with cracks--Figure 33 . . . . . 204
36	Boundary tractions and conditions for cantilever linear elasticity solution (Appendix D) . . . . . 205

## NOTATION

The specific use and meaning of symbols is defined in the text where they are introduced.

The summation convention holds for subscripted variables with repeated lower case indices; it does not apply to repeated upper case indices. The range of summation is indicated where the variables are first introduced.

The lower case letter  $\ell$  which is also frequently used for element length or diameter appears as  $l$  in the text and the tables and as  $\ell$  in the figures.

The Greek symbol  $\epsilon$  implies "belongs to" unless otherwise specified.

### ACKNOWLEDGEMENTS

The author wishes to express his gratitude to his advisor, Dr. M. D. Olson, for his invaluable advice and guidance during the research and preparation of this thesis. He also expresses thanks to Dr. D. L. Anderson and Dr. N. D. Nathan for their valuable suggestions during the research work.

The financial support of the Defence Research Board and the National Research Council of Canada, University of British Columbia Fellowships (1973-75) and Killam Predoctoral Fellowship (1975-76) is gratefully acknowledged.

Finally, many thanks to Ruth Mirza for tremendous inspiration, assistance and diligent typing of this thesis.

## CHAPTER 1

### INTRODUCTION

#### 1.1 Background

The finite element method has proved to be an extremely powerful tool for the analysis of engineering problems for which no closed form solutions exist. A good introduction to the subject, which is still undergoing continuing development, can be found in the books by Zienkiewicz [41], Gallagher [9], Cook [4], Strang and Fix [33], Huebner [14], and Oden [19], etc.

For more than a decade now, the use of either displacement or equilibrium finite element methods have dominated in the analysis of problems in continuum and structural mechanics. These methods precipitate from well-established extremum principles; the displacement method from the principle of minimum potential energy or Rayleigh-Ritz method and the equilibrium method from the principle of minimum complementary energy. Both energy principles mentioned here, involve positive definite operators with well-developed mathematical properties, such as lower and upper bounds, completeness requirements, convergence in the energy sense, etc., and provided tremendous assistance in establishing the convergence of the displacement and equilibrium finite element methods. Hutton and Anderson [16] used the Galerkin method in the finite element analysis and established the convergence properties for the problems which may not have any variational principle, i.e. for non-self-adjoint operators. This encouraged many researchers to use the Galerkin method in the finite element analysis of incompressible viscous flow problems with velocities and pressure as basic dependent variables, Taylor and Hood [34], Olson and Tuann [26], etc. But the use of pressure as a dependent variable amounts to a mixed formulation which has caused some difficulties regarding the degree of the polynomial assumed for pressure within the element in relation to the polynomials used for approximating the

velocity field . This is also observed in the derivation of the variational theorem for incompressible and nearly incompressible materials by Herrmann [13] where the pressure, taken as the mean of the normal stresses, is considered as a dependent variable along with the displacements. The earlier applications of the mixed method in the finite element analysis date back to the mid-1960's when the use of mixed finite element models for plate bending were proposed, independently, by Herrmann [12] and Hellan [10]. These involved the simultaneous approximation of two dependent variables, the bending moment and the transverse deflection of thin elastic plates and were based on stationary rather than extremum variational principles. Dunham and Pister [6] used the Hellinger-Reissner variational principle to develop mixed finite element models for plane elasticity and plate bending problems while Wunderlich [40] exploited the idea of mixed models in a finite element analysis of non-linear shell behaviour. Somewhat similar to mixed finite elements was the development of the hybrid elements by Pian and Tong [28] and Tong [36]. However the assumed approximations for stresses and displacements were not considered over the entire domain as in the mixed finite elements mentioned above. In all these studies, higher accuracies as well as rapid convergence were obtained for certain quantities, e.g., stresses, than from the corresponding displacement elements.

However, the mixed methods involve indefinite systems and despite their wide spread use their mathematical properties are not as well understood as those of the displacement and equilibrium methods. This situation has caused considerable difficulties in establishing completeness requirements and convergence proofs for the mixed methods. Consequently the theoretical basis for these methods is far behind that for the displacement and equilibrium methods. See for example Tong and Pian [37] and Oliveira [25].

More recently, Oden [20] has discussed some generalizations of the

theory of mixed methods and Reddy and Oden [30] established the convergence of dependent variables, i.e., stresses and displacements, by decomposing the linear, positive definite operator into two self-adjoint linear operators ( $A=T^*T$ ) and then applied the theory of projections in order to formulate the mixed method. However, their numerical examples were limited to one dimensional problems and further, the convergence of the strain energy was not explored.

## 1.2 Purpose and Scope

The purpose of this thesis is to extend the work of previous investigators in the field of mixed finite element method and to define the mathematical framework in which the procedure can be used most advantageously.

A new energy product and the associated energy norm are defined which are then used in establishing the energy convergence of mixed methods in continuum mechanics. The completeness requirements for the approximating solutions are also established. The theory is then extended to its application in the finite element analysis. The continuity requirement for displacements and stresses and their influence on error in the energy product is also discussed. The forced and natural boundary conditions seem to be interchangeable depending on the boundary integrals and how these are treated during the derivation of the mixed variational principle. In the case of the mixed Galerkin method, which provides exactly the same results as the mixed variational principle for self-adjoint linear boundary-value problems, the forced and natural boundary conditions will depend on how the boundary residuals are accounted for, i.e. either through the displacement boundary residual or the stress boundary residual.

In the mixed finite element formulation, some approximations for the dependent variables can lead to mechanisms in general and self-equilibrating systems for incompressible cases. In order to explain this, the eigenvalues and the composition of the eigenvectors for the linear elasticity plane

stress and linear part of the Navier-Stokes equations are studied for various combinations of polynomial approximations of the dependent variables. These are stress and displacement for plane stress, and stress, pressure and velocity for the incompressible, viscous flow. The latter is very similar to the plane strain elasticity problem for incompressible material.

A number of numerical examples for one and two dimensional problems are presented. In the one dimensional case, the fourth order beam equation is first decomposed into two second order equations and then into four first order equations. The different combinations of the forced boundary conditions are also demonstrated for the beam problem. The plane stress mixed finite element is formulated, using linear stresses and displacements, and used in the analysis of a square plate with parabolically varying end loads, a cantilever with parabolic end load and a rectangular plate with symmetric edge cracks. Also, the plane strain problem of stresses around a circular hole, both isotropic and orthotropic cases, is analysed. The latter orthotropic case only requires slight adjustments to the element matrix of plane stress case. Finally, the stress intensity factor  $K_I$  for both symmetric edge cracks and a central crack is determined from the energy release rates.

### 1.3 Limitations

In the development, analysis and applications of the mixed methods carried out in this thesis, the linear boundary-value problems of self-adjoint operators are considered. These cover the largest class of problems in continuum and structural mechanics. It is hoped that the theory developed here will provide better grounds for extension to problems involving non-self-adjoint non-linear operators.

## CHAPTER 2

### MATHEMATICAL PRELIMINARIES

In this chapter basic concepts, definitions and theorems are presented to recapitulate some of the mathematical fundamentals which shall be used later in the development of the theory of mixed methods. For further clarification and proofs of the theorems, the texts by Lorch [17], Mikhlin [18], Balakrishnan [43] and Hellwig [11] are hereby referred to and shall not be repeated again.

#### 2.1 Basic Concepts

The first step in predicting the behaviour of a physical system by mathematical analysis is to idealize the system so as to obtain a mathematical model. In many cases it is a differential equation with some boundary conditions. The purpose of the finite element method is to provide an approximate solution to the differential equation and boundary conditions that will converge to the right solution in some sense, e.g. energy, mean square, etc.

The solution of a given equation is obtained by finding that function which, when acted upon by the given operator, yields a known function. Attention will be restricted to those functions that are square integrable over a given domain  $\Omega$ , i.e. functions  $u_i$  such that the Lebesgue integral

$$\int_{\Omega} u_i u_i d\Omega < \infty. \quad (2.1)$$

The functions considered will, in general, be vector valued and  $u_i$  is the  $i^{\text{th}}$  component of a column vector  $\underline{u}$ , i.e.

$$\underline{u} = \langle u_1 \quad u_2 \quad . \quad . \quad . \quad u_n \rangle^T.$$

The class of square integrable functions over  $\Omega$ , denoted by  $L_2(\Omega)$ , constitutes a vector space over the field of real numbers.

In order to compare different approximations of a given equation, it is necessary to introduce a norm. This can be accomplished by first defining an inner product. (Only real vector spaces are considered.)

### Definition 2.1.1

A real vector space  $H$  is called an inner product space (also pre-Hilbert space) if there is defined a real-valued function of pairs of vectors  $\underline{u}$  and  $\underline{v}$  in  $H$  denoted by  $(\underline{u}, \underline{v})$  which satisfies the following conditions:

- (i)  $(\underline{u}_1 + \underline{u}_2, \underline{v}) = (\underline{u}_1, \underline{v}) + (\underline{u}_2, \underline{v})$
- (ii)  $(\alpha \underline{u}, \underline{v}) = \alpha (\underline{u}, \underline{v})$ ;  $\alpha = \text{a constant}$
- (iii)  $(\underline{u}, \underline{v}) = (\underline{v}, \underline{u})$
- (iv)  $(\underline{u}, \underline{u}) \geq 0$ , where the equality holds if, and only if,  $\underline{u} \equiv \underline{0}$ .

### Definition 2.1.2

An inner product space in which every Cauchy sequence is a convergent sequence is said to be complete. A complete inner product space is called a Hilbert space.

If the  $L_2$  norm of  $\underline{u}$  is defined as

$$\|\underline{u}\| = \sqrt{(\underline{u}, \underline{u})} \quad (2.2)$$

then the following theorem holds:

### Theorem 2.1.1

For any vectors  $\underline{u}$ ,  $\underline{v}$  and  $\underline{w} \in H$

- (i)  $\|\underline{u}\| \geq 0$ ; and  $\|\underline{u}\| = 0$ , if, and only if,  $\underline{u} \equiv \underline{0}$ ;
- (ii)  $\|\alpha \underline{u}\| = |\alpha| \|\underline{u}\|$ ;  $\alpha = \text{constant}$ ;
- (iii)  $|(\underline{u}, \underline{v})| \leq \|\underline{u}\| \|\underline{v}\|$  (Schwarz inequality);
- (iv)  $\|\underline{u} + \underline{v}\| \leq \|\underline{u}\| + \|\underline{v}\|$  (triangle inequality).

The difference between two approximating functions can be characterized by the norm of their difference, i.e.  $\|\underline{u} - \underline{v}\|$ .

## 2.2 The Limit Process in Hilbert Spaces

### Definition 2.2.1

Let there be given a Hilbert space  $H$  and let  $\{\underline{u}_n\}$  be a sequence of its elements. This sequence converges, or tends to  $\underline{u}$  if  $\underline{u}$  is an element of  $H$  and

$$\lim_{n \rightarrow \infty} \|\underline{u}_n - \underline{u}\| = 0. \quad (2.3)$$

The element  $\underline{u}$  is called the limit of the sequence  $\{\underline{u}_n\}$ , and is written as

$$\underline{u}_n \rightarrow \underline{u}, \quad \lim_{n \rightarrow \infty} \underline{u}_n = \underline{u}.$$

The following are examples of the above definition:

(a) In the space  $L_2(\Omega)$  the convergence  $\underline{u}_n \rightarrow \underline{u}$  means that

$$\lim_{n \rightarrow \infty} \int_{\Omega} |\underline{u}_n - \underline{u}|^2 d\Omega = 0$$

i.e. that  $\underline{u}_n$  converges to  $\underline{u}$  in the mean.

(b) Convergence  $\underline{L}_2^r(\Omega) = \underline{W}_2^r(\Omega)$  denotes convergence in the mean of the functions of the sequence  $\{\underline{u}_n\}$  and all their derivatives up to order  $r$  inclusive to a limiting function and all its corresponding derivatives.

### Theorem 2.2.1

If  $\underline{u}_n$  and  $\underline{v}_n \in L_2(\Omega)$  converge to  $\underline{u}$  and  $\underline{v}$ , respectively, in the  $L_2$  norm, then

$$(\underline{u}_n, \underline{v}_n) \rightarrow (\underline{u}, \underline{v}). \quad (2.4)$$

Corollary 1. If  $\underline{u}_n \rightarrow \underline{u}$  then  $(\underline{u}_n, \underline{v}) \rightarrow (\underline{u}, \underline{v})$ ;

Corollary 2. If  $\underline{u}_n \rightarrow \underline{u}$  then  $\|\underline{u}_n\| \rightarrow \|\underline{u}\|$ .

If  $\{\underline{u}_n\}$  is a specified sequence in a Hilbert space  $H$  which converges to an element  $\underline{u}$ , then by definition 2.2.1  $\lim_{n \rightarrow \infty} \|\underline{u}_n - \underline{u}\| = 0$ . This means that for any specified  $\epsilon > 0$  it is possible to find a number  $n_0(\epsilon)$  such that for  $n > n_0(\epsilon)$ ,

$$\|\underline{u}_n - \underline{u}\| < \epsilon.$$

Let  $k > \eta_0(\frac{\epsilon}{2})$  and  $n > \eta_0(\frac{\epsilon}{2})$ , then

$$\|\underline{u}_k - \underline{u}\| < \frac{\epsilon}{2} \quad \text{and} \quad \|\underline{u}_n - \underline{u}\| < \frac{\epsilon}{2}.$$

Now, the norm of the difference of  $\underline{u}_k$  and  $\underline{u}_n$  can be estimated by the triangular inequality

$$\|\underline{u}_k - \underline{u}_n\| = \|(\underline{u}_k - \underline{u}) - (\underline{u}_n - \underline{u})\| < \|\underline{u}_k - \underline{u}\| + \|\underline{u}_n - \underline{u}\| < \epsilon.$$

The last equation by virtue of the arbitrariness of  $\epsilon$  implies that

$$\lim_{\substack{k \rightarrow \infty \\ n \rightarrow \infty}} \|\underline{u}_k - \underline{u}_n\| = 0. \quad (2.5)$$

Thus if  $\underline{u}_n \rightarrow \underline{u}$ , then equation (2.5) is necessarily satisfied. Since, in the space  $L_2(\Omega)$ , equation (2.5) necessitates the existence of a limiting element  $\underline{u}$ , the converse also holds.

### 2.3 Orthogonality and Orthonormal Basis

An important notion in any inner product space is that of orthogonality. Two vector functions  $\underline{u}$  and  $\underline{v}$  are said to be orthogonal if their inner product is zero, i.e.

$$(\underline{u}, \underline{v}) = 0.$$

#### Definition 2.3.1

The orthogonal complement of a set  $\Theta$  in a Hilbert space is the set of all elements orthogonal to every element in  $\Theta$ . It is denoted by  $\Theta^\perp$ .

#### Definition 2.3.2

An orthonormal set is one in which any two elements are orthogonal to each other, and each element of the set is of unit norm.

#### Theorem 2.3.1

Every non-trivial Hilbert space has an orthonormal basis. (For proof, see Balakrishnan [43]).

Definition 2.3.3

A set is said to be dense in a Hilbert space  $H$ , if its closure is equal to  $H$ .

Definition 2.3.4

A Hilbert space is said to be separable if it has a countable dense set.

Definition 2.3.5

A sequence of functions  $u_1, u_2, \dots, u_N$  is said to be complete in  $L_2(\Omega)$  if for a function  $u$  with a finite  $L_2$  norm and any  $\epsilon > 0$  it is possible to find a natural number  $N$  and constants  $\alpha_1, \alpha_2, \dots, \alpha_N$  such that

$$\|u - (\alpha_1 u_1 + \alpha_2 u_2 + \dots + \alpha_N u_N)\| = \|u - \sum_{i=1}^N \alpha_i u_i\| < \epsilon. \quad (2.6)$$

Theorem 2.3.2

If an orthonormal sequence of functions  $u_1, u_2, \dots, u_N$  is complete, then the Fourier series  $\sum_{i=1}^N a_i u_i$  of some function  $u$  with a finite  $L_2$  norm converges to this function in  $L_2$  norm. The coefficients  $a_i$  are given by

$$a_i = (u, u_i). \quad (2.7)$$

In this case there occurs the so-called Parseval equation;

$$\|u\|^2 = \sum_{i=1}^{\infty} a_i^2 = \sum_{i=1}^{\infty} (u, u_i)^2. \quad (2.8)$$

2.4 Subspaces and Projections

Consider the space  $L_2(\Omega)$  of scalar or vector functions which are defined in a certain finite domain  $\Omega$  and have a finite  $L_2$  norm. Select some linear set of functions belonging to this class and add all of its limiting elements to this set (i.e., functions which are the limits in the mean of a sequence of functions belonging to the given linear set). Such linear sets

of functions are called closed subspaces of the basic space  $L_2(\Omega)$  (e.g. Let  $\Omega$  be equivalent to the segment  $(0, 2\pi)$  of the x-axis. The set of functions whose Fourier series contains only  $\sin(nx), n=1, 2, \dots$  constitute a subspace. Obviously the functions of this subspace are characterized by the fact that they are orthogonal to the functions  $\cos(nx), n=1, 2, \dots$ ). Sometimes the linear set leads to a subspace which coincides with  $L_2(\Omega)$ . Thus adding all the limiting functions to the set of all polynomials (which is obviously linear) would constitute the class  $L_2(\Omega)$ .

Let there be given a separable Hilbert space  $H$  and one of its subspaces  $H_1$ . Then from definition 2.3.4, there exists in  $H_1$  a complete finite or enumerable orthonormalized system  $u_1, u_2, \dots, u_n$ . Take an arbitrary function  $u$ , which has a finite norm but does not necessarily belong to  $H_1$ , and construct its Fourier series in terms of the functions  $u_1, u_2, \dots, u_n$ .

$$\sum_{n=1}^{\infty} a_n u_n; a_n = (u, u_n). \quad (2.9)$$

The sequence  $\{u_n\}$  may be composed of a finite number of terms.

In such a case the sum in (2.9) will contain only a finite number of terms.

From theorem 2.3.2, the series converges in the  $L_2$  norm. Let its sum be

denoted by  $\bar{u}$ , that is,  $\bar{u} = \sum_{n=1}^{\infty} a_n u_n$ . In fact,  $\bar{u}$  is the limit as  $N \rightarrow \infty$

of the functions

$$\sum_{n=1}^N a_n u_n$$

which belong to the subspace  $H_1$ , since the sequence  $\{u_n\} \in H_1$ . Therefore,

$\bar{u} \in H_1$ . The function  $\bar{u}$  is called the orthogonal projection, or simply the

projection of the function  $u$  onto the subspace  $H_1$ . The difference  $\bar{\bar{u}} = u - \bar{u}$  is

orthogonal to the subspace  $H_1$ .

Therefore any function  $u \in H$  can be represented as the sum of two terms, i.e.  $u = \bar{u} + \bar{\bar{u}}$ , of which the first is the projection of the given function  $u$  onto the given subspace  $H_1$  and the second one is orthogonal to this subspace. The projection of  $u$  onto  $H_1$  does not change when one system of functions  $\{u_n\}$ , which is complete and orthonormalized, is replaced by some other complete, orthonormal system  $\{w_n\}$  in  $H_1$ .

A projection possesses an extremal property. If  $u \in L_2(\Omega)$  and  $\bar{u}$  is the projection of the function  $u$  onto a subspace  $H_1$ , then the norm of the difference  $\bar{\bar{u}} = u - \bar{u}$  where  $v$  is an arbitrary function from  $H_1$ , becomes a minimum for  $v = \bar{u}$ . In fact

$$\|u - v\|^2 = \|\bar{\bar{u}} + (\bar{u} - v)\|^2 = \|\bar{\bar{u}}\|^2 + \|\bar{u} - v\|^2 \quad (2.10)$$

since  $(\bar{u} - v) \in H_1$  and thus  $(\bar{\bar{u}}, \bar{u} - v) = 0$ . It becomes obvious now that  $\|u - v\|^2$  becomes a minimum at  $v = \bar{u}$ ; this minimum equals  $\|\bar{\bar{u}}\|^2$ .

Consider all possible functions  $u \in L_2(\Omega)$  and their projections  $\bar{u}$  onto a given subspace  $H_1$ . The differences  $\bar{\bar{u}} = u - \bar{u}$  constitute some new subspace  $H_2$ . Every function from  $H_2$  is orthogonal to every function from  $H_1$  and it is said that the subspaces  $H_1$  and  $H_2$  are orthogonal. Further, any function  $u \in L_2(\Omega)$  expands into a sum  $u = \bar{u} + \bar{\bar{u}}$ , where  $\bar{u} \in H_1$  and  $\bar{\bar{u}} \in H_2$ . This fact is usually formulated by saying that  $L_2(\Omega)$  is an orthogonal sum of the subspaces  $H_1$  and  $H_2$ , and each of the subspaces  $H_1$  and  $H_2$  is the orthogonal complement of the other subspace.

The properties mentioned about  $L_2(\Omega)$  in this section apply without change to any arbitrary Hilbert space. If a given Hilbert space is the orthogonal sum of the subspaces  $H_1$  and  $H_2$  then it can be written as

$$H = H_1 \oplus H_2$$

or 
$$H_1 = H \ominus H_2; H_2 = H \ominus H_1.$$

## 2.5 Application to Linear Elasticity

A typical differential equation in linear elasticity is of the form

$$\underline{A}\underline{w} = \underline{f} \quad \text{in } \Omega \quad (2.11)$$

where  $\underline{w}$  and  $\underline{f}$  are members of some Hilbert space  $H(\Omega)$  and  $\underline{f}$  is known. A solution  $\underline{w}$  sought for the differential equation (2.11) will also be required to satisfy certain boundary conditions. A class of functions that satisfy exactly all the boundary conditions of the problem and possess sufficient continuity so that  $\underline{A}\underline{w}$  is defined is known as the field of definition of the operator  $\underline{A}$  and is denoted by  $D_A$ . In general,  $\underline{A}$  is considered defined for a dense set of  $H(\Omega)$ .

For a large majority of problems in linear elasticity, the operator  $\underline{A}$  has the following properties:

- (i) linear;  $\underline{A}(\alpha\underline{u} + \beta\underline{v}) = \alpha\underline{A}\underline{u} + \beta\underline{A}\underline{v}$ ; where  $\alpha, \beta$  are constants and  $\underline{u}, \underline{v} \in D_A$ ;
- (ii) symmetric;  $(\underline{A}\underline{u}, \underline{v}) = (\underline{u}, \underline{A}\underline{v})$  for all  $\underline{u}, \underline{v} \in D_A$ ;
- (iii) positive definite;  $(\underline{A}\underline{u}, \underline{u}) \geq 0$  for all  $\underline{u} \in D_A$ , where the equality holds if, and only if,  $\underline{u} \equiv 0$ ;
- (iv) positive bounded below;  $(\underline{A}\underline{u}, \underline{u}) \geq r^2(\underline{u}, \underline{u})$  for all  $\underline{u} \in D_A$ , where  $r$  is a positive constant.

Let  $\underline{u}$  and  $\underline{v}$  be two functions in  $D_A$ . One convenient measure of closeness of these functions is the square root of the energy of their difference, i.e. the energy norm of  $\underline{u} - \underline{v}$ . This is now defined.

### Definition 2.5.1

For a positive definite operator  $\underline{A}$ , the energy product of functions  $\underline{u}$  and  $\underline{v} \in D_A$  over  $\Omega$  is given by

$$[\underline{u}, \underline{v}] = (\underline{A}\underline{u}, \underline{v}) = \int_{\Omega} \underline{v}^T \underline{A}\underline{u} d\Omega. \quad (2.12)$$

The energy norm  $|\underline{u}|$  is defined as

$$|\underline{u}| = \sqrt{[\underline{u}, \underline{v}]}. \quad (2.13)$$

The energy product and the energy norm defined above satisfy the properties of an inner product and a norm presented in definition 2.1.1 and theorem 2.1.1, respectively. Thus a measure of closeness of the functions  $\underline{u}, \underline{v} \in D_A$  is

$$|\underline{u} - \underline{v}| = \sqrt{[\underline{u} - \underline{v}, \underline{u} - \underline{v}]} = \sqrt{(A(\underline{u} - \underline{v}), \underline{u} - \underline{v})}. \quad (2.14)$$

The space  $D_A$  may be incomplete with respect to the energy norm, i.e. not all Cauchy sequences in  $D_A$  converge to a function in  $D_A$  in the energy norm. If so, a function  $\underline{u}$  is defined to be a member of the space  $D_A$  by the following limiting process:

$$|\underline{u}_n - \underline{u}| \rightarrow 0 \quad \text{as } n \rightarrow \infty, \quad (2.15)$$

where  $\underline{u}_n$  is a typical member of a sequence  $\{\underline{u}_n\} \in D_A$ . Thus, the space  $D_A$  is completed by including all the limiting elements. The completed space so obtained is a Hilbert space and is denoted by  $H_A$  to emphasize its dependence upon the operator  $\underline{A}$ . The definition of the energy product in equation (2.12) can be extended to all functions in  $H_A$ :

$$[\underline{u}, \underline{v}]_A = \lim_{n \rightarrow \infty} (\underline{A}\underline{u}_n, \underline{v}_n) = \lim_{n \rightarrow \infty} \int_{\Omega} \underline{v}_n^T \underline{A}\underline{u}_n d\Omega; \quad \underline{u}_n, \underline{v}_n \in D_A. \quad (2.16)$$

The completeness definition 2.3.5 and theorem 2.3.2 can now be rewritten as:

#### Definition 2.5.2

A sequence of functions  $u_1, u_2, \dots, u_N$  is said to be complete in  $H_A$  if for a function  $u$  with a finite energy norm and any  $\epsilon > 0$  it is possible to find a natural number  $N$  and constants  $\alpha_1, \alpha_2, \dots, \alpha_N$  such that

$$|u - (\alpha_1 u_1 + \alpha_2 u_2 + \dots + \alpha_N u_N)| = |u - \sum_{i=1}^N \alpha_i u_i| < \epsilon. \quad (2.17)$$

Theorem 2.5.1

If an orthonormal sequence of functions  $u_1, u_2, \dots, u_N$  is complete, then the Fourier series  $\sum_{i=1}^N a_i u_i$  of some function  $u \in H_A$  with a finite energy norm converges to this function in the energy norm. The coefficients  $a_i$  are given by

$$a_i = [u, u_i]. \quad (2.18)$$

In this case there occurs the so-called Parseval equation

$$|u|^2 = \sum_{i=1}^{\infty} [u, u_i]^2. \quad (2.19)$$

## CHAPTER 3

### MIXED METHODS

In this chapter, a brief introduction to the theory of mixed methods is presented first. Then the definitions and theorems given in Chapter 2 are used to establish the convergence of these mixed methods. Since these methods involve indefinite operators, their fields of definition have to be restricted in order to define their energy products and energy norms. The procedure for doing this is illustrated for a typical indefinite operator, and the resulting energy norm is then used to prove convergence in energy and to establish an error estimate. In the process the completeness requirements are also laid out.

A remarkably large class of problems in mathematical physics involves equations of the form

$$-Au - f = 0 \quad (3.1a)$$

$$Bu - g_1 = 0 \text{ on } \partial R_1 \text{ and } B^*Tu - g_2 = 0 \text{ on } \partial R_2, \quad (3.1b)$$

where  $u = u(\underline{x})$  is a function defined on a bounded region  $R$  of  $E^n$ ;  $\partial R$  is the smooth boundary of  $R$ . The operator  $A$  is assumed to have the following properties:

- (i)  $A$  is factorable, i.e.  $A = T^*T$ , and
- (ii)  $A$  is positive definite.

$B$  and  $B^*$  are linear boundary operators. Thus equation (3.1a) can be written as

$$-T^*T - f = 0. \quad (3.2)$$

Here  $T$  is a linear operator whose domain  $D_T$  is in a Hilbert space  $U$  and its range in another Hilbert space  $V$ . The operator  $T^*$  is the formal adjoint of  $T$ ; its domain  $D_{T^*}$  is in  $V$  and its range is in  $U$ . If the boundary conditions in (3.1b) are homogeneous then, as the operator  $T^*$  is the formal adjoint of  $T$ , the following Green's formula holds:

$$(Tu, v)_V = (T^*v, u)_U \quad \{\text{for every } u \in U \text{ and } v \in V\} \quad (3.3)$$

where  $(\ , \ )_U$  and  $(\ , \ )_V$  represent inner products in the spaces  $U$  and  $V$ , respectively

Through equations of the form (3.2), by using direct integral methods, a collection of variational principles can be developed, Oden [21],

which generalize the classical ones existing in the theory of linear elasticity. In many cases, bounds on the solution or some other quantity of interest can be obtained even if the problem is not explicitly solvable.

### 3.1 Mixed Variational Principle

A mixed variational principle associated with equation (3.2) can be developed by splitting this equation into canonical form, equivalent to the following pair of equations:

$$\begin{aligned} Tu &= v \text{ in } R; \text{ and } B(u) = g_1 \text{ on } \partial R_1 \\ T^*v &= -f(u) \text{ in } R; \text{ and } B^*(v) = g_2 \text{ on } \partial R_2 \end{aligned} \quad (3.4)$$

where  $\partial R_1 + \partial R_2 = \partial R$ , and the linear boundary operator  $B$  (and  $B^*$ ) depends upon  $T$ . For the non-homogeneous boundary condition of (3.4),  $T^*$  is the formal adjoint of  $T$  if it satisfies the generalized Green's formula

$$(v, Tu)_V = (u, T^*v)_U + (v, Bu)_{V\partial R} \quad (3.5)$$

where  $(v, Bu)_{V\partial R}$  denotes an inner product in the space  $V$  associated with the boundary terms. The only difference between (3.3) and (3.5) is the addition of the boundary term to the right hand side. The boundary operator  $B^*$  is the adjoint of  $B$  in the sense that

$$(v, Bu)_{V\partial R} = (u, B^*v)_{U\partial R}. \quad (3.5a)$$

In certain cases it is also possible to write equations (3.4) in a generalized Hamiltonian form. Assume that there exists a Gateaux differentiable, (Balakrishnan [43]), bilinear functional  $H(u, v)$ , called the generalized Hamiltonian, whose total Gateaux differential is of the form

$$\delta H(u, v; \eta, w) = (-f(u), \eta)_U + (v, w)_V \quad (3.6)$$

where  $\eta$  is the variation of  $u$  and  $w$  that of  $v$ . In equation (3.6),  $H(u, v)$  is assumed to have the property that its partial Gateaux derivatives with

respect to  $u$  and  $v$ ,  $\delta H/\delta u$  and  $\delta H/\delta v$ , respectively, coincide with the right hand sides of the canonical equations (3.4), i.e.

$$\frac{\delta H(u,v)}{\delta u} = v; \quad \frac{\delta H(u,v)}{\delta v} = -f(u). \quad (3.7)$$

Then the generalized Hamiltonian forms are analogous to those of analytical dynamics,

$$\begin{aligned} T u &= \frac{\delta H}{\delta v} \\ T^* v &= \frac{\delta H}{\delta u} \end{aligned} \quad (3.8)$$

with  $B(u) = g_1$  on  $\partial R_1$  and  $B^*(v) = g_2$  on  $\partial R_2$ .

The direct integral method can now be employed to derive a functional for (3.4) or (3.8). Let  $W$  denote the tensor product space,

$$W = U \times V.$$

Then elements  $\underline{\Lambda}$  of  $W$  are the ordered pairs

$$\underline{\Lambda} = \langle u \ v \rangle^T; \quad u \in U, \ v \in V. \quad (3.9)$$

The equations (3.4) can be put into a compact form (Oden [21])

$$\underline{P}(\underline{\Lambda}) - \underline{\Gamma} = 0 \quad (3.10)$$

where the matrix operator  $\underline{P}$  and  $\underline{\Gamma}$  are:

$$\underline{P} = \begin{bmatrix} 0 & T^* \\ T & 0 \end{bmatrix} \quad \text{and} \quad \underline{\Gamma} = \begin{Bmatrix} -f(u) \\ v \end{Bmatrix}. \quad (3.11)$$

Similarly the general boundary conditions can be written symbolically as

$$\underline{B}(\underline{\Lambda}) - \underline{T}_{\partial R} = 0 \quad \text{on } \partial R \quad (3.12)$$

where

$$\underline{B} = \begin{bmatrix} 0 & B^* \\ -B & 0 \end{bmatrix}; \quad \underline{T}_{\partial R} = \begin{Bmatrix} g_2 \\ -g_1 \end{Bmatrix}. \quad (3.13)$$

Denote the inner product of elements  $\underline{\Lambda} \in W=U \times V$  as

$$(\underline{\Lambda}_1, \underline{\Lambda}_2) = (u_1, u_2)_U + (v_1, v_2)_V, \quad (3.14)$$

and  $\underline{\Lambda} = \langle u_1 \ v_1 \rangle^T$ ,  $\underline{\Lambda}_2 = \langle u_2 \ v_2 \rangle^T$  are the ordered pairs.

A functional can now be constructed by integrating the inner product of the residual of equations (3.10) and (3.12) and a variation of an arbitrary element  $\delta \underline{\Lambda}$  in  $W$ , i.e.

$$\begin{aligned}
 J(u, v) &= J(\underline{\Lambda}) = \int_R \{ [\underline{P}(\underline{\Lambda}) - \underline{T}] + [\underline{B}(\underline{\Lambda}) - \underline{T}_{\partial R}] \} \delta \underline{\Lambda} dR \\
 &= 1/2 (Tu, v)_V + 1/2 (T^*v, u)_U + F(u) - 1/2 (v, v)_V \\
 &\quad + 1/2 (B^*v, u)_{U\partial R_2} - 1/2 (Bu, v)_{V\partial R_2} - 1/2 (g_2, u)_{U\partial R_2} \\
 &\quad + 1/2 (g_1, v)_{V\partial R_1}
 \end{aligned} \tag{3.15}$$

Here

$$F(u) = (f, u)_U. \tag{3.16}$$

In computing the boundary terms in (3.15), it is important to realize that both  $B$  and  $B^*$  depend upon  $T$ . Moreover  $B(u(\underline{x})) \equiv 0$  if  $\underline{x} \in \partial R_2$  and  $B^*(v(\underline{x})) \equiv 0$  if  $\underline{x} \in \partial R_1$  for the boundary conditions given in (3.4).

In the formulation of the variational statement (3.15) inclusion of the boundary terms is analogous to the boundary residual concept presented by Finlayson and Scriven [8] and to the principle of virtual work.

### Theorem 3.1.1

The functional  $J(u, v)$  of (3.15) assumes a stationary value at the point  $(\bar{u}, \bar{v})$  which satisfies the canonical pair (3.4), where the operator  $\underline{P}$  is defined for some dense set  $D_{\underline{A}}^W$  of the space  $W$ .

Proof:

Let the varied solution be  $u = \bar{u} + \alpha \eta$  and  $v = \bar{v} + \beta w$ , where  $u, \eta$  and  $v, w \in D_{\underline{A}}^W$ . Substitute it into the expression (3.15) for  $J(u, v)$ ,

$$\begin{aligned}
J(\bar{u}+\alpha\eta, \bar{v}+\beta w) &= 1/2(T(\bar{u}+\alpha\eta), \bar{v}+\beta w) + 1/2(T^*(\bar{v}+\beta w), \bar{u}+\alpha\eta)_U + F(\bar{u}+\alpha\eta) \\
&- 1/2(\bar{v}+\beta w, \bar{v}+\beta w)_V + 1/2(B^*(\bar{v}+\beta w), \bar{u}+\alpha\eta)_{U\partial R_2} - 1/2(B(\bar{u}+\alpha\eta), \bar{v}+\beta w)_{V\partial R_1} \\
&- (g_2, \bar{u}+\alpha\eta)_{U\partial R_2} + (g_1, \bar{v}+\beta w)_{V\partial R_1}.
\end{aligned} \tag{3.17}$$

Then for a stationary point of  $J(\bar{u}+\alpha\eta, \bar{v}+\beta w)$ ;

$$\begin{aligned}
\delta J(\bar{u}, \bar{v}; \eta, w) &= \lim_{\alpha \rightarrow 0} \frac{\partial J(\bar{u}+\alpha\eta, \bar{v})}{\partial \alpha} + \lim_{\beta \rightarrow 0} \frac{\partial J(\bar{u}, \bar{v}+\beta w)}{\partial \beta} = 0 \\
&= [1/2(T\bar{u}, w)_V + 1/2(T^*\bar{v}, \eta)_U + (f(\bar{u}), \eta) + 1/2 (B^*\bar{v}, \eta)_{U\partial R_2} \\
&- 1/2(B\bar{u}, w)_{V\partial R_1} - (g_2, \eta)_{U\partial R_2}] + [1/2(T\bar{u}, w)_{V\partial R_1} + 1/2(T^*\bar{v}, \eta)_{U\partial R_2} \\
&- (\bar{v}, w)_V + 1/2(B^*\bar{v}, \eta)_{U\partial R_2} - 1/2(B\bar{u}, w)_{V\partial R_1} + (g_1, w)_{V\partial R_1}] \\
&= [(T\bar{u}, w)_V - (\bar{v}, w)_V - (B\bar{u}, w)_{V\partial R_1} + (g_1, w)_{V\partial R_1}] + [(T^*\bar{v}, \eta)_U \\
&+ (f(\bar{u}), \eta)_U + (B^*\bar{v}, \eta)_{U\partial R_2} - (g_2, \eta)_{U\partial R_2}] \\
&= [(T^*\bar{v}+f(\bar{u}), \eta)_U + (B^*\bar{v}-g_2, \eta)_{U\partial R_2}] + [(T\bar{u}-\bar{v}, w)_V \\
&- (B\bar{u}-g_1, w)_{V\partial R_1}] = 0
\end{aligned} \tag{3.18}$$

Since the variations  $\eta$  and  $w$  are arbitrary, then from Lagrange's lemma

$$\begin{aligned}
T^*\bar{v} + f(\bar{u}) &= 0; & B^*\bar{v} &= g_2 \text{ on } \partial R_2 \\
T\bar{u} - \bar{v} &= 0; & B\bar{u} &= g_1 \text{ on } \partial R_1.
\end{aligned}$$

Hence the equations obtained are the same as equations (3.4),

and therefore the solution at the stationary point  $(\bar{u}, \bar{v})$  does satisfy the canonical pair (3.4).

### Boundary Conditions

Rewriting equation (3.5) by splitting the boundary inner product

$$(Tu, v)_V = (u, T^*v)_U + (B^*v, u)_{U\partial R_2} + (Bu, v)_{V\partial R_1} \tag{3.19}$$

the variational statement in (3.15) can be rewritten as

$$J(u, v) = (Tu, v)_V - 1/2(v, v)_V + F(u) - (Bu-g_1, v)_{V\partial R_1} - (g_2, u)_{U\partial R_2} \tag{3.20a}$$

$$\begin{aligned} \text{or } J(u,v) = & (T^*v,u)_U - 1/2(v,v)_V + F(u) + (B^*v-g_2,u)_{U\partial R_2} \\ & - (Bu-g_1,v)_{V\partial R_1} + (B^*v,u)_{V\partial R_1}. \end{aligned} \quad (3.20b)$$

The equivalent forms of  $J(u,v)$  in equations (3.20a) and (3.20b) provide some flexibility as to how boundary conditions can be incorporated. In (3.20a) the boundary integrals are extracted from the second of the canonical pair (3.4) (the equilibrium equation), and in (3.20b), from the first of (3.4) (the constitutive-compatibility combined equation). This idea shall be explained later in detail (Chapter 5 on boundary conditions).

It is worthwhile noting that under the assumption  $Tu=v$  being exactly satisfied, the functional  $(Ju,v)$  in (3.20a) reduces to

$$I(u) = 1/2(Tu,Tu) + F(u) - (g_2,u)_{\partial R_2} \quad (3.21)$$

This is the functional for the principle of minimum potential energy, the completeness, energy convergence and bounds for which are well established, Mikhlin [18].

### 3.2 Projection Operators

The orthogonal projection, or projection of a function into subspaces was discussed in Section 2.4. The method of orthogonal projections can also be used for estimating errors in approximations of linear boundary value problems, Mikhlin [18]. The idea of projections of linear operators has been exploited by Reddy and Oden [30] in establishing convergence rates for the basic variables involved in the mixed methods.

In general, there exists a number of possible projections for a given operator, e.g.,  $T^*T$ . The four important projections are cited here:

- (i) Primal Projection (equivalent to the conventional Ritz-Galerkin approximation)
  - (ii) Dual Projection (similar to the Equilibrium Finite Element method)
  - (iii) Primal-Dual Projection
  - (iv) Dual-Primal Projection
- (both together lead to the mixed formulation)

Consider two linear vector spaces,  $U$  and  $V$ , defined over the same field, and let  $\{\phi_m\}$ , ( $m=1,2, \dots M$ ) denote a set of  $M$  linearly independent elements in  $U$  and  $\{\psi_n\}$ , ( $n=1,2, \dots N$ ) a set of  $N$  linearly independent elements in  $V$ . The sets  $\{\phi_m\}$  and  $\{\psi_n\}$  define an  $M$ -dimensional subspace  $\Phi_M \in U$  and an  $N$ -dimensional subspace  $\Psi_N \in V$ , respectively. The Gram matrices associated with the subspaces  $\Phi_M$  and  $\Psi_N$  are

$$G_{ij} = (\phi_i, \phi_j)_U; H_{ij} = (\psi_i, \psi_j)_V \quad (3.22)$$

which are not singular since  $\{\phi_m\}$  and  $\{\psi_n\}$  are linearly independent and the biorthogonal bases can be computed directly

$$\phi^i = G_{ij}^{-1} \phi_j; \psi^i = H_{ij}^{-1} \psi_j. \quad (3.23)$$

From equations (3.22) and (3.23), it can be seen that the bi-orthogonality conditions are

$$(\phi_i, \phi^j)_U = \delta_i^j; (\psi_i, \psi^j)_V = \delta_i^j. \quad (\delta_i^j=1, \text{ when } i=j \text{ and zero otherwise}). \quad (3.24)$$

Note that there is no relation between the spaces  $U$  and  $V$ , and the biorthogonal bases in  $\Phi_M$  and  $\Psi_N$  are completely independent, unless some additional information is provided.

### Definition 3.2.1

The orthogonal projection operators  $\Pi: U \rightarrow \Phi_M$  and  $P: V \rightarrow \Psi_N$  can now be defined in the following sense: if  $u$  is an arbitrary element in  $U$  and  $v$  is an arbitrary element in  $V$ , the projection  $\bar{u}$  of  $u$  into subspace  $\Phi_M$  and the projection  $\bar{v}$  of  $v$  into subspace  $\Psi_N$  are of the form

$$\Pi(u) = \bar{u} = \sum_{i=1}^M a^i \phi_i \quad \text{and} \quad P(v) = \bar{v} = \sum_{i=1}^N b^i \psi_i \quad (3.25)$$

where  $a^i = (u, \phi_i)_U$  and  $b^i = (v, \psi_i)_V$ . (3.26)

Now let  $U$  be a Hilbert space consisting of functions  $u$  defined on a compact, convex subset  $R$  of  $E^n$  with a smooth boundary  $\partial R$ , and let  $T$  be a bounded linear operator mapping  $U$  into another Hilbert space  $V$ , and  $T^*: V \rightarrow U$  its formal adjoint satisfying equation (3.5) while  $B^*$  and  $B$  are their boundary operators which satisfy equation (3.5a). Consider the cases in which  $\phi_M \in D_T$ , the domain of  $T$ , and  $\psi_N \in D_{T^*}$ . In general,  $T(\phi_M)$  is not a subspace of  $\psi_N$ , and  $T^*(\psi_N)$  is not a subspace of  $\phi_M$ .

Operators  $T$  and  $T^*$  can be approximated by projecting  $T(\phi_M)$  into  $\psi_N$  and  $T^*(\psi_N)$  into  $\phi_M$ . This projection process leads to rectangular matrices of the following type:

$$PT(\phi_M): PT(\phi_i) = m_i^j \psi_j \quad (\text{Dual-Primal}) \quad (3.27)$$

$$\Pi T^*(\psi_N): \Pi T^*(\psi_i) = n_j^i \phi_j \quad (\text{Primal-Dual}) \quad (3.28)$$

Here  $P: V \rightarrow \psi_N$  and  $\Pi: U \rightarrow \phi_M$  are projection operators defined by bases  $\phi^i$  and  $\psi^i$ , and

$$m_i^j = (T\phi_i, \psi_j)_V; \quad n_j^i = (T^*\psi_i, \phi_j)_U. \quad (3.29)$$

Similar projections can also be obtained for  $B$  and  $B^*$ .

### 3.3 Mixed Galerkin Method

Consider the problem of equation (3.4) where  $f$  is a function of spatial coordinates  $\underline{x}$  only. That is,

$$T^*v + f = 0 \quad (3.30)$$

$$Tu - v = 0. \quad (3.31)$$

Choose linearly independent sequences of coordinate function  $\phi_1, \phi_2, \dots, \phi_M \in U^0$  for approximating  $u$  and  $\psi_1, \psi_2, \dots, \psi_N \in V^0$  for  $v$  over the same

domain  $R$  which are continuously differentiable in the closed domain  $\bar{R}=R+\partial R$  as many times as required for the specified problem, and satisfy all the boundary conditions of the problem. Then the functions

$$\begin{aligned} u_M &= \sum_{i=1}^M a_i \phi_i \\ v_N &= \sum_{i=1}^N b_i \psi_i \end{aligned} \quad (3.32)$$

where  $a_i$  and  $b_i$  are arbitrary constants, also satisfy all the boundary conditions of the problem.

In the mixed Galerkin method, the coefficients  $a_i$  and  $b_j$  are determined from the requirement that the residual of equation (3.30), is made orthogonal to the coordinate functions for  $u_M$  and the residual of equation (3.31) is made orthogonal to the coordinate functions for  $v_N$  over  $R$ . This then leads to the following system of algebraic equations:

$$\sum_{j=1}^N b_j (T^* \psi_j, \phi_i) = -(f, \phi_i); \quad i=1, 2, 3, \dots, M \quad (3.33)$$

$$\begin{aligned} \sum_{j=1}^M a_j (T \phi_j, \psi_i) - \sum_{k=1}^N b_k (\psi_j, \psi_i) &= 0; \\ i &= 1, 2, 3, \dots, N \end{aligned} \quad (3.34)$$

which consists of  $(M+N)$  equations with  $(M+N)$  unknowns ( $a_i, i=1, 2, \dots, M; b_j, j=1, 2, \dots, N$ ).

For equations (3.30) and (3.31), the operator  $T$  and its adjoint  $T^*$  are defined for sets which are dense in some separable Hilbert spaces  $U^0$  and  $V^0$ , respectively, and the sequences  $\{\phi_M\} \in D_T$  and  $\{\psi_N\} \in D_{T^*}$  are complete. The derivation of equations (3.33) and (3.34) is the same as the estimation of  $T$  and  $T^*$  by projection operators in the previous

section, equations (3.27) to (3.29), except here the bases are not bi-orthogonal. Furthermore, equations (3.33) and (3.34) would be identical to those derived from the functional  $J(u,v)$  of equation (3.15), since  $T^*$  is the formal adjoint of  $T$ .

Before the completeness and the convergence of mixed methods are presented, certain definitions and concepts have to be introduced.

### 3.4 Concepts and Definitions

The differential equations and boundary conditions in equation (3.4) can be put into matrix forms somewhat similar to equations (3.10) and (3.12) as

$$\begin{bmatrix} 0 & T^* \\ T & -1 \end{bmatrix} \begin{Bmatrix} u \\ v \end{Bmatrix} = \begin{Bmatrix} +f \\ 0 \end{Bmatrix} \text{ in } R \text{ and } \begin{bmatrix} 0 & B^* \\ B & 0 \end{bmatrix} \begin{Bmatrix} u \\ v \end{Bmatrix} = \begin{Bmatrix} g_1 \\ g_2 \end{Bmatrix} \text{ on } \partial R \quad (3.35)$$

$$\text{or} \quad \underline{A}\underline{\Lambda} = \underline{p} \text{ in } R \text{ and } \underline{B}\underline{\Lambda} = \underline{g} \text{ on } \partial R \quad (3.36)$$

$$\text{where} \quad \underline{A} = \begin{bmatrix} 0 & T^* \\ T & -1 \end{bmatrix} \text{ and } \underline{B} = \begin{bmatrix} 0 & B^* \\ B & 0 \end{bmatrix} \quad (3.36a)$$

which are linear operators,

$$\underline{\Lambda} = \begin{Bmatrix} u \\ v \end{Bmatrix}, \quad \underline{g} = \begin{Bmatrix} g_1 \\ g_2 \end{Bmatrix}$$

and

$$\underline{p} = \begin{Bmatrix} +f \\ 0 \end{Bmatrix}$$

where  $\underline{\Lambda}$  forms ordered pairs  $\langle u \ v \rangle^T$  just like in equation (3.9).

#### Definition 3.4.1

The class of functions that satisfy all the boundary conditions of the problem (3.35) and possess sufficient continuity to make the evaluation of  $\underline{A}\underline{\Lambda}$  possible is known as the field of definition of  $\underline{A}$  and is denoted

by  $W_{\underline{A}}$ . For example if  $A=T^*T$  were a fourth order differential operator, then  $T$  and  $T^*$  would be second order differential operators and the functions  $u$  and  $v$  in  $W_{\underline{A}}$  would have continuous second derivatives in  $R$  and would satisfy the boundary conditions in (3.35) on  $\partial R$ .

#### Definition 3.4.2

The operator  $\underline{A}$  is called symmetric if for any elements  $\underline{\Lambda}$  and  $\tilde{\underline{\Lambda}}$  from the field of definition of this operator  $W_{\underline{A}}$ , the following identity is valid:

$$(\underline{\underline{\Lambda}}, \tilde{\underline{\Lambda}})_{W_{\underline{A}}} = (\underline{\underline{\Lambda}}, \underline{\underline{\Lambda}})_{W_{\underline{A}}} \quad (3.37)$$

#### Theorem 3.4.1

Operator  $\underline{A}$  as defined in (3.36a) is a symmetric operator.

#### Proof:

For  $\underline{\Lambda}$  and  $\tilde{\underline{\Lambda}} \in W_{\underline{A}}$ , form the product

$$\begin{aligned} (\underline{\underline{\Lambda}}, \tilde{\underline{\Lambda}})_{W_{\underline{A}}} &= (T^*v, \tilde{u})_U + (Tu-v, \tilde{v})_V \\ &= (T^*v, \tilde{u})_U + (Tu, \tilde{v})_V - (v, \tilde{v})_V. \end{aligned}$$

Using equation (3.5)

$$(\underline{\underline{\Lambda}}, \tilde{\underline{\Lambda}})_{W_{\underline{A}}} = -(v, B\tilde{u})_{V\partial R} + (T\tilde{u}, v)_V + (\tilde{v}, Bu)_{V\partial R} + (T^*\tilde{v}, u)_U - (v, \tilde{v})_V.$$

Since  $\underline{\Lambda}$  and  $\tilde{\underline{\Lambda}}$  satisfy the same boundary conditions, then

$$(\underline{\underline{\Lambda}}, \tilde{\underline{\Lambda}})_{W_{\underline{A}}} = (T^*\tilde{v}, u)_U + (T\tilde{u}-\tilde{v}, v)_V = (\underline{\underline{\Lambda}}, \underline{\underline{\Lambda}})_{W_{\underline{A}}}$$

Hence, as long as  $T^*$  is the formal adjoint of  $T$ , the operator  $\underline{A}$  is symmetric.

In order to define a norm in the product space  $W_{\underline{A}}$ , an inner product has to be introduced. In the following it is assumed that the approximations  $u_M$  and  $v_N$  given in equations (3.32) are to be used for  $u$  and  $v$ , respectively. Then when the Mixed Galerkin Method is applied to equations (3.35), the second equation yields:

$$(v_N, \psi_j)_V = (Tu_M, \psi_j)_V; j=1, 2, \dots, N \quad (3.38)$$

where  $u_M = \sum_{i=1}^M a_i \phi_i; \phi_i \in U$  and  $\psi_j \in V$ .

This equation may be best understood by thinking of  $Tu_M$  as a known function  $f$ . Then if the  $\psi_j$  are orthonormal, equation (3.38) reduces to  $b_j = (f, \psi_j)_V$ , i.e. the Fourier coefficients. Further, if the sequence of functions  $\{\psi_N\}$  is complete and  $Tu_M \in V$ , then  $v_N$  can be made arbitrarily close to  $Tu_M$ , Lorch [17].

However, in formulating an energy product for the mixed method, another question arises and that is: is  $Tu_M=0$  when  $v_N=0$ ? This may be answered by noting that for  $v_N=0$  (which implies that the coefficients  $b_j=0$ ), equation (3.38) yields

$$(Tu_M, \psi_j)_V = 0, \text{ for each } j. \quad (3.39)$$

Then, if the sequence of functions  $\{\psi_N\}$  is complete and if  $Tu_M$  is restricted to be in  $V$ ,  $Tu_M=0$  necessarily, Lorch [17]. This is now used to define a restricted field of definition  $D_{\underline{A}}^W$  for the operator  $\underline{A}$ .

#### Definition 3.4.3

The restricted field of definition  $D_{\underline{A}}^W$  for the operator  $\underline{A}$  is defined as the product space  $\tilde{U} \times \tilde{V}$  where the restricted spaces  $\tilde{U}$  and  $\tilde{V}$  are subspaces of  $U$  and  $V$ , respectively. A sequence of functions  $\{\phi_M\} \in U$

are used for the approximation of  $u$ , i.e.  $u_M = \sum_{i=1}^M a_i \phi_i$ . Then the space  $\tilde{V}$  may be defined somewhat arbitrarily provided it includes  $Tu_M$ . That is, there is a minimum requirement that  $Tu_M \in \tilde{V}$ . Thereafter, any sequence of functions  $\{\psi_N\}$  used for approximating  $v$ , i.e.  $v_N = \sum_{j=1}^N b_j \psi_j$ , are assumed to be complete and to belong to  $\tilde{V}$ , i.e.  $\{\psi_N\} \in \tilde{V}$ . Conversely, any sequence  $\{\psi_N\} \in \tilde{V}$  restricts the choice of  $\{\phi_M\} \in U$ . Such restricted sequences  $\{\phi_M\}$  then constitute the restricted subspace  $\tilde{U}$ . Furthermore equations (3.38) are always to be enforced and therefore

$$(v_N, v_N)_{\tilde{V}} = (Tu_M, v_N)_{\tilde{V}} \quad (3.40)$$

where  $v_N$  and  $u_M$  now belong to the restricted space  $D_{\underline{A}}^W$ .

Now the energy product can be defined for this restricted space.

#### Definition 3.4.4

The energy product is defined as

$$\begin{aligned} [\underline{\Lambda}_1, \underline{\Lambda}_2] &= (\underline{A}\underline{\Lambda}_1, \underline{\Lambda}_2) = \int_R \langle u_2 \quad v_2 \rangle \begin{bmatrix} 0 & T^* \\ T & -1 \end{bmatrix} \begin{Bmatrix} u_1 \\ v_1 \end{Bmatrix} dR \\ &= (T^*v_1, u_2)_{\tilde{U}} + (Tu_1, v_2)_{\tilde{V}} - (v_1, v_2)_{\tilde{V}} \end{aligned} \quad (3.41)$$

where  $\underline{\Lambda}_1 = \langle u_1 \quad v_1 \rangle^T$  and  $\underline{\Lambda}_2 = \langle u_2 \quad v_2 \rangle^T \in D_{\underline{A}}^W$ .

(Note: If  $Tu=v$  is satisfied exactly it can be shown that  $[\underline{\Lambda}, \underline{\Lambda}] = (Tu, Tu)$ , i.e. the above energy product is twice the strain energy).

The energy product so defined has to satisfy the properties of an inner product in definition 2.1.1. The properties (i), (ii) and (iii)

follow from linearity and symmetry of the operator  $\underline{A}$  whereas the property (iv), which follows from positivity of the inner product, is not as obvious.

This is proved here.

The energy product in (3.41) can be rewritten as

$$[\underline{\tilde{A}}, \underline{\tilde{A}}] = (T^* \tilde{v}, \tilde{u})_{\tilde{U}} + (T \tilde{u}, \tilde{v})_{\tilde{V}} - (\tilde{v}, \tilde{v})_{\tilde{V}}; \{ \underline{\tilde{A}} \in D_{\underline{A}}^W = \tilde{U} \times \tilde{V} \}. \quad (3.41a)$$

Assuming homogeneous boundary conditions, therefore from (3.3)

$$(T^* \tilde{v}, \tilde{u})_{\tilde{U}} = (T \tilde{u}, \tilde{v})_{\tilde{V}}$$

and substitution into (3.41a) yields

$$[\underline{\tilde{A}}, \underline{\tilde{A}}] = 2(T \tilde{u}, \tilde{v})_{\tilde{V}} - (\tilde{v}, \tilde{v})_{\tilde{V}}. \quad (3.41b)$$

Since  $\underline{\tilde{A}} \in D_{\underline{A}}^W$  and equation (3.40) is satisfied, replacing  $(T \tilde{u}, \tilde{v})_{\tilde{V}}$  by  $(\tilde{v}, \tilde{v})_{\tilde{V}}$  in (3.41b) leads to

$$[\underline{\tilde{A}}, \underline{\tilde{A}}] = (\tilde{v}, \tilde{v})_{\tilde{V}}. \quad (3.42)$$

The right hand side of (3.42) is always greater than zero and equals zero if, and only if,  $\tilde{v}=0$ . Further, for any  $\underline{\tilde{A}}$  in the restricted space  $D_{\underline{A}}^W$ , if  $\tilde{v}=0$  then also  $T \tilde{u}=0$  and it follows from the homogeneous boundary conditions that  $\tilde{u}=0$ .

Hence, the positive definiteness of the mixed operator  $\underline{A}$ , when every  $\underline{A}$  is chosen from the restricted space  $D_{\underline{A}}^W$ , can be ascertained as

$$[\underline{A}, \underline{A}] \geq 0, \text{ where the equality holds if, and only if, } \underline{A} \equiv 0. \quad (3.43)$$

Further it is bounded below as

$$[\underline{A}, \underline{A}] \geq v^2 \|v\|^2 \quad (3.43a)$$

where  $v$  is a positive constant. This then proves that the property (iv)

of an inner product in definition 2.1.1 also holds.

The energy norm can now be defined as

$$|\underline{\Lambda}| = \sqrt{[\underline{\Lambda}, \underline{\Lambda}]}; \{\underline{\Lambda} \in D_{\underline{\Lambda}}^W\}$$

and the following theorem holds.

### Theorem 3.4.2

If the energy norm is defined as  $|\underline{\Lambda}| = \sqrt{[\underline{\Lambda}, \underline{\Lambda}]}$  and the conditions of the energy product in definition 3.4.3 are satisfied, i.e.  $\underline{\Lambda}$  is chosen from the restricted space  $D_{\underline{\Lambda}}^W$ , then

- (i)  $|\underline{\Lambda}| \geq 0$ , the equality holds if, and only if  $\underline{\Lambda} \equiv \underline{0}$ ;
- (ii)  $|a\underline{\Lambda}| = |a| |\underline{\Lambda}|$ ,  $a = \text{constant}$ ;
- (iii)  $|[\underline{\Lambda}_1 \underline{\Lambda}_2]| \leq |\underline{\Lambda}_1| |\underline{\Lambda}_2|$  (Schwarz inequality);
- (iv)  $|\underline{\Lambda}_1 + \underline{\Lambda}_2| \leq |\underline{\Lambda}_1| + |\underline{\Lambda}_2|$  (triangle inequality).

#### Proof (i):

This property of the energy norm follows from the positive definiteness of the energy product.

#### Proof (ii):

From linearity of the operator  $\underline{A}$  and substituting  $\underline{\Lambda}_1 = \underline{\Lambda}_2 = a\underline{\Lambda}$  in equation (3.38), where  $a$  is constant

$$[a\underline{\Lambda}, a\underline{\Lambda}] = a^2 [\underline{\Lambda}, \underline{\Lambda}].$$

By taking the square root of both sides

$$|a\underline{\Lambda}| = \sqrt{[a\underline{\Lambda}, a\underline{\Lambda}]} = |a| |\underline{\Lambda}|.$$

#### Proof (iii):

Consider an arbitrary positive real number  $\lambda$  and construct the

non-zero function  $\underline{\Lambda}_1 + \lambda \underline{\Lambda}_2$ . The energy product of this function, by using linearity and symmetry of the operator  $\underline{A}$  yields

$$[\underline{\Lambda}_1 + \lambda \underline{\Lambda}_2, \underline{\Lambda}_1 + \lambda \underline{\Lambda}_2] = [\underline{\Lambda}_1, \underline{\Lambda}_2] + 2\lambda [\underline{\Lambda}_1, \underline{\Lambda}_2] + \lambda^2 [\underline{\Lambda}_2, \underline{\Lambda}_2].$$

By virtue of property (i)

$$[\underline{\Lambda}_1 + \lambda \underline{\Lambda}_2, \underline{\Lambda}_1 + \lambda \underline{\Lambda}_2] \geq 0. \quad (3.44)$$

Therefore

$$[\underline{\Lambda}_1, \underline{\Lambda}_1] + 2\lambda [\underline{\Lambda}_1, \underline{\Lambda}_2] + \lambda^2 [\underline{\Lambda}_2, \underline{\Lambda}_2] \geq 0. \quad (3.45)$$

The left hand side of (3.45) is quadratic in  $\lambda$ , and all its values are non-negative. Hence it follows that its discriminant is less than or equal to zero

$$[\underline{\Lambda}_1, \underline{\Lambda}_2]^2 - [\underline{\Lambda}_1, \underline{\Lambda}_1] [\underline{\Lambda}_2, \underline{\Lambda}_2] \leq 0$$

or

$$[\underline{\Lambda}_1, \underline{\Lambda}_2]^2 \leq [\underline{\Lambda}_1, \underline{\Lambda}_1] [\underline{\Lambda}_2, \underline{\Lambda}_2].$$

Taking the square root of both sides yields the required inequality

$$|[\underline{\Lambda}_1, \underline{\Lambda}_2]| \leq |\underline{\Lambda}_1| |\underline{\Lambda}_2|.$$

Proof (iv):

If  $\lambda=1$  in proof (iii), the following results:

$$[\underline{\Lambda}_1 + \underline{\Lambda}_2, \underline{\Lambda}_1 + \underline{\Lambda}_2] = [\underline{\Lambda}_1, \underline{\Lambda}_1] + 2[\underline{\Lambda}_1, \underline{\Lambda}_2] + [\underline{\Lambda}_2, \underline{\Lambda}_2]$$

or

$$|\underline{\Lambda}_1 + \underline{\Lambda}_2|^2 \leq |\underline{\Lambda}_1|^2 + 2|[\underline{\Lambda}_1, \underline{\Lambda}_2]| + |\underline{\Lambda}_2|^2.$$

Substituting the Schwarz inequality  $|[\underline{\Lambda}_1, \underline{\Lambda}_2]| \leq |\underline{\Lambda}_1| |\underline{\Lambda}_2|$ ;

$$|\underline{\Lambda}_1 + \underline{\Lambda}_2|^2 \leq |\underline{\Lambda}_1|^2 + 2|\underline{\Lambda}_1| |\underline{\Lambda}_2| + |\underline{\Lambda}_2|^2$$

or

$$|\underline{\Lambda}_1 + \underline{\Lambda}_2|^2 \leq (|\underline{\Lambda}_1| + |\underline{\Lambda}_2|)^2.$$

Taking the square root of both sides gives the required inequality

$$|\underline{\Lambda}_1 + \underline{\Lambda}_2| \leq |\underline{\Lambda}_1| + |\underline{\Lambda}_2|.$$

Similarly it can be shown that

$$|\underline{\Lambda}_1 - \underline{\Lambda}_2| \leq |\underline{\Lambda}_1| + |\underline{\Lambda}_2|.$$

### 3.5 Convergence of the Mixed Method

The mixed variational principle of equation (3.15) for homogeneous boundary conditions, i.e.,  $g_1 = g_2 = 0$  in equations (3.4), in lieu of definition 3.4.3 of the energy product, can be rewritten in the following form:

$$F(\underline{\Lambda}) = (\underline{A}\underline{\Lambda}, \underline{\Lambda}) - 2(\underline{p}^T, \underline{\Lambda}) \quad (3.46)$$

where  $\underline{\Lambda} \in D_{\underline{A}}^W$ . From theorem 3.1.1, let  $\underline{\Lambda}_0 = (u_0, v_0)$  satisfy the canonical pair (3.4) for which the functional  $F(\underline{\Lambda}_0)$  assumes a stationary value, and has a finite value in general. Then the matrix form (3.36) becomes

$$\underline{A}\underline{\Lambda}_0 = \underline{p}. \quad (3.47)$$

Substituting for  $\underline{p}$  in (3.46),

$$F(\underline{\Lambda}) = (\underline{A}\underline{\Lambda}, \underline{\Lambda}) - 2(\underline{A}\underline{\Lambda}_0, \underline{\Lambda}) = [\underline{\Lambda}, \underline{\Lambda}] - 2[\underline{\Lambda}_0, \underline{\Lambda}]. \quad (3.48)$$

Adding and subtracting  $[\underline{\Lambda}_0, \underline{\Lambda}_0]$  from the right hand side of (3.48)

$$F(\underline{\Lambda}) = [\underline{\Lambda}, \underline{\Lambda}] - 2[\underline{\Lambda}_0, \underline{\Lambda}] + [\underline{\Lambda}_0, \underline{\Lambda}_0] - [\underline{\Lambda}_0, \underline{\Lambda}_0]$$

which can be formally shown to be

$$F(\underline{\Lambda}) = [\underline{\Lambda} - \underline{\Lambda}_0, \underline{\Lambda} - \underline{\Lambda}_0] - [\underline{\Lambda}_0, \underline{\Lambda}_0]. \quad (3.49)$$

Now if  $\underline{\Lambda} = \underline{\Lambda}_0$  the exact solution, then

$$F(\underline{\Lambda}_0) = -[\underline{\Lambda}_0, \underline{\Lambda}_0]. \quad (3.50)$$

Let  $d$ , some real number be the exact stationary value of the functional.

Therefore

$$d = F(\underline{\Lambda}_0) = -[\underline{\Lambda}_0, \underline{\Lambda}_0]. \quad (3.51)$$

In general, the functional  $F(\underline{\Lambda})$  does not lead to a minimum problem.

However, as a consequence of the conditions imposed on the energy product, it's positive definiteness provides the sufficient condition for the minimum.

Therefore the following minimum functional theorem is presented.

### Theorem 3.5.1

Let  $\underline{A}$  be a symmetric and indefinite operator as defined in equation (3.35) and further that this equation has a solution. Then of all the values which are given to the quadratic functional

$$F(\underline{\Lambda}) = (\underline{A}\underline{\Lambda}, \underline{\Lambda}) - 2(\underline{p}^T, \underline{\Lambda}) \quad (3.52)$$

by all possible functions from the restricted field of definition  $D_{\underline{A}}$  of the operator  $\underline{A}$ , the actual minimum occurs only for the solution of equations (3.35).

### Converse:

If there exists in  $D_{\underline{A}}^W$  a function  $\underline{\Lambda} = \langle u \ v \rangle^T$  which also satisfies the conditions of the definition 3.4.3 and gives the minimal value to the functional (3.52), then this function is also the solution of equation (3.35).

### Proof:

Assume that  $\underline{\Lambda}, \underline{\Lambda}_1 \in D_{\underline{A}}^W$  and  $\underline{\Lambda} = \langle u \ v \rangle^T$  and  $\underline{\Lambda}_1 = \langle \mu \ \eta \rangle^T$ . Set  $\underline{\Lambda} - \underline{\Lambda}_0 = \underline{\Lambda}_1$  where  $\underline{\Lambda}_0$  is the solution of equations (3.35). Thus  $\underline{\Lambda} = \underline{\Lambda}_0 + \underline{\Lambda}_1$ . Therefore from linearity and symmetry of the operator,

$$\begin{aligned} F(\underline{\Lambda}) &= [\underline{\Lambda}, \underline{\Lambda}] - 2(\underline{p}^T, \underline{\Lambda}) \\ &= (\underline{A}(\underline{\Lambda}_0 + \underline{\Lambda}_1), \underline{\Lambda}_0 + \underline{\Lambda}_1) - 2(\underline{p}^T, \underline{\Lambda}_0 + \underline{\Lambda}_1) \\ &= [\underline{\Lambda}_0, \underline{\Lambda}_0] - 2(\underline{p}^T, \underline{\Lambda}_0) + 2(\underline{A}\underline{\Lambda}_0 - \underline{p}^T, \underline{\Lambda}_1) + [\underline{\Lambda}_1, \underline{\Lambda}_1] \\ &= F(\underline{\Lambda}_0) + 2(\underline{A}\underline{\Lambda}_0 - \underline{p}, \underline{\Lambda}_1) + [\underline{\Lambda}_1, \underline{\Lambda}_1]. \end{aligned}$$

But  $\underline{\Lambda}_0 - \underline{p} = 0$  by hypothesis. Hence

$$F(\underline{\Lambda}) = F(\underline{\Lambda}_0) + [\underline{\Lambda}_1, \underline{\Lambda}_1].$$

Now from positive definiteness of the energy product

$$[\underline{\Lambda}_1, \underline{\Lambda}_1] \geq 0, \text{ where the equality holds if, and only if, } \underline{\Lambda}_1 = 0.$$

Thus  $F(\underline{\Lambda}) \geq F(\underline{\Lambda}_0)$  with equality only valid if  $\underline{\Lambda}_1 = 0$  or  $\underline{\Lambda} = \underline{\Lambda}_0$ . Hence the functional attains its minimum value when  $\underline{\Lambda} = \underline{\Lambda}_0$  and from (3.49)

$$\min F(\underline{\Lambda}) = F(\underline{\Lambda}_0) = -[\underline{\Lambda}_0, \underline{\Lambda}_0] = -|\underline{\Lambda}_0|^2.$$

The converse follows from theorem 3.1.1. The functional  $F(\underline{\Lambda})$  assumes a stationary value at  $\underline{\Lambda} = \langle \underline{u} \quad \underline{v} \rangle^T$  which satisfies the equation (3.35) and further, this stationary value is a minimum when the conditions of the definition 3.4.3 are satisfied. Therefore the function  $\underline{\Lambda}_0 \in D_{\underline{A}}^W$  which gives the functional in (3.52) the minimal value is also the solution of equation (3.35).

### Theorem 3.5.2

The approximate solution  $\underline{\Lambda}_{-m}^n = \langle \underline{\bar{u}}_m \quad \underline{\bar{v}}_n \rangle^T \in D_{\underline{A}}^W$  of equation (3.35) constitutes a minimizing sequence for the functional (3.52) provided that equation (3.35) has a solution with finite energy and that the conditions of definition 3.4.3 are satisfied.

### Proof:

From theorem 3.5.1 let  $d$  be the minimum value of  $F(\underline{\Lambda})$ , i.e.

$$d = \min F(\underline{\Lambda}) = -|\underline{\Lambda}_0|^2.$$

Let the approximation  $\underline{\Lambda}_{-m}^n = \langle \underline{\bar{u}}_m \quad \underline{\bar{v}}_n \rangle^T$  be given by

$$\underline{\bar{u}}_m = \sum_{i=1}^m \phi_i u_i$$

$$\underline{\bar{v}}_n = \sum_{j=1}^n \psi_j v_j$$

(3.53a)

Therefore  $F(\underline{\Lambda}_{-m}^n) \geq d$ , since  $\underline{\Lambda}_{-m}^n \in D_{\underline{A}}^W$  and  $\bar{u}_m$  and  $\bar{v}_n$  are linear combinations of the sequences  $\{\phi_m\}$  and  $\{\psi_n\}$ , respectively, which enter into  $D_{\underline{A}}^W$ . The quantity  $d$  is the exact lower bound of the function  $F(\underline{\Lambda})$ . If  $\varepsilon$  is an arbitrary small positive number, then, by definition of the exact lower bound, there exists a function  $\tilde{\underline{\Lambda}} \in D_{\underline{A}}^W$  such that  $d < F(\tilde{\underline{\Lambda}}) < d + \frac{\varepsilon}{2}$ . The task now reduces to choosing natural numbers  $m$  and  $n$  and constants  $\bar{u}_1, \bar{u}_2, \dots, \bar{u}_m$  and  $\bar{v}_1, \bar{v}_2, \dots, \bar{v}_n$  such that they satisfy the inequality

$$F(\underline{\Lambda}_{-m}^n) - F(\tilde{\underline{\Lambda}}) < \frac{\varepsilon}{2}. \quad (3.53b)$$

Using equation (3.49) this inequality reduces to

$$[\underline{\Lambda}_{-m}^n - \underline{\Lambda}_0, \underline{\Lambda}_{-m}^n - \underline{\Lambda}_0] - [\tilde{\underline{\Lambda}} - \underline{\Lambda}_0, \tilde{\underline{\Lambda}} - \underline{\Lambda}_0] < \frac{\varepsilon}{2}. \quad (3.53c)$$

Consider the left hand side

$$\begin{aligned} [\underline{\Lambda}_{-m}^n - \underline{\Lambda}_0, \underline{\Lambda}_{-m}^n - \underline{\Lambda}_0] - [\tilde{\underline{\Lambda}} - \underline{\Lambda}_0, \tilde{\underline{\Lambda}} - \underline{\Lambda}_0] &= |\underline{\Lambda}_{-m}^n - \underline{\Lambda}_0|^2 - |\tilde{\underline{\Lambda}} - \underline{\Lambda}_0|^2 \\ &= \{|\underline{\Lambda}_{-m}^n - \underline{\Lambda}_0| + |\tilde{\underline{\Lambda}} - \underline{\Lambda}_0|\} \{|\underline{\Lambda}_{-m}^n - \underline{\Lambda}_0| - |\tilde{\underline{\Lambda}} - \underline{\Lambda}_0|\}. \end{aligned} \quad (3.54)$$

By the triangle inequality, property (iv) of theorem 2.4.2

$$|\underline{\Lambda}_{-m}^n - \underline{\Lambda}_0| \leq |\underline{\Lambda}_{-m}^n - \tilde{\underline{\Lambda}}| + |\tilde{\underline{\Lambda}} - \underline{\Lambda}_0|.$$

Therefore

$$|\underline{\Lambda}_{-m}^n - \underline{\Lambda}_0| - |\tilde{\underline{\Lambda}} - \underline{\Lambda}_0| \leq |\underline{\Lambda}_{-m}^n - \tilde{\underline{\Lambda}}|.$$

Substitution into (3.54) yields

$$[\underline{\Lambda}_{-m}^n - \underline{\Lambda}_0, \underline{\Lambda}_{-m}^n - \underline{\Lambda}_0] - [\tilde{\underline{\Lambda}} - \underline{\Lambda}_0, \tilde{\underline{\Lambda}} - \underline{\Lambda}_0] \leq \{|\underline{\Lambda}_{-m}^n - \underline{\Lambda}_0| + |\tilde{\underline{\Lambda}} - \underline{\Lambda}_0|\} |\underline{\Lambda}_{-m}^n - \tilde{\underline{\Lambda}}|.$$

Select  $m, n$  and coefficients  $u_1, u_2, \dots, u_m; v_1, v_2, \dots, v_n$  such that

$$|\underline{\Lambda}_{-m}^n - \tilde{\underline{\Lambda}}| < \frac{\varepsilon}{k}.$$

The value of  $k$  will be chosen later. Also from the triangle inequality

$$|\underline{\Lambda}_{-m}^n - \tilde{\underline{\Lambda}}| \leq |\underline{\Lambda}_{-m}^n| + |\tilde{\underline{\Lambda}}|.$$

Therefore 
$$|\tilde{\Lambda}_{-m}^n - \Lambda_0| + |\tilde{\Lambda} - \Lambda_0| \leq |\tilde{\Lambda}_{-m}^n| + |\tilde{\Lambda}| + 2|\Lambda_0|.$$

Now 
$$|\tilde{\Lambda}_{-m}^n| < |\tilde{\Lambda}| + \frac{\varepsilon}{k}$$

and 
$$[\tilde{\Lambda}_{-m}^n - \Lambda_0, \tilde{\Lambda}_{-m}^n - \Lambda_0] - [\tilde{\Lambda} - \Lambda_0, \tilde{\Lambda} - \Lambda_0] < \{2|\tilde{\Lambda}| + 2|\Lambda_0| + \frac{\varepsilon}{k}\} \frac{\varepsilon}{k}. \quad (3.54a)$$

By taking  $k$  such that

$$\frac{1}{k} \{2|\tilde{\Lambda}| + 2|\Lambda_0| + \frac{\varepsilon}{k}\} < \frac{1}{2}$$

inequality (3.54a) reduces to (3.53), i.e.

$$[\tilde{\Lambda}_{-m}^n - \Lambda_0, \tilde{\Lambda}_{-m}^n - \Lambda_0] - [\tilde{\Lambda} - \Lambda_0, \tilde{\Lambda} - \Lambda_0] < \frac{\varepsilon}{2}.$$

Therefore 
$$F(\tilde{\Lambda}_{-m}^n) - F(\tilde{\Lambda}) < \frac{\varepsilon}{2}.$$

Hence, it follows that

$$d \leq F(\tilde{\Lambda}_{-m}^n) \leq F(\tilde{\Lambda}) + \frac{\varepsilon}{2} < d + \varepsilon. \quad (3.55)$$

Let  $\tilde{\Lambda}_{-m}^n$  be the solution obtained by minimizing the functional  $F(\tilde{\Lambda})$  in (3.46).

Then

$$d \leq F(\tilde{\Lambda}_{-m}^n) \leq F(\tilde{\Lambda}_{-m}^n) \quad (3.56a)$$

or 
$$d \leq F(\tilde{\Lambda}_{-m}^n) \leq d + \varepsilon. \quad (3.56b)$$

Thus by letting  $\varepsilon \rightarrow 0$ , the functional  $F(\tilde{\Lambda}_{-m}^n)$  converges to the exact value  $d$ ,

i.e. the sequence  $\tilde{\Lambda}_{-m}^n = \langle \tilde{u}_m, \tilde{v}_n \rangle^T$  is minimizing.

Rewriting inequality (3.56b) as

$$0 \leq F(\tilde{\Lambda}_{-m}^n) - d \leq \varepsilon,$$

and using equations (3.49), (3.51) and positive definiteness of the energy product, this inequality reduces to

$$[\tilde{\Lambda}_{-m}^n - \Lambda_0, \tilde{\Lambda}_{-m}^n - \Lambda_0] \leq \varepsilon,$$

or 
$$|\underline{\Lambda}_m^n - \underline{\Lambda}_0| \leq \varepsilon.$$

Again as  $\varepsilon \rightarrow 0$ , therefore

$$|\underline{\Lambda}_m^n - \underline{\Lambda}_0| \rightarrow 0. \quad (3.57)$$

But from equation (3.42)

$$[\underline{\Lambda}_m^n - \underline{\Lambda}_0, \underline{\Lambda}_m^n - \underline{\Lambda}_0] = (\bar{v}_m - v_0, \bar{v}_m - v_0)_V.$$

Therefore 
$$\|\bar{v}_m - v_0\| \rightarrow 0 \quad (3.58)$$

Hence convergence in energy also implies the mean square convergence of the approximating stress  $\bar{v}_m$  to the exact value  $v_0$ .

In order to show the mean convergence of the displacement, consider a free vibration problem for which the equation (3.35) takes the form

$$\begin{bmatrix} 0 & T^* \\ T & -1 \end{bmatrix} \begin{bmatrix} u \\ v \end{bmatrix} = \omega^2 \begin{bmatrix} 1 & 0 \\ 0 & 0 \end{bmatrix} \begin{bmatrix} u \\ v \end{bmatrix} \quad (3.59)$$

where  $\omega$  is the frequency of vibration. Alternatively,

$$\underline{A}\underline{\Lambda} = \lambda \underline{B}\underline{\Lambda}. \quad (3.60)$$

Here  $\underline{A}$  is a symmetric operator as before,  $\omega^2 = \lambda$  and  $\underline{B} = \begin{bmatrix} 1 & 0 \\ 0 & 0 \end{bmatrix}$ .

Let  $\lambda_0$  and  $\underline{\Lambda}_0 = \langle u_0 \ v_0 \rangle^T$  be an eigenvalue and its eigenfunction, respectively. Then

$$\underline{A}\underline{\Lambda}_0 = \lambda_0 \underline{B}\underline{\Lambda}_0, \quad (3.61)$$

and substituting into the energy product (3.41) yields

$$[\underline{\Lambda}_0, \underline{\Lambda}_0] = \lambda_0 (\underline{B}\underline{\Lambda}_0, \underline{\Lambda}_0)_{D_{\underline{A}}^W}. \quad (3.62)$$

But 
$$(\underline{B}\underline{\Lambda}_0, \underline{\Lambda}_0)_{D_{\underline{A}}^W} = (u_0, u_0)_{\tilde{U}}. \quad (3.63)$$

Therefore 
$$\lambda_0 = \frac{[\underline{\Lambda}_0, \underline{\Lambda}_0]}{(u_0, u_0)_{\tilde{U}}}. \quad (3.64)$$

Since the energy product  $[\underline{\Lambda}_0, \underline{\Lambda}_0]$  represents strain energy, equation (3.64) is similar to the Rayleigh's quotient. Further, from the positive definiteness of  $[\underline{\Lambda}_0, \underline{\Lambda}_0]$  and observing that  $(u_0, u_0)$  is always a positive number,  $\lambda_0$  is also a positive real number.

In general for any  $\underline{\Lambda} \in D_{\underline{A}}^W$ , the equation (3.64) can be rewritten as

$$\lambda = \frac{[\underline{\Lambda}, \underline{\Lambda}]}{(u, u)_U} \quad (3.65)$$

Let  $\underline{\Lambda}_0 = \langle u_0, v_0 \rangle^T$  be the exact solution and consider the energy product of the difference  $\underline{\Lambda}_m^n - \underline{\Lambda}_0$ , where  $\underline{\Lambda}_m^n$  and  $\underline{\Lambda}_0$  satisfy the same boundary conditions. Then from symmetry of the operator  $\underline{A}$

$$[\underline{\Lambda}_m^n - \underline{\Lambda}_0, \underline{\Lambda}_m^n - \underline{\Lambda}_0] = [\underline{\Lambda}_m^n, \underline{\Lambda}_m^n] + [\underline{\Lambda}_0, \underline{\Lambda}_0] - 2[\underline{\Lambda}_0, \underline{\Lambda}_m^n].$$

Using equations (3.62), (3.64) and (3.65)

$$[\underline{\Lambda}_m^n - \underline{\Lambda}_0, \underline{\Lambda}_m^n - \underline{\Lambda}_0] = \lambda (\bar{u}_m, \bar{u}_m)_U + \lambda_0 (u_0, u_0)_U - 2\lambda_0 (u_0, \bar{u}_m)_U.$$

Therefore from equation (3.42)

$$(\bar{v}_n - v_0, \bar{v}_n - v_0)_V = \lambda (\bar{u}_m, \bar{u}_m)_U + \lambda_0 (u_0, u_0)_U - 2\lambda_0 (u_0, \bar{u}_m)_U.$$

Because of the definition 3.4.3, the problem becomes that of a minimum.

Therefore  $\lambda > \lambda_0$  and replacing  $\lambda$  by  $\lambda_0$  yields the following inequality:

$$\lambda_0 (\bar{u}_m - u_0, \bar{u}_m - u_0)_U \leq (\bar{v}_n - v_0, \bar{v}_n - v_0)_U$$

or 
$$\omega_0 \|\bar{u}_m - u_0\| < \|\bar{v}_n - v_0\|.$$

Since  $\omega_0$  is not zero, from (3.58) also

$$\|\bar{u}_m - u_0\| \rightarrow 0. \quad (3.66)$$

Hence convergence in energy also implies the mean square convergence of the approximation  $\bar{u}_m$  to the exact value  $u_0$  of the displacement.

The following theorem can now be stated for convergence of stress and displacement when the approximate solution converges in the energy sense.

### Theorem 3.5.3

If the approximations  $\Lambda_{-m}^n = \langle \bar{u}_m, \bar{v}_n \rangle^T \in D_{\underline{A}}^W$  for the displacement and stress converge in the energy sense, i.e.  $|\Lambda_{-m}^n - \Lambda_0| \rightarrow 0$  as  $m$  and  $n \rightarrow \infty$ , then it follows that the displacement  $\bar{u}_m$  and stress  $\bar{v}_n$  converge to the exact values  $u_0$  and  $v_0$ , respectively, in the mean square sense.

So far the energy convergence and the convergence of displacement and stress have been discussed in general terms. Now in order to establish the completeness in energy, it is sufficient to reiterate the requirements in definition 3.4.3. In defining the restricted space  $D_{\underline{A}}^W$ , it was required that  $T\bar{u}_m \in \tilde{V}$ . Also the sequence of functions  $\{\psi_n\}$  used for approximating  $v$ , i.e.  $\bar{v}_n = \sum_{j=1}^n \psi_j v_j$  must belong to  $\tilde{V}$ . Thus, when the Mixed Galerkin Method is applied to equations (3.35) using the approximations in (3.53a), the second equation yields

$$\sum_{j=1}^n (\psi_i, \psi_j) v_j = \sum_{j=1}^m (\psi_i, T\phi_j) u_j; \quad i=1, 2, \dots, n. \quad (3.67)$$

Assuming  $\psi_j \in \tilde{V}$  are orthonormal for convenience, i.e.

$$(\psi_i, \psi_j) = \begin{cases} 1 & \text{if } i = j \\ 0 & \text{if } i \neq j, \end{cases}$$

equation (3.67) then reduces to

$$v_i = \sum_{j=1}^m (\psi_i, T\phi_j) u_j = (T\bar{u}_m, \psi_i). \quad (3.67a)$$

These are the Fourier coefficients for  $T\bar{u}_m$  with respect to the orthonormal sequence  $\{\psi_n\} \in \tilde{V}$ . The equation (3.67a) can also be obtained by minimizing the  $L_2$  norm  $\|T\bar{u}_m - \bar{v}_n\|$ , Mikhlin [18], given by

$$\|T\bar{u}_m - \bar{v}_n\|^2 = \int_R (T\bar{u}_m - \bar{v}_n)^2 dR, \quad (3.68)$$

with respect to the unknown constants  $v_j$ . This represents the mean square convergence of  $\bar{v}_n$  to  $T\bar{u}_m$  and plays an important role in defining completeness in energy of the mixed methods. Unless, for any  $T\bar{u}_m \in \tilde{V}$  the set of functions

$\{\psi_n\}$  is complete for convergence in the mean square sense, the energy product in definition 3.4.4 is not positive definite. Therefore, the mean square convergence of the approximation of  $v$ , i.e.  $\bar{v}_n = \sum_{j=1}^n \psi_j v_j$  to  $T\bar{u}_m$  ( $\bar{u}_m = \sum_{i=1}^m \phi_i u_i$ ;  $\phi_i \in \tilde{U}$ ) acts as a prerequisite for completeness in energy.

### 3.6 Completeness

The sequences of functions  $\phi_1, \phi_2, \dots$  and  $\psi_1, \psi_2, \dots$  are said to be complete in  $D_A^W$  if for a function  $\underline{\Lambda}$  with a finite energy norm and any  $\varepsilon_1 > 0$ ,  $\varepsilon_2 > 0$ , it is possible to find positive integers  $M$  and  $N$  and constants  $\alpha_1, \alpha_2, \dots, \alpha_M$ ;  $\beta_1, \beta_2, \dots, \beta_N$  such that the following inequalities are satisfied:

$$(i) \quad \|T\bar{u}_M - (\beta_1\psi_1 + \beta_2\psi_2 + \dots + \beta_N\psi_N)\| < \varepsilon_2$$

$$(ii) \quad \|\underline{\Lambda} - \underline{\Lambda}_M^N\| < \varepsilon_1$$

where  $\underline{\Lambda} = \langle u \quad v \rangle^T$ ,  $\underline{\Lambda}_M^N = \langle \bar{u}_M \quad \bar{v}_N \rangle^T$  and  $\bar{u}_M = \sum_{i=1}^M \alpha_i \phi_i$ ,  $\bar{v}_N = \sum_{i=1}^N \beta_i \psi_i$ .

The first inequality (which comes from the second of equations (3.35), the constitutive equation) implies that the approximation of the stress function  $v$ , i.e.  $\bar{v}_n = \sum_{i=1}^N \beta_i \psi_i$  for finite  $N$  should contain all the stress modes that correspond to strain modes present in the strain  $T\bar{u}_M$  obtained from the displacement approximation  $\bar{u}_M$ , and only then  $\underline{\Lambda}_M^N$  will converge to  $\underline{\Lambda}$  in energy.

### 3.7 Estimation of Error in the Energy Product

It was shown in Section 3.5 that the mixed approximation  $\underline{\Lambda}_m^n \in D_A^W$  of equation (3.53a) does converge in the energy sense. Therefore it is desirable to seek some estimate of error in the energy product (or strain energy). From equation (3.41)

$$\begin{aligned} [\underline{\Lambda}_m^n - \underline{\Lambda}_0, \underline{\Lambda}_m^n - \underline{\Lambda}_0] &= \int_R \langle \bar{u}_m - u_0 \quad \bar{v}_n - v_0 \rangle \begin{bmatrix} 0 & T^* \\ T & -1 \end{bmatrix} \begin{Bmatrix} \bar{u}_m - u_0 \\ \bar{v}_n - v_0 \end{Bmatrix} dR \\ &= (\bar{u}_m - u_0, T^*(\bar{v}_n - v_0))_{\tilde{U}} + (\bar{v}_n - v_0, T(\bar{u}_m - u_0))_{\tilde{V}} - (\bar{v}_n - v_0, \bar{v}_n - v_0)_{\tilde{V}} \quad (3.69) \end{aligned}$$

where  $\underline{\Lambda}_0 = \langle \underline{u}_0 \quad \underline{v}_0 \rangle^T$  is the exact solution. Consider homogeneous boundary conditions. Therefore from (3.3)

$$(\bar{\underline{u}}_m - \underline{u}_0, T^* \bar{\underline{v}}_n - \underline{v}_0)_{\tilde{U}} = (\bar{\underline{v}}_n - \underline{v}_0, T \bar{\underline{u}}_m - \underline{u}_0)_{\tilde{V}}$$

and reduces equation (3.69) to

$$[\underline{\Lambda}_{-m}^n - \underline{\Lambda}_0, \underline{\Lambda}_{-m}^n - \underline{\Lambda}_0] = 2(\bar{\underline{v}}_n - \underline{v}_0, T \bar{\underline{u}}_m - \underline{u}_0)_{\tilde{V}} - (\bar{\underline{v}}_n - \underline{v}_0, \bar{\underline{v}}_n - \underline{v}_0)_{\tilde{V}}. \quad (3.70)$$

But from (3.42)

$$(\bar{\underline{v}}_n - \underline{v}_0, T(\bar{\underline{u}}_m - \underline{u}_0))_{\tilde{V}} = (\bar{\underline{v}}_n - \underline{v}_0, \bar{\underline{v}}_n - \underline{v}_0)_{\tilde{V}}.$$

Substituting this into (3.70) yields

$$[\underline{\Lambda}_{-m}^n - \underline{\Lambda}_0, \underline{\Lambda}_{-m}^n - \underline{\Lambda}_0] = (\bar{\underline{v}}_n - \underline{v}_0, \bar{\underline{v}}_n - \underline{v}_0)_{\tilde{V}}.$$

Therefore, when the conditions in definition 3.4.3 of the energy product are satisfied, the error in the energy product is given by the mean square error in the stress  $\underline{v}$ ;

$$[\underline{\Lambda}_{-m}^n - \underline{\Lambda}_0, \underline{\Lambda}_{-m}^n - \underline{\Lambda}_0] = \|\bar{\underline{v}}_n - \underline{v}_0\|^2 \quad (3.71)$$

and the error in the energy norm as

$$|\underline{\Lambda}_{-m}^n - \underline{\Lambda}_0| = \|\bar{\underline{v}}_n - \underline{v}_0\|. \quad (3.72)$$

Perhaps it should be noted that if the second of the matrix equations (3.35) is satisfied exactly, the following are obtained for the energy product and energy norm:

$$[\underline{\Lambda}_{-m}^n - \underline{\Lambda}_0, \underline{\Lambda}_{-m}^n - \underline{\Lambda}_0] = (A(\bar{\underline{u}}_m - \underline{u}_0), \bar{\underline{u}}_m - \underline{u}_0) = \|T \bar{\underline{u}}_m - T \underline{u}_0\|^2,$$

and 
$$|\bar{\underline{u}}_m - \underline{u}_0| = \sqrt{(A(\bar{\underline{u}}_m - \underline{u}_0), \bar{\underline{u}}_m - \underline{u}_0)} = \|T \bar{\underline{u}}_m - T \underline{u}_0\|.$$

The last two equations can be recognized as the errors in the energy product and the energy norm, respectively, as one would obtain in the Ritz method where  $A$  is a positive definite operator as in equation (2.11).

### 3.8 Extension

It can occur that for some functions  $f \in W$  there does not exist a function  $\underline{\Lambda}$  in the restricted field of definition  $D_{\underline{A}}^W$  that will satisfy equations (3.35). Further, it is important that an approximation be so chosen that only the kinematic boundary conditions are required to be satisfied. Such situations arise in the majority of problems in continuum mechanics. The governing differential equations of the type in (3.35) are derived under the assumption that the load  $f$  is continuous. This then requires that the field of definition of the operator  $\underline{A}$  be the totality of functions  $u$  and  $v$  defined over  $\bar{R} = R + \partial R$  that possess continuous  $m^{\text{th}}$  derivatives and satisfy all the boundary conditions of the problem on  $u$  and  $v$ . Here  $m$  is the order of derivatives in  $T$ .

Thus if  $f$  is continuous then there exists a solution in  $D_{\underline{A}}^W$  but if  $f$  is discontinuous, no solution can be found in  $D_{\underline{A}}^W$ . This difficulty can be overcome by considering limits of functions that lie in  $D_{\underline{A}}^W$ . Then it is possible to formulate the functional  $F(\underline{\Lambda})$  in such a manner that a generalized solution of equations (3.35) is obtained. Just as a discontinuous load may be considered as a limit of a sequence of continuous loads, so functions with discontinuous  $m^{\text{th}}$  derivatives are introduced that are the limits of sequences of functions with continuous  $m^{\text{th}}$  derivatives. Thus it can be said that amongst the new set of functions lies the solution (or generalized solution if it is not in  $D_{\underline{A}}^W$ ) of equations (3.35) for any  $f \in H_{\underline{A}}^W$ . These ideas are now developed.

Using equation (3.5), the first term on the right hand side in the energy product of equation (3.41) is replaced by

$$(T^*v_1, u_2)_{\tilde{U}} = (v_1, Tu_2)_{\tilde{V}} - (v_1, Bu_2)_{\tilde{V}\partial R}.$$

The boundary term is then deleted and the modified energy product in the symmetric form, denoted by  $[\underline{\Lambda}_1, \underline{\Lambda}_2]_{\underline{A}}$ , is given by

$$[\underline{\Lambda}_1, \underline{\Lambda}_2]_A = (v_1, Tu_2)_{\tilde{V}} + (Tu_1, v_2)_{\tilde{V}} - (v_1, v_2)_{\tilde{V}}. \quad (3.73)$$

In which  $\underline{\Lambda}_1 = \langle u_1 \quad v_1 \rangle^T$  and  $\underline{\Lambda}_2 = \langle u_2 \quad v_2 \rangle^T \in D_{\underline{A}}^W$ . The conditions of definition 3.4.3 are still required to be satisfied so that the positive definiteness holds.

The energy product in (3.73) also satisfies the properties of an inner product (definition 2.1.1). The energy norm is now defined as

$$|\underline{\Lambda}|_A = \sqrt{[\underline{\Lambda}, \underline{\Lambda}]_A} \quad (3.74)$$

and also satisfies the axioms of a norm presented in theorem 3.4.2. The space  $D_{\underline{A}}^W$  may be incomplete with respect to the energy norm, i.e. not all Cauchy sequences in  $D_{\underline{A}}^W$  converge to a function in  $D_{\underline{A}}^W$ . If this is so,  $D_{\underline{A}}^W$  is completed by defining  $\underline{\Lambda}$  to be a member of the space if

$$|\underline{\Lambda}_m^n - \underline{\Lambda}| \rightarrow 0, \text{ as } m \rightarrow \infty \text{ and } n \rightarrow \infty. \quad (3.75)$$

Where  $\underline{\Lambda}_m^n = \langle \bar{u}_m \quad \bar{v}_n \rangle^T \in D_{\underline{A}}^W$  since  $\bar{u}_m$  and  $\bar{v}_n$  are linear combinations of the sequences  $\{\phi_m\}$  and  $\{\psi_n\}$ , respectively, which are in  $D_{\underline{A}}^W$ . The completed cross product space so obtained is denoted by  $H_{\underline{A}}^W$  where the subscript emphasizes the dependence on the operator  $\underline{A}$ . The energy product in (3.73) is only defined for  $D_{\underline{A}}^W$  but may now be extended for all functions in  $H_{\underline{A}}^W$ ;

$$[\underline{\Lambda}_1, \underline{\Lambda}_2]_A = \lim_{\substack{m \rightarrow \infty \\ n \rightarrow \infty}} \{ (v_{1n}, Tu_{2m})_{\tilde{V}} + (Tu_{1m}, v_{2n})_{\tilde{V}} - (v_{1n}, v_{2n})_{\tilde{V}} \} \quad (3.76)$$

where  $\underline{\Lambda}_1 = \langle u_{1m} \quad v_{1n} \rangle^T$  and  $\underline{\Lambda}_2 = \langle u_{2m} \quad v_{2n} \rangle^T \in D_{\underline{A}}^W$ . Thus the energy product and the energy norm have meaning for a function  $\underline{\Lambda} \in H_{\underline{A}}^W$ .

The field of definition of the functional  $F(\underline{\Lambda})$  in equation (3.46) can now be extended from  $D_{\underline{A}}^W$  to  $H_{\underline{A}}^W$  and theorem 3.5.1 becomes:

Theorem 3.8.1

For a symmetric and indefinite operator  $\underline{A}$  as defined in equation (3.35), of all the values which are given to the functional

$$F(\underline{\Lambda}) = [\underline{\Lambda}, \underline{\Lambda}]_{\underline{A}} - 2(\underline{p}^T, \underline{\Lambda}) \quad (3.77)$$

by all possible functions  $\underline{\Lambda}$  in  $H_{\underline{A}}^W$  which also satisfy the conditions in definition 3.4.3 of the energy product, the minimum occurs only for the solution of equations (3.35).

Proof:

According to theorem 3.5.1 if equation (3.35) has a solution  $\underline{\Lambda}$  in  $D_{\underline{A}}^W$ , this solution uniquely determines the minimum value of  $F(\underline{\Lambda})$  in  $D_{\underline{A}}^W$ . It will be shown that the minimum value of  $F(\underline{\Lambda})$  in the wider class  $H_{\underline{A}}^W$  is not altered and that the functions  $u$  and  $v$  only give this value.

Let  $d$  denote the minimum value of  $F(\underline{\Lambda})$  in  $D_{\underline{A}}^W$  and  $\bar{d}$  that in  $H_{\underline{A}}^W$ . Then as  $H_{\underline{A}}^W$  includes  $D_{\underline{A}}^W$ ,  $\bar{d} \leq d$ .

Assume  $\bar{d} < d$ . Then there exists a function  $\bar{\Lambda} = \langle \bar{u} \quad \bar{v} \rangle^T \in H_{\underline{A}}^W$  such that  $F(\bar{\Lambda}) < d$ , i.e.

$$F(\bar{\Lambda}) = [\bar{\Lambda}, \bar{\Lambda}] - 2(\underline{p}^T, \bar{\Lambda}) = \|\bar{\Lambda}\|^2 - 2(f, \bar{u}) < d.$$

But as  $\bar{\Lambda} \in H_{\underline{A}}^W$  then there exist sequences  $\Lambda_{-m}^n = \langle u_m \quad v_n \rangle^T \in D_{\underline{A}}^W$  such that  $\|\Lambda_{-m}^n - \bar{\Lambda}\| \rightarrow 0$ . Therefore from theorem 3.5.3  $\|u_m - \bar{u}\| \rightarrow 0$ . Thus  $\|\Lambda_{-m}^n\| \rightarrow \|\bar{\Lambda}\|$  and  $(f, u_m) \rightarrow (f, \bar{u})$ . Therefore for sufficiently large  $m$  and  $n$ ,  $F(\bar{\Lambda})$  and  $F(\Lambda_{-m}^n)$  differ by an arbitrary small amount and it follows that  $F(\Lambda_{-m}^n) < d$ . This is impossible as  $\Lambda_{-m}^n \in D_{\underline{A}}^W$ . Hence the contradiction shows that  $\bar{d} = d$ .

To show that the minimum value of the functional is unique assume that  $\bar{\Lambda} \in H_{\underline{A}}^W$  also minimizes the functional. From the proof of theorem 3.1.1, if the boundary conditions are homogeneous, equation (3.18) reduces to

$$[(T^*v - f, \eta)_{\tilde{U}} + (Tu - v, w)_{\tilde{V}}] = 0 \quad (3.78)$$

where  $u, \eta$  and  $v, w \in D_A^W$ , and  $\eta$  and  $w$  are arbitrary variations of  $u$  and  $v$ , respectively. Equation (3.78) can also be written as

$$[\underline{\Lambda}, \hat{\underline{\Lambda}}] = (\underline{p}^T, \hat{\underline{\Lambda}}) \quad (3.79)$$

where  $\hat{\underline{\Lambda}} = \langle \eta \quad w \rangle^T$ . If  $\hat{\underline{\Lambda}}$  is set equal to  $\underline{\Lambda}$ , i.e.  $u=\eta, v=w$ , the equation (3.79) becomes

$$[\underline{\Lambda}, \underline{\Lambda}] = (\underline{p}^T, \underline{\Lambda}). \quad (3.80)$$

Equation (3.79) is also valid for any function in  $H_A^W$ . In fact if  $\hat{\underline{\Lambda}} \in H_A^W$  then there exists  $\hat{\underline{\Lambda}}_m^n \in D_A^W$  such that  $|\hat{\underline{\Lambda}} - \hat{\underline{\Lambda}}_m^n| \rightarrow 0$ ,  $\|\hat{u} - \hat{u}_m^n\| \rightarrow 0$  and  $[\underline{\Lambda}, \hat{\underline{\Lambda}}_m^n] = (\underline{p}^T, \hat{\underline{\Lambda}}_m^n)$ .

Proceeding to the limit gives equation (3.79) which is also valid for arbitrary functions in  $H_A^W$ . Thus

$$[\underline{\Lambda}, \bar{\underline{\Lambda}}] = (\underline{p}^T, \bar{\underline{\Lambda}}). \quad (3.81)$$

By repeating the proof of theorem 3.1.1 with  $F(\underline{\Lambda})$  expressed in (3.77) the relation  $[\bar{\underline{\Lambda}}, \hat{\underline{\Lambda}}] = (\underline{p}^T, \hat{\underline{\Lambda}})$  is obtained where  $\hat{\underline{\Lambda}} = \langle \eta \quad w \rangle^T$  is now an arbitrary function in  $H_A^W$ . Putting  $\hat{\underline{\Lambda}} = \bar{\underline{\Lambda}}$  and  $\underline{\Lambda}$  separately yields

$$[\bar{\underline{\Lambda}}, \bar{\underline{\Lambda}}] = (\underline{p}^T, \bar{\underline{\Lambda}}) \quad (3.82)$$

$$\text{and} \quad [\bar{\underline{\Lambda}}, \underline{\Lambda}] = (\underline{p}^T, \underline{\Lambda}). \quad (3.83)$$

Subtracting (3.82) from (3.81) and (3.83) from (3.80) gives

$$[\underline{\Lambda} - \bar{\underline{\Lambda}}, \bar{\underline{\Lambda}}] = 0; [\underline{\Lambda} - \bar{\underline{\Lambda}}, \underline{\Lambda}] = 0.$$

Finally subtracting one from the other of the last two equations yields

$$[\underline{\Lambda} - \bar{\underline{\Lambda}}, \underline{\Lambda} - \bar{\underline{\Lambda}}] = 0.$$

This implies that  $\bar{\underline{\Lambda}} = \underline{\Lambda}$ . Therefore the minimum value of the functional and the function from  $H_A^W$  which gives this minimum are the same as in  $D_A^W$  and from theorem 3.5.1 such a function is also the solution of the equations (3.35).

If the minimum of the functional  $F(\underline{\Lambda})$  in (3.77) is given by a function  $\underline{\Lambda}$  that is not in  $D_A^W$ , then this function is known as a generalized

solution of equation (3.35).

To illustrate these concepts, consider the example of uniaxial tension of a bar with uniform cross-section. The differential equations are expressed in the matrix form as

$$\begin{bmatrix} 0 & -D \\ D & -\frac{1}{EA} \end{bmatrix} \begin{Bmatrix} u \\ P \end{Bmatrix} = \begin{Bmatrix} f(x) \\ 0 \end{Bmatrix}. \quad (3.84)$$

and the boundary conditions are

$$u(0) = 0, P(L) = 0 \quad (3.85)$$

where  $D = \frac{d}{dx}$ ;  $P$  is the axial load;  $u$ , the elongation;  $f(x)$ , the distributed axial load and  $EA$ , the axial stiffness. For this example, the operators  $\underline{A}$ ,  $T$  and  $T^*$  and  $\underline{\Lambda}$ ,  $\underline{p}$  are given by

$$\underline{A} = \begin{bmatrix} 0 & -D \\ D & -\frac{1}{EA} \end{bmatrix}, T = -T^* = D; \underline{\Lambda} = \langle u \ P \rangle^T \text{ and } \underline{p} = \langle f(x) \ 0 \rangle^T.$$

Now the energy product in (3.41) is given by

$$[\underline{\Lambda}_1, \underline{\Lambda}_2] = \int_0^L \{-u_2 D P_1 + P_2 D u_1 - \frac{P_1 P_2}{EA}\} dx. \quad (3.86)$$

Integrating by parts the first term on the right hand side yields

$$[\underline{\Lambda}_1, \underline{\Lambda}_2] = -u_2 P_1 \Big|_0^L + \int_0^L \{P_1 D u_2 + P_2 D u_1 - \frac{P_1 P_2}{EA}\} dx,$$

and deleting the boundary term gives the modified, symmetric energy product of (3.73);

$$[\underline{\Lambda}_1, \underline{\Lambda}_2]_A = \int_0^L \{P_1 D u_2 + P_2 D u_1 - \frac{P_1 P_2}{EA}\} dx. \quad (3.87)$$

The functional  $F(\underline{\Lambda})$  in (3.77), for the example considered, becomes

$$F(\underline{\Lambda}) = \int_0^L \{2 P D u - \frac{P^2}{EA}\} dx - 2 \int_0^L f(x) u dx. \quad (3.88)$$

If the solution  $\underline{\Lambda}$  for equation (3.84) with  $f(x)$  continuous and the boundary conditions (3.85) was sought in  $D_{\underline{A}}^W$ , then both boundary conditions on  $u$  and  $P$  have to be satisfied by  $\underline{\Lambda} \in D_{\underline{A}}^W$ . However, the functions  $\bar{\underline{\Lambda}} = \langle \bar{u} \ \bar{P} \rangle^T$  in  $H_{\underline{A}}^W$  are defined such that

$$\|\bar{\underline{\Lambda}} - \underline{\Lambda}_m^n\| = \sqrt{\int_0^L 2(\bar{P} - P_n)D(\bar{u} - u_m) - \frac{1}{EA} (\bar{P} - P_n)^2 dx} \rightarrow 0; \text{ as } m \text{ and } n \rightarrow \infty \quad (3.89)$$

in which  $\underline{\Lambda}_m^n = \langle u_m \ P_n \rangle^T \in D_{\underline{A}}^W$  and therefore  $u_m$  and  $P_n$  have continuous first derivatives and satisfy all the boundary conditions of the problem. Such a definition means that functions  $\bar{u}$  need only have generalized or piecewise first derivatives which in this case implies that  $\bar{u}$  itself be continuous and  $\bar{P}$ , piecewise continuous for  $\bar{\underline{\Lambda}} = \langle \bar{u} \ \bar{P} \rangle^T \in H_{\underline{A}}^W$ . While the boundary condition to be satisfied is that on  $u$  only, e.g. kinematic boundary condition  $u(0)=0$ , whereas  $P$  on the boundary turns out to be a natural boundary condition at the extremum of  $F(\underline{\Lambda})$  and  $\bar{P}$  need not satisfy  $P(L)=0$ .

In lieu of theorem 3.8.1, theorems 3.5.2 and 3.5.3 and the completeness definition of section 3.6 still hold. The only changes needed are the modified definition of the energy norm as in equation (3.74) and the extension of the field of definition of the functional from  $D_{\underline{A}}^W$  to  $H_{\underline{A}}^W$ .

In concluding this chapter, it should be pointed out that in the development of the theory and the consequent proofs of the theorems, the problem considered involved single dependent variables,  $u$  for displacement and  $v$  for stress. However, the theory is not limited to one dimensional problems and the extension to problems involving multi-dependent variables in displacements and stresses is only a simple matter.

## CHAPTER 4

### FORMULATION AND CONVERGENCE OF THE MIXED FINITE ELEMENT METHOD

It is well established that the formulation of a finite element method is a purely topological construction of a function sought as an approximate solution of a well-posed problem in mathematical physics, Oden [22,23]. The approximate solution is expressed in terms of known coordinate functions and unknown parameters which can be determined by applying various different techniques, i.e. Ritz method, Galerkin method, least square method, etc. The technique employed here is the mixed method discussed in Chapter 3.

A complete formulation of the mixed finite element method, its convergence and completeness criteria are presented in this chapter. The strain energy convergence of the mixed finite element method for problems with stress singularities is also established and a method for determining the stress intensity factor  $K_I$  is laid out.

#### 4.1 Generation of a Finite Element Approximation

In the finite element method, the first step is to replace the domain of the problem  $\bar{\Omega} = \Omega + S$  by  $\bar{\Omega}^*$  such that  $\bar{\Omega}^*$  may be exactly subdivided into a number  $E$  of non-overlapping subdomains of simple geometrical forms called elements. Here,  $\bar{\Omega}$  is the closed domain,  $\Omega$ , the open domain and  $S$ , the boundary. The domain of a typical element will be denoted by  $\Omega^e$  and adjacent elements are specified to have a common boundary. Thus

$$\Omega^m \cap \Omega^n = \emptyset, \quad m \neq n; \quad m, n = 1, 2, \dots, E$$

where  $\emptyset$  is the empty set, and

$$\bar{\Omega}^* = \bigcup_{e=1}^E \bar{\Omega}^e.$$

Further

$$\lim_{E \rightarrow \infty} \bar{\Omega}^* = \bar{\Omega}.$$

The elements are chosen, if possible, such that  $\bar{\Omega}^*$  coincides with  $\bar{\Omega}$ , but if not, in such a manner that for a finite number  $E$  the error in the last equation is acceptable. If so, for notation purposes  $\bar{\Omega}$  and  $\Omega$  will be used to represent  $\bar{\Omega}^*$  and  $\Omega^*$ .

The second step in the method involves the assumption of approximate solutions for  $u$  and  $v$  in each of the elements and can be expressed in the form

$$\begin{aligned}\bar{u}^e &= \sum_{k=1}^m u_k^e \phi_k^e \\ \bar{v}^e &= \sum_{k=1}^n v_k^e \psi_k^e\end{aligned}\quad e=1,2, \dots E \quad (4.1)$$

where  $\phi_k^e$  and  $\psi_k^e$  are the coordinate functions defined only in  $\bar{\Omega}^e$  and  $u_k^e, v_k^e$  are the values  $\bar{u}^e$  and  $\bar{v}^e$ , or one of its derivatives, respectively, at certain nodal points generally situated on the boundary of the element. For example, if the  $u_k^e, k=1,2, \dots m$  correspond to the values of  $\bar{u}^e$  at the nodes with coordinates  $x_i^m$  then

$$\begin{aligned}\phi_k^e(x_i^m) &= 1, \quad \text{if } k = m \\ &= 0, \quad \text{if } k \neq m\end{aligned}\quad k=1,2, \dots M. \quad (4.2)$$

A similar relation also holds for  $\psi_k^e$ . Such a definition ensures that  $\phi_k^e$  and  $\psi_k^e$  are linearly independent throughout  $\bar{\Omega}^e$ . A polynomial, which always contains linearly independent terms, with an appropriate number of coefficients (i.e., equal to the number of degrees of freedom in  $u$  or  $v$ ) can always be put into the form (4.1) and leads to linearly independent  $\phi_k^e$  and  $\psi_k^e$ .

It is only necessary to assume coordinate functions defined over individual elements to obtain a solution in the finite element procedure. However, it can be rigorously shown that approximate solutions of the form (4.1) in fact do lead to approximations of the form (3.32) in terms of global degrees of freedom. It is convenient to introduce two functions

$\phi_k^e$  and  $\psi_k^e$  defined over the entire domain  $\bar{\Omega}$  such that

$$\begin{aligned}\phi_k^e(x_i) &= \phi_k^e(x_i) & \text{for } x_i \in \bar{\Omega}^e \\ &= 0 & \text{otherwise;} \end{aligned} \quad (4.3)$$

and

$$\begin{aligned}\psi_k^e(x_i) &= \psi_k^e(x_i) & \text{for } x_i \in \bar{\Omega}^e \\ &= 0 & \text{otherwise;} \end{aligned} \quad (4.4)$$

where the  $x_i$ 's represent a point in the domain. Then the assumed approximations for  $u$  and  $v$  throughout the whole domain  $\bar{\Omega}$  can be written as

$$\begin{aligned}\bar{u} &= \sum_{e=1}^E \sum_{k=1}^m u_k^e \phi_k^e \\ \bar{v} &= \sum_{e=1}^E \sum_{k=1}^n v_k^e \psi_k^e. \end{aligned} \quad (4.5)$$

There has not been introduced any type of continuity in the generation of approximate solutions  $\bar{u}$  and  $\bar{v}$  in (4.5). Clearly  $\bar{u}$  has  $(m \times E)$  unknowns in  $u_k^e$  and  $\bar{v}$  has  $(n \times E)$  unknowns in  $v_k^e$ . On interelement boundaries where nodes of adjacent elements coincide, it is customary to specify that these nodal values should be the same. Assume that there are  $M$  and  $N$  independent degrees of freedom for  $u$  and  $v$  over  $\bar{\Omega}$  denoted by  $u_i$  and  $v_i$ , respectively. Then the element degrees of freedom are related to the global degrees of freedom by the relationship

$$u_k^e = \sum_{i=1}^M F_{ik}^e u_i \quad (4.5a)$$

and

$$v_k^e = \sum_{j=1}^N G_{jk}^e v_j$$

where

$$\begin{aligned}F_{ik}^e &= 1, \quad \text{if nodal value } u_k^e \text{ coincides with } u_i \\ &= 0, \quad \text{otherwise.} \end{aligned}$$

Similarly

$$G_{jk}^e = 1, \text{ if nodal value } v_k^e \text{ coincides with } v_j \\ = 0, \text{ otherwise.}$$

Therefore  $F_{ik}^e$  and  $G_{jk}^e$  are rectangular matrices in general and compare with the compatibility matrix one obtains in the usual displacement method relating the element degrees of freedom to global degrees of freedom.

Then

$$\bar{u} = \sum_{e=1}^E \sum_{k=1}^m \sum_{j=1}^M u_j F_{jk}^e \phi_k^e$$

and

$$\bar{v} = \sum_{e=1}^E \sum_{k=1}^n \sum_{j=1}^N v_j G_{jk}^e \psi_k^e.$$

Defining

$$\phi_j = \sum_{e=1}^E \sum_{k=1}^m F_{jk}^e \phi_k^e$$

and

$$\psi_j = \sum_{e=1}^E \sum_{k=1}^n G_{jk}^e \psi_k^e$$

allows equation (4.5) to be written as

$$\begin{aligned} \bar{u} &= \sum_{i=1}^M u_i \phi_i \\ \bar{v} &= \sum_{j=1}^N v_j \psi_j \end{aligned} \tag{4.6}$$

in which  $\phi_j$  and  $\psi_j$  are linearly independent throughout  $\bar{\Omega}$ .

Thus the finite element approximations of (4.6) have the same form as (3.32). The approximations for  $u$  and  $v$  within each element are chosen according to a certain continuity requirement and completeness so that the convergence of the finite element method in some sense can be guaranteed. This has been excluded in the discussion above and will be discussed later.

## 4.2 Generation of an Element Matrix

The derivation of an element matrix is described here for the problem of equation (3.30) and (3.31) over  $\Omega^e$

$$T^*v - f = 0 \quad (4.7)$$

$$Tu - v = 0. \quad (4.8)$$

The element matrix can be derived either by using the variational principle  $F(\underline{\Lambda})$  of theorem 3.8.1 or by using the mixed Galerkin method of section 3.3 in which both residuals, that of the differential equations within the open domain  $\Omega^e$  and boundary  $S^e$  are included. Since the linear operators  $T$  and  $T^*$  are self-adjoint, the matrices obtained by both methods will be identical.

Consider the variational formulation

$$F(\underline{\Lambda}) = [\underline{\Lambda}, \underline{\Lambda}]_A - 2(\underline{p}^T, \underline{\Lambda}) \quad (4.9)$$

where  $\underline{\Lambda} = \langle u \ v \rangle^T$ ,  $\underline{p} = \langle f \ 0 \rangle^T$  and

$$[\underline{\Lambda}, \underline{\Lambda}] = \int_{\Omega} [2vTu - v^2] d\Omega \quad (4.10)$$

$$(\underline{p}^T, \underline{\Lambda}) = \int_{\Omega} f u d\Omega. \quad (4.11)$$

Let  $u$  and  $v$  be approximated by  $\bar{u}^e = \sum_{i=1}^m \phi_i^e u_i^e$  and  $\bar{v}^e = \sum_{j=1}^n \psi_j^e v_j^e$  within the element.

Substitution of these into (4.10) yields,

$$[\underline{\Lambda}^e, \underline{\Lambda}^e]_A = \int_{\Omega^e} \left[ 2 \sum_{i=1}^m \sum_{j=1}^n \psi_j^e T \phi_i^e u_i^e v_j^e - \sum_{i=1}^n \sum_{j=1}^n \psi_i^e \psi_j^e v_i^e v_j^e \right] d\Omega^e$$

$$\text{or } [\underline{\Lambda}^e, \underline{\Lambda}^e]_A = 2 \sum_{i=1}^m \sum_{j=1}^n u_i^e v_j^e \int_{\Omega^e} \psi_j^e T \phi_i^e d\Omega^e - \sum_{i=1}^n \sum_{j=1}^n v_i^e v_j^e \int_{\Omega^e} \psi_i^e \psi_j^e d\Omega^e \quad (4.12)$$

and (4.11) gives

$$(\underline{p}^T, \underline{\Lambda}^e) = \sum_{i=1}^m u_i^e \int_{\Omega^e} f \phi_i^e d\Omega^e. \quad (4.13)$$

Now  $F(\underline{\Lambda}^e)$  in terms of  $u_i^e$  and  $v_j^e$  takes the form

$$\begin{aligned} F(\underline{\Lambda}^e) &= 2 \sum_{i=1}^m \sum_{j=1}^n u_i^e v_j^e \int_{\Omega^e} \psi_j^e T \phi_i^e d\Omega^e - \sum_{i=1}^n \sum_{j=1}^n v_i^e v_j^e \int_{\Omega^e} \psi_i^e \psi_j^e d\Omega^e \\ &\quad - 2 \sum_{i=1}^m u_i^e \int_{\Omega^e} f \phi_i^e d\Omega^e \end{aligned} \quad (4.14)$$

and for a stationary point its derivatives  $\frac{\partial F(\underline{\Lambda}^e)}{\partial u_i^e}$  and  $\frac{\partial F(\underline{\Lambda}^e)}{\partial v_j^e}$  must equal zero.

This results in the following equations:

$$\sum_{j=1}^n \int_{\Omega^e} T \phi_i^e \psi_j^e d\Omega^e v_j^e - \int_{\Omega^e} f \phi_i^e d\Omega^e = 0; \quad i=1,2, \dots, m \quad (4.15)$$

$$\sum_{j=1}^m \int_{\Omega^e} \psi_i^e T \phi_j^e d\Omega^e u_j^e - \sum_{j=1}^n \int_{\Omega^e} \psi_i^e \psi_j^e d\Omega^e v_j^e = 0; \quad i=1,2, \dots, n. \quad (4.16)$$

Equations (4.15) and (4.16) together yield  $(m+n)$  equations for  $(m+n)$

unknowns and can be put into a matrix form by defining  $a_{ij}^e$  and  $b_{ij}^e$  as

$$\begin{aligned} a_{ij}^e &= \int_{\Omega^e} T \phi_i^e \psi_j^e d\Omega^e; \quad i=1,2, \dots, m, \\ &\quad j=1,2, \dots, n. \\ b_{ij}^e &= \int_{\Omega^e} \psi_i^e \psi_j^e d\Omega^e; \quad i=j=1,2, \dots, n \\ p_i^e &= \int_{\Omega^e} f \phi_i^e d\Omega^e; \quad i=1,2, \dots, m. \end{aligned} \quad (4.17)$$

The matrix form is

$$\begin{bmatrix} \begin{matrix} \underline{0} \\ (m \times m) \end{matrix} & \begin{matrix} \underline{a}^e \\ (m \times n) \end{matrix} \\ \hline \begin{matrix} \underline{a}^{eT} \\ (n \times m) \end{matrix} & \begin{matrix} \underline{-b}^e \\ (n \times n) \end{matrix} \end{bmatrix} \begin{bmatrix} u_1^e \\ u_2^e \\ \vdots \\ u_m^e \\ v_1^e \\ v_2^e \\ \vdots \\ v_n^e \end{bmatrix} = \begin{bmatrix} p_1^e \\ p_2^e \\ \vdots \\ p_m^e \\ 0 \\ 0 \\ \vdots \\ 0 \end{bmatrix} \quad (4.18)$$

In general  $m$  need not be equal to  $n$  and matrix  $\underline{a}^e$  can be rectangular. Furthermore, from equations (4.17), matrix  $\underline{b}^e$  is symmetric and positive definite as long as the functions  $\psi_i$  are square summable over  $\Omega^e$ . It can be observed that the matrix of coefficients of equation (4.18), i.e.

$$\begin{array}{c}
 \left[ \begin{array}{cc}
 \begin{array}{c} 0 \\ (m \times m) \end{array} & \begin{array}{c} \underline{a}^e \\ (m \times n) \end{array} \\
 \hline
 \begin{array}{c} \underline{a}^{eT} \\ (n \times m) \end{array} & \begin{array}{c} -\underline{b}^e \\ n \times n \end{array}
 \end{array} \right] \quad (4.19)
 \end{array}$$

(m+n)

is symmetric but indefinite. The latter property follows from the non-extremum character of the mixed operators.

### 4.3 Assemblage of Element Matrices

In the displacement approach, the stiffness matrix relates the nodal forces to nodal displacements. Hence during assemblage of element stiffness matrices, the addition of columns corresponds to equating the nodal displacements of adjacent elements to achieve certain compatibility

and addition of rows corresponds to equilibrium of the nodal forces. In the present case, the matrix of (4.19) relates both stresses and displacements ( $v$  and  $u$ , respectively) to the generalized applied loads. Although, the mechanics of the process of adding columns and rows is still the same, the additions of both corresponding rows and columns of the element matrices are due to equating the nodal variables in stresses and displacements with respect to certain continuity requirements. This, in fact, transforms the mixed problem of equation (4.14) from local (element) degrees of freedom in  $u$  and  $v$  to global degrees of freedom. This is analogous to the transformation of approximate solutions for each element of (4.1) in  $u_i^e$  and  $v_j^e$  to approximate solutions in global degrees of freedom  $u_j$  and  $v_j$  of (4.6). Similarly for the mixed Galerkin method, in which the residual of equation (4.7), after substitution of an approximate solution is made orthogonal to  $\phi_i^e$  and that of equation (4.8) is made orthogonal to  $\psi_i^e$ , the addition of corresponding rows and columns extends the orthogonalizing process from the element domain  $\Omega^e$  to the overall domain  $\Omega$ .

The submatrices  $\underline{a}$  and  $\underline{b}$  can be assembled separately or the complete matrix (4.10) can be assembled as a whole. The latter is used in this thesis for analyzing problems. This requires interchanging of rows and columns of the matrix so that the degrees of freedom in matrix equation (4.18)  $u_1^e, u_2^e, \dots, u_m^e; v_1^e, v_2^e, \dots, v_n^e$  appear as  $u_1^e, v_1^e, u_2^e, v_2^e, \dots, u_m^e, v_m^e, v_{m+1}^e, \dots, v_n^e$  for  $n \geq m$ . This is demonstrated in Appendix A. By suitably arranging the global degrees of freedom  $u_i$  and  $v_j$  the master matrix can be obtained in an optimum banded form. It was mentioned in the previous section that the matrix of (4.19) is indefinite. Therefore the method of Gaussian elimination with partial pivoting is used to solve the global equations.

#### 4.4. Convergence Criteria

In Chapter 3 and especially section 3.8, the requirements that would ensure energy convergence in mixed methods for a continuum were presented. The same results are now used to provide sufficient convergence criteria for a finite element approximation.

Theorem 3.8.1 implies that the convergence of the mixed approximation in the energy norm of equation (3.74) is ensured when applied to the equations (4.7) and (4.8) if the coordinate functions  $\phi_m \in \tilde{U}_{\underline{A}}$  and  $\psi_n \in \tilde{V}_{\underline{A}}$  used for approximating  $u$  and  $v$ , respectively, are complete in  $H_{\underline{A}}^W$ . This is explained for a finite element approximation by considering the following example (similar to (3.84)) representing the one dimensional linear elasticity problem with unit stiffness  $EA=1$ ;  $u, v$  are displacement and stress, respectively, and  $f(x)$  is the applied load in the  $x$ -direction.

$$\begin{bmatrix} 0 & -\frac{d}{dx} \\ \frac{d}{dx} & -1 \end{bmatrix} \begin{bmatrix} u \\ v \end{bmatrix} = \begin{bmatrix} -f \\ 0 \end{bmatrix}. \quad (4.20)$$

Therefore  $T^* = -\frac{d}{dx}$ ;  $T = \frac{d}{dx}$ . (4.21)

The homogeneous boundary conditions are  $u(0)=u(L)=0$ . It is convenient to construct a cross product space  $H_{\underline{A}}^W = \tilde{U}_{\underline{A}} \times \tilde{V}_{\underline{A}}$  in which

$$|\underline{\Lambda}|_{\underline{A}} = \sqrt{[\underline{\Lambda}, \underline{\Lambda}]_{\underline{A}}} = \sqrt{\int_0^1 (2v \frac{du}{dx} v^2) dx}. \quad (4.22)$$

Then the functions  $\underline{\Lambda} = \langle u \ v \rangle^T$  that are in  $H_{\underline{A}}^W$  must satisfy the condition

$$d(\underline{\Lambda}, \underline{\Lambda}_{-m}^n) = \|\underline{\Lambda} - \underline{\Lambda}_{-m}^n\|_{\underline{A}} \rightarrow 0, \text{ as } m \rightarrow \infty, n \rightarrow \infty; \underline{\Lambda}_{-m}^n \in D_{\underline{A}}^W. \quad (4.23)$$

The space  $H_{\underline{A}}^W$  therefore contains the exact solution according to theorem 3.8.1.

Thus the convergence would be ensured if the coordinate functions  $\phi_m$  and  $\psi_n$  are complete in  $H_{\underline{A}}^W$ .

From section 4.1, a finite element approximation for  $u$  and  $v$  is obtained by dividing the interval  $(0,L)$  into  $E$  elements of lengths  $l^e$  and within each element, assuming solutions of the form

$$\begin{aligned}\bar{u}^e &= \sum_{k=1}^m u_k^e \phi_k^e \\ \bar{v}^e &= \sum_{k=1}^n v_k^e \psi_k^e\end{aligned}\quad e=1,2, \dots E. \quad (4.24)$$

The equations obtained within each element (section 4.2) are

$$\sum_{j=1}^n \int_0^{l^e} \phi_i^{e'} \psi_j^e dx v_j^e = \int_0^{l^e} f \phi_i^e dx; \quad i=1,2, \dots m \quad (4.25)$$

$$\sum_{j=1}^m \int_0^{l^e} \psi_i^e \phi_j^{e'} dx u_j^e - \sum_{j=1}^n \int_0^{l^e} \psi_i^e \psi_j^e dx v_j^e = 0; \quad i=1,2, \dots n \quad (4.26)$$

where the prime denotes a derivative with respect to  $x$ . The equations

(4.25) and (4.26) can be assembled to yield the following global equations:

$$\sum_{j=1}^N \int_0^L \phi_i^{e'} \psi_j^e dx v_j^e = \int_0^L f \phi_i^e dx; \quad i=1,2, \dots M \quad (4.27)$$

$$\sum_{j=1}^M \int_0^L \psi_i^e \phi_j^{e'} dx u_j^e - \sum_{j=1}^N \int_0^L \psi_i^e \psi_j^e dx v_j^e = 0; \quad i=1,2, \dots N. \quad (4.28)$$

Here  $\phi_i$  and  $\psi_j$  are the same as in equation (4.6) and  $M,N$  are the numbers of global degrees of freedom in  $u$  and  $v$ , respectively. Thus the global approximate solutions for  $u$  and  $v$

$$\begin{aligned}\bar{u} &= \sum_{i=1}^M \phi_i^u u_i \\ \bar{v} &= \sum_{i=1}^N \psi_i^v v_i\end{aligned} \quad (4.29)$$

converge in the energy norm if the  $\phi_k$  and  $\psi_k$  are complete in  $H_{\underline{A}}^W$ . The conditions that must be satisfied by the assumed solution within each element in order to ensure that the coordinate functions defining the global solution

be complete in  $H_{\underline{A}}^W$  must therefore be established.

For the example considered, the equations (4.22) and (4.23) suggest that functions  $\phi_i$  in  $H_{\underline{A}}^W$  must have generalized first derivatives and therefore are continuous over  $(0,L)$ . However,  $\psi_j$  in  $H_{\underline{A}}^W$  over  $(0,L)$  may only be piecewise continuous. Further, these functions must also satisfy the forced boundary conditions as all functions in  $H_{\underline{A}}^W$  are required to do so, and since  $u$  on the boundary takes on forced or kinematic boundary conditions, therefore  $\phi_i$  are to satisfy these conditions.

In order to establish a criterion which leads to satisfying the completeness requirements of section 3.6, their definition in terms of finite element approximations is necessary. This is done next.

#### Completeness for Finite Element Approximations

The finite element approximations for  $u$  and  $v$  as linear combinations of sequences of functions  $\phi_m$  and  $\psi_n$ ,  $m$  and  $n = 1, 2, \dots$ , in  $H_{\underline{A}}^W$  are complete if for a  $\tilde{\underline{\Lambda}}$  with a finite energy norm and any  $\epsilon_1 > 0$ ,  $\epsilon_2 > 0$ , there exists a subdivision of the domain of the problem corresponding to  $M$  and  $N$  degrees of freedom in  $u$  and  $v$ , respectively, such that

$$(i) \quad \left\| Tu_M - \sum_{i=1}^N v_i \psi_i \right\| < \epsilon_2$$

$$(ii) \quad \left| \tilde{\underline{\Lambda}} - \underline{\Lambda}_M^N \right| < \epsilon_1$$

where  $\tilde{\underline{\Lambda}} = \langle \tilde{u} \tilde{v} \rangle^T$ ,  $\underline{\Lambda}_M^N = \langle u_M v_N \rangle^T$  and  $u_M = \sum_{i=1}^M u_i \phi_i$ ,  $v_N = \sum_{j=1}^N v_j \psi_j$ .

Again, the completeness requirement (i) implies that the stress approximation,  $v_N = \sum_{j=1}^N v_j \psi_j$ , should contain all the stress modes that correspond to strain modes present in the strain  $Tu_M$  for finite degrees of freedom  $N$  in stress  $v$ .

If the operator  $T$  involves derivatives of order  $m_T$ , then the energy

product in equation (3.73) for  $\underline{\Lambda}_i = \langle \underline{u}_i \ \underline{v}_i \rangle^T$  and  $\underline{\Lambda}_j = \langle \underline{u}_j \ \underline{v}_j \rangle^T$

$$[\underline{\Lambda}_i, \underline{\Lambda}_j]_A = (\underline{v}_{jn}, Tu_{im})_V + (\underline{v}_{in}, Tu_{jm})_V - (\underline{v}_{in}, \underline{v}_{jn})_V \quad (4.30)$$

is symmetric and involves derivatives of order  $m_T$  in  $u$  and zero in  $v$ . To establish certain completeness criterion for finite element approximations for  $u$  and  $v$  within each element, interest lies in the least requirement that would allow the energy norm in (4.22) to be evaluated, i.e. requirement (ii), and also enable the mean convergence of approximation for  $v$  to  $Tu$ , i.e. requirement (i) of completeness. Therefore continuity of  $(m_T-1)$  derivatives is required for  $u$ . However  $v$  can be piecewise continuous.

Completeness criterion for the finite element approximations within the element is presented in the following section for linear elasticity plane stress. The explanation of the notation used for certain quantities can be found in the beginning of Chapter 5.

#### 4.5 Completeness Criterion

A general criterion for completeness is stated and justified here and is analogous to the one presented by Oliveira [24,25]. Let  $H_0^W A$  be the set of compatible and equilibrated elastic fields where  $\underline{u}_i$  have continuous and bounded second order derivatives and  $\underline{v}_i$  have continuous and bounded first order derivatives within each element. It is to be demonstrated that the completeness for a finite element approximation  $\underline{\Lambda}_m^{ne} = \langle \underline{u}_m^e \ \underline{\tau}_n^e \rangle^T$  where  $\underline{u}_m^e$  is the vector of displacement components and  $\underline{\tau}_n^e$ , the stress components, within the element with respect to any  $\underline{\Lambda} = \langle \underline{u} \ \underline{\tau} \rangle^T \in H_0^W A$  will be obtained if:

- (a) the general analytical expression for  $\underline{u}_i$  and  $\tau_{ij}$  within each element are polynomials with the number of arbitrary parameters equal to the number of unit modes corresponding to the element,

- (b) the terms of degree higher than the first in  $u_i^e$  and the constants in  $\tau_{ij}^e$  can vanish regardless of the values taken by the constant terms and the coefficients which affect the linear terms in  $u_i^e$  and the constant terms in  $\tau_{ij}^e$ .
- (c) the constant terms and the coefficients which affect the linear terms in  $u_i^e$  and the constant terms in  $\tau_{ij}^e$  are completely arbitrary.
- (d)  $\tau_{ij}^e$  should at least possess all the modes that are present in  $T_{ij}u_j^e$ .

The conditions (a) to (c) result in displacements  $u_i^e$  or their first derivatives and stresses  $\tau_{ij}^e$  to take up any arbitrary value throughout the element. The condition (d) assures convergence of  $\tau_{ij}^e$  to  $T_{ij}u_j^e$  in the mean square sense, i.e. completeness requirement (i).

The displacements  $u_i$  belonging to  $H_0^W$  can be represented inside  $\Omega^e$  by the following Taylor's expansion

$$u_i = u_i(P) + u_{i,j}(P)(x_j - x_j^P) + 1/2! u_{i,jk}(\bar{P})(x_j - x_j^P)(x_k - x_k^P) \quad (4.31)$$

where  $P$  and  $\bar{P}$  are points in  $\Omega^e$  and  $\bar{P}$  depends upon the coordinates of the point where the  $u_i$  are to be determined. Similarly  $\tau_{ij}$  can be represented by the following Taylor's expansion

$$\tau_{ij} = \tau_{ij}(P) + \tau_{ij,k}(\bar{P})(x_k - x_k^P). \quad (4.32)$$

Now consider the displacement field with components

$$u_{ti}^e = u_i(P) + u_{i,j}(P)(x_j - x_j^P) \quad (4.33)$$

within  $\Omega^e$  and call it a tangent field to  $u_i$  at  $P$ . Similarly consider the stress field

$$\tau_{cij}^e = \tau_{cij}(P) \quad (4.34)$$

within  $\Omega^e$  and call it a constant field at  $P$ . From hypotheses, all second derivatives of  $u_i$  and first derivatives of  $\tau_{ij}$  are supposed to be bounded inside  $\Omega^e$ . Then equations (4.31) and (4.33) yield

$$|u_i - u_{ti}^e| < \frac{d}{2!} L_1^e (l_e)^2 \quad (4.35)$$

where  $L_1^e$  is the upper bound for all the second derivatives of  $u_i$ ,  $l_e$  is the maximum diameter of element  $e$  and  $d$  is the total number of second order derivatives. Similarly from equations (4.32) and (4.34)

$$|\tau_{ij} - \tau_{cij}^e| < f L_2^e (l_e) \quad (4.36)$$

where  $L_2^e$  is the upper bound for all  $f$  first derivatives of  $\tau_{ij}$ .

By considering similar expansions for the first derivatives of  $u_i$ , it is possible to derive the inequality

$$|u_{i,j} - u_{ti,j}^e| < d L_1^e (l_e). \quad (4.37)$$

The distance between  $\underline{\Lambda}$  and  $\tilde{\underline{\Lambda}}$  over the entire domain  $\Omega$  can be evaluated from the energy norm of equation (3.74)

$$d(\underline{\Lambda}, \tilde{\underline{\Lambda}}) = \sqrt{\sum_{e=1}^E [\underline{\Lambda} - \tilde{\underline{\Lambda}}, \underline{\Lambda} - \tilde{\underline{\Lambda}}]_A}$$

where  $E$  is the total number of elements and  $\tilde{\underline{\Lambda}} = \langle \underline{u}^e \quad \underline{\tau}^e \rangle^T$ . By using equation (5.13)

$$d(\underline{\Lambda}, \tilde{\underline{\Lambda}}) = \sqrt{\sum_{e=1}^E \int_{\Omega^e} [2(\underline{\tau}^e - \underline{\tau}_c^e)^T \underline{T}(\underline{u}^e - \underline{u}_t^e) - (\underline{\tau}^e - \underline{\tau}_c^e)^T \underline{C}(\underline{\tau}^e - \underline{\tau}_c^e)] d\Omega^e}$$

or

$$d(\underline{\Lambda}, \tilde{\underline{\Lambda}}) < \sqrt{\sum_{e=1}^E [2 \left| \int_{\Omega^e} (\underline{\tau}^e - \underline{\tau}_c^e)^T \underline{T}(\underline{u}^e - \underline{u}_t^e) d\Omega^e \right| + \left| \int_{\Omega^e} (\underline{\tau}^e - \underline{\tau}_c^e)^T \underline{C}(\underline{\tau}^e - \underline{\tau}_c^e) d\Omega^e \right|]}.$$

As the operator  $\underline{T}$  involves first derivatives and  $\underline{C}$  is a compliance matrix which involves no derivatives, by virtue of equations (4.36) and (4.37)

$$d(\underline{\Lambda}, \tilde{\underline{\Lambda}}) < \sqrt{\sum_{e=1}^E [\{L_3^e (l_e)^2 + L_4^e (l_e)^2\} \Omega^e]}$$

for  $l_e$  sufficiently small.  $L_3^e$  and  $L_4^e$  are positive numbers. The inequality above can be further simplified;

$$d(\underline{\Lambda}, \tilde{\underline{\Lambda}}) < \sqrt{(L_3^n + L_4^n) l_n^2 \sum_{e=1}^{\Omega} \Omega^e} \quad (4.38)$$

where  $L_3^n, L_4^n$  and  $l_n$  denote the maximum values of  $L_3^e, L_4^e$  and  $l_e$  in the whole set of elements. Now if  $\alpha = (L_3^n + L_4^n)$ , then

$$d(\underline{\Lambda}, \tilde{\underline{\Lambda}}) < \sqrt{\alpha l_n^2 \Omega}. \quad (4.39)$$

Therefore the energy distance between  $\underline{\Lambda}$  and  $\tilde{\underline{\Lambda}}$  tends to zero when the size of elements decreases indefinitely or the number of elements  $E$  goes to infinity.

Consider now a type of element generating a sequence of families of fields,  $H_A^W$ , whose completeness is to be investigated. Let  $\underline{\Lambda}_M^N = \langle \underline{u}_M \quad \underline{\tau}_N \rangle^T$  be one of these fields whose generalized parameters or nodal degrees of freedom take the same values as that of  $\underline{\Lambda}$  from  $H_A^W$ , and  $\underline{\Lambda}_m^n$  corresponds to  $\underline{\Lambda}_M^N$  within  $\Omega^e$ . If the general criterion is satisfied then  $\tilde{\underline{\Lambda}}$  is one of the family of fields which can occur within the finite element. Let such a field correspond to values  $u_{tik}^e$  and  $\tau_{cij}^e$  of the parameters, i.e.

$$\tilde{u}_{ti}^e = \sum_{k=1}^m \phi_i^{ke} u_{tik}^e; \quad \text{in } \Omega^e, \quad (4.40)$$

$$\tilde{\tau}_{cij}^e = \sum_{k=1}^n \psi_{ij}^{ke} \tau_{cij}^e; \quad \text{in } \Omega^e, \quad (4.41)$$

or

$$\tilde{\underline{\Lambda}}^e = \langle \underline{u}_t^e \quad \underline{\tau}_c^e \rangle^T; \quad \text{in } \Omega^e.$$

On the other hand for  $\underline{\Lambda}_m^n$ ,

$$u_{mi}^e = \sum_{k=1}^m \phi_i^{ke} u_{mik}^e; \quad \text{in } \Omega^e, \quad (4.42)$$

$$\tau_{nij}^e = \sum_{k=1}^n \psi_{ij}^{ke} \tau_{nij}^e; \quad \text{in } \Omega^e, \quad (4.43)$$

or

$$\underline{\Lambda}_m^{ne} = \langle \underline{u}_m^e \quad \underline{\tau}_n^e \rangle^T; \quad \text{in } \Omega^e.$$

From equations (4.40) and (4.42)

$$|\tilde{u}_{ti}^e - u_{mi}^e| = \left| \sum_{k=1}^m \phi_i^{ke} (u_{tik}^e - u_{mik}^e) \right|$$

which then leads to a difference of derivatives as

$$|\tilde{u}_{ti,j}^e - u_{mi,j}^e| = \left| \sum_{k=1}^m \phi_{i,j}^{ke} (u_{tik}^e - u_{mik}^e) \right|; \text{ in } \Omega^e. \quad (4.44)$$

Similarly

$$|\tilde{\tau}_{cij}^e - \tau_{nij}^e| = \left| \sum_{k=1}^n \psi_{ij}^{ke} (\tau_{cijk}^e - \tau_{nijk}^e) \right|; \text{ in } \Omega^e. \quad (4.45)$$

Since the coordinate functions  $\phi_i^{ke}, \phi_{i,j}^{ke}$  and  $\psi_{ij}^{ke}$  can be expressed in dimensionless form, i.e. as a function of  $\frac{x_i}{l_e}$ , these functions remain bounded as the size of the element decreases. Assume that the moduli of the magnitudes of all functions  $\phi_i^{ke}, \phi_{i,j}^{ke}$  and  $\psi_{ij}^{ke}$  remain below  $L_5^e$ , a positive number. Then

$$|\tilde{u}_{ti}^e - u_{mi}^e| < L_5^e \sum_{k=1}^m |u_{tik}^e - u_{mik}^e| \quad (4.46)$$

$$|\tilde{u}_{ti,j}^e - u_{mi,j}^e| < \frac{L_5^e}{l_e} \sum_{k=1}^m |u_{tik}^e - u_{mik}^e| \quad (4.47)$$

$$|\tilde{\tau}_{cij}^e - \tau_{nij}^e| < L_5 \sum_{k=1}^n |\tau_{cijk}^e - \tau_{nijk}^e| \quad (4.48)$$

within  $\Omega^e$ .

Since  $\underline{\Lambda}$  and  $\underline{\Lambda}^e$  take the same values at nodes, i.e.  $u_{ik}^e$  and  $\tau_{ijk}^e$ ; equations (4.35) and (4.36) permit one to write

$$|u_{tik}^e - u_{mik}^e| < \frac{d}{2!} L_1^e (l_e)^2 \quad (4.49)$$

$$|\tau_{cijk}^e - \tau_{nijk}^e| < f L_2^e (l_e). \quad (4.50)$$

Introducing (4.49) and (4.50) into (4.47) and (4.48) yields

$$|\tilde{u}_{ti,j}^e - u_{mi,j}^e| < \frac{dL_j^e L_m^e}{2!} (l^e) = L_6^e l^e \quad (4.51)$$

$$|\tau_{cij}^e - \tau_{nij}^e| < f L_2^e L_5^e (l^e) = L_7^e l^e. \quad (4.52)$$

Equations (4.51) and (4.52) still hold even if  $u_{mi,j}$  and  $\tau_{nij}$  are discontinuous, as long as they are bounded. From similarity between (4.36), (4.37) and (4.52), (4.51), respectively, the following inequality which is analogous to (4.39) can be written directly

$$d(\tilde{\Lambda}, \Lambda_M^N) < \sqrt{\beta l_n^2 \Omega}. \quad (4.53)$$

Combining equations (4.39) and (4.53) and using the triangle inequality of the energy norm

$$d(\Lambda_M^M, \Lambda) < d(\Lambda_M^N, \tilde{\Lambda}) + d(\tilde{\Lambda}, \Lambda) < l_n \sqrt{\Omega} (\sqrt{\alpha} + \sqrt{\beta})$$

or 
$$|\Lambda_M^N - \Lambda| < (\sqrt{\alpha} + \sqrt{\beta}) \sqrt{\Omega} (l_n). \quad (4.54)$$

Equation (4.54) means that the energy distance between  $\Lambda_M^N$  and  $\Lambda$  tends to zero as the size of the largest element decreases indefinitely. Note, condition (d) of completeness criterion is satisfied for the case where  $u_{i,j}$  and  $\tau_{ij}$  are piecewise continuous and taken as constants within each element, i.e. the best  $u_i^e$  can represent is constant strain and  $\tau_{ij}^e$  constant stress. Although, from the completeness criterion, continuity of  $\tau_{ij}$  is not required; improved accuracy in the energy convergence is observed in the results (Chapter 7) by making  $\tau_{ij}$  continuous across element boundaries. Also, if the stresses  $\tau_{ij}$  are not continuous, and completeness requirements satisfied, the mixed finite element method yields the same results as the displacement method would using identical interpolations for the displacements.

Theorem 4.5.1

The mixed finite element method, with approximations for the displacements and stresses satisfying completeness requirements, yields exactly the same results as the displacement method would using the same approximations for displacements if the stresses were not continuous across the interelement boundaries.

Proof:

Suppose with the finite element solution of equations (4.5) for  $u$  and  $v$  the functional  $F(\underline{\Lambda}^e)$  of (4.9) has been arrived at. Using (4.17) and  $f=0$ ,  $F(\underline{\Lambda}^e)$  can be expressed in the matrix form

$$F(\underline{\Lambda}^e) = \underline{u}^e \underline{a}^T \underline{v}^e + \underline{v}^e \underline{a}^T \underline{u}^e - \underline{v}^e \underline{b}^T \underline{v}^e. \quad (4.55)$$

Assume  $u$  and  $v$  to be continuous and let

$$\underline{\tilde{u}}^e = \underline{r} \underline{u} \quad (4.56)$$

$$\underline{\tilde{v}}^e = \underline{s} \underline{v} \quad (4.57)$$

where  $\underline{r}$  and  $\underline{s}$  relate the total element degrees of freedom  $\underline{\tilde{u}}^e$  and  $\underline{\tilde{v}}^e$  to the global degrees of freedom  $\underline{u}$  and  $\underline{v}$  so as to restore interelement continuity for  $u$  and  $v$ , respectively, equations (4.5a). Therefore  $F(\underline{\Lambda}_{-M}^N)$  for the entire domain can be expressed as

$$F(\underline{\Lambda}_{-M}^N) = \underline{u}^T \underline{r}^T \underline{a} \underline{v} + \underline{v}^T \underline{s}^T \underline{a}^T \underline{r} \underline{u} - \underline{v}^T \underline{s}^T \underline{b} \underline{v} \quad (4.58)$$

where  $\underline{a}$  and  $\underline{b}$  matrices are formed by collecting the  $\underline{a}^e$  and  $\underline{b}^e$  matrices for each element in uncoupled form, respectively, and substituting (4.56) and (4.57) to couple them.  $M$  and  $N$  are the global degrees of freedom in  $u$  and  $v$ , respectively.

If only the displacement  $u$  is continuous, then

$$F(\underline{\Lambda}_{-M}^{N_1}) = \underline{u}^T \underline{r}^T \underline{a} \underline{\tilde{v}}^e + \underline{\tilde{v}}^e \underline{a}^T \underline{r} \underline{u} - \underline{\tilde{v}}^e \underline{b} \underline{\tilde{v}}^e \quad (4.59)$$

where  $N_1 = eN$  because at common nodes the stresses are not equated.

But within each element

$$\underline{a}^e \underline{u}^e = \underline{b}^e \underline{v}^e$$

and since  $\underline{b}$  is an  $(n \times n)$  symmetric positive definite matrix, it can be inverted to give

$$\underline{v}^e = \underline{b}^{e-1} \underline{a}^e \underline{u}^e$$

$$\text{also } \underline{\tilde{v}}^e = \underline{b}^{-1} \underline{a}^T \underline{\tilde{u}}^e = \underline{b}^{-1} \underline{a}^T \underline{r_u}. \quad (4.60)$$

Substitution of (4.60) into (4.59) yields

$$F(\underline{\Lambda}_M^{N1}) = \underline{u}^T \underline{r}^T \underline{a} \underline{b}^{-1} \underline{a}^T \underline{r_u} + \underline{u}^T \underline{r}^T \underline{a} \underline{b}^{-1} \underline{a}^T \underline{r_u} - \underline{u}^T \underline{r}^T \underline{a} \underline{b}^{-1} \underline{b} \underline{b}^{-1} \underline{a}^T \underline{r_u}.$$

Since  $\underline{b}^{-1} \underline{b} = \underline{I}$ ; therefore

$$F(\underline{\Lambda}_M^{N1}) = \underline{u}^T \underline{r}^T \underline{a} \underline{b}^{-1} \underline{a}^T \underline{r_u}. \quad (4.61)$$

If it can be shown that the elimination of  $\underline{v}^e$  in the matrix equation (4.18), i.e.

$$\underline{a}^e \underline{b}^{e-1} \underline{a}^e \underline{u}_e^e = \underline{k}^e \underline{u}_e^e = \underline{p}^e \quad (4.62)$$

and that  $\underline{k}^e$  is the same as the element stiffness matrix one would obtain from the displacement method using the same approximation for  $u$ , then the theorem would hold.

In a system of finite degrees of freedom, the requirement (i) of completeness requires that the approximation for stress  $\bar{v}_n$  should contain all the modes present in  $\bar{Tu}_m$ , the strain field from  $\bar{u}_m$ . Then no matter how much better the stress field  $\bar{v}_n$  is chosen to be, for discontinuous stress fields across the element boundaries, the Fourier type convergence of the strain field from  $\bar{v}_n$  cannot be better than  $\bar{Tu}_m$ . Further, from equation (3.68)

$$\left\| \bar{u}'_m - \sum_{i=1}^n v_i \psi_i \right\|^2 = \left\| u'_m \right\|^2 - \sum_{i=1}^n v_i^2 = 0. \quad (4.63)$$

Here  $\bar{Tu}_m = \frac{d\bar{u}_m}{dx} = \bar{u}'_m$  for the example considered in equation (4.20).

Then, for orthonormal  $\psi_i$ , equation (4.28) yields

$$v_i = (\bar{u}'_m, \psi_i); \quad i=1,2, \dots n. \quad (4.64)$$

Also matrix  $\underline{b}^e$  is just an identity matrix  $\underline{I}$ . Therefore

$$\underline{a}^e \underline{b}^{e-1} \underline{a}^{eT} = \underline{a}^e \underline{I} \underline{a}^{eT} = \underline{a}^e \underline{a}^{eT}. \quad (4.65)$$

From (4.63)

$$\|\bar{u}'_m\|^2 = \sum_{i=1}^n v_i^2. \quad (4.66)$$

But from (4.1),  $\bar{u}'_m = \sum_{i=1}^m \phi_i^{e'} u_i^e$ , therefore

$$\|\bar{u}'_m\|^2 = \sum_{i=1}^m \sum_{j=1}^m \int \phi_i^{e'} \phi_j^{e'} dx u_i^e u_j^e$$

and from (4.64)

$$\sum_{i=1}^n v_i^2 = \sum_{i=1}^m \sum_{j=1}^m (\phi_i^{e'}, \psi_k) (\psi_k, \phi_j^{e'}) u_i^e u_j^e; \quad k=1,2, \dots n.$$

For the problem considered

$$k_{ij}^e = (\phi_i^{e'}, \phi_j^{e'})$$

and

$$a_{ij}^e = (\phi_i^{e'}, \psi_j).$$

Therefore the matrix form of equation (4.66) is

$$\underline{u}^{eT} \underline{k}^e \underline{u}^e = \underline{u}^{eT} \underline{a}^e \underline{a}^{eT} \underline{u}^e$$

or

$$\underline{k}^e = \underline{a}^e \underline{a}^{eT}. \quad (4.67)$$

The functions  $\psi_i$ 's used, were assumed to be orthonormal for convenience.

However, no generality is lost and for any linearly independent  $\psi_i$ 's equation (4.67) can be written as

$$\underline{k}^e = \underline{a}^e \underline{b}^{e-1} \underline{a}^{eT}. \quad (4.68)$$

Therefore equation (4.61) takes the form

$$F(\Lambda_{-m}^{N_1}) = \underline{u}^T \underline{r}^T \underline{k} \underline{r} \underline{u} = \underline{u}^T \underline{K} \underline{u} \quad (4.69)$$

where  $\underline{k}$  is the assembled uncoupled global stiffness matrix and  $\underline{K}$  is the coupled form as one would obtain from the displacement approach. Therefore, the energy convergence cannot be any better in the mixed method when the stresses are discontinuous across the interelement boundaries. This then completes the proof.

#### 4.6 Stress Singularities

Stress singularity at the crack tip in plane elasticity problems, it's influence on strain energy convergence and estimation of its crack intensity factor of mode type I (the opening mode, Figure 1) are considered in this section. The displacements and stresses near the tip of a sharp crack (mode type I) are given by

$$\begin{bmatrix} u \\ v \end{bmatrix} = \frac{K_I \sqrt{2r}}{8G\sqrt{\pi}} \begin{bmatrix} (2\kappa-1)\cos\frac{\theta}{2} - \cos\frac{3\theta}{2} \\ (2\kappa+1)\sin\frac{\theta}{2} - \sin\frac{3\theta}{2} \end{bmatrix} + O(r); \quad (4.70)$$

$$\begin{bmatrix} \tau_{xx} \\ \tau_{yy} \\ \tau_{xy} \end{bmatrix} = \frac{K_I}{\sqrt{2\pi r}} \begin{bmatrix} \cos\frac{\theta}{2} \cdot (1 - \sin\frac{\theta}{2} \cdot \sin\frac{3\theta}{2}) \\ \cos\frac{\theta}{2} \cdot (1 + \sin\frac{\theta}{2} \cdot \sin\frac{3\theta}{2}) \\ \sin\frac{\theta}{2} \cdot \cos\frac{\theta}{2} \cdot \cos\frac{3\theta}{2} \end{bmatrix} + \begin{bmatrix} S_{xx} \\ S_{yy} \\ S_{xy} \end{bmatrix} + O(\sqrt{r}). \quad (4.71)$$

Here,  $K_I$  is the stress intensity factor;  $\kappa$  takes the value  $(3-4\nu)$  for plane strain and  $(3-\nu)/(1+\nu)$  for plane stress state;  $\nu$  is Poisson's ratio and  $G$ , the shear modulus. As for the constant stresses  $S_{xx}$ ,  $S_{yy}$  and  $S_{xy}$  in equation (4.71), the stress free condition on the crack surface near the tip leads to  $S_{yy} = S_{xy} = 0$ , whereas the component  $S_{xx}$  in the direction of the crack line remains unknown.

The strain energy convergence of the mixed finite element method for stress singular plane elasticity is established first, and then a procedure for determining the stress intensity factor  $K_I$  is presented which is somewhat similar to the one presented by Parks [27] for displacement method.

#### 4.6.A Strain Energy Convergence for Problems with Stress Singularity

In plane elasticity with stress singularities, the convergence rate for the displacement finite element method is often controlled by the nature of the solution near the singularities. Unless the singularities are properly handled, the regular so-called high accuracy element will not be able to improve the convergence rate. Tong and Pian [38] showed that the convergence in strain energy for displacement and hybrid type elements is only of order  $l_e$  or  $O(l_e)$  where  $l_e$  is the maximum size of the elements near the crack tip. They established it by arguing that in stress singular problems, the typical polynomial type approximations for the displacements lead to strain fields which exclude the singular stresses near the crack tip. Hence the missing terms govern the error in strain and consequently lead to slower convergence of the strain energy.

A similar argument is followed for establishing the strain energy convergence for mixed methods applied to problems with stress singularities. In linear elasticity, twice the potential energy for zero body forces can be written as (from equation (3.77))

$$F(\underline{\Lambda}) = [\underline{\Lambda}, \underline{\Lambda}]_A - 2 \int_{S_\tau} \bar{T}_i^T u_i ds \quad (4.72)$$

where

$$[\underline{\Lambda}, \underline{\Lambda}]_A = \int_V (2[\underline{T}u]^T \underline{T} - \underline{T}^T \underline{C} \underline{T}) dV \quad (4.73)$$

represents twice the strain energy and  $\underline{C}$ ,  $\underline{T}^*$ ,  $\underline{T}$ ,  $\underline{u}$  and  $\underline{\tau}$  are the extensions

to three dimensions from plane stress elasticity, equations (5.10) and  $\bar{T}_i$ 's are the surface stresses specified on  $S_\tau$  part of the boundary. Let  $\underline{\Lambda}_0 = \langle \underline{u}_0 \quad \underline{\tau}_0 \rangle^T$  be the exact solution of the problem over a domain  $V$ . For simplicity, assume that the solution is sufficiently smooth except that

$$\underline{u}_0 = r^\alpha \underline{g}(\underline{x}) \quad (4.74a)$$

$$\underline{\tau}_0 = r^{\alpha-1} \underline{h}(\underline{x}) \quad (4.74b)$$

near the point of the singularity  $R$  in  $V$ . In equations (4.74),  $r$  is the radial distance from  $R$ ,  $\underline{g}$  and  $\underline{h}$  are smooth functions,  $\underline{x}$  are the spatial coordinates,  $\alpha$  is not an integer and

$$p_1 + 1 > \alpha + \frac{n}{2} \geq 1 \text{ and } p_2 + 2 > \alpha + \frac{n}{2} \geq 1 \quad (4.75)$$

where  $n$  is the spatial dimension of the domain  $V$ ,  $p_1$  and  $p_2$  are the degrees of polynomials used as approximations for  $\underline{u}$  and  $\underline{\tau}$ , (satisfying completeness) respectively. The finite element approximations can be put into the form (section 4.1)

$$\begin{aligned} \underline{u} &= \sum_{i=1}^m \phi_i(\underline{x}) \underline{u}_i \\ \underline{\tau} &= \sum_{i=1}^n \psi_i(\underline{x}) \underline{\tau}_i. \end{aligned} \quad (4.76)$$

Let the solution obtained from the mixed finite element method be

$$\begin{aligned} \bar{\underline{u}} &= \sum_{i=1}^m \phi_i(\underline{x}) \bar{\underline{u}}_i \\ \bar{\underline{\tau}} &= \sum_{i=1}^n \psi_i(\underline{x}) \bar{\underline{\tau}}_i \end{aligned} \quad (4.77)$$

and the solution by forcing the nodal degrees of freedom to take the exact values of  $\underline{\Lambda}_0$  at the nodes, be

$$\underline{\tilde{u}} = \sum_{i=1}^m \phi_i(\underline{x}) \underline{\tilde{u}}_i \quad (4.78)$$

$$\underline{\tilde{\tau}} = \sum_{i=1}^n \psi_i(\underline{x}) \underline{\tilde{\tau}}_i.$$

Using equation (3.49), inequality (3.56a) yields

$$[\underline{\tilde{\Lambda}} - \underline{\Lambda}_0, \underline{\tilde{\Lambda}} - \underline{\tilde{\Lambda}}] \leq [\underline{\tilde{\Lambda}} - \underline{\Lambda}_0, \underline{\tilde{\Lambda}} - \underline{\Lambda}_0] \quad (4.79)$$

where  $\underline{\tilde{\Lambda}} = \langle \underline{\tilde{u}} \quad \underline{\tilde{\tau}} \rangle^T$ ,  $\underline{\tilde{\Lambda}} = \langle \underline{\tilde{u}} \quad \underline{\tilde{\tau}} \rangle^T$  and  $\underline{\Lambda}_0 = \langle \underline{u}_0 \quad \underline{\tau}_0 \rangle^T$ .

Then from theorem 3.5.3

$$\int_V (\underline{\tilde{u}}_i - \underline{u}_{i0})^2 dV \leq \lambda_1 [\underline{\tilde{\Lambda}} - \underline{\Lambda}_0, \underline{\tilde{\Lambda}} - \underline{\Lambda}_0] \quad (4.80)$$

$$\int_V (\underline{\tilde{\tau}}_{ij} - \underline{\tau}_{ij0})^2 dV \leq \lambda_2 [\underline{\tilde{\Lambda}} - \underline{\Lambda}_0, \underline{\tilde{\Lambda}} - \underline{\Lambda}_0] \quad (4.81)$$

where  $\lambda_1$  and  $\lambda_2$  are positive constants and  $\lambda_1$  depends on the lowest non-zero vibration frequency. The inequalities (4.79) to (4.81) show that the mixed finite element solution is bounded by the rate at which  $|\underline{\tilde{\Lambda}} - \underline{\Lambda}_0|$  approaches zero. If the interpolations are chosen such that the equations (4.78) can exactly represent any polynomial of degree  $p_1$  for displacements and  $p_2$  for stresses; further that way from the singularity, the  $p_1+1$  derivatives of  $\underline{u}_0$  and  $p_2+1$  derivatives of  $\underline{\tau}_0$  are bounded then it can be shown (section 4.5)

$$|\underline{\tilde{u}}_{i,j} - \underline{u}_{i,j}^0| \leq A_i r^{\alpha-1} \quad \text{in } V_1 \quad (4.82)$$

$$|\underline{\tilde{u}}_{i,j} - \underline{u}_{i,j}^0| \leq \frac{A_i h^{p_1}}{r^{p_1+1-\alpha}} \quad \text{in } V-V_1;$$

$$|\underline{\tilde{\tau}}_{ij} - \underline{\tau}_{ij}^0| \leq B_{ij} r^{\alpha-1} \quad \text{in } V_1 \quad (4.83)$$

$$|\underline{\tilde{\tau}}_{ij} - \underline{\tau}_{ij}^0| \leq \frac{B_{ij} h^{p_2+1}}{r^{p_2+2-\alpha}} \quad \text{in } V-V_1.$$

The positive constants  $A_i$  and  $B_{ij}$  are, respectively, the combinations of the upper bounds of all  $p_1+1$  derivatives in the Taylor expansions of  $u_i^0$  and all  $p_2+1$  derivatives for  $\tau_{ij}^0$ .  $V_1$  is the domain covered by the elements adjacent to  $R$  and  $h$  is the maximum size of the elements.

From equation (4.73), the energy product for  $\tilde{\Lambda}-\Lambda_0$  is given by

$$[\tilde{\Lambda}-\Lambda_0, \tilde{\Lambda}-\Lambda_0]_A = \int_V \{2[T(\tilde{u}-u_0)]^T(\tilde{\tau}-\tau_0) - (\tilde{\tau}-\tau_0)^T \underline{C}(\tilde{\tau}-\tau_0)\} dV \quad (4.84)$$

$$\text{or } [\tilde{\Lambda}-\Lambda_0, \tilde{\Lambda}-\Lambda_0] \leq 2 \int_V |[T(\tilde{u}-u_0)]^T| |(\tilde{\tau}-\tau_0)| dV + \int_V |(\tilde{\tau}-\tau_0)^T| |\underline{C}| |(\tilde{\tau}-\tau_0)| dV. \quad (4.85)$$

As the operator  $\underline{T}$  involves first derivatives and  $\underline{C}$  is a positive definite compliance matrix, by virtue of (4.82) and (4.83)

$$[\tilde{\Lambda}-\Lambda_0, \tilde{\Lambda}-\Lambda_0] \leq \int_{V_1} \{c_1 r^{2(\alpha-1)} + c_2 r^{2(\alpha-1)}\} dV + \int_{V-V_1} \{c_1 \frac{h^{p_1+p_2+1}}{r^{p_1+p_2+3-2\alpha}} + c_2 \frac{h^{2(p_2+1)}}{r^{2(p_2+2-\alpha)}}\} dV \quad (4.86)$$

The constants  $c_1$  and  $c_2$  are positive;  $c_1$  depends on  $A_i$  and  $B_{ij}$  and  $c_2$  depends on  $B_{ij}$  and the compliance matrix  $\underline{C}$ .

Assuming that the inequalities in (4.75) are satisfied, integration of the right hand side of (4.86) yields

$$[\tilde{\Lambda}-\Lambda_0, \tilde{\Lambda}-\Lambda_0] \leq k_1(c_1+c_2)r_{\max}^{2(\alpha-1)+n} + k_2 c_1 \frac{h^{p_1+p_2+1}}{r_{\min}^{p_1+p_2+3-2\alpha-n}} + k_3 c_2 \frac{h^{2(p_2+1)}}{r_{\min}^{2(p_2+2-\alpha)-n}}. \quad (4.87)$$

The constants  $k_1, k_2$  and  $k_3$  are also positive and depend on the geometry and the arrangement of the finite element mesh;  $r_{\max}$  and  $r_{\min}$  are the maximum and the minimum radial distances from  $R$  to the boundaries of  $V_1$ , respectively.

From inequality (4.87), the contribution to error in the energy product from the elements immediately adjacent to the point of singularity is of order

$r_{\max}^{2(\alpha-1)+n}$  and the contribution from the rest of the domain is of order either  $\frac{h^{p_1+p_2+1}}{r_{\min}^{p_1+p_2+3-2\alpha-n}}$  or  $\frac{h^{2(p_2+1)}}{r_{\min}^{2(p_2+2-\alpha)-n}}$ , whichever is smaller.

Further, the main contribution from the latter part is from the elements that are close to the singularity. In the finite element analysis,  $r_{\max}$ ,  $r_{\min}$  and  $h$  are usually of the same order, i.e.  $r_{\max} \sim r_{\min} \sim h$ . Thus inequality (4.87) can be rewritten as

$$[\bar{\Lambda}-\bar{\Lambda}_0, \bar{\Lambda}-\bar{\Lambda}_0] < \{c_1(k_1+k_2) + c_2(k_1+k_3)\} h^{2(\alpha-1)+n}. \quad (4.88)$$

It should be noted that the constants  $c_1$  and  $c_2$ , through their dependence on  $A_i$  and  $B_{ij}$ , also depend on the behaviour of  $\underline{u}$  and  $\underline{\tau}$  near the point of singularity. Now from inequality (4.79)

$$[\bar{\Lambda}-\bar{\Lambda}_0, \bar{\Lambda}-\bar{\Lambda}_0] < \{c_1(k_1+k_2) + c_2(k_1+k_3)\} h^{2(\alpha-1)+n}. \quad (4.89)$$

Inequality (4.89) shows that the order of convergence of the energy product is controlled by the order of singularity, rather than by the order of the polynomials used for interpolation of  $\underline{u}$  and  $\underline{\tau}$  provided the inequalities (4.75) hold and completeness criterion (section 4.5) is satisfied.

For plane elasticity, from equations (4.70) and (4.71),  $n=2$  and  $\alpha=1/2$ . Therefore  $2(\alpha-1)+n=1$  and for any  $p_1 \geq 1$  and  $p_2 \geq 0$ , the inequalities (4.75) are satisfied. Inequality (4.89) now becomes

$$[\bar{\Lambda}-\bar{\Lambda}_0, \bar{\Lambda}-\bar{\Lambda}_0] < \{c_1(k_1+k_2) + c_2(k_1+k_3)\} h. \quad (4.90)$$

Therefore it can be concluded that the strain energy will converge at least as  $h$  and perhaps faster if there is a cancellation of errors in the energy product of (4.84) due to singular terms which are left out when regular polynomials are used for approximating displacements and stresses.

#### 4.6.B Determination of Stress Intensity Factor $K_I$

The crack intensity factor  $K_I$  (mode type I crack, Figure 1) is related to the potential energy release rate  $G_I$ , i.e. the rate of change in the potential energy due to crack extension. For plane stress and plane strain problems with unit thickness; this relationship is given by the following equation, Rice [29].

$$G_I = \frac{\partial \pi}{\partial a} = \frac{(\kappa+1)}{8G} K_I^2 \quad (4.91)$$

where  $\pi$  is the potential energy,  $a$  the crack length and  $G$  and  $\kappa$  are the same as defined for equations (4.70) and (4.71). It has been concluded by many investigators, Watwood [39], Anderson, *et al.* [1], Parks [27], etc. that the most accurate finite element scheme for determining the stress intensity factor is by means of the evaluation of the energy release rate without requiring any special elements to model the stress singularities. This method is now applied to determine  $K_I$  for plane strain linear elasticity using the mixed finite elements. For plane strain, the equation (4.91) reduces to

$$G_I = \frac{\partial \pi}{\partial a} = \frac{(1-\nu^2)}{E} K_I^2, \quad (4.92)$$

where  $E$  is the Young's modulus.

The procedure used in the application of the mixed finite element

method is somewhat similar to the one presented by Parks [27]. For two dimensional planar configurations, an alternative computation of  $G_I$  can be based on the path independent J-integral, Rice [29];

$$J = \int_{\Gamma} W dy - \underline{T} \cdot \frac{\partial \underline{u}}{\partial x} ds. \quad (4.93)$$

Here  $W$  is the strain energy density ( $W=1/2 \tau_{ij} \epsilon_{ij}$  for linear elasticity);  $\Gamma$  is an arbitrary contour enclosing the crack tip, Figure 2;  $\underline{T}$  is the traction vector associated with  $\underline{n}$ , the outward unit normal and  $\underline{u}$  is the displacement vector, and  $ds$  is an element of arc-length along  $\Gamma$ . Near the crack tip, the parameters comprising the integrand of the J-integral as determined from a finite element solution are likely to be in greatest error. However, the path independence allows the contour to be chosen farther away from the crack tip, hopefully resulting in improved accuracy. Rice [29] also showed that the J-integral in fact is equal to the potential energy release rate, equation (4.91).

$$J = G_I = \left( \frac{1-\nu^2}{E} \right) k_I^2 = \frac{-\partial \pi}{\partial a}. \quad (4.94)$$

Suppose that the finite element analysis has been performed on a given planar linear elastic body of unit thickness containing a crack. In the discrete form, the potential energy in the mixed method can be expressed as

$$\pi_M = \underline{f}^T \underline{A} \underline{u} - \frac{1}{2} \underline{f}^T \underline{B} \underline{f} - \underline{f}^T \underline{u} \quad (4.95)$$

where the matrices  $\underline{A}$  and  $\underline{B}$  are separately assembled element sub-matrices  $\underline{a}^e$  and  $\underline{b}^e$  of equation (4.18),  $\underline{f}$  is the generalized load vector, and  $\underline{u}$  and  $\underline{f}$  are the solution vectors. The equation (4.95) is analogous to the expression for twice the potential energy in a continuum, equation (5.12). The potential energy release rate can now be obtained by differentiating  $\pi_M$  with respect

to the crack length  $a$ :

$$\frac{\partial \pi_M}{\partial a} = \frac{\partial \underline{\tau}^T}{\partial a} [\underline{A}\underline{u} - \underline{B}\underline{\tau}] + [\underline{A}\underline{\tau} - \underline{f}] \frac{\partial \underline{u}}{\partial a} + \underline{\tau}^T \frac{\partial \underline{A}}{\partial a} \underline{u} - \frac{1}{2} \underline{\tau}^T \frac{\partial \underline{B}}{\partial a} \underline{\tau} - \frac{\partial \underline{f}^T}{\partial a} \underline{u}. \quad (4.96)$$

But from the finite element analysis,  $\underline{A}\underline{u} = \underline{B}\underline{\tau}$  and  $\underline{A}\underline{\tau} = \underline{f}$ ; therefore the first two terms on the right hand side are zero and (4.96) reduces to

$$\frac{\partial \pi_M}{\partial a} = \frac{1}{2} \underline{u}^T \underline{\tau}^T \frac{\partial}{\partial a} \begin{bmatrix} 0 & \underline{A} \\ \underline{A}^T & -\underline{B} \end{bmatrix} \begin{bmatrix} \underline{u} \\ \underline{\tau} \end{bmatrix} - \frac{\partial \underline{f}^T}{\partial a} \underline{u}. \quad (4.97)$$

Furthermore, if the loading on the body is accomplished by surface tractions applied on the boundary other than the crack face, then the load vector  $\underline{f}$  is independent of the infinitesimal crack advance, i.e.  $\frac{\partial \underline{f}}{\partial a} = 0$ . Therefore, from the equations (4.94) and (4.97)

$$-\frac{\partial \pi_M}{\partial a} = \left( \frac{1-\nu^2}{E} \right) k_I^2 = -\frac{1}{2} \underline{u}^T \underline{\tau}^T \frac{\partial \underline{S}}{\partial a} \begin{bmatrix} \underline{u} \\ \underline{\tau} \end{bmatrix}, \quad (4.98)$$

where  $\underline{S}$  is the master finite element matrix;

$$\underline{S} = \begin{bmatrix} 0 & \underline{A} \\ \underline{A}^T & -\underline{B} \end{bmatrix} \quad (4.99)$$

and  $\frac{\partial \underline{S}}{\partial a}$  represents the change in the master finite element matrix per unit crack advance.  $\Delta a$ , the infinitesimal extension of the crack tip can be approximated by rigidly translating all nodes on and within a contour  $\Gamma_0$  about the crack tip in the  $x$ -direction, Figure 3. All other nodes remain in their initial positions. Thus the master finite element matrix, which depends on individual element geometries and elastic material properties, remains unchanged in the regions interior to  $\Gamma_0$  and exterior to  $\Gamma_1$ , and the only contributions to  $\frac{\partial \underline{S}}{\partial a}$  come from the band of elements between the contours  $\Gamma_0$  and  $\Gamma_1$ . Thus

$$\frac{\partial \pi M}{\partial a} = \langle \underline{u}^T \quad \underline{\tau}^T \rangle \frac{\partial \underline{S}}{\partial a} \begin{bmatrix} \underline{u} \\ \underline{\tau} \end{bmatrix} = \langle \underline{u}^T \quad \underline{\hat{\tau}}^T \rangle \sum_{i=1}^{E^0} \frac{\partial \underline{S}_{-i}^0}{\partial a} \begin{bmatrix} \underline{u} \\ \underline{\hat{\tau}} \end{bmatrix} \quad (4.100)$$

where  $\underline{u}$  and  $\underline{\hat{\tau}}$  are the nodal variables for the nodes on  $\Gamma_0$  and  $\Gamma_1$ ;  $E^0$  is the number of elements between the contours  $\Gamma_0$  and  $\Gamma_1$ ; and  $\underline{S}_{-i}^0$  their element matrices. The change in the element matrices can be calculated directly as

$$\frac{\partial \underline{S}_{-i}^0}{\partial a} = \frac{\partial \underline{S}_{-i}^0}{\partial x_j} \frac{\partial x_j}{\partial a} \quad (4.101)$$

where the nodal coordinates  $x_j$  are thought of as functions of the crack length  $a$ . The derivatives  $\partial x_j / \partial a$  are then unity or zero, depending on whether or not  $x_j$  is the  $x$ -coordinate of a node located on  $\Gamma_0$ , respectively. Alternatively,  $\partial \underline{S}_{-i}^0 / \partial a$  may be approximated by a simple forward finite difference scheme

$$\frac{\partial \underline{S}_{-i}^0}{\partial a} \approx \frac{\Delta \underline{S}_{-i}^0}{\Delta a} = \frac{1}{\Delta a} [\underline{S}_{-i}^0 \bigg|_{a+\Delta a} - \underline{S}_{-i}^0 \bigg|_a] \quad (4.102)$$

Here  $\underline{S}_{-i}^0$  are the element matrices for the elements between the contours  $\Gamma_0$  and  $\Gamma_1$ , calculated for the initial crack length  $a$ , and  $\underline{S}_{-i}^0 \big|_{a+\Delta a}$  when  $x$  coordinate of each of the nodes lying on  $\Gamma_0$  have been incremented by  $\Delta a$ .

The equations (4.98) and (4.100) suggest that to calculate the stress intensity factor  $K_I$ , the master finite element matrix equation need only be solved once, i.e. for the initial crack length  $a$ . After obtaining this solution, pre- and post-multiplying the differentiated element matrices of equation (4.102) with the solution vectors for the corresponding nodal variables and then summing these over all the elements between  $\Gamma_0$  and  $\Gamma_1$  yields the rate of change of potential energy in the discrete sense  $\Delta \pi_M / \Delta a$ . Alternatively, the differentiated matrices can be assembled and then pre- and post-multiplied by the solution vectors  $\underline{u}$  and  $\underline{\hat{\tau}}$  for the nodal displacements and stresses, respectively, for the nodes on  $\Gamma_0$  and  $\Gamma_1$ , as in

equation (4.100)

$$\frac{\Delta \pi_M}{\Delta a} = \langle \hat{u}^T \quad \underline{1}^T \rangle \sum_{i=1}^{E^0} \frac{1}{\Delta a} [S_{-i}^0 \quad -S_{-i}^0] \begin{bmatrix} \hat{u} \\ \underline{1} \end{bmatrix}. \quad (4.103)$$

Finally, the stress intensity factor  $K_I$  for plane strain state can be computed from

$$K_I = \sqrt{\frac{E}{1-\nu^2} \left[ -\frac{\Delta \pi_M}{\Delta a} \right]}. \quad (4.104)$$

The contour  $\Gamma_0$  to be translated is thus far arbitrary except for the requirement that it be internal to the body and enclose the crack tip. It can also be shrunk to a single node at the crack tip so that the summation in (4.100) extends over the elements adjacent to the crack tip only. A glance at Figure 3 and the procedure outlined above for determining the potential energy release rate indicate that it is an area-analogue of the path independent J-integral.

## CHAPTER 5

### APPLICATION OF BOUNDARY CONDITIONS

So far only the homogeneous boundary conditions have been considered in the development of the theory of mixed methods. The treatment of homogeneous, mixed homogeneous and non-homogeneous boundary conditions, how these can be incorporated in the mixed finite element method, and equivalence to boundary residual concept are presented in this chapter. For illustration purposes the plane stress linear elasticity problem with unit thickness is considered. The governing differential equations are

$$-\tau_{ij,j} = f_i \quad (5.1a)$$

$$\tau_{ij} = 2\mu\epsilon_{ij} + \lambda\epsilon_{kk}\delta_{ij} \quad (5.1b)$$

$$\epsilon_{ij} = 1/2(u_{i,j} + u_{j,i}) \quad (5.1c)$$

where  $\tau_{ij}$  and  $\epsilon_{ij}$  are symmetric second order tensors, and  $i,j=1,2$ .

Equations (5.1a) are the equilibrium equations relating stress gradients to the body forces  $f_i$ , (5.1b) are the constitutive equations where  $\lambda$  and  $\mu$  are Lamé's constants and (5.1c) are the kinematic equations relating strains to displacement gradients. Assuming that the equations (5.1c) are satisfied identically equations (5.1) reduce to the following set of equations

$$-\tau_{ij,j} = f_i; \quad i,j=1,2 \quad (5.2)$$

$$1/2(u_{i,j} + u_{j,i}) - C_{ijkl}\tau_{kl} = 0; \quad i,j,k,l=1,2. \quad (5.3)$$

Where  $C_{ijkl}$  is the fourth order compliance tensor. For  $E$ , the Young's modulus and  $\nu$ , the Poisson's ratio defined as

$$E = \frac{\mu(3\lambda+\mu)}{(\lambda+\mu)}; \quad \nu = \frac{\lambda}{2(\lambda+\mu)}$$

the equations (5.2) and (5.3), for a plane stress problem, can be written in the following form:

$$-\tau_{xx,x} - \tau_{xy,y} = f_x \quad (5.4)$$

$$-\tau_{xy,x} - \tau_{yy,y} = f_y \quad (5.5)$$

$$u_{,x} - \frac{1}{E} (\tau_{xx} - \nu\tau_{yy}) = 0 \quad (5.6)$$

$$v_{,y} - \frac{1}{E} (-\nu\tau_{xx} + \tau_{yy}) = 0 \quad (5.7)$$

$$u_{,y} + v_{,x} - \frac{2(1+\nu)}{E} \tau_{xy} = 0. \quad (5.8)$$

The equations (5.4) to (5.8) can now be put into matrix form

$$\begin{bmatrix} 0 & 0 & -\frac{\partial}{\partial x} & 0 & -\frac{\partial}{\partial y} \\ 0 & 0 & 0 & -\frac{\partial}{\partial y} & -\frac{\partial}{\partial x} \\ \frac{\partial}{\partial x} & 0 & -\frac{1}{E} & \frac{\nu}{E} & 0 \\ 0 & \frac{\partial}{\partial y} & \frac{\nu}{E} & -\frac{1}{E} & 0 \\ \frac{\partial}{\partial y} & \frac{\partial}{\partial x} & 0 & 0 & -\frac{2(1+\nu)}{E} \end{bmatrix} \begin{bmatrix} u \\ v \\ \tau_{xx} \\ \tau_{yy} \\ \tau_{xy} \end{bmatrix} = \begin{bmatrix} f_x \\ f_y \\ 0 \\ 0 \\ 0 \end{bmatrix} \quad (5.9)$$

which takes the equivalent form of (3.35) as

$$\begin{bmatrix} \underline{0} & \underline{T}^* \\ \underline{T} & -\underline{C} \end{bmatrix} \begin{bmatrix} \underline{u} \\ \underline{\tau} \end{bmatrix} = \begin{bmatrix} \underline{f} \\ 0 \end{bmatrix} \quad (5.10)$$

or

$$\underline{A}\underline{\Lambda} = \underline{p}. \quad (5.10a)$$

Where

$$\underline{u} = \langle u \quad v \rangle^T; \text{ or } u_1 = u \text{ and } u_2 = v \quad (5.10b)$$

$$\underline{\tau} = \langle \tau_{xx} \quad \tau_{yy} \quad \tau_{xy} \rangle^T, \quad (5.10c)$$

$$\underline{T}^* = -\underline{T}^T = \begin{bmatrix} -\frac{\partial}{\partial x} & 0 & -\frac{\partial}{\partial y} \\ 0 & -\frac{\partial}{\partial y} & -\frac{\partial}{\partial x} \end{bmatrix}, \quad (5.10d)$$

$$\underline{\Lambda} = \langle \underline{u}^T \quad \underline{\tau}^T \rangle \quad \text{and} \quad \underline{f} = \langle f_x \quad f_y \rangle^T,$$

and the compliance matrix  $\underline{C}$  is a symmetric positive definite matrix

$$\underline{C} = \frac{1}{E} \begin{bmatrix} 1 & -\nu & 0 \\ -\nu & 1 & 0 \\ 0 & 0 & 2(1+\nu) \end{bmatrix}. \quad (5.10e)$$

The energy product of definition 3.4.3, for unit thickness,

becomes

$$(\underline{\Lambda}, \underline{\Lambda}) = [\underline{\Lambda}, \underline{\Lambda}] = \int_{\Omega} [\underline{u}^T \underline{\tau}^* \underline{\tau} + \underline{\tau}^T \underline{\tau} \underline{u} - \underline{\tau}^T \underline{C} \underline{\tau}] d\Omega. \quad (5.11)$$

This, on integration by parts of the first term on the right hand side, yields

$$[\underline{\Lambda}, \underline{\Lambda}] = - \oint_S \tau_{nn} \underline{u} \cdot \underline{n} ds - \oint_S \tau_{ns} \underline{u} \cdot \underline{s} ds + \int_{\Omega} [2 \underline{\tau}^T \underline{\tau} \underline{u} - \underline{\tau}^T \underline{C} \underline{\tau}] d\Omega \quad (5.12)$$

where  $\tau_{nn}$  and  $\tau_{ns}$  are stresses normal and tangential to the boundary and  $\underline{n}$  and  $\underline{s}$  are unit outward normal and tangential vectors, respectively. If the boundary conditions are homogeneous, the boundary integrals in (5.12) can be dropped resulting in the energy product of equation (3.73).

$$[\underline{\Lambda}, \underline{\Lambda}]_A = \int_{\Omega} [2 \underline{\tau}^T \underline{\tau} \underline{u} - \underline{\tau}^T \underline{C} \underline{\tau}] d\Omega. \quad (5.12a)$$

The mixed variational principle of (3.77) for plane stress linear elasticity can now be written as

$$F(\underline{\Lambda}) = \int_{\Omega} [2 \underline{\tau}^T \underline{\tau} \underline{u} - \underline{\tau}^T \underline{C} \underline{\tau}] d\Omega - 2 \int_{\Omega} \underline{f}^T \underline{u} d\Omega. \quad (5.13)$$

and  $\underline{\Lambda} = \langle \underline{u} \quad \underline{\tau} \rangle^T \in H_A^W$ .

### 5.1 Homogeneous Boundary Conditions

The homogeneous boundary conditions for plane stress can be expressed as

$$\begin{aligned} \tau_{ij} n_j &= 0 & \text{on } S_T \\ u_i &= 0 & \text{on } S_u \end{aligned} \quad (5.14)$$

where  $n_j$ 's are the components of unit outward normal,  $S_T$  and  $S_u$  are the portions of the boundary  $S$  where the stresses and the displacements are prescribed to be zero, respectively.

The element matrices can be generated directly from (5.13) (Appendix A) and assembled by using the procedure discussed in Chapter 4. Since the stresses are incorporated into the functional  $F(\underline{\Lambda})$  as natural boundary conditions only the kinematic boundary conditions on  $\underline{u}$  are to be satisfied. This can be achieved by forcing the corresponding displacement nodal variables to be zero on the boundary  $S_u$ . The process is identical to forcing the homogeneous kinematic boundary conditions in the displacement method.

## 5.2 Homogeneous Mixed Boundary Conditions

The boundary conditions for the plane stress problem of equations (5.4) to (5.8) in this case are

$$\begin{aligned} u_i &= 0 & \text{on } S_u \\ \tau_{ij} n_j &= 0 & \text{on } S_T \\ \tau_{ij} n_j + \alpha u_i &= 0 & \text{on } S_M \end{aligned} \quad (5.15)$$

where  $S_u$ ,  $S_T$  and  $S_M$  are the portions of the boundary  $S$  on which displacements, stresses and mixed conditions are specified, respectively, and  $\alpha$  is a constant.

Consider the energy product of (5.11). Since the variable  $\underline{u}$  and  $\underline{\tau}$  are in the field of definition of operator  $\underline{A}$ , they must satisfy all the boundary conditions in equations (5.15). The energy product of two elements  $\underline{\Lambda}$  and  $\tilde{\underline{\Lambda}}$  from  $D_{\underline{A}}^W$  is

$$[\underline{\Lambda}, \tilde{\underline{\Lambda}}] = \int_{\Omega} [\tilde{\underline{u}}^T \underline{\tau}^* \underline{\tau} + \tilde{\underline{\tau}}^T \underline{T} \underline{u} - \tilde{\underline{\tau}}^T \underline{C} \underline{\tau}] d\Omega.$$

Integration by parts of the first two terms on the right hand side yields

$$\begin{aligned}
[\underline{\Lambda}, \underline{\tilde{\Lambda}}] = & - \oint_S \underline{\tau}_{nn} \underline{\tilde{u}} \cdot \underline{n} ds + \oint_S \underline{\tilde{\tau}}_{nn} \underline{u} \cdot \underline{n} ds - \oint_S \underline{\tau}_{ns} \underline{\tilde{u}} \cdot \underline{s} ds + \oint_S \underline{\tilde{\tau}}_{ns} \underline{u} \cdot \underline{s} ds \\
& + \int_{\Omega} [\underline{u}^T \underline{T}^* \underline{\tilde{\tau}} + \underline{\tau}^T \underline{T} \underline{u} - \underline{\tilde{\tau}}^T \underline{C} \underline{\tau}] d\Omega.
\end{aligned} \tag{5.16}$$

Since  $\underline{\Lambda}$  and  $\underline{\tilde{\Lambda}}$  satisfy the same boundary conditions, the boundary integrals above cancel each other. Further, since  $\underline{C}$  is symmetric, therefore

$$\underline{\tilde{\tau}}^T \underline{C} \underline{\tau} = \underline{\tau}^T \underline{C} \underline{\tilde{\tau}}$$

and

$$[\underline{\Lambda}, \underline{\tilde{\Lambda}}] = \int_{\Omega} [\underline{u}^T \underline{T}^* \underline{\tilde{\tau}} + \underline{\tau}^T \underline{T} \underline{u} - \underline{\tau}^T \underline{C} \underline{\tilde{\tau}}] d\Omega$$

or

$$[\underline{\Lambda}, \underline{\tilde{\Lambda}}] = [\underline{\tilde{\Lambda}}, \underline{\Lambda}]$$

which proves that the operator  $\underline{A}$  is symmetric. Therefore the energy product in the space  $H_A^W$  is given by

$$[\underline{\Lambda}, \underline{\Lambda}]_A = \int_{\Omega} [2 \underline{\tau}^T \underline{T} \underline{u} - \underline{\tau}^T \underline{C} \underline{\tau}] d\Omega + \int_{S_M} \alpha \underline{u}^T \underline{u} ds \tag{5.17}$$

since the contribution to the line integral arises only from the  $S_M$  part of the boundary. In this case, the mixed boundary conditions give rise to a line integral in the energy product. The element matrices can be obtained by substitution of the approximate finite element solution into (5.17), which would still be symmetric. However, some of the zero entries of the matrix (4.19) are now replaced by the boundary contribution from the non-zero line integral.

The energy convergence would be ensured if the coordinate functions are complete in  $H_A^W$ . Further, since the boundary conditions prescribed on  $S_T$  and  $S_M$  contain stress terms they are therefore natural. The coordinate functions then need not satisfy these boundary conditions whereas the homogeneous kinematic boundary conditions on  $S_u$  are enforced in the same manner as discussed in section 5.1.

### 5.3 Nonhomogeneous Boundary Conditions

The nonhomogeneous boundary conditions for a plane stress problem are usually prescribed as

$$u_i = u_i^0 \quad \text{on } S_u \quad (5.18a)$$

$$\tau_{ij} n_j = T_i^0 \quad \text{on } S_T \quad (5.18b)$$

$$\tau_{ij} n_j + \alpha u_i = C_i^0 \quad \text{on } S_M. \quad (5.18c)$$

These can be incorporated by changing variables in such a way that the problem reduces to one with homogeneous boundary conditions. Thus, assume that there exists functions  $\underline{\Lambda}' = \langle \underline{u}', \underline{\tau}' \rangle^T$ , i.e. functions  $u_i'$  and  $\tau_{ij}'$ , both continuous, such that

$$u_i' = u_i^0 \quad \text{on } S_u$$

$$\tau_{ij}' n_j = T_i^0 \quad \text{on } S_T \quad (5.19)$$

$$\tau_{ij}' n_j + \alpha u_i' = C_i^0 \quad \text{on } S_M.$$

Define new variables  $u_i^2$  and  $\tau_{ij}^2$  in the following way

$$u_i'' = u_i - u_i' \quad (5.20)$$

$$\tau_{ij}'' = \tau_{ij} - \tau_{ij}'$$

$$\text{or} \quad \underline{\Lambda}'' = \underline{\Lambda} - \underline{\Lambda}'. \quad (5.20a)$$

Substituting equations (5.20) into (5.2), (5.3) and (5.18) yields

$$-\tau_{ij,j}'' = f_i + \tau_{ij,j}' = f_i'' \quad (5.21)$$

$$1/2(u_{i,j}'' + u_{j,i}'') - C_{ijkl} \tau_{kl}'' = -1/2(u_{i,j}' + u_{j,i}') + C_{ijkl} \tau_{kl}' = g_{kl}'' \quad (5.22)$$

$$u_i'' = 0 \quad \text{on } S_u$$

$$\tau_{ij}'' n_j = 0 \quad \text{on } S_T \quad (5.23)$$

$$\tau_{ij}'' n_j + \alpha u_i'' = 0 \quad \text{on } S_M.$$

Thus the problem in  $\underline{\Lambda}''$  has homogeneous boundary conditions, and the only difference in (5.2), (5.3) and (5.21), (5.22), respectively, is the introduction of the term  $\tau'_{ij,j}$  on the right hand side of (5.21) and  $[-1/2 (u'_{i,j} + u'_{j,i}) + C_{ijkl} \tau'_{kl}]$  in (5.22). If these terms were known, it would be possible to obtain an approximate solution for  $\underline{\Lambda}''$  and convergence would be ensured if the coordinate functions were complete in the space  $H_A^W$  and the associated energy product as given in equation (5.17).

Let the finite element approximations for  $\underline{\Lambda}'' = \langle \underline{\bar{u}}'' \quad \underline{\bar{\tau}}'' \rangle^T$  be

$$\bar{u}_i'' = \sum_{k=1}^M \phi_{ik}^k \bar{u}_{ik}''; \quad i=1,2. \quad (5.24)$$

$$\bar{\tau}_{ij}'' = \sum_{l=1}^N \psi_{ij}^l \bar{\tau}_{ijl}''; \quad i,j=1,2. \quad (5.25)$$

or

$$\underline{\bar{\Lambda}}'' = \underline{\Phi}_{-M}^N \underline{w}_{-M}^N \quad (5.26)$$

where

$$\underline{\Phi}_{-M}^N = \langle \phi_i^k \quad \psi_{ij}^l \rangle$$

and

$$\underline{w}_{-M}^N = \langle \bar{u}_{ik}'' \quad \bar{\tau}_{ijl}'' \rangle^T.$$

Then the required element matrix equation, from section 4.2, is

$$[\underline{\bar{\Lambda}}'', \underline{\Phi}_{-M}^N]_A = (\underline{p}^T, \underline{\Phi}_{-M}^N) \quad (5.27)$$

here

$$\underline{p}^T = \begin{bmatrix} f_i'' & 0 \\ 0 & g_{ij}'' \end{bmatrix}.$$

Thus a solution for  $\underline{\Lambda}''$  can be obtained such that

$$\|\underline{\bar{\Lambda}}'' - \underline{\Lambda}''\|_A \rightarrow 0, \text{ as } M \text{ and } N \rightarrow \infty. \quad (5.28)$$

It is worth noting that here the kinematic nonhomogeneous boundary conditions are conveniently incorporated through the load vector. Such a procedure cannot be achieved in the displacement approach because it would

require displacements to satisfy the nonhomogeneous boundary conditions and have continuous first derivatives.

However, a solution may be obtained directly for  $u_i$  and  $\tau_{ij}$  without actually knowing  $\underline{\Lambda}'$ . This is accomplished by assuming approximations for  $u_i$  and  $\tau_{ij}$  as

$$\begin{aligned}\bar{u}_i &= \sum_{k=1}^M \bar{\phi}_i^k u_{ik}; \quad i=1,2. \\ \bar{\tau}_{ij} &= \sum_{l=1}^N \bar{\psi}_{ij}^l \tau_{ijl}; \quad i,j=1,2.\end{aligned}\tag{5.29}$$

and

$$\bar{\underline{\Lambda}} = \begin{bmatrix} \bar{\phi}_M^N \\ \bar{\psi}_M^N \end{bmatrix}^T$$

where

$$\bar{\phi}_M^N = \langle \bar{\phi}_1^k \quad \bar{\psi}_{ij}^l \rangle$$

and

$$\bar{\psi}_M^N = \langle u_{ik} \quad \tau_{ijl} \rangle^T.$$

The sets of functions  $\{\bar{\phi}_i^k\}$  and  $\{\bar{\psi}_{ij}^l\}$  are complete in  $H_A^W$  space considered with respect to the nonhomogeneous boundary conditions. Therefore as the function  $\bar{\underline{\Lambda}}'' + \underline{\Lambda}'$  satisfies such nonhomogeneous boundary conditions, it follows that there exist  $u_{ik}$  and  $\tau_{ijl}$  such that

$$\left| \bar{\underline{\Lambda}} - (\bar{\underline{\Lambda}}'' + \underline{\Lambda}') \right|_A \rightarrow 0, \text{ as } M \text{ and } N \rightarrow \infty.\tag{5.30}$$

Now the function  $\bar{\underline{\Lambda}} - (\bar{\underline{\Lambda}}'' + \underline{\Lambda}')$  has homogeneous forced boundary conditions; therefore the energy product of it with any arbitrary function  $\underline{\Theta}_M^N$  in the space  $H_A^W$ , with homogeneous forced boundary conditions, would also vanish in lieu of (5.30). Therefore

$$[\bar{\underline{\Lambda}} - (\bar{\underline{\Lambda}}'' + \underline{\Lambda}'), \underline{\Theta}_M^N]_A = 0.\tag{5.31}$$

Since  $\underline{\Theta}_M^N$  is arbitrary, it can be replaced by  $\bar{\phi}_M^N$  in (5.26) and equation (5.31) can be written as

$$[\bar{\Lambda} - (\bar{\Lambda}'' + \Lambda'), \phi_{-M}^N]_A = 0. \quad (5.32)$$

From linearity of the operator  $\underline{A}$ ,

$$[\bar{\Lambda}'', \phi_{-M}^N]_A = [\bar{\Lambda} - \Lambda', \phi_{-M}^M]_A \quad (5.33)$$

and substituting this into equation (5.27) yields

$$[\bar{\Lambda}, \phi_{-M}^N]_A = (\underline{p}^T, \phi_{-M}^N) + [\Lambda', \phi_{-M}^N]_A. \quad (5.34)$$

But

$$(\underline{p}^T, \phi_{-M}^N) = \int_{\Omega} \begin{bmatrix} f''_i & 0 \\ 0 & g''_{ij} \end{bmatrix} \begin{Bmatrix} \phi_i^k \\ \psi_{ij}^l \end{Bmatrix} d\Omega$$

or

$$(\underline{p}^T, \phi_{-M}^N) = \int_{\Omega} \begin{Bmatrix} (f''_i \phi_i^k) \\ (g''_{ij} \psi_{ij}^l) \end{Bmatrix} d\Omega.$$

Therefore from (5.21)

$$\int_{\Omega} (f''_i, \phi_i^k) d\Omega = \int_{\Omega} (f_i + \tau'_{ij,j}) \phi_i^k d\Omega$$

and integrating by parts the second term on the right hand side yields

$$\int_{\Omega} (f''_i, \phi_i^k) d\Omega = \int_{\Omega} (f_i \phi_i^k - \tau'_{ij} \phi_{i,j}^k) d\Omega + \oint_S \tau'_{ij} n_j \phi_i^k ds.$$

Using equations (5.19) and the fact that  $\phi_i^k=0$  on  $S_u$  gives

$$\int_{\Omega} (f''_i, \phi_i^k) d\Omega = \int_{\Omega} (f_i \phi_i^k - \tau'_{ij} \phi_{i,j}^k) d\Omega + \int_{S_T} T_i^0 \phi_i^k ds + \int_{S_M} (C_i^0 - \alpha u'_i) \phi_i^k ds \quad (5.35)$$

and from (5.22)

$$\int_{\Omega} (g''_{ij} \psi_{ij}^q) d\Omega = \int_{\Omega} \{-1/2(u'_{i,j} + u'_{j,i}) + C_{ijkl} \tau'_{kl}\} \psi_{ij}^q d\Omega. \quad (5.36)$$

Therefore

$$(\underline{p}^T, \phi_{-M}^N) = \{\int_{\Omega} f_i \phi_i^k d\Omega + \int_{S_T} T_i^0 \phi_i^k ds + \int_{S_M} C_i^0 \phi_i^k ds\} - [\Lambda', \phi_M^N]_A \quad (5.37)$$

because, from (5.17)

$$[\underline{\Lambda}', \phi_M^N]_A = \left\{ \begin{array}{l} \int_{\Omega} \tau'_{ij} \phi_{i,j}^k d\Omega + \int_{S_M} \alpha u'_i \phi_i^k ds \\ \int_{\Omega} \{1/2(u'_{i,j} + u'_{j,i}) - C_{ijkl} \tau'_{kl}\} \psi_{ij}^q d\Omega \end{array} \right\}. \quad (5.38)$$

Now equation (5.37) enables (5.34) to be written as

$$[\bar{\Lambda}, \phi_M^N]_A = \left\{ \begin{array}{l} \int_{\Omega} f_i \phi_i^k d\Omega + \int_{S_T} T_i^0 \phi_i^k ds + \int_{S_M} C_i^0 \phi_i^k ds \\ 0 \end{array} \right\} \quad (5.39)$$

which are the mixed Galerkin equations that govern a solution for  $\bar{\Lambda} = \langle \bar{u} \ \bar{\tau} \rangle^T$  in  $H_A^W$  when the boundary conditions are nonhomogeneous. Writing out in full the equation (5.39)

$$\int_{\Omega} \bar{\tau}_{ij} \phi_{i,j}^k d\Omega + \int_{S_M} \alpha \bar{u}_i \phi_i^k ds = \int_{\Omega} f_i \phi_i^k d\Omega + \int_{S_T} T_i^0 \phi_i^k ds + \int_{S_M} C_i^0 \phi_i^k ds; \quad k=1,2, \dots M. \quad (5.40)$$

$$\int_{\Omega} [1/2(\bar{u}_{i,j} + \bar{u}_{j,i}) - C_{ijkl} \bar{\tau}_{kl}] \psi_{ij}^q d\Omega = 0; \quad q=1,2, \dots N. \quad (5.41)$$

The equations (5.40) and (5.41) require that the approximate solution for  $\bar{u}_i$  given by (5.29) should satisfy the nonhomogeneous forced boundary conditions and the coordinate functions  $\phi_i^k$  the homogeneous forced boundary conditions on  $S_u$ .

In the finite element method it is not necessary to introduce different approximations  $\underline{\Lambda}$  corresponding to  $\phi_M^N$  and  $\bar{\phi}_M^N$  coordinate functions. The coordinate functions  $\bar{\phi}_M^N$  of a finite element approximation associated with the degrees of freedom that do not lie on  $S_u$  satisfy homogeneous conditions on  $S_u$ , i.e. vanish on  $S_u$ . Therefore the equations (5.40) and (5.41) can be solved by specifying the values of  $u_{ik}$  of (5.29), the nodal degrees of freedom on  $S_u$ . The remaining coordinate functions satisfy homogeneous forced boundary conditions and thus only one set of coordinate functions need be introduced.

To show that the approximate solution  $\bar{\Lambda}$  of (5.29) converges in the energy norm, rewrite (5.31) from linearity of the operator  $\underline{A}$  in the form

$$[\bar{\Lambda}, \underline{\Theta}_M^N]_A = [\bar{\Lambda}'' + \Lambda', \underline{\Theta}_M^N]_A. \quad (5.42)$$

Also from equation (5.20a)

$$[\Lambda, \underline{\Theta}_M^N]_A = [\Lambda'' + \Lambda', \underline{\Theta}_M^N]_A. \quad (5.43)$$

Subtracting (5.42) from (5.43) and from linearity of the operator  $\underline{A}$ ;

$$[\Lambda - \bar{\Lambda}, \underline{\Theta}_M^N]_A = [\Lambda'' - \bar{\Lambda}'', \underline{\Theta}_M^N]_A.$$

Using property (iii) of theorem 3.4.2 (Schwarz inequality)

$$|[\Lambda'' - \bar{\Lambda}'', \underline{\Theta}_M^N]_A| \leq |\Lambda'' - \bar{\Lambda}''|_A |\underline{\Theta}_M^N|_A.$$

But from (5.28),  $|\Lambda'' - \bar{\Lambda}''| \rightarrow 0$ ; as  $M$  and  $N \rightarrow \infty$ ; therefore

$$[\Lambda - \bar{\Lambda}, \underline{\Theta}_M^N]_A \rightarrow 0, \text{ as } M \text{ and } N \rightarrow \infty.$$

Since  $\underline{\Theta}_M^N$  is an arbitrary function with homogeneous forced boundary conditions, it may be set equal to  $\Lambda - \bar{\Lambda}$ . Then

$$[\Lambda - \bar{\Lambda}, \Lambda - \bar{\Lambda}]_A \rightarrow 0, \text{ as } M \text{ and } N \rightarrow \infty,$$

which implies that

$$|\Lambda - \bar{\Lambda}|_A \rightarrow 0, \text{ as } M \text{ and } N \rightarrow \infty. \quad (5.44)$$

That is, the approximate solution to the nonhomogeneous boundary condition problem converges in the energy norm of  $H_A^W$ .

One of the advantages that the mixed method offers lies in different ways of incorporating the boundary conditions. So far the natural boundary conditions have been associated with stresses, a consequence of extracting the boundary integrals from the equilibrium equations. This led to constraining of forced boundary conditions on  $\underline{u}$  on  $S_u$  through the nodal variables.

It will be demonstrated here that in fact all nonhomogeneous

boundary conditions can be incorporated through boundary integrals from both equilibrium and constitutive-kinematic equations through the Hellinger-Reissner's mixed variational principle since it yields the same equations as the mixed Galerkin method for T\*T theory (Chapter 3).

The Hellinger-Reissner mixed variational principle for plane stress with unit thickness and zero body forces  $f_x$  and  $f_y$  can be written as

$$I = \int_{\Omega} [\tau_{xx} u_{,x} + \tau_{yy} v_{,y} + \tau_{xy} (u_{,y} + v_{,x}) - \frac{1}{2E} \{\tau_{xx}^2 + \tau_{yy}^2 - 2\nu \tau_{xx} \tau_{yy} + 2(1+\nu) \tau_{xy}^2\}] d\Omega - \int_{S_1} (u \bar{p}_x + v \bar{p}_y) ds - \int_{S_2} [(u - \bar{u}) p_x + (v - \bar{v}) p_y] ds \quad (5.45)$$

where  $p_i = \tau_{ij} n_j$ .  $S_1$  is the portion of the boundary  $S$  on which the stresses  $\bar{\tau}_{ij}$  or  $\bar{p}_i$  are prescribed. The part  $S_2$  has the displacements  $\bar{u}_i$  ( $\bar{u}$  and  $\bar{v}$ ) prescribed on it. The stress boundary conditions of (5.18a) and (5.18b) on  $S_T$  and  $S_M$  can be considered to be on part  $S_1$  while  $S_u$  would coincide with  $S_2$ . Therefore

$$\begin{aligned} \bar{p}_i &= \bar{\tau}_{ij} n_j = T_i^0 & \text{on } S_T \\ \bar{p}_i &= \bar{\tau}_{ij} n_j = C_i^0 - \alpha u_i & \text{on } S_M \end{aligned} \quad (5.46)$$

and the first variation of  $I$  with respect to  $u_i$  and  $\tau_{ij}$  gives

$$\begin{aligned} \delta I &= \int_{\Omega} [\tau_{ij} \delta u_{i,j}] d\Omega + \int_{\Omega} [1/2 (u_{i,j} + u_{j,i}) - C_{ijkl} \tau_{kl}] \delta \tau_{ij} d\Omega - \int_{S_T} T_i^0 \delta u_i ds \\ &\quad - \int_{S_M} (C_i^0 - \alpha u_i) \delta u_i - \int_{S_u} (u_i - u_i^0) \delta (\tau_{ij} n_j) ds - \int_{S_u} \tau_{ij} n_j \delta u_i = 0. \end{aligned} \quad (5.47)$$

Now assume approximations for  $u_i$  and  $\tau_{ij}$  as

$$\bar{u}_i = \sum_{k=1}^M \phi_i^k u_{ik}; \quad i=1,2. \quad (5.48)$$

$$\text{and} \quad \bar{\tau}_{ij} = \sum_{l=1}^N \psi_{ij}^l \tau_{ijl}; \quad i,j=1,2. \quad (5.49)$$

Therefore

$$\delta \bar{u}_i = \sum_{k=1}^M \phi_i^k \delta u_{ik}; \quad \delta \bar{\tau}_{ij} = \sum_{l=1}^N \psi_{ij}^l \delta \tau_{ijl} \quad (5.50)$$

and

$$\delta \bar{u}_{i,j} = \sum_{k=1}^N \phi_{i,j}^k \delta u_{ik}. \quad (5.51)$$

Substitution of (5.48) to (5.51) into (5.47) yields

$$\begin{aligned} \delta I = & \sum_{k=1}^M \left[ \int_{\Omega} \bar{\tau}_{ij} \phi_{i,j}^k d\Omega - \int_{S_T} T_i^0 \phi_i^k ds - \int_{S_M} (C_i^0 - \bar{u}_i) \phi_i^k ds - \int_{S_u} \bar{\tau}_{ij} n_j \phi_i^k ds \right] \delta u_{ik} \\ & + \sum_{q=1}^N \left[ \int_{\Omega} \{1/2(\bar{u}_{i,j} + \bar{u}_{j,i}) - C_{ijkl} \bar{\tau}_{kl}\} \psi_{ij}^q d\Omega - \int_{S_u} \bar{u}_i \psi_{ij}^q n_j ds + \int_{S_u} u_i^0 \psi_{ij}^q n_j ds \right] \delta \tau_{ijq} \\ & \delta \tau_{ijq} = 0. \end{aligned} \quad (5.52)$$

Since  $\delta I$  vanishes for arbitrary variations  $\delta u_{ik}$  and  $\delta \tau_{ijq}$ , the following equations are obtained:

$$\begin{aligned} \int_{\Omega} \bar{\tau}_{ij} \phi_{i,j}^k d\Omega + \int_{S_M} \alpha \bar{u}_i \phi_i^k ds - \int_{S_u} \bar{\tau}_{ij} n_j \phi_i^k ds = \int_{S_T} T_i^0 \phi_i^k ds + \int_{S_M} C_i^0 \phi_i^k ds; \\ k=1, 2, \dots, M. \end{aligned} \quad (5.53)$$

$$\begin{aligned} \int_{\Omega} [1/2(\bar{u}_{i,j} + \bar{u}_{j,i}) - C_{ijkl} \bar{\tau}_{kl}] \psi_{ij}^q d\Omega - \int_{S_u} \bar{u}_i \psi_{ij}^q n_j ds = \int_{S_u} u_i^0 \psi_{ij}^q n_j ds; \\ q=1, 2, \dots, N. \end{aligned} \quad (5.54)$$

The equations (5.53) and (5.54) contain  $2M+3N$  equations for  $2M+3N$  unknowns with a symmetric matrix of coefficients. It is interesting to note that the nonhomogeneous forced boundary conditions are applied through the displacement vector in (5.54) and hence need not be constrained as was done in the previous case. Except for boundary integrals over  $S_u$  these equations are exactly the same as (5.40) and (5.41).

#### 5.4 Boundary Residual Concept

An alternate procedure for incorporating boundary conditions in the mixed Galerkin method is similar to the boundary residual concept presented by Finlayson and Scriven [8] and Finlayson [7] in which the domain residual together with boundary residuals are made orthogonal to the shape functions of the approximate solution.

Consider the plane stress linear elasticity problem of equation (5.9) with nonhomogeneous boundary conditions of equations (5.18) and approximations for  $u_i$  and  $\tau_{ij}$  of equations (5.48) and (5.49). The substitution of  $\bar{u}_i$  and  $\bar{\tau}_{ij}$  into the field equations (5.9) and boundary conditions (5.18) yields the following residuals:

$$R_{ei} = [-\bar{\tau}_{ij,j} - f_i] \quad \text{in } \Omega \quad (5.55)$$

$$R_{ci} = [1/2(\bar{u}_{i,j} + \bar{u}_{j,i}) - C_{ijkl}\bar{\tau}_{kl}] \quad \text{in } \Omega \quad (5.56)$$

$$R_{ui} = -[\bar{u}_i - u_i^0] \quad \text{on } S_u \quad (5.57)$$

$$R_{Ti} = [\bar{\tau}_{ij}n_j - T_i^0] \quad \text{on } S_T \quad (5.58)$$

$$R_{Mi} = [\bar{\tau}_{ij}n_j + \alpha\bar{u}_i - C_i^0] \quad \text{on } S_M \quad (5.59)$$

where  $R_{ei}$  and  $R_{ci}$  are the domain residuals for the equilibrium and kinematic-constitutive equations, respectively;  $R_u$ ,  $R_T$  and  $R_M$  are the boundary residuals on  $S_u$ ,  $S_T$  and  $S_M$ , respectively.

If the residuals  $R_{ei}$  from equation (5.55) along with  $R_{Ti}$  and  $R_{Mi}$  from equations (5.58) and (5.59) are made orthogonal to the shape functions for  $\bar{u}_i$  and residuals  $R_{ci}$  from (5.56) along with residual  $R_{ui}$  from (5.57) to the shape functions for  $\bar{\tau}_{ij}$ , the following equations result:

$$\int_{\Omega} (-\bar{\tau}_{ij,j} - f_i) \phi_i^k d\Omega + \int_S (\bar{\tau}_{ij}n_j - T_i^0) \phi_i^k ds + \int_{S_M} (\bar{\tau}_{ij}n_j + \alpha\bar{u}_i - C_i^0) \phi_i^k ds = 0; \quad k=1,2, \dots M. \quad (5.60)$$

$$\int_{\Omega} [1/2(\bar{u}_{i,j} + \bar{u}_{j,i}) - C_{ijkl} \bar{\tau}_{ij}] \psi_{ij}^q d\Omega - \int_{S_u} (\bar{u}_i - u_i^0) \psi_{ij}^q n_j ds = 0;$$

$$q=1,2, \dots N. \quad (5.61)$$

Assuming  $f_i=0$ ; and applying Gauss' theorem to (5.60) yields

$$\int_{\Omega} \bar{\tau}_{ij} \phi_{i,j}^k d\Omega + \int_{S_M} \alpha \bar{u}_i \phi_i^k ds - \int_{S_u} \bar{\tau}_{ij} n_j \phi_i^k ds = \int_{S_T} T_i^0 \phi_i^k ds + \int_{S_M} C_i^0 \phi_i^k ds;$$

$$k=1,2, \dots M. \quad (5.62)$$

$$\int_{\Omega} [1/2(u_{i,j} + u_{j,i}) - C_{ijkl} \tau_{kl}] \psi_{ij}^q d\Omega - \int_{S_u} \bar{u}_i \psi_{ij}^q n_j ds = \int_{S_u} u_i^0 \psi_{ij}^q n_j ds;$$

$$q=1,2, \dots N. \quad (5.63)$$

The equations (5.62) and (5.63) are the same as equations (5.53) and (5.54) in the previous section. Therefore in linear elasticity, the equations obtained by the mixed Galerkin method, the mixed variational principle and the boundary residual concept are the same. In the displacement approach, Hutton [15] showed that the equations obtained from the Galerkin Method and the boundary residual concept for approximations from wider class  $H_A$  would be identical if the forced boundary conditions were either homogeneous or were identically satisfied by the finite element approximations when nonhomogeneous. However, the flexibility offered by the mixed methods in incorporating the boundary conditions, forced or natural, provides a wider equivalence.

## CHAPTER 6

### EIGENVALUE ANALYSIS OF THE ELEMENT MATRIX

An eigenvalue-eigenvector analysis of the element matrix arising from the mixed method is presented in this chapter. Various combinations of displacement and stress approximations over a triangular and a rectangular element are considered. Two problems are included, namely the linear elasticity plane stress and the linear part of the Navier-Stokes equations. It is anticipated that the analysis of eigenvalues will provide some insight as to choice of approximations for the dependent variables involved so that completeness is achieved.

#### 6.1 Linear Elasticity Problem

Consider the matrix equation (5.9) for the plane stress problem with zero body forces, i.e.  $f_x = f_y = 0$ ,

$$\begin{bmatrix} 0 & 0 & -\frac{\partial}{\partial x} & 0 & -\frac{\partial}{\partial y} \\ 0 & 0 & 0 & -\frac{\partial}{\partial y} & -\frac{\partial}{\partial x} \\ \frac{\partial}{\partial x} & 0 & -\frac{1}{E} & \frac{\nu}{E} & 0 \\ 0 & \frac{\partial}{\partial y} & \frac{\nu}{E} & -\frac{1}{E} & 0 \\ \frac{\partial}{\partial y} & \frac{\partial}{\partial x} & 0 & 0 & -\frac{2(1+\nu)}{E} \end{bmatrix} \begin{bmatrix} u \\ v \\ \tau_{xx} \\ \tau_{yy} \\ \tau_{xy} \end{bmatrix} = \begin{bmatrix} 0 \\ 0 \\ 0 \\ 0 \\ 0 \end{bmatrix}. \quad (6.1)$$

The variational principle for (6.1) with homogeneous boundary conditions (section 5.1) can be written as

$$I = \int_{\Omega} [\tau_{xx} u_{,x} + \tau_{yy} v_{,y} + \tau_{xy} (u_{,y} + v_{,x}) - \frac{1}{2E} (\tau_{xx}^2 + \tau_{yy}^2 - 2\nu \tau_{xx} \tau_{yy} + 2(1+\nu) \tau_{xy}^2)] d\Omega. \quad (6.2)$$

Since  $I$  represents strain energy, inspection of the right hand side in (6.2) suggests the following three rigid body modes which yield zero strain energy:

$$\begin{aligned}
\text{(i)} \quad u &= \text{constant}, v = 0 & ; \tau_{xx} = \tau_{yy} = \tau_{xy} = 0 \\
\text{(ii)} \quad u &= 0, v = \text{constant}; \tau_{xx} = \tau_{yy} = \tau_{xy} = 0 \\
\text{(iii)} \quad u &= -cy, v = cx & ; \tau_{xx} = \tau_{yy} = \tau_{xy} = 0
\end{aligned} \tag{6.3}$$

These rigid body modes are expected to be removed by the specified kinematic boundary conditions. Furthermore, it is required by the functional of (6.2) that the displacements satisfy the kinematic boundary conditions while the stresses emerge as natural boundary conditions. Therefore the finite element approximations should be in compliance with these requirements, i.e. the matrix of equations (4.19) should exhibit the rigid body modes of (6.3).

The independently chosen approximations for the stresses and the displacements have to comply with the completeness requirement (i) of section 4.4. The mean convergence of strains from the assumed stresses to the strains derived from the assumed displacements would be assured for a finite number of degrees of freedom if the former contains all the strain modes and perhaps more than the strain modes in the latter. It is assumed that the displacements possess all the rigid body and constant strain modes and that the stresses possess all the constant stress modes. It is now asserted that the violation of the completeness requirement (i) results in a hypersingular element matrix, i.e. the number of zero eigenvalues greater than the rigid body modes expected in a problem. The eigenvectors for the extra zero eigenvalues correspond to mechanisms which are defined as the kinematic freedoms possible when the material has no elastic stiffness. This is illustrated by the following example.

Consider one element domain  $\Omega^e$  and the approximate solutions for  $u, v, \tau_{xx}, \tau_{yy}$  and  $\tau_{xy}$  as

$$\begin{aligned}
\bar{u} &= ax + by + cx^2 + dxy + ey^2 \\
\bar{v} &= bx + fy + gx^2 + hxy + iy^2 \\
\bar{\tau}_{xx} &= j \\
\bar{\tau}_{yy} &= k \\
\bar{\tau}_{xy} &= l.
\end{aligned} \tag{6.4}$$

The polynomials for  $u$  and  $v$  are so chosen that the rigid body modes have been eliminated by satisfying the kinematic boundary conditions. Therefore

$$\begin{aligned}
\bar{\epsilon}_{xx} &= \bar{u}_{,x} = a + 2cx + dy \\
\bar{\epsilon}_{yy} &= \bar{v}_{,y} = f + hx + 2iy \\
\bar{\gamma}_{xy} &= \bar{u}_{,y} + \bar{v}_{,x} = 2b + (d+2g)x + (2e+h)y.
\end{aligned} \tag{6.5}$$

From the equations (6.5) the strains derived from  $\bar{u}$  and  $\bar{v}$  are complete linear polynomials. Therefore the mean convergence of constant strains from  $\bar{\tau}_{xx}$ ,  $\bar{\tau}_{yy}$  and  $\bar{\tau}_{xy}$  in (6.4) to the strains in (6.5) would not occur and the completeness requirement (i) is violated. The parameters in (6.4) are to be determined from the variational formulation. The substitution of the expressions in equations (6.4) into (6.2) yields

$$\begin{aligned}
I &= [j(Aa+2\alpha c+\beta d) + k(Af+\alpha h+2\beta i) + l(2Ab+\alpha d+2\alpha g+2\beta e+\beta h)] \\
&\quad - \frac{A}{2E}[j^2+k^2-2\nu jk+2(1+\nu)l^2]
\end{aligned} \tag{6.6}$$

where  $A = \int_{\Omega} e \, d\Omega$ ,  $\alpha = \int_{\Omega} e \, x d\Omega$  and  $\beta = \int_{\Omega} e \, y d\Omega$ .

The system of equations governing the one element domain is obtained by making  $I$  stationary with respect to the unknowns  $a, b, c, d, \dots, l$ . This is

$$\begin{bmatrix}
 0 & 0 & 0 & 0 & 0 & 0 & 0 & 0 & 0 & A & 0 & 0 \\
 & 0 & 0 & 0 & 0 & 0 & 0 & 0 & 0 & 0 & 0 & 2A \\
 & & 0 & 0 & 0 & 0 & 0 & 0 & 0 & 2\alpha & 0 & 0 \\
 & & & 0 & 0 & 0 & 0 & 0 & 0 & \beta & 0 & \alpha \\
 & & & & 0 & 0 & 0 & 0 & 0 & 0 & 0 & 2\beta \\
 & & & & & 0 & 0 & 0 & 0 & 0 & A & 0 \\
 & & & & & & 0 & 0 & 0 & 0 & 0 & 2\alpha \\
 & & & & & & & 0 & 0 & 0 & \alpha & \beta \\
 \text{--- symmetric ---} & & & & & & & 0 & 0 & 2\beta & 0 & \text{---} \\
 & & & & & & & & \frac{A}{E} & \frac{\nu A}{E} & 0 & \\
 & & & & & & & & & \frac{A}{E} & 0 & \\
 & & & & & & & & & & \frac{-2(1+\nu)A}{E} & 
 \end{bmatrix}
 \begin{bmatrix}
 a \\
 b \\
 c \\
 d \\
 e \\
 f \\
 g \\
 h \\
 i \\
 j \\
 k \\
 l
 \end{bmatrix}
 = \underline{0}. \quad (6.7)$$

It is observed that the first and the third rows; second, fifth and the seventh rows; and sixth and the ninth rows are the same except for some multiples, while the fourth and the eighth rows are linear combinations of the first and the second rows and the second and the sixth rows, respectively. Therefore only six of the twelve equations in (6.7) are linearly independent. Hence the element matrix has a rank of 6 instead of 12 and therefore is singular. As a consequence  $c, d, e, g, h$  and  $i$  are indeterminate and these are the coefficients of the quadratic terms in the polynomials for  $u$  and  $v$ , equations (6.4).

For a matrix of the form (4.19),

$${}_{(m+n)}\bar{S}_{(m+n)} = \begin{bmatrix} \frac{0}{m \times m} & \frac{a}{m \times n} \\ \frac{a^T}{n \times m} & -\frac{b}{n \times n} \end{bmatrix} \quad (6.8)$$

which is real and symmetric, the eigenvalues are real and because of the indefiniteness of the matrix these can be either positive, zero or negative. Further, if the  $n \times n$  submatrix is positive definite and  $r$  the rank of the matrix  $\underline{S}$ , it is shown in Appendix B that the eigenvalue distribution is of the following type:

- (i)  $m$  positive and  $n$  negative eigenvalues if  $r = m + n$ ;
- (ii)  $(r - n)$  positive,  $(m + n - r)$  zero and  $n$  negative eigenvalues if  $r < m + n$ .

Thus the matrix of equation (6.7) which has  $r = 6$ ,  $m = 9$ ,  $n = 3$ , would yield three positive, six zero and three negative eigenvalues. Also from the functional in equation (6.6) with indeterminate  $c, d, e, g, h$  and  $i$ , for eigenvalues to be zero, the stresses  $j, k$  and  $l$  must be zero. It is, therefore, obvious that with the displacements and stresses of equations (6.4), the element can strain with zero stresses (i.e. forming mechanisms). The non-stressing strain modes arise from the quadratic terms in  $\underline{u}$  and  $\underline{v}$  giving rise to the linear terms in strains, equations (6.5), which are not contained by the assumed stresses. This violates the completeness requirement (i) and it is this violation which leads to mechanisms. Further the number of mechanisms corresponds to the number of terms present in the derived strains, equations (6.5), but which are not included in the strains obtained from the assumed stresses using the constitutive laws.

It was shown in the proof of theorem 4.5.1 that the elimination of stresses from the matrix equation (4.18), i.e.

$$\begin{bmatrix} 0 & \underline{a}^e \\ \underline{a}^{eT} & -\underline{b}^e \end{bmatrix} \begin{bmatrix} \underline{u}^e \\ \underline{\tau}^e \end{bmatrix} = \begin{bmatrix} \underline{p}^e \\ 0 \end{bmatrix} \quad (6.9)$$

gives

$$\underline{a}^e \underline{b}^e{}^{-1} \underline{a}^{eT} \underline{u}^e = \underline{k}^e \underline{u}^e \quad (6.10)$$

where the matrix  $\underline{k}^e$  is identical to the element stiffness matrix one would obtain from the displacement finite element method using the same approximating polynomials for the displacements, provided the assumed displacements and stresses in the mixed method were complete.

In the example considered here, obviously the completeness is violated. However, the static condensation of the matrix equation (6.7) by eliminating stress degrees of freedom  $j, k$  and  $l$  is performed to obtain the following matrix equation:

$$\frac{E}{1-\nu^2} \begin{bmatrix} A & 0 & 2\alpha & \beta & 0 & \nu A & 0 & \nu\alpha & 2\nu\beta \\ (1-\nu)A & 0 & (1-\nu)\alpha & 2(1-\nu)\beta & 0 & 2(1-\nu)\alpha & (1-\nu)\beta & 0 & \\ \frac{4\alpha^2}{A} & \frac{2\alpha\beta}{A} & & 0 & 2\nu\alpha & 0 & \frac{2\nu\alpha^2}{A} & \frac{4\nu\alpha\beta}{A} & \\ \frac{\beta^2}{A} + \frac{(1-\nu)\alpha^2}{2A} & \frac{(1-\nu)\alpha\beta}{A} & \nu\beta & \frac{(1-\nu)\alpha^2}{A} & \frac{(1+\nu)\alpha\beta}{2A} & \frac{2\nu\beta^2}{A} & & & \\ \frac{2(1-\nu)\beta^2}{A} & 0 & \frac{2(1-\nu)\alpha\beta}{A} & \frac{(1-\nu)\beta^2}{A} & 0 & & & & \\ & & A & 0 & \alpha & 2\beta & & & \\ & & \frac{2(1-\nu)\alpha^2}{A} & \frac{(1-\nu)\alpha\beta}{A} & 0 & & & & \\ & & & \frac{\alpha^2}{A} + \frac{(1-\nu)\beta^2}{2A} & \frac{2\alpha\beta}{A} & & & & \\ & & & & \frac{4\beta^2}{A} & & & & \end{bmatrix} \begin{bmatrix} a \\ b \\ c \\ d \\ e \\ f \\ g \\ h \\ i \end{bmatrix} = \underline{0}. \quad (6.11)$$

symmetric

The very same linear dependence of equations is observed in (6.11) as was for (6.7) and again c,d,e,g,h and i are indeterminate. The rank of the 9×9 matrix is 3 instead of 9. Therefore it cannot be the same matrix as one would obtain from the displacement approach using the same approximations for u and v as in equations (6.4), since it is well known that the stiffness matrix is positive definite after the rigid body modes have been eliminated. Now if the quadratic terms in  $\underline{u}$  and  $\underline{v}$  were dropped, then the completeness requirement (i) is satisfied thus resulting in the following non-singular equation with rank 6.

$$\begin{bmatrix} 0 & 0 & 0 & A & 0 & 0 \\ 0 & 0 & 0 & 0 & 0 & 2A \\ 0 & 0 & 0 & 0 & A & 0 \\ A & 0 & 0 & -\frac{A}{E} & \frac{\nu A}{E} & 0 \\ 0 & 0 & A & \frac{\nu A}{E} & -\frac{A}{E} & 0 \\ 0 & 2A & 0 & 0 & 0 & \frac{-2(1+\nu)A}{E} \end{bmatrix} \begin{bmatrix} a \\ b \\ f \\ j \\ k \\ l \end{bmatrix} = \underline{0}. \quad (6.12)$$

The matrix of equation (6.12) would yield three negative and three positive eigenvalues. The static condensation of the matrix by elimination of the stress degrees of freedom j,k and l gives

$$\frac{E}{1-\nu^2} \begin{bmatrix} A & 0 & \nu A \\ 0 & 2(1-\nu)A & 0 \\ \nu A & 0 & A \end{bmatrix} \begin{bmatrix} a \\ b \\ f \end{bmatrix} = \underline{0}. \quad (6.12a)$$

The matrix of equation (6.12a) is exactly the same as the stiffness matrix one would obtain from the displacement approach for constant stress triangles.

To further demonstrate what has been explained so far, various combinations of interpolations for the displacements and the stresses over a triangular and a rectangular element are considered. The typical node

numbering and nodal degrees of freedom for both triangular and rectangular elements are shown in Figures 4 and 5. The derivation of the element matrices is demonstrated in Appendix A. An eigenvalue routine, which uses Householder transformations, is then used to solve the following eigenvalue problem.

$$\begin{bmatrix} S \end{bmatrix} \begin{Bmatrix} \underline{\delta} \\ \underline{\tau} \end{Bmatrix} - \lambda \begin{bmatrix} I \end{bmatrix} \begin{Bmatrix} \underline{\delta} \\ \underline{\tau} \end{Bmatrix} = \underline{0}. \quad (6.13)$$

where  $\underline{\delta}^T = \langle \underline{u}^T \quad \underline{v}^T \rangle$  and  $\underline{\tau}^T = \langle \tau_{xx}^T \quad \tau_{yy}^T \quad \tau_{xy}^T \rangle$  and  $[S] = \begin{bmatrix} 0 & a \\ a^T & b \end{bmatrix}$  as in (6.8), and  $[I]$  is the identity matrix.

The qualitative description of the eigenvalues and the composition of the eigenvectors for all the combinations of interpolations used for the displacements and stresses over a triangular element appears in Table I and that for a rectangular element is listed in Table II. For both triangular and rectangular elements, the number of negative eigenvalues corresponded to the number of stress degrees of freedom, whereas the three zero eigenvalues for the expected rigid body modes are obtained only for the displacement stress combinations which satisfy the completeness requirement (i). In the cases where more than three zero eigenvalues are obtained the number of extra zeroes corresponded to the number of modes present in the strains derived from the assumed displacements that were not contained in the strains from the assumed stresses. The eigenvectors are composed of the same distribution as the assumed approximations for displacements and stresses in all cases except for rigid body modes where  $u$  and  $v$  satisfied  $u_{,x}=0$ ,  $v_{,y}=0$ ,  $u_{,y}+v_{,x}=0$  and stresses were zero.

It is essential for convergence in the energy sense that a mixed finite element formulation conform to the completeness requirements of

section 4.4, and be able to represent rigid body modes and the constant strains (with completeness requirement (i) satisfied and assumed displacements that possess constant strains, it is implied that the corresponding assumed stresses would contain the constant stresses). To include rigid body modes and constant strains in the assumed displacements is a simple matter. However for certain combinations of assumed displacements and stresses, it is not quite obvious that completeness is achieved, especially for incomplete polynomials. For example using biquadratic displacements and bilinear stresses over a rectangular element yields four zero eigenvalues. A scheme to check completeness requirement (i) and trace the terms in the polynomials used for the displacements which correspond to strains not included in the assumed stresses is presented here. The polynomials considered are the ones mentioned in the example above.

The assumed biquadratic displacements  $u$  and  $v$  are

$$\begin{aligned}\bar{u} &= a_1 + a_2x + a_3y + a_4x^2 + a_5xy + a_6y^2 + a_7x^2y + a_8xy^2 \\ \bar{v} &= b_1 + b_2x + b_3y + b_4x^2 + b_5xy + b_6y^2 + b_7x^2y + b_8xy^2\end{aligned}\tag{6.14}$$

and the bilinear stresses are

$$\begin{aligned}\bar{\tau}_{xx} &= c_1 + c_2x + c_3y + c_4xy \\ \bar{\tau}_{yy} &= d_1 + d_2x + d_3y + d_4xy \\ \bar{\tau}_{xy} &= e_1 + e_2x + e_3y + e_4xy.\end{aligned}\tag{6.15}$$

The strains derived from  $\bar{u}$  and  $\bar{v}$  are

$$\epsilon_{xx} = \bar{u}_{,x} = a_2 + 2a_4x + a_5y + 2a_7xy + a_8y^2\tag{6.16a}$$

$$\epsilon_{yy} = \bar{v}_{,y} = b_3 + b_5x + 2b_6y + b_7x^2 + 2b_8xy\tag{6.16b}$$

$$\gamma_{xy} = \bar{u}_{,y} + \bar{v}_{,x} = (a_3 + b_2) + (a_5 + 2b_4)x + (2a_6 + b_5)y + a_7x^2 + 2(a_8 + b_7)xy + b_8y^2.\tag{6.16c}$$

Now using the generalized Hooke's Law for the plane stress problem, the strains corresponding to the assumed stresses in (6.15) are

$$\bar{\epsilon}_{xx} = \frac{1}{E}[\bar{\tau}_{xx} - \nu\bar{\tau}_{yy}] = \frac{1}{E}[(c_1 - \nu d_1) + (c_2 - \nu d_2)x + (c_3 - \nu d_3)y + (c_4 - \nu d_4)xy] \quad (6.17a)$$

$$\bar{\epsilon}_{yy} = \frac{1}{E}[-\nu\bar{\tau}_{xx} + \bar{\tau}_{yy}] = \frac{1}{E}[(d_1 - \nu c_1) + (d_2 - \nu c_2)x + (d_3 - \nu c_3)y + (d_4 - \nu c_4)xy] \quad (6.17b)$$

$$\bar{\gamma}_{xy} = \frac{2(1+\nu)}{E}\bar{\tau}_{xy} = \frac{2(1+\nu)}{E}[e_1 + e_2x + e_3y + e_4xy]. \quad (6.17c)$$

If the displacements were assumed to be a complete polynomial of degree  $p$  and stresses to be a complete polynomial of degree  $(p-1)$ , then completeness would be achieved. However, the polynomials considered here are not complete and comparison of equations (6.16) with (6.17) shows that certain terms in the derived strains are not contained in the corresponding strains from the assumed stresses, i.e.  $a_8y^2$  in (6.16a),  $b_7x^2$  (6.16b),  $a_7x^2$  and  $b_8y^2$  in (6.16c). But  $a_7$  and  $b_8$  as coefficients of the bilinear terms in the derived strains  $\epsilon_{xx}$  and  $\epsilon_{yy}$  match with the coefficients of the bilinear terms in  $\bar{\epsilon}_{xx}$  and  $\bar{\epsilon}_{yy}$  of (6.17), respectively; while  $(a_8 + a_7)$  appearing as coefficient of the bilinear term in the derived shear strain  $\gamma_{xy}$  matches with the coefficient of the bilinear term in  $\bar{\gamma}_{xy}$  of (6.17). Therefore only one of the coefficients  $a_7, a_8, b_7$  and  $b_8$  is indeterminate, hence it leads to only one mechanism besides the three rigid body modes. This is confirmed by the results obtained for biquadratic  $u$  and  $v$  and bilinear stresses over a rectangular element, Table II. For the same combination, the mode shape for the mechanism after elimination of the rigid body modes, is illustrated in Figure 6.

The static condensation by elimination of stresses was performed for all of the combinations of displacements and stresses appearing in Tables I and II. The condensed element matrix is found to be exactly the same as the stiffness matrix one would obtain from the displacement method using identical assumed displacements over an element except for the combinations

where the completeness requirement (i) is violated which possess the same number of mechanisms.

## 6.2 Linear Part of the Navier-Stokes Equations

The basic equations governing the two dimensional, steady, incompressible flow are the well-known Navier-Stokes equations

$$\rho(uu_{,x} + vu_{,y}) + p_{,x} - \mu \nabla^2 u = 0 \quad \text{in } \Omega \quad (6.18)$$

$$\rho(uv_{,x} + vv_{,y}) + p_{,y} - \mu \nabla^2 v = 0 \quad \text{in } \Omega \quad (6.19)$$

$$u_{,x} + v_{,y} = 0 \quad \text{in } \Omega \quad (6.20)$$

where  $u, v$  are the  $x, y$  components of velocity, respectively,  $\rho$  is the fluid density,  $p$ , the pressure,  $\mu$ , the dynamic viscosity, and  $\Omega$  the open domain of the problem. In terms of deviatoric stresses directly, the equations (6.18) and (6.19) can be written as

$$\rho(uu_{,x} + vu_{,y}) + (p_{,x} - \tau_{xx,x} - \tau_{xy,y}) = 0 \quad \text{in } \Omega \quad (6.21)$$

$$\rho(uv_{,x} + vv_{,y}) + (p_{,y} - \tau_{xy,x} - \tau_{yy,y}) = 0 \quad \text{in } \Omega \quad (6.22)$$

where  $\tau_{xx}$  and  $\tau_{yy}$  are the normal deviatoric stresses in the  $x$  and  $y$  directions, respectively; and  $\tau_{xy}$  is the shear stress. The equations relating deviatoric stresses to velocities for a Newtonian fluid are

$$\tau_{xx} = -\frac{2}{3}\mu(u_{,x} + v_{,y}) + 2\mu u_{,x} \quad (6.23)$$

$$\tau_{yy} = -\frac{2}{3}\mu(u_{,x} + v_{,y}) + 2\mu v_{,y} \quad (6.24)$$

$$\tau_{xy} = \mu(u_{,y} + v_{,x}). \quad (6.25)$$

These equations can be put into an alternate form by solving for the velocity gradients as

$$\begin{aligned}
u_{,x} &= \frac{1}{\mu}(\tau_{xx} - \frac{1}{2}\tau_{yy}) & \text{in } \Omega \\
v_{,y} &= \frac{1}{\mu}(-\frac{1}{2}\tau_{xx} + \tau_{yy}) & \text{in } \Omega \\
u_{,y} + v_{,x} &= \frac{1}{\mu}\tau_{xy} & \text{in } \Omega.
\end{aligned} \tag{6.26}$$

Now the equations (6.21), (6.22), (6.20) and (6.26) can be put into the matrix operator form for mixed formulation as

$$\begin{bmatrix}
\rho(u\frac{\partial}{\partial x} + v\frac{\partial}{\partial y}) & 0 & \frac{\partial}{\partial x} & -\frac{\partial}{\partial x} & 0 & -\frac{\partial}{\partial y} \\
0 & \rho(u\frac{\partial}{\partial x} + v\frac{\partial}{\partial y}) & \frac{\partial}{\partial y} & 0 & -\frac{\partial}{\partial y} & -\frac{\partial}{\partial x} \\
\frac{\partial}{\partial x} & \frac{\partial}{\partial y} & 0 & 0 & 0 & 0 \\
\frac{\partial}{\partial x} & 0 & 0 & -\frac{1}{\mu} & \frac{1}{2\mu} & 0 \\
0 & \frac{\partial}{\partial y} & 0 & \frac{1}{2\mu} & -\frac{1}{\mu} & 0 \\
\frac{\partial}{\partial y} & \frac{\partial}{\partial x} & 0 & 0 & 0 & -\frac{1}{\mu}
\end{bmatrix}
\begin{bmatrix}
u \\
v \\
p \\
\tau_{xx} \\
\tau_{yy} \\
\tau_{xy}
\end{bmatrix}
= \underline{0} \quad \text{in } \Omega. \tag{6.27}$$

For steady creeping flow, a special case of incompressible, steady Newtonian flow, the nonlinear part of the matrix operator above, which makes it non-symmetric, can be dropped. Thus the following first order, linear differential equations result and involve a symmetric matrix differential operator

$$\begin{bmatrix}
0 & 0 & \frac{\partial}{\partial x} & -\frac{\partial}{\partial x} & 0 & -\frac{\partial}{\partial y} \\
0 & 0 & \frac{\partial}{\partial y} & 0 & -\frac{\partial}{\partial y} & -\frac{\partial}{\partial x} \\
-\frac{\partial}{\partial x} & -\frac{\partial}{\partial y} & 0 & 0 & 0 & 0 \\
\frac{\partial}{\partial x} & 0 & 0 & -\frac{1}{\mu} & \frac{1}{2\mu} & 0 \\
0 & \frac{\partial}{\partial y} & 0 & \frac{1}{2\mu} & -\frac{1}{\mu} & 0 \\
\frac{\partial}{\partial y} & \frac{\partial}{\partial x} & 0 & 0 & 0 & \frac{1}{\mu}
\end{bmatrix}
\begin{bmatrix}
u \\
v \\
p \\
\tau_{xx} \\
\tau_{yy} \\
\tau_{xy}
\end{bmatrix}
= \underline{0} \quad \text{in } \Omega; \tag{6.28}$$

comprising six equations for six unknowns. Here, in lieu of  $T^*T$  theory

$$T^* = -T^T = \begin{bmatrix} \frac{\partial}{\partial x} & -\frac{\partial}{\partial x} & 0 & -\frac{\partial}{\partial y} \\ \frac{\partial}{\partial y} & 0 & -\frac{\partial}{\partial y} & -\frac{\partial}{\partial x} \end{bmatrix}$$

and for  $\underline{u} = \langle u \ v \rangle^T$  and  $\underline{\tau} = \langle p \ \tau_{xx} \ \tau_{yy} \ \tau_{xy} \rangle^T$ , the analogous form of equations (6.28) to the plane stress elasticity equations (5.10) is

$$\begin{bmatrix} 0 & \underline{T}^* \\ \underline{T} & -\underline{F} \end{bmatrix} \begin{bmatrix} \underline{u} \\ \underline{\tau} \end{bmatrix} = \underline{0} \quad (6.29)$$

$$\text{or} \quad \underline{A}\underline{\Lambda} = \underline{0} \quad (6.29a)$$

where

$$\underline{F} = \begin{bmatrix} 0 & 0 & 0 & 0 \\ 0 & \frac{1}{\mu} & -\frac{1}{2\mu} & 0 \\ 0 & -\frac{1}{2\mu} & \frac{1}{\mu} & 0 \\ 0 & 0 & 0 & \frac{1}{\mu} \end{bmatrix} \quad (6.30)$$

which is a positive semidefinite matrix.

In tensor notation, the equations (6.28) take the form

$$p_{,i} - \tau_{ij,j} = 0; \quad i=j=1,2; \quad \text{in } \Omega \quad (6.31a)$$

$$u_{i,i} = 0; \quad i=1,2; \quad \text{in } \Omega \quad (6.31b)$$

$$\frac{1}{2}(u_{i,j} + u_{j,i}) - C_{ijkl}\tau_{kl} = 0; \quad i=j=k=l=1,2; \quad \text{in } \Omega \quad (6.31c)$$

and can be subjected to some boundary conditions analogous to equations

(5.18);

$$\begin{aligned} u_i &= u_i^0 && \text{on } S_u \\ (-p\delta_{ij} + \tau_{ij})n_j &= T_i^0 && \text{on } S_T \\ (-p\delta_{ij} + \tau_{ij})n_j + \alpha u_i &= C_i^0 && \text{on } S_M \end{aligned} \quad (6.32)$$

where  $S_u + S_T + S_M = S$ , the boundary of domain  $\Omega$ .

The matrix equation (6.28) is similar to matrix equation (6.1) except for pressure  $p$ , the continuity equation as zero divergence of velocities and the deviatoric normal stresses. The mixed variational principle for these equations for homogeneous boundary conditions can be derived as

$$I = \int_{\Omega} [-p(u_{,x} + v_{,y}) + \tau_{xx}u_{,x} + \tau_{yy}v_{,y} + \tau_{xy}(u_{,y} + v_{,x}) - \frac{1}{2\mu}\{\tau_{xx}^2 + \tau_{yy}^2 - \tau_{xx}\tau_{yy} + \tau_{xy}^2\}]d\Omega \quad (6.33)$$

which is also similar to the mixed variational principle for the linear elasticity plane stress problem in (6.2) except for the term  $p(u_{,x} + v_{,y})$  and requires velocities to satisfy the kinematic boundary conditions. The variational principle of (6.33) also gives the three rigid body modes as in (6.3);

$$\begin{aligned} \text{(i)} \quad & u = \text{constant}, v = 0; & \tau_{xx} = \tau_{yy} = \tau_{xy} = 0 \\ \text{(ii)} \quad & u = 0, v = \text{constant}; & \tau_{xx} = \tau_{yy} = \tau_{xy} = 0 \\ \text{(iii)} \quad & u = -cy; v = cx; & \tau_{xx} = \tau_{yy} = \tau_{xy} = 0 \end{aligned} \quad (6.34)$$

while pressure can be arbitrary, since the incompressibility leads to the divergence of  $u$  and  $v$  to be zero rather than be proportional to pressure.

If the finite element approximations for the variables involved in (6.33) are chosen over an element domain  $\Omega^e$  as

$$\bar{u} = \sum_{i=1}^m \phi_i \bar{u}_i \quad (6.35a)$$

$$\bar{v} = \sum_{i=1}^m \phi_i \bar{v}_i$$

$$\bar{p} = \sum_{i=1}^l \phi_i \bar{p}_i \quad (6.35b)$$

$$\begin{aligned}
 \bar{\tau}_{xx} &= \sum_{i=1}^n \psi_i \bar{\tau}_{xxi} \\
 \bar{\tau}_{yy} &= \sum_{i=1}^n \psi_i \bar{\tau}_{yyi} \\
 \bar{\tau}_{xy} &= \sum_{i=1}^n \psi_i \bar{\tau}_{xyi}.
 \end{aligned} \tag{6.35c}$$

Then the substitution into the functional I of (6.33) and setting its first variation  $\delta I$  to zero for stationarity yields the following matrix equation:

$$\begin{bmatrix}
 \underline{0} & \underline{0} & \underline{e} & \underline{a} & \underline{0} & \underline{b} \\
 \underline{0} & \underline{0} & \underline{f} & \underline{0} & \underline{b} & \underline{a} \\
 \underline{e}^T & \underline{f}^T & \underline{0} & \underline{0} & \underline{0} & \underline{0} \\
 \underline{a}^T & \underline{0} & \underline{0} & -\frac{1}{\mu} \underline{d} & \frac{1}{2\mu} \underline{d} & \underline{0} \\
 \underline{0} & \underline{b}^T & \underline{0} & \frac{1}{2\mu} \underline{d} & -\frac{1}{\mu} \underline{d} & \underline{0} \\
 \underline{b}^T & \underline{a}^T & \underline{0} & \underline{0} & \underline{0} & -\frac{1}{\mu} \underline{d}
 \end{bmatrix}
 \begin{bmatrix}
 \underline{u} \\
 \underline{v} \\
 \underline{p} \\
 \underline{\tau}_{xx} \\
 \underline{\tau}_{yy} \\
 \underline{\tau}_{xy}
 \end{bmatrix}
 = \underline{0}. \tag{6.36}$$

Here  $\underline{u} = \langle u_1 \ u_2 \ \dots \ u_m \rangle^T$ ,  $\underline{v} = \langle v_1 \ v_2 \ \dots \ v_m \rangle^T$ ,  $\underline{p} = \langle p_1 \ p_2 \ \dots \ p_I \rangle^T$ ,  $\underline{\tau}_{xx} = \langle \tau_{xx1} \ \tau_{xx2} \ \dots \ \tau_{xxn} \rangle^T$ , etc., are the linear vectors of nodal degrees of freedom. The submatrices  $\underline{a}, \underline{b}, \underline{d}, \underline{e}$  and  $\underline{f}$  are obtained in the following manner:

$$\begin{aligned}
 a_{ij} &= \int_{\Omega} e \phi_{i,x} \psi_j d\Omega^e & i=1,2, \dots, m; \\
 b_{ij} &= \int_{\Omega} e \phi_{i,y} \psi_j d\Omega^e & j=1,2, \dots, n. \\
 d_{ij} &= \int_{\Omega} e \psi_i \psi_j d\Omega^e & i,j=1,2, \dots, n. \\
 e_{ij} &= -\int_{\Omega} e \phi_{i,x} \xi_j d\Omega^e & i=1,2, \dots, m; \\
 f_{ij} &= -\int_{\Omega} e \phi_{i,y} \xi_j d\Omega^e & j=1,2, \dots, 1.
 \end{aligned} \tag{6.37}$$

Note that the matrix  $\underline{d}$  is symmetric and positive definite.

The matrix of equation (6.36) is symmetric, therefore the eigenvalues of the matrix are real. Further, it is indefinite and if the rank of the matrix is  $(2m+1+3n)$ , then from Appendix B it has  $2m$  positive and  $(1+3n)$  negative eigenvalues. The choice of polynomials for  $u, v, \tau_{xx}, \tau_{yy}$  and  $\tau_{xy}$  still has to comply with the same completeness requirements set out in the previous section. However the requirements on the pressure field are dubious because it is not related to the strains. The obvious question that arises here is: what are the completeness requirements on  $p$ ? Further it is not possible to ask for mean convergence of pressure to the volumetric strain as was done for the stresses in the plane stress linear elasticity problem because of the incompressibility constraint.

In the finite element application to the Navier-Stokes equations (6.18) to (6.20) using the primitive dependent variables  $u, v$  and  $p$ , a similar situation was faced by Taylor and Hood [34] and Olson and Tuann [26]. One of the possible variational principles for the linear part of these equations used in the reference [26] is

$$J(u, v, p) = \int_{\Omega} \left[ \frac{1}{\text{Re}} \{ u_{,x}^2 + v_{,y}^2 + \frac{1}{2} (u_{,y} + v_{,x})^2 \} - p(u_{,x} + v_{,y}) \right] d\Omega - \int_{S_{\tau}} (\bar{X}u + \bar{Y}v) ds \quad (6.38)$$

where  $(\bar{X}, \bar{Y})$  are the specified traction on the boundary  $S_{\tau}$ . The term  $\int_{\Omega} p(u_{,x} + v_{,y}) d\Omega$  appears in both variational principles, I of (6.33) and  $J(u, v, p)$  of (6.38). Therefore the requirement that the pressure interpolation should be one degree less than those for the velocity components, as found by Olson and Tuann [26], is also expected here and indeed confirmed by the numerical results. A different explanation for such a requirement is presented here.

Since the divergence of  $u$  and  $v$  in equation (6.20) is zero, it acts as a constraint equation. If the approximations used for  $u$  and  $v$  involve complete polynomials of degree  $m$ , then  $u_{,x}$  and  $v_{,y}$  would involve complete polynomials of degree  $(m-1)$ . Therefore the unknowns corresponding to the  $(m-1)$  complete polynomial for  $u_{,x}$  must be related to the unknowns corresponding to  $(m-1)$  complete polynomial for  $v_{,y}$  in order to satisfy continuity in the discrete sense. Assuming that  $u, v, \tau_{xx}, \tau_{yy}$  and  $\tau_{xy}$  have been chosen properly, i.e. do not yield any mechanisms except for the rigid body modes, then the discretized continuity equations

$$\begin{bmatrix} \underline{e}^T & \underline{f}^T \end{bmatrix} \begin{Bmatrix} \underline{u} \\ \underline{v} \end{Bmatrix} = \underline{0} \quad (6.39)$$

should have a rank not less than  ${}^{m+1}C_2$ , i.e. combinations of  $(m+1)$  taken 2 at a time. However in the finite element formulation, equation (6.36), the number of discretized continuity equations is associated with the number of degrees of freedom for pressure thus limiting it to  ${}^{m+1}C_2$ . As a consequence, the pressure should have degrees of freedom not more than  ${}^{m+1}C_2$ , which implies a complete polynomial of degree not higher than  $(m-1)$ .

Consider the following schematic representation of the complete polynomials for  $u, v$  and  $p$ .

Velocity $u$				
1	Constant	$a_1$		
$x \quad y$	Linear	$a_2 \quad a_3$		
$x^2 \quad xy \quad y^2$	Quadratic	$a_4 \quad a_5 \quad a_6$		
$x^3 \quad x^2y \quad xy^2 \quad y^3$	Cubic	$a_7 \quad a_8 \quad a_9 \quad a_{10}$		
$x^4 \quad x^3y \quad x^2y^2 \quad xy^3 \quad y^4$	Quartic	$a_{11} \quad a_{12} \quad a_{13} \quad a_{14} \quad a_{15}$		
etc.	etc.	etc.		

(a)

Thus if the  $a_i$ 's are the coefficients of the polynomial for  $u$ , the complete quadratic for  $u$  can be written as

$$u = a_1 + a_2x + a_3y + a_4x^2 + a_5xy + a_6y^2. \quad (6.40)$$

Replacing  $a_i$ 's by  $b_i$ 's in scheme (a) for  $v$ ; the complete quadratic for  $v$  is

$$v = b_1 + b_2x + b_3y + b_4x^2 + b_5xy + b_6y^2. \quad (6.41)$$

Similarly for pressure  $p$ ;

$$p = c_1 + c_2x + c_3y + c_4x^2 + c_5xy + c_6y^2. \quad (6.42)$$

The partial derivatives  $u_{,x}$  and  $v_{,y}$  can also be written schematically as complete polynomials,

$\begin{array}{c} 0 \\ 1 \quad 0 \\ x \quad y \quad 0 \\ x^2 \quad xy \quad y^2 \quad 0 \\ x^3 \quad x^2y \quad xy^2 \quad y^3 \quad 0 \\ \text{etc.} \end{array}$	$\begin{array}{c} u_{,x} \\ \text{Constant} \\ \text{Linear} \\ \text{Quadratic} \\ \text{Cubic} \\ \text{etc.} \end{array}$	$\begin{array}{c} a_1 \\ a_2 \quad a_3 \\ 2a_4 \quad a_5 \quad a_6 \\ 3a_7 \quad 2a_8 \quad a_9 \quad a_{10} \\ 4a_{11} \quad 3a_{12} \quad 2a_{13} \quad a_{14} \quad a_{15} \\ \text{etc.} \end{array}$	(b)
--	--	---	-----

$\begin{array}{c} 0 \\ 0 \quad 1 \\ 0 \quad x \quad y \\ 0 \quad x^2 \quad xy \quad y^2 \\ 0 \quad x^3 \quad x^2y \quad xy^2 \quad y^3 \\ \text{etc.} \end{array}$	$\begin{array}{c} v_{,y} \\ \text{Constant} \\ \text{Linear} \\ \text{Quadratic} \\ \text{Cubic} \\ \text{etc.} \end{array}$	$\begin{array}{c} b_1 \\ b_2 \quad b_3 \\ b_4 \quad b_5 \quad 2b_6 \\ b_7 \quad b_8 \quad 2b_9 \quad 3b_{10} \\ b_{11} \quad b_{12} \quad 2b_{13} \quad 3b_{14} \quad 4b_{15} \\ \text{etc.} \end{array}$	(c)
--	--	---	-----

Consider only the non-zero terms to obtain  $u_{,x} + v_{,y}$  as

$\begin{array}{c} 1 \\ x \quad y \\ x^2 \quad xy \quad y^2 \\ x^3 \quad x^2y \quad xy^2 \quad y^3 \\ \text{etc.} \end{array}$	$\begin{array}{c} (u_{,x} + v_{,y}) \\ \text{Constant} \\ \text{Linear} \\ \text{Quadratic} \\ \text{Cubic} \\ \text{etc.} \end{array}$	$\begin{array}{c} (a_2 + b_3) \\ (2a_4 + b_5) \quad (a_5 + 2b_6) \\ (3a_7 + b_8) \quad (2a_8 + 2b_9) \quad (a_9 + 3b_{10}) \\ (4a_{11} + b_{12}) \quad (3a_{12} + 2b_{13}) \quad (2a_{13} + 3b_{14}) \quad (a_{14} + 4b_{15}) \\ \text{etc.} \end{array}$	(d)
---	---	---	-----

and p;

		Pressure p	
1	Constant	$c_1$	
x y	Linear	$c_2$	$c_3$
$x^2$ xy $y^2$	Quadratic	$c_4$	$c_5$ $c_6$
$x^3$ $x^2y$ $xy^2$ $y^3$	Cubic	$c_7$ $c_8$ $c_9$	$c_{10}$
$x^4$ $x^3y$ $x^2y^2$ $xy^3$ $y^4$	Quartic	$c_{11}$ $c_{12}$ $c_{13}$ $c_{14}$	$c_{15}$
etc.	etc.	etc.	

(e)

The discretized continuity equations can now be obtained over the domain in the following manner:

$$\frac{\partial}{\partial c_i} \int_{\Omega^e} p(u, x + v, y) d\Omega^e = 0. \quad (6.43)$$

Let

$$\alpha_{ij} = \int_{\Omega^e} x^i y^j d\Omega^e; \quad i, j = 0, 1, 2, 3, \dots$$

then from schemes (d) and (e) the following matrix form for the discretized continuity equations is obtained;

$$\begin{bmatrix} \alpha_{00} & 2\alpha_{10} & \alpha_{01} & 3\alpha_{20} & 2\alpha_{11} & \alpha_{02} & \dots & \alpha_{00} & \alpha_{10} & 2\alpha_{01} & \alpha_{20} & 2\alpha_{11} & 3\alpha_{02} & \dots \\ \alpha_{10} & 2\alpha_{20} & \alpha_{11} & 3\alpha_{30} & 2\alpha_{21} & \alpha_{12} & \dots & \alpha_{10} & \alpha_{20} & 2\alpha_{11} & \alpha_{30} & 2\alpha_{21} & 3\alpha_{12} & \dots \\ \alpha_{01} & 2\alpha_{11} & \alpha_{02} & 3\alpha_{21} & 2\alpha_{12} & \alpha_{03} & \dots & \alpha_{01} & \alpha_{11} & 2\alpha_{02} & \alpha_{21} & 2\alpha_{12} & 3\alpha_{03} & \dots \\ \alpha_{20} & 2\alpha_{30} & \alpha_{21} & 3\alpha_{40} & 2\alpha_{31} & \alpha_{22} & \dots & \alpha_{20} & \alpha_{30} & 2\alpha_{21} & \alpha_{40} & 2\alpha_{31} & 3\alpha_{22} & \dots \\ \alpha_{11} & 2\alpha_{21} & \alpha_{12} & 3\alpha_{31} & 2\alpha_{22} & \alpha_{13} & \dots & \alpha_{11} & \alpha_{21} & 2\alpha_{12} & \alpha_{31} & 2\alpha_{22} & 3\alpha_{13} & \dots \\ \alpha_{02} & 2\alpha_{12} & \alpha_{03} & 3\alpha_{22} & 2\alpha_{13} & \alpha_{04} & \dots & \alpha_{02} & \alpha_{12} & 2\alpha_{03} & \alpha_{22} & 2\alpha_{13} & 3\alpha_{04} & \dots \\ \alpha_{30} & 2\alpha_{40} & \alpha_{31} & 3\alpha_{50} & 2\alpha_{41} & \alpha_{32} & \dots & \alpha_{30} & \alpha_{40} & 2\alpha_{31} & \alpha_{50} & 2\alpha_{41} & 3\alpha_{32} & \dots \\ \alpha_{21} & 2\alpha_{31} & \alpha_{22} & 3\alpha_{41} & 2\alpha_{32} & \alpha_{23} & \dots & \alpha_{21} & \alpha_{31} & 2\alpha_{22} & \alpha_{41} & 2\alpha_{32} & 3\alpha_{23} & \dots \\ \alpha_{12} & 2\alpha_{22} & \alpha_{13} & 3\alpha_{32} & 2\alpha_{23} & \alpha_{14} & \dots & \alpha_{12} & \alpha_{22} & 2\alpha_{13} & \alpha_{32} & 2\alpha_{23} & 3\alpha_{14} & \dots \\ \alpha_{03} & 2\alpha_{13} & \alpha_{04} & 3\alpha_{23} & 2\alpha_{14} & \alpha_{05} & \dots & \alpha_{03} & \alpha_{13} & 2\alpha_{04} & \alpha_{23} & 2\alpha_{14} & 3\alpha_{05} & \dots \\ \vdots & \vdots & \vdots & \vdots & \vdots & \vdots & \vdots & \vdots & \vdots & \vdots & \vdots & \vdots & \vdots & \vdots \\ \vdots & \vdots & \vdots & \vdots & \vdots & \vdots & \vdots & \vdots & \vdots & \vdots & \vdots & \vdots & \vdots & \vdots \end{bmatrix} \begin{bmatrix} a_2 \\ a_4 \\ a_5 \\ a_7 \\ a_8 \\ a_9 \\ \vdots \\ b_3 \\ b_5 \\ b_6 \\ b_8 \\ b_9 \\ b_{10} \\ \vdots \end{bmatrix} = \underline{0}. \quad (6.44)$$

(N×2Q)

Here  $N = \binom{n+2}{2} C_2$ , where  $n$  is the degree of complete polynomial for  $p$ ;  $Q = \binom{m+1}{2} C_2$ ,  $m$  being the degree of polynomials used for velocities  $u$  and  $v$ ; e.g. for  $u$  and  $v$  cubic,  $m=3$  and  $Q=6$ . It can be observed that every  $(Q+j)^{\text{th}}$  column is either equal to or a simple multiple of the  $j^{\text{th}}$  column. Therefore the rank of the matrix of coefficients in (6.44) is at most  $Q$ . Further the rank of the matrix is still  $Q$  even if  $N$  is greater than  $Q$ . Thus for  $N$  greater than  $Q$ , all the discretized continuity equations of (6.44) are not independent.

Now consider the case where  $u, v$  and  $p$  are complete quadratics, i.e.  $m=n=2$  and  $Q=3$ ,  $N=6$ . The resulting discretized incompressibility constraints are

$$\begin{bmatrix} \alpha_{00} & 2\alpha_{10} & \alpha_{01} & \alpha_{00} & \alpha_{10} & 2\alpha_{01} \\ \alpha_{10} & 2\alpha_{20} & \alpha_{11} & \alpha_{10} & \alpha_{20} & 2\alpha_{11} \\ \alpha_{01} & 2\alpha_{11} & \alpha_{02} & \alpha_{01} & \alpha_{11} & 2\alpha_{02} \\ \alpha_{20} & 2\alpha_{30} & \alpha_{21} & \alpha_{20} & \alpha_{30} & 2\alpha_{21} \\ \alpha_{11} & 2\alpha_{21} & \alpha_{12} & \alpha_{11} & \alpha_{21} & 2\alpha_{12} \\ \alpha_{02} & 2\alpha_{12} & \alpha_{03} & \alpha_{02} & \alpha_{12} & 2\alpha_{03} \end{bmatrix} \begin{bmatrix} a_2 \\ a_4 \\ a_5 \\ b_3 \\ b_5 \\ b_6 \end{bmatrix} = \underline{0}. \quad (6.45)$$

Clearly the rank of the matrix of coefficients in (6.45) is 3. Therefore three of the constraints in (6.45) are not independent.

The corresponding contribution from  $\int_{\Omega} p(u_x + v_y) d\Omega$  to the equilibrium equations is

$$\begin{bmatrix} \alpha_{00} & \alpha_{10} & \alpha_{01} & \alpha_{20} & \alpha_{11} & \alpha_{02} \\ 2\alpha_{10} & 2\alpha_{20} & 2\alpha_{11} & 2\alpha_{30} & 2\alpha_{21} & 2\alpha_{12} \\ \alpha_{01} & \alpha_{11} & \alpha_{02} & \alpha_{21} & \alpha_{12} & \alpha_{03} \\ \alpha_{00} & \alpha_{10} & \alpha_{01} & \alpha_{20} & \alpha_{11} & \alpha_{02} \\ \alpha_{10} & \alpha_{20} & \alpha_{11} & \alpha_{30} & \alpha_{21} & \alpha_{12} \\ 2\alpha_{01} & 2\alpha_{11} & 2\alpha_{02} & 2\alpha_{21} & 2\alpha_{12} & 2\alpha_{03} \end{bmatrix} \begin{bmatrix} c_1 \\ c_2 \\ c_3 \\ c_4 \\ c_5 \\ c_6 \end{bmatrix} = \underline{\underline{ac.}} \quad (6.46)$$

where the matrix of coefficients is simply the transpose of the matrix in (6.45). This is the equivalent of

$$\begin{bmatrix} \underline{e} \\ \underline{f} \end{bmatrix} \{ \underline{p} \}$$

part of the equilibrium equations in (6.36). In general,  $\underline{\alpha c}$  cannot be equal to zero, i.e. pressure cannot be in equilibrium by itself. Therefore

$$\underline{\alpha c} = 0 \quad (6.47)$$

should not have any non-zero solutions. This can be possible if the rank of matrix  $\underline{\alpha}$  is the same as the degrees of freedom  $c_i$ 's, i.e. 6 in the example considered. But the rank of  $\underline{\alpha}$  is obviously 3, thus leading to indeterminate  $c_i$ 's which causes a self-equilibrating pressure field and non-unique solutions. However, this situation can be avoided if the rank of the matrix  $\underline{\alpha}$  is equal to the number of constraints. This is possible if the pressure distribution is taken as linear for quadratic distributions in  $u$  and  $v$ . The equations (6.45) and (6.46) then reduce to

$$\begin{bmatrix} \alpha_{00} & 2\alpha_{10} & \alpha_{01} & \alpha_{00} & \alpha_{10} & 2\alpha_{01} \\ \alpha_{10} & 2\alpha_{20} & \alpha_{11} & \alpha_{10} & \alpha_{20} & 2\alpha_{11} \\ \alpha_{01} & 2\alpha_{11} & \alpha_{02} & \alpha_{01} & \alpha_{11} & 2\alpha_{02} \end{bmatrix} \begin{bmatrix} a_2 \\ a_4 \\ a_5 \\ b_3 \\ b_5 \\ b_6 \end{bmatrix} = \underline{0}, \quad (6.48)$$

and

$$\begin{bmatrix} \alpha_{00} & \alpha_{10} & \alpha_{01} \\ 2\alpha_{10} & 2\alpha_{20} & 2\alpha_{11} \\ \alpha_{01} & \alpha_{11} & \alpha_{02} \\ \alpha_{00} & \alpha_{10} & \alpha_{01} \\ \alpha_{10} & \alpha_{20} & \alpha_{11} \\ 2\alpha_{01} & 2\alpha_{11} & 2\alpha_{02} \end{bmatrix} \begin{bmatrix} c_1 \\ c_2 \\ c_3 \end{bmatrix} = \underline{\alpha c}, \quad (6.49)$$

respectively.

It can now be concluded that in general  $N$  should not be greater than  $Q$  in equation (6.44) to avoid self-equilibrating systems in pressure and is equivalent to saying that the degree of interpolating polynomial for pressure should not be larger than  $(m-1)$  where  $m$  is the degree of complete polynomials used for the velocity components  $u$  and  $v$ .

The pressure on the boundary is incorporated as a natural boundary condition in the functional of (6.33). However, inspection of equations (6.31) reveals that pressure needs to be fixed at some point in the domain  $\Omega$  as adatum. If the approximating polynomial in the finite element formulation fails to comply with the requirement concluded above, then to avoid self-equilibrating systems, the pressure needs to be specified at more than one point on the boundary depending on the number of self-equilibrating modes present. At the same time the completeness requirement (i) for mean convergence of the stresses to velocities should not be overlooked. Therefore a consistent formulation of the element matrix would have only three rigid body modes, as in equations (6.34).

Various combinations of interpolations for the velocities, pressure and stresses ( $u, v, p, \tau_{xx}, \tau_{yy}$  and  $\tau_{xy}$ ) over a triangular and a rectangular element (Figures 4 and 5, expect for addition of pressure degree of freedom at the nodes) are considered. The following eigenvalue problem is then solved:

$$\begin{bmatrix} \underline{0} & \underline{\alpha} & \underline{\beta} \\ \underline{\alpha}^T & \underline{0} & \underline{0} \\ \underline{\beta}^T & \underline{0} & -\underline{b} \end{bmatrix} \begin{bmatrix} \underline{\delta} \\ \underline{p} \\ \underline{\tau} \end{bmatrix} - \lambda \begin{bmatrix} \underline{I}_{\delta} & \underline{0} & \underline{0} \\ \underline{0} & \underline{I}_p & \underline{0} \\ \underline{0} & \underline{0} & \underline{I}_{\tau} \end{bmatrix} \begin{bmatrix} \underline{\delta} \\ \underline{p} \\ \underline{\tau} \end{bmatrix} = 0 \quad (6.50)$$

$(2m+1+3n) \times (2m+1+3n)$ 
 $(2m+1+3n) \times (2m+1+3n)$

$$\text{where } \underline{\underline{\delta}}_{1 \times 2m}^T = \langle \underline{u}^T \quad \underline{v}^T \rangle, \quad \underline{\underline{\tau}}_{1 \times 3n}^T = \langle \underline{\tau}_{xx}^T \quad \underline{\tau}_{yy}^T \quad \underline{\tau}_{xy}^T \rangle,$$

$$\underline{\underline{\beta}}_{2m \times 3n} = \begin{bmatrix} \underline{a} & \underline{0} & \underline{b} \\ \underline{0} & \underline{b} & \underline{a} \end{bmatrix}, \quad \underline{\underline{\alpha}}_{2m \times 1} = \begin{bmatrix} \underline{e} \\ \underline{f} \end{bmatrix} \quad \text{and} \quad \underline{\underline{b}}_{3n \times 3n} = \frac{1}{\mu} \begin{bmatrix} \underline{d} & -\frac{1}{2}\underline{d} & \underline{0} \\ -\frac{1}{2}\underline{d} & \underline{d} & \underline{0} \\ \underline{0} & \underline{0} & \underline{d} \end{bmatrix}.$$

The submatrices  $\underline{a}, \underline{b}, \underline{d}, \underline{e}, \underline{f}$ , and the sub-column vectors are the same as in the matrix equation (6.36) whose derivation is similar to that of plane stress problem (Appendix A), where as  $\underline{I}_{2m \times 2m}$ ,  $\underline{U}_{1 \times 1}$  and  $\underline{I}_{3n \times 3n}$  are the identity matrices. It was mentioned earlier in this section that if the rank of this matrix is  $(2m+1+3n)$ , then it has  $2m$  positive and  $(1+3n)$  negative eigenvalues. If there are  $q$  rigid body modes and  $r$  mechanisms which correspond to zero eigenvalues, and since these correspond to indeterminacies of the  $u$  and  $v$  degrees of freedom ( $2m$ ), then only  $(2m-q-r)$  eigenvalues are positive. Similarly, if there are  $p$  indeterminacies of pressure degrees of freedom ( $1$ ), then  $(1+3n-p)$  eigenvalues are negative.

The distribution of negative, zero and positive eigenvalues and the composition of eigenvectors for different combinations of interpolations for  $u, v, p$  and the stresses  $\tau$ 's are presented in Tables III and IV for a triangular and a rectangular element, respectively. It can be observed that the combinations of interpolations which do not comply with the requirements on pressure and stresses resulted in more than three eigenvalues required for rigid body modes. The self-equilibrating modes in pressure are obtained when the pressure interpolation polynomial is of the same degree as the polynomials for  $u$  and  $v$  and with the exception of linear  $u, v, p, \tau_{xx}, \tau_{yy}$  and  $\tau_{xy}$  over a triangular element, have the same distribution as the interpolation polynomial while  $u, v$  and the  $\tau$ 's are zero. The mechanisms are obtained when  $u, v$  are quadratic and  $\tau$ 's constant over a triangular element;  $u, v$  biquadratic,  $\tau$ 's bilinear over a rectangular element, as in the plane stress

problem of the previous section. In addition self-equilibrating pressure modes result when the pressure is quadratic for the triangular element. Again, when the rigid body modes are eliminated, the mechanisms seem to possess the same distribution for  $u$  and  $v$  as the assumed interpolations while pressure and the stresses are zero.

In recognizing the rigid body modes of equations (6.34), the pressure was said to be arbitrary. However, the eigenvectors for zero eigenvalues associated with the rigid body modes and mechanisms displayed zero pressure in the element. This can be explained by splitting the eigenvalue problem of equation (6.50) in the following manner:

$$-\lambda \underline{I}_{\delta} \underline{\delta} + \underline{\alpha} p + \underline{\beta} \underline{\tau} = 0 \quad (6.51a)$$

$$\underline{\alpha}^T \underline{\delta} - \lambda \underline{I}_p p = 0 \quad (6.51b)$$

$$\underline{\beta}^T \underline{\delta} - [\underline{b} + \lambda \underline{I}_{\tau}] = 0. \quad (6.51c)$$

Now the rigid body modes consist of  $u=a-cy$  and  $v=b+cy$ , therefore it is clear that  $\underline{\alpha}^T \underline{\delta}$  and  $\underline{\beta}^T \underline{\delta}$  are zero since these involve derivatives  $u_{,x}$ ,  $v_{,y}$  and  $(u_{,y}+v_{,x})$ . The stresses are zero from (6.34), hence from equation (6.51a)

$$\underline{\alpha} p = 0. \quad (6.52)$$

If the rank of  $\underline{\alpha}$  is equal to the number of constraints, i.e. the degrees of freedom in pressure, then the equation (6.52) is only true if  $p=0$ . Therefore pressure is zero everywhere in the domain. Hence the equations (6.34) for rigid body modes are modified here

$$\begin{aligned} \text{(i)} \quad & u = \text{Constant}, v = 0; & p = \tau_{xx} = \tau_{yy} = \tau_{xy} = 0 \\ \text{(ii)} \quad & u = 0, v = \text{constant}; & p = \tau_{xx} = \tau_{yy} = \tau_{xy} = 0 \\ \text{(iii)} \quad & u = cy, v = cx; & p = \tau_{xx} = \tau_{yy} = \tau_{xy} = 0. \end{aligned} \quad (6.53)$$

Thus a consistent formulation should not have more than three zero eigenvalues for the rigid modes of equations (6.53). Finally static condensation

of the matrix equation (6.36) by eliminating the stresses, for the cases where no mechanisms are present, gives exactly the same matrix equation as one would obtain from the functional of (6.38) using the same  $u, v$  and  $p$  interpolation polynomials. In fact, the results of the eigenvalue analysis for such cases are very similar to those presented by Olson and Tuann [25].

In concluding this chapter it should be pointed out that for certain combinations of approximate displacements and stresses (which indeed comply with the completeness requirement (i) and exhibit proper eigenvalues and eigenvectors over one element domain) the assembled element matrices according to certain continuity requirements yield self-equilibrating modes over the full domain. The typical example is that of plane linear elasticity with quadratic displacements, linear stresses over a triangular element and both continuous across the interelement boundaries. In this case, the boundary integrals on the common boundaries amongst adjacent elements cancel each other. Thus the element matrices for the elements, which do not have edges coinciding with the boundary of the problem domain, can be formulated without extracting the boundary integrals from the energy product. Then the contribution to the energy product from the integrals like  $\int_{\Omega^e} u_i \tau_{ij,j} d\Omega^e$  is zero for the degrees of freedom at the vertex nodes. Thus zero rows and columns are obtained for displacement degrees of freedom at all internal vertices of the triangular elements when the element matrices are assembled. This then gives self-equilibrating modes over the full domain. To check the existence of such modes, the element matrices for a certain formulation can be assembled so that there is at least one internal vertex node for the triangular elements and a corner node for the quadrilateral elements, and then an eigenvalue-eigenvector analysis performed on the resulting matrix.

## CHAPTER 7

### APPLICATIONS OF THE MIXED FINITE ELEMENT METHOD

The applications of the mixed finite element method to beam bending, plane linear elasticity and the problems with stress concentrations and singularities are presented in this chapter. The strain energy convergence rates for various formulations are predicted and compared with the numerical results obtained from the finite element analysis. The energy convergence of the mixed finite element method for plane elasticity with stress singularities, established in section 4.6, is also demonstrated with a numerical example. Finally the stress intensity factor  $K_I$  for plates with symmetric edge cracks and a central crack are calculated and compared with the nearly exact values available.

#### 7.1 Beam Problem

Using the nomenclature of Figure 7, the following four first order field differential equations for simple beam theory result:

$$-\frac{dV}{dx} - q = 0 \quad (7.1)$$

$$-\frac{dM}{dx} - V = 0 \quad (7.2)$$

$$\frac{d\theta}{dx} - \frac{M}{EI} = 0 \quad (7.3)$$

$$\frac{dv}{dx} - \theta = 0 \quad (7.4)$$

where (7.1) and (7.2) are the equilibrium equations (7.3) is the constitutive relationship ( $E$ =Young's Modulus,  $I$ =moment of inertia) and (7.4) is the constraint equation arising from the assumption of plane sections remaining plane after deformation. If equations (7.2) and (7.4) are satisfied exactly,  $V$  and  $\theta$  in equations (7.1) and (7.3) can be eliminated and two second order equations are obtained

$$\frac{d^2 M}{dx^2} - q = 0 \quad (7.5)$$

$$\frac{d^2 v}{dx^2} - \frac{M}{EI} = 0. \quad (7.6)$$

The mixed method is applied to both systems, namely the four first order equations (7.1) to (7.4) and the two second order equations (7.5) and (7.6).

### 7.1.A Two Second Order Equations

The equations (7.5) and (7.6) can be put into the matrix form as

$$\begin{bmatrix} 0 & D^2 \\ D^2 & -\frac{1}{EI} \end{bmatrix} \begin{bmatrix} v \\ M \end{bmatrix} = \begin{bmatrix} q \\ 0 \end{bmatrix} \quad (7.7)$$

or  $\underline{\underline{A}} \underline{\underline{\Lambda}} = \underline{\underline{f}} \quad (7.7a)$

where  $D = \frac{d}{dx}$ .

Here the matrix operator  $\underline{\underline{A}}$  is symmetric, i.e.  $(\underline{\underline{A}}\underline{\underline{\Lambda}}, \underline{\underline{\Lambda}}) = (\underline{\underline{\Lambda}}, \underline{\underline{A}}\underline{\underline{\Lambda}})$ ,

and the energy product is given by

$$(\underline{\underline{A}}\underline{\underline{\Lambda}}, \underline{\underline{\Lambda}}) = \int_{x_1}^{x_2} [M''v + v''M - \frac{M^2}{EI}] dx. \quad (7.8)$$

Integration of the first and the second term by parts yields

$$(\underline{\underline{A}}\underline{\underline{\Lambda}}, \underline{\underline{\Lambda}}) = M'v \Big|_{x_1}^{x_2} + v'M \Big|_{x_1}^{x_2} - \int_{x_1}^{x_2} [2M'v' + \frac{M^2}{EI}] dx. \quad (7.9)$$

The mixed variational principle can now be expressed as

$$I_M = - \int_{x_1}^{x_2} [2M'v' + \frac{M^2}{EI} - 2qv] dx. \quad (7.10)$$

It can be observed from (7.10) that the continuity requirement has been reduced by one order compared to the Potential Energy approach with the variational form as

$$I_D = \int_{x_1}^{x_2} [EIv''^2 - 2qv] dx. \quad (7.11)$$

This allows one to use lower order polynomials for approximating  $v$  and  $M$ .

For a stationary point, the first variation of  $I_M$  in (7.10) is zero

$$\delta I_M = -\int_{x_1}^{x_2} [2M'\delta v' + 2v'\delta M' + \frac{2M}{EI}\delta M - 2q\delta v]dx = 0.$$

Again integration of the first and the second term on the right hand side yields

$$\delta I_M = \int_{x_1}^{x_2} 2(M''-q)\delta v dx + \int_{x_1}^{x_2} 2(v'' - \frac{M}{EI})\delta M dx - M'\delta v \Big|_{x_1}^{x_2} - v'\delta M \Big|_{x_1}^{x_2} = 0. \quad (7.12)$$

This indicates that the forced boundary conditions are implied on the variables  $v$  and  $M$  which are different from  $v$  and  $v'$ , one would find from the variational principle in equation (7.11) (ordinary Potential Energy Theorem). The two boundary terms in (7.9) could have also been obtained by twice integrating by parts the first term in (7.8) giving a variational principle of the form

$$J_M = \int_{x_1}^{x_2} [2v''M - \frac{M^2}{EI} - 2qv]dx \quad (7.13)$$

which involves a second derivative  $v$ , thereby requiring the same continuity requirement on  $v$  as the potential energy approach. It can be shown that the forced boundary conditions for the mixed variational principle  $J_M$  in (7.13) are implied on  $v$  and  $v'$ . Thus the mixed method offers flexibility not just in incorporating the boundary conditions as mentioned in Chapter 5, but also in continuity requirements when dealing with higher order operators.

The mixed variational principle in (7.10) should be distinguished from the one in (7.13) in that the latter follows from the energy product in symmetric form as defined in equation (3.73). As it is advantageous to have reduced continuity requirements in finite element analysis for problems involving higher order operators, e.g. (7.7), the boundary terms have to be extracted from both the equilibrium (7.5) and the constitutive (7.6) equations. The effect of such a formulation on the convergence is considered.

In the simple beam bending theory the stress, which is the bending

moment  $M$ , is proportional to the curvature, the second derivative of displacement, equation (7.6). In order to obtain improved convergence in the strain energy the approximations for  $M$  and  $v$  have to comply with the requirement for mean square convergence of  $M$  to  $v''$ , so that the error in strain energy can be estimated from equation (3.71). This can be rewritten as

$$[\underline{\Lambda} - \underline{\Lambda}_0, \underline{\Lambda} - \underline{\Lambda}_0] = (\bar{M} - M_0, \bar{M} - M_0) \quad (7.14)$$

for two second order beam equations. Here  $M_0 = EIV''$  is the exact bending moment distribution,  $\bar{M}$ , the finite element approximation, and  $v_0$ , the exact solution for the deflection  $v$ . Let the approximations for  $v$  and  $M$  be

$$\begin{aligned} \bar{v} &= \sum_{i=1}^M \phi_i v_i \\ \bar{M} &= \sum_{j=1}^N \psi_j M_j, \end{aligned} \quad (7.15)$$

where  $\phi_i$  and  $\psi_j \in H_{\underline{\Lambda}}^W = \tilde{V} \times \tilde{M}$ , the cross product space ( $\phi_i \in \tilde{V}$ ,  $\psi_j \in \tilde{M}$ ).

The substitution of (7.15) into (3.68) gives

$$\|\bar{v}'' - \frac{\bar{M}}{EI}\|^2 = (\bar{v}'', \bar{v}'') - 2(\bar{v}'', \frac{\bar{M}}{EI}) + (\frac{\bar{M}}{EI}, \frac{\bar{M}}{EI})$$

and minimization with respect to  $M_j$  yields

$$\sum_{j=1}^N (\psi_i, \psi_j) M_j = \sum_{j=1}^M (\psi_i, \phi_j'') v_j, \quad i=1, 2, \dots, N. \quad (7.16)$$

However, the mixed variational principle in (7.10) gives the following equation at extremum instead of (7.16), i.e.

$$\sum_{j=1}^N (\psi_i, \psi_j) M_j = - \sum_{j=1}^N (\psi_i', \phi_j') v_j, \quad i=1, 2, \dots, N. \quad (7.17)$$

The right sides of (7.16) and (7.17) imply that

$$(\psi_i, \bar{v}'') = - (\psi_i', \bar{v}'), \quad (7.17a)$$

which means that the derivative of  $\bar{v}'$ , which is  $\bar{v}''$ , is taken as a generalized derivative. This is because  $\bar{v}'$  is only required to be piecewise continuous and therefore would not possess an ordinary derivative everywhere.

As was done in Chapter 6, inspection of the functional  $I_M$  in (7.10), for  $g=0$ , reveals that the element matrix should have the following rigid body mode

$$v = \text{constant}, M = 0.$$

After trying out different polynomials for  $v$  and  $M$ , it is found that the interpolations should be of the same degree in order to achieve the only rigid body mode as mentioned above. Such approximations also meet the requirement (i) of completeness. If the boundary conditions are homogeneous equations (7.16) and (7.17) are equivalent and the error in the energy product can be estimated from (7.14).

A beam of uniform cross section with constant stiffness  $EI$ , length  $l$  is subjected to constant load per unit length  $q$ . The following four cases of boundary conditions are considered, Figure 8:

- (1) simply supported beam (S.S);  $v(0)=M(0)=v(l)=M(l)=0$ .
- (2) cantilever;  $v(0)=M(l)=0$ .
- (3) both ends clamped (fixed-fixed);  $v(0)=v(l)=0$ .
- (4) one end clamped and the other in a vertical guide (fixed-guided);  
 $v(0)=0$ . (Tangent to the elastic curve at vertical guide remains horizontal).

Three different combinations for approximating  $v$  and  $M$  within the element are chosen

- (i)  $v$ -linear,  $M$ -linear;
- (ii)  $v$ -quadratic,  $M$ -quadratic;
- (iii)  $v$ -cubic,  $M$ -cubic.

The nodes per element and the number of degrees of freedom per node for the combinations (i), (ii) and (iii) are shown in Figure 9. The derivation of the element matrices in all three cases is analogous to that of plane stress problem presented in Appendix A. In each case the beam is divided into

elements of equal length,  $l_e$ .

The following quantities, where necessary, are tabulated for presentation purposes:

$\delta$  = deflection (v);

$\theta$  = rotation (v');

M = moment;

V = shear (M');

U = strain energy.

The subscript M stands for middle, Q for quarter point, E for end, RE for right hand end, and LE for left hand end.

#### (i) v-linear, M-linear

The results are shown in Table V and the plots of quantities of interest versus the number of elements to show convergence appear in Figures 10. Linear approximations for v and M provide the continuity of v and M across the nodes and do not violate the completeness requirement (i). Since the second derivative of linear approximation for v vanishes, equation (7.16) is satisfied only in a generalized sense, i.e. equation (7.17). For linear approximations within the element, the error in both v and M can be shown to be  $O(l_e^2)$  and  $O(l_e^4)$  in  $\|\bar{M}\|^2$ , where  $l_e$  is the element length ( $l_e = \frac{1}{N}$ ). From Figure 10(a), the relative error in strain energy converges as  $N^{-2}$  for the simply supported and cantilever configurations (cases 1 and 2, respectively), from below in case 1 (Table V(a)) and from above in case 2 (Table V(b)); and  $N^{-4}$  from below for the fixed-fixed and fixed-guided ones (cases 3 and 4, respectively) (Tables V(c) and V(d)). The expected rate of strain energy convergence is obtained when the moments are not forced to be zero (not as the forced homogeneous boundary condition on stress). Perhaps, for the cases when the bending moment is forced to be zero on the boundary, some lower

order error terms prevail. Figure 10(b) illustrates the monotonic convergence of mid-point deflection  $\delta_M$  for the simply supported beam from below and tip deflection  $\delta_E$  for the cantilever from above, whereas the relative error converges as  $N^{-2}$ , Figure 10(c). The bending moments at the nodes are exact for both cases 1 and 2. However, the reverse is true for the other two cases, as can be observed from Tables V(c) and V(d). The computed deflections at the nodes are exact, whereas the relative error in the fixed moment converges as  $N^{-2}$ , as illustrated in Figure 10(d). The other quantities, appearing in Tables V, seem to converge with increasing number of elements  $N$  for all four cases.

#### (ii) v-quadratic, M-quadratic

With  $v$  and  $M$  both quadratic, the completeness requirements for the energy convergence are satisfied since the variables  $v$  and  $M$  are continuous across the nodes and have piecewise continuous first and second derivatives. The errors in  $v$  and  $M$  can be shown to be  $O(l_e^3)$  which leads to an error of  $O(l_e^6)$  in  $\|\bar{M}\|^2$ . However, a quadratic approximation for  $\bar{M}$  is capable of representing the exact solution  $M_0$  for the constant load  $q$  along the beam length. Therefore the strain energy from the finite element solution is expected to be exact. This is confirmed by the results in Tables VI for all four cases. Also the moments and the derived shears obtained are exact. It is interesting to note that the mid-deflections  $\delta_M$ , in all four cases, for an even number of elements obtained are exact and the relative error for an odd number of elements along the beam length converges as  $N^{-4}$ , Figure 11; while the end computed deflection  $\delta_{RE}$  for cases 2 and 4 are exact for odd and even number of elements. When a faster convergence is observed for the displacement, the relative error in the derived rotation, in all four cases appears to converge as  $N^{-2}$ , Figure 11. Tables VI also indicate convergence

of other nodal variables.

### (iii) v-cubic, M-cubic

With cubic approximations, both M and v and their first derivatives are continuous. Here again, the completeness requirements are satisfied and like the previous approximations (ii) the strain energy is expected to be exact as well as the moments and the shears. The numerical results presented in Tables VII confirm this. The end deflections in the cases 2 and 4 are also exact. However, the relative error in the mid-deflection  $\delta_M$  converges as  $N^{-4}$  and in rotations as  $N^{-3}$  for all four cases; Figure 12.

### 7.1.B Four First Order Equations

The four first order beam equations (7.1) to (7.4) can be put into the matrix form as

$$\begin{bmatrix} 0 & 0 & 0 & -D \\ 0 & 0 & -D & -1 \\ 0 & D & -\frac{1}{EI} & 0 \\ D & -1 & 0 & 0 \end{bmatrix} \begin{bmatrix} v \\ \theta \\ M \\ V \end{bmatrix} = \begin{bmatrix} q \\ 0 \\ 0 \\ 0 \end{bmatrix} \quad (7.18)$$

$$\text{or} \quad \underline{\underline{A}} \underline{\underline{\Lambda}} = \underline{\underline{f}} \quad (7.18a)$$

where the matrix operator  $\underline{\underline{A}}$  is symmetric, i.e.  $(\underline{\underline{A}}\underline{\underline{\Lambda}}, \underline{\underline{\Lambda}}) = (\underline{\underline{\Lambda}}, \underline{\underline{A}}\underline{\underline{\Lambda}})$ .

The energy product is given by

$$(\underline{\underline{A}}\underline{\underline{\Lambda}}, \underline{\underline{\Lambda}}) = \int_1 [-\frac{dV}{dx}v - \frac{dM}{dx}\theta - 2v\theta + \frac{d\theta}{dx}M - \frac{M^2}{EI} + \frac{dv}{dx}V] dx. \quad (7.19)$$

Integrating by parts the first and the fourth terms on the right hand side gives

$$\begin{aligned} (\underline{\underline{A}}\underline{\underline{\Lambda}}, \underline{\underline{\Lambda}}) &= -Vv \Big|_{x_1}^{x_2} + \theta M \Big|_{x_1}^{x_2} + \int_1 [2V\frac{dv}{dx} - 2\frac{dM}{dx}\theta - 2v\theta - \frac{M^2}{EI}] dx \\ &= -Vv \Big|_{x_1}^{x_2} + \theta M \Big|_{x_1}^{x_2} + [\underline{\underline{\Lambda}}, \underline{\underline{\Lambda}}]_A. \end{aligned} \quad (7.20)$$

Here  $[\underline{\Lambda}, \underline{\Lambda}]_A$  is the modified energy product of equation (3.73);

$$[\underline{\Lambda}, \underline{\Lambda}]_A = \int_I \left[ 2V \frac{dv}{dx} - 2 \frac{dM}{dx} \theta - 2v\theta - \frac{M^2}{EI} \right] dx. \quad (7.20a)$$

The equation (7.20a) then leads to the mixed variational principle for the equations (7.18)

$$I_M = \int_I \left[ 2V \frac{dv}{dx} - 2 \frac{dM}{dx} \theta - 2V\theta - \frac{M^2}{EI} - 2qv \right] dx \quad (7.21)$$

with forced boundary conditions on  $v$  and  $M$ . The mixed Galerkin Method (by adding boundary residuals to the residuals of equations (7.1) and (7.3), section 5.4) and the mixed variational principle (7.21) would yield the same element matrix since the problem is linear and self-adjoint. Appendix C shows that the linear elasticity equation (5.9) yields the same energy product (7.19) as equations (7.18) when the basic assumptions of the simple beam bending theory are incorporated and the shear strain energy term, involving  $V^2$ , is neglected. Therefore the error in the energy product can be predicted from equation (3.71) provided approximations for the displacements  $(v, \theta)$  and stresses  $(M, V)$  are complete.

Linear approximations are chosen for  $v, \theta, M$  and  $V$ . The element nodes and the nodal degrees of freedom are the same as illustrated in Figure 9, combination (iii). Further, the approximations chosen are complete and the error in the energy product is governed by the mean square error in  $M$ , i.e. error in  $\|\bar{M}\|^2$ , which is  $O(l_e^4)$  for the linear  $M$  distribution. Again four cases of boundary conditions (Figure 8) are considered. The results obtained from the finite element analysis are tabulated in Table VIII and convergence plots are shown in Figures 13. It is observed from Figure 13(a) that the relative error in strain energy converges as  $N^{-4}$  for all four cases. Moments and shears at the nodes in cases 1 and 2 for both even and odd number of elements  $N$  are exact. However for cases 3 and 4, shears

are exact for both even and odd  $N$  but only end moments are exact for  $N$  even and they converge as  $N^{-4}$  for  $N$  odd in case 3. From Figure 13(b), the relative error in rotation  $\theta$  converges as  $N^{-2}$  in all cases. Deflections  $\delta_{RE}$  at the free end for  $N$  even in case 2 and the guided end for  $N$  odd and even in case 4 are exact, converging as  $N^{-4}$  for odd  $N$  in case 2; whereas the mid-deflections  $\delta_M$  appear to converge to the exact value in an oscillatory manner.

It has been mentioned in Chapters 3 and 5 and section 7.1.A that the mixed methods allow flexibility in incorporating the boundary conditions. If the first and the second terms on the right hand side of equation (7.19) are integrated by parts, the following mixed variational principle results:

$$I_M = \int_1 [2V \frac{dv}{dx} + 2M \frac{d\theta}{dx} - 2v\theta - \frac{M^2}{EI} - 2qv] dx \quad (7.22)$$

with forced boundary conditions on  $v$  and  $\theta$ , the same as for the Potential Energy Theorem. Again linear  $v, \theta, M$  and  $V$  are used. Since the completeness requirements are not altered by shifting the forced boundary condition from  $M$  to  $\theta$ , the convergence of strain energy is still expected to be  $N^{-4}$ . The strain energy for cases 1, 2 and 3 is computed and tabulated in Table IX. The relative error in strain energy versus  $N$  is then plotted in Figure 14 and in all cases the strain energy is found to converge as  $N^{-4}$ .

Next the shear strain energy term  $V^2$  is also included and the mixed variational principle of (7.22) now includes an additional term (Appendix C)

$$I_M = \int [2V \frac{dv}{dx} + 2M \frac{d\theta}{dx} - 2v\theta - \frac{M^2}{EI} - \frac{(1+\nu)}{5EI} h^2 V^2 - 2qv] dx \quad (7.23)$$

where  $\nu$  is poisson's ratio and  $h$  the height of the beam. Again the forced boundary conditions are on the variables  $v$  and  $\theta$ . Using the same linear

approximations for  $v, \theta, M$  and  $V$  within an element, which still complies with the completeness requirements, cases 1, 2 and 3 are analysed and the results appear in Tables X. In the analysis,  $\nu$  is taken as 0.25 and  $h$  as  $\frac{1}{2}$ . The relative error in strain energy converges as  $N^{-4}$  in all three cases as shown in Figure 15(a). The shear  $V$ , in cases 1 and 3, is exact and converges as  $N^{-2}$  for the cantilever, case 2; the relative errors in the mid-moment for case 1, the fixed moment for case 2 and the end moments for case 3 converge as  $N^{-2}$ ; the mid-deflection  $\delta_M$  for cases 1 and 3 converges as  $N^{-2}$  while the free end deflection  $\delta_{RE}$  of the cantilever converges as  $N^{-4}$  as shown in Figures 15. However, the end rotation  $\theta$  for the cases 1 and 2 is exact for  $N$  even (Tables X) and from Figure 15(b) it appears to converge as  $N^{-4}$  for  $N$  odd in case 2.

Despite the several different convergence rates observed for basic variables  $v, \theta, M$  and  $V$  for the three different formulations considered above, the relative error in the strain energy in all cases converges as  $N^{-4}$ . Further, where the boundary integrals were taken out from the equilibrium equations, i.e. forced boundary conditions on  $v$  and  $\theta$ , the strain energy converges from below. Alternately it is from above in the case where the forced boundary conditions are on the displacement  $v$  and the moment  $M$ .

## 7.2 Plane Linear Elasticity

The stress and the displacement are chosen to be linear within a three node triangular element with five degrees of freedom per node (Figure 4) and are forced to be continuous across the interelement boundaries by equating the nodal variables at common nodes. These approximations satisfy the completeness requirements.

The derivation of the element matrix and the consistent load vector arising either from body forces or nonhomogeneous stress boundary conditions are given in Appendix A. The finite element thus formulated is then applied to solve the following problems.

#### 7.2.A Plane Stress: Square Plate with Parabolically Varying End Loads

A square plate with parabolically varying end loads is shown in Figure 16. Since the problem is symmetric about the  $x$  and  $y$  axes, only a quarter of the plate ABCD is considered in the finite element analysis with the forced boundary conditions  $u=0$  on AD and  $v=0$  on AB.

Since the displacements  $u$ ,  $v$  and the stresses  $\tau_{xx}$ ,  $\tau_{yy}$  and  $\tau_{xy}$  are assumed linear, the error in the stresses is  $O(l_e^2)$ , where  $l_e$  is the largest diameter within the element. Further, since such approximations satisfy the completeness requirements, and displacements and stresses are continuous across the interelement boundaries, equation (3.71) holds and error in the strain energy is expected to be the mean square error in the stresses, i.e.  $O(l_e^4)$ , which is  $O(N^{-4})$  for a uniform grid, Figure 16.

The numerical results for some of the stresses and displacements at points A,B,C, and D and the strain energy from the mixed finite element analysis for various grids are presented in Table XI. Also presented in Table XI are the results from the displacement element, obtained by Cowper, Lindberg and Olson [5], (using full cubics for  $u$  and  $v$  displacements over a triangular element with six degrees of freedom  $(u, u_x, u_y, v, v_x, v_y)$  at vertices and two  $(u,v)$  at the centroid) for comparison. Since no attempt is made to satisfy the stress boundary conditions, the correct values of stresses on the boundary are obtained only in the limit of  $N \rightarrow \infty$ .

The convergence plots for the mixed element are shown in Figures 17

and those for the displacement element in Figure 18, [5]. The energy convergence rate for the former appears to be very close to  $N^{-4}$  (Figure 17(a)) as predicted. Although the error in strain energy from the displacement element is much smaller than from the mixed, owing to the fact that the former is a much more refined element, the energy convergence rate is slightly less than  $N^{-5}$ , Figure 18, which is lower than the predicted asymptotic rate of  $N^{-6}$ . The other interesting observation about the energy convergence for the mixed finite element is the convergence from below when the forced boundary conditions are on the displacement variables which has also been observed in section 7.1.B.

The convergence rate for the stresses from the mixed element, Figure 17(c), appears to be close to  $N^{-2}$  for  $N$  larger than 8. However, peculiar kinks are observed and can be associated with the fact that certain stresses were fortuitously close to their exact values for a certain grid; e.g.  $N_{yyB}$  for  $N=6$ , etc. Figure 17(b) shows the convergence of displacements indicating faster convergence for  $u_c$  and  $v_c$  (close to  $N^{-4}$ ) than  $u_B$  and  $v_D$  (close to  $N^{-2}$ ). This is also observed for the displacement element and  $N$  greater than 6, Figure 18. In the mixed element, the kinks are observed in the convergence plots for the displacement  $u_B$  at  $N=6$  and  $v_c$  at  $N=6$  and  $N=10$ , which can be associated with slightly larger errors for such grids.

### 7.2.B Cantilever (Plane Stress)

The dimensions, loading and the material properties are detailed in Figure 19(a). Two types of boundary conditions are considered at the fixed end as indicated in Figures 19(b) and 19(c); B.C.1 and B.C.2. The latter is used for comparison purposes since the solutions using various finite elements for B.C.2 are available in the literature, while the former is considered to investigate the energy convergence.

(a) Cantilever with Boundary Conditions B.C.1

In an effort to investigate the energy convergence, the exact value of strain energy is necessary. Besides such boundary conditions being easily incorporated in the finite element analysis, it is also possible to obtain an elasticity plane stress solution under the assumption of bilinear normal stress in the x-direction and the shear stress independent of x and quadratic in y. The solutions for the displacements u and v along with the strain energy for the boundary conditions B.C.1 are presented in Appendix D.

Since the part of the boundary between A and F, and E and F can move in either direction and if the stresses on the left face were not included in the finite element analysis through a consistent load vector, a stress-free boundary will be simulated. This violates the assumptions of the elasticity solution which shall put in doubt the validity of the exact strain energy to be used in the error analysis. Therefore the stresses on the left end are included in the consistent load vector.

The typical mesh used in the analysis is shown in Figure 22 and the numerical results are presented in Table XII. The results indicate that the stress  $\tau_{xx}$  at  $x=12$  inches and  $y=-6$  inches, and the tip deflection are converging to the exact values in an oscillatory manner. However, the strain energy is converging to the correct value from below. The convergence plots are shown in Figures 20. In Figure 20(a), the plot of relative error in strain energy versus N the number of elements in the beam depth, the inclusion of  $N=6$  leads to a kink in the plot. Note the grid for  $N=6$  does not contain the previous grids for  $N=2$  and  $N=4$ , and excluding this the energy appears to converge as  $N^{-4}$  as predicted. The same behaviour is also observed in Figure 20(c) for the relative error in the stress  $\tau_{xx}$  versus N for  $N>4$  (close to  $N^{-2}$  without  $N=6$ ). This is not surprising since the error in strain energy is governed by the mean square error in the stresses. It is gratifying

that the energy convergence rate is about double that for stress as predicted. Figure 20(b) does not indicate any definite convergence rate for the tip deflection  $\delta$  and perhaps, more data is required to establish any trend of convergence.

#### (b) Cantilever with Boundary Conditions B.C.2

Unfortunately the exact solution for the boundary conditions B.C.2 is not available and hence the exact strain energy is not known. The problem is solved to compare with the solutions obtained by using different displacement finite elements for various grids. These are readily available in literature, e.g. Gallagher [9]. Here the boundary AE (Figures 19) is prevented from moving in either direction and leads to stress singularities at corners A and E. Furthermore the shear stress and normal stress distributions at the fixed boundary are not the same as assumed in the beam theory. However the results are compared with the beam theory [35] which provides an upper bound for the tip deflection from the displacement finite element.

The numerical results from the mixed finite element analysis for various grids (Figure 22) are tabulated in Table XIII. Again the stress  $\tau_{xx}$  at  $x=12$  inches and  $y=-6$  inches, and the tip deflection appear to converge in an oscillatory manner. The strain energy for  $N=8$  is slightly higher than the strain energy  $1/2P\delta$  obtained from the beam theory whereas in the previous examples, when the boundary integrals were extracted from the equilibrium equations, the energy converged from below. Since the exact numerical value is not known, the convergence of strain energy is rather difficult to establish.

Table XIV shows the comparison of numerical results from the mixed finite element with those from the displacement models, e.g. constant stress triangle (C.S.T.), linear stress triangle (L.S.T.) and quadratic stress

triangle (Q.S.T.) elements, for the various grids shown in Figures 21. The mixed finite element used here appears to perform slightly poorer than the L.S.T., which uses quadratic approximations for the displacements and much better than the C.S.T., using linear displacements. The Figures 23(a) and 23(c) also indicate fast convergence of the tip deflection with increasing degrees of freedom and  $N$ , the number of elements in the beam depth, respectively, relative to the other elements. The graph of strain energy versus  $N$  shown in Figure 23(b) also shows rapid convergence. Finally the relative error in tip deflection is plotted against  $N$  for the mixed finite element and other displacement finite elements in Figure 24. It appears as in case (a) that more data is required to establish the convergence rate. However the plot does exhibit fast convergence. It should be noted that the tip deflection from beam theory is used as exact solution in plotting these curves, and it is in error itself.

### 7.2.C Stress Concentration around a Circular Hole (Plane Strain)

A square plate (plane strain) with a circular hole in the middle (Figures 25) loaded by a uniform uniaxial stress  $\tau_0$  is considered. The diameter of the hole is one eighth of the plate width and the plate is of unit thickness. The plane strain state is analysed for both isotropic and orthotropic cases. It is demonstrated in Appendix A, how the element matrix for a plane stress isotropic case is modified for plane strain isotropic and orthotropic cases. The procedure is much simpler than for a displacement finite element. Because of symmetry only a quarter of the problem is considered. The grid and the boundary conditions used in the finite element analysis are shown in Figure 26. This is essentially the same as used by Zienkiewicz, Cheung and Stagg [42] for constant stress triangular elements.

A comparison between the analytical solutions (for the isotropic case, Timoshenko and Goodier [35], and the orthotropic case, Savin [31]) for an infinite plate with a circular hole in the middle ( $\tau_{xx}$  along edge BC and  $\tau_{yy}$  along edge AE) and the solutions obtained from the mixed finite element analysis is shown in Figure 27. A similar comparison with the solutions from the constant stress triangles [42] are shown in Figure 28. The mixed finite element solution shows excellent agreement with the analytical solution, and further the stresses are obtained directly at the nodes. The constant stress triangles also show good agreement with the exact solution, but the stresses are computed by averaging at nodes from the neighbouring elements, assuming the constant stress within the element to be the stress level at the node. Further the concentrations occurring at the boundaries are obtained by extrapolation.

### 7.3 Stress Singularities

The strain energy convergence for plane stress elasticity with stress singularities, established in section 4.6.A, is demonstrated by a numerical example. The stress intensity factor  $K_I$  is then determined from the method described in section 4.6.B for rectangular plates with symmetric edge cracks and a central crack (mode type I, Figure 1).

#### 7.3.A Strain Energy Convergence

The problem of a square plate with symmetric edge cracks (mode type I) is considered. Figure 29(a) shows the problem description and Figure 29(b) illustrates the finite element idealization of the quarter of the plate considered because of the symmetry about the x and y axes. The problem is solved using mixed finite elements for various grid sizes for two cases. The stress  $\tau_{yy}$  is kept continuous across point D (the crack tip) in the first case and

in the second case, an extra node is introduced along the x-axis next to the original one at D and only  $u, v, \tau_{xx}$  and  $\tau_{xy}$  degrees of freedom are equated at the two nodes, thus allowing  $\tau_{yy}$  to be discontinuous across point D, the crack tip. (See distributions in Figure 32).

The numerical results for both cases are presented in Tables XV. The strain energy is converging from below in both cases, while the peak stress  $\tau_{yyD}$  at the crack tip is about 28 percent higher when the normal stress is discontinuous across the point D, than for the case when it is continuous. The plots of strain energy versus the mesh size appear in Figures 30. The shape of the curves in both cases are very similar and they exhibit faster convergence than just linear as might have been expected. Figure 30(a) shows a comparison with the solutions obtained using various other elements. The present mixed element definitely shows a faster strain energy convergence than the constant stress triangles, the linear stress triangles, and the hybrid stress rectangles with cubic stress distribution within the element and quadratic displacements along the boundaries. The convergence rate is indicated by the plot of the relative error in strain energy (exact  $U = 3.228 \frac{\tau^2 L^2}{Et}$ , Tong and Pian [38]) versus  $N$ , the number of elements along the edge OA, Figure 31. It can be observed that the convergence rate approaches  $N^{-2}$  as  $N$  gets larger, for both cases. It is clearly faster than  $N^{-1}$  indicating the cancellation of the errors in the energy product of equation (4.84) due to stress singular terms. Further, a slightly larger error is observed in the case of discontinuous normal stress at the crack tip. Finally the normal stress  $\tau_{yy}$  is plotted along the edge OA in Figures 32. In both cases, a small zone of compression is observed on the stress free edge of the crack with a peak value of about  $\tau_0$  (the applied stress on edge BC) close to the crack tip.

### 7.3.B Evaluation of the Stress Intensity Factor $K_I$

Two plane strain problems, rectangular plates one with symmetric edge cracks and the other with a central crack are considered. The details for these are shown in Figures 33 and the finite element idealization in Figure 34. The layout of the mesh, used in both problems, is analogous to the one used by Parks [27] with the exception that the present elements are triangular. Also indicated in Figure 34 are the ratios of the radii  $\gamma_{\Gamma_0}$  to the crack length  $a$  (0, 0.1, 0.2 and 0.5). These are then used to calculate the potential energy release rate for a crack extension of  $\Delta a$  in the finite element analysis as described in section 4.6.B. Because of symmetry about the  $x$  and  $y$  axes, only a quarter of the problem is considered in each case and this is shown in Figures 33 as shaded areas along with the respective boundary conditions.

Although, it is sufficient to solve each problem once for the initial crack length  $a$  (section 4.6.B), at present the finite element analysis is performed every time when the contour  $\Gamma_0$  is translated along with the interior nodes by the amount  $\Delta a = 5 \times 10^{-6}a$  in the  $x$ -direction. The potential energy release rate, in the discretized form can be expressed as

$$G_I = - \frac{\Delta \pi_M}{\Delta a} \quad (7.55)$$

and

$$\Delta \pi_M = \pi_{M_{\Gamma_0}} - \pi_{M_0}$$

where  $\pi_{M_0}$  is the potential energy associated with the initial crack and  $\pi_{M_{\Gamma_0}}$  when the crack tip has been moved by the amount  $\Delta a$ . Then the crack intensity factor is calculated by

$$K_I = \sqrt{\frac{E}{1-\nu^2} \left( - \frac{\Delta \pi_M}{\Delta a} \right)}. \quad (7.56)$$

The numerical results for the plate with symmetric edge cracks are listed in Table XVI and those for the plate with a central crack in Table VII. The crack intensity factor for the former is compared with the nearly exact  $K_I$  obtained by Bowie [2] and for the latter, with  $K_I$  by Bowie and Neal [3]. In both cases the results obtained are in excellent agreement with the references. It is seen that the least percentage error is obtained for the contour  $\Gamma_0$  with radius  $\gamma_{\Gamma_0}=0.1a$ , and the worst for  $\gamma_{\Gamma_0}=0$ , i.e. only the crack tip node is translated. The former is also associated with the highest potential energy release rate which varies for different sets of nodes defining  $\Gamma_0$ .

When the calculated value of  $G_I$  or J-integral is in fact independent of the particular set of nodes defining  $\Gamma_0$ , the mesh may be called optimal. Thus, it suffices, for optimal meshes, to move only the exterior node defining the crack tip, thereby altering the boundary, regardless of the particular set of interior nodes comprising the contour  $\Gamma_0$ . Alternatively, non-optimal meshes will exhibit some path dependence in the calculated values of  $G_I$ . In such cases, personal judgement and experience can help determine the best value of  $G_I$ .

In Table XVIII, a comparison with stress intensity factors obtained from the energy release rate by other authors is presented. It can be seen that excellent accuracy is obtained with much fewer mixed finite elements and degrees of freedom than the corresponding displacement models. Finally the plots of normal stress on the cracked face OA (Figures 33) are shown in Figures 35. Note that a higher peak stress is obtained at the crack tip than the peak stress indicated in Figure 32(a), probably because of the refined mesh near the crack tip.

## CHAPTER 8

### CONCLUSIONS

A detailed investigation of the theoretical foundation and practical aspects of applying mixed methods of approximate analysis for continuum and finite element analysis has been presented.

Mixed methods always involve indefinite operators and consequently a new energy product and its associated energy norm had to be introduced for these special operators. The fields of definition of such operators were so restricted that when obeyed, the energy product was found to be positive definite and represented twice the strain energy.

These new concepts then formed the bases for establishing the energy convergence of complete approximations for displacements and stresses. It was found that the energy convergence implied the mean square convergence of such approximations to the exact values.

The completeness requirements for continuum analysis were defined in two steps: (i) the mean square convergence of the strains from the approximate stresses to the strains derived from the approximate displacements; (ii) convergence of the energy norm. The alternate form of the requirement (i) is as follows: *The strains from the stress approximations should possess at least all the strain modes that are present in the strains derived from the displacement approximations.* It was also concluded that a violation of this requirement leads to mechanisms and this was confirmed by the eigenvalue-eigenvector analysis of an element matrix. The presence of mechanisms also indicates the breakdown of positive definiteness of the energy product, hence requirement (i) is the prerequisite of (ii). The error in the energy product was shown to be proportional to the mean square error in the stress approximation when completeness is satisfied. This leads to much faster convergence in the

strain energy calculated from the mixed method than obtainable from the corresponding displacement method, i.e. the latter with identical displacement approximations as used in the mixed method.

The foregoing concepts for the continuum were then extended to the finite element method and the corresponding completeness criteria were established. These were found to be as follows:

- a) the displacement approximations should include all rigid body and constant strain modes;
- b) the stress approximations should include all constant stress modes;
- c) the same as requirement (i) for the continuum, i.e. all the displacement strain modes should be included in the stress (strain) approximations.

It was also concluded that for complete approximations the strain energy convergence cannot be any faster than for that calculated from the corresponding displacement model, unless the stresses are made continuous across the interelement boundaries.

In the example of beam bending with four first order equations the use of linear interpolations for the four basic variables resulted in a predicted mean square error in stresses of  $O(N^{-4})$ . Therefore the predicted error in strain energy was also of  $O(N^{-4})$  and this was confirmed by the numerical examples.

The plane stress triangular element using linear interpolations for both displacements and stresses yielded a predicted error in stresses of  $O(N^{-2})$ , and a mean square error and strain energy error of  $O(N^{-4})$ . In the numerical applications of this element, the energy convergence rate was indeed found to be  $O(N^{-4})$  for the plane stress square plate with parabolic end loads and nearly the same for the plane stress cantilever. In comparison the corresponding displacement element (C.S.T.) yields a convergence rate of only  $O(N^{-2})$ . A faster energy convergence rate (nearly  $O(N^{-2})$ ) was also

observed for the plane stress square plate with symmetric edge cracks for which the strain energy converges only linearly with  $N$ , even with higher order displacement or hybrid-type finite elements, Tong and Pian [38].

Excellent accuracy was also obtained for the stresses around a circular hole in the middle of a square plate subjected to uniaxial compression for plane strain isotropic and orthotropic cases. Finally the crack intensity factors ( $K_I$ ) computed for plane strain rectangular plates, one with symmetric edge cracks and the other with a central crack, yielded errors of only 1.97% and 0.89%, respectively.

The matrix equations to be solved in the mixed finite element analysis are always indefinite and have zeroes on the diagonals for the displacement degrees of freedom. The method of Gaussian elimination with partial pivoting was successfully employed to solve such equations. Hence it is concluded that the indefinite nature of the mixed method equations presents no special difficulties.

In general, methods involving indefinite operators preclude obtaining upper or lower bounds on energy. In the applications of the mixed finite element method discussed herein, the energy was observed to converge in some cases from above and in some from below. However, in the examples where the variational principle was formed by extracting the boundary integrals from the equilibrium equations, the strain energy always converged from below.

In the examples solved, far more accurate results were obtained by using the mixed finite element method than the corresponding displacement method with the same displacement approximations. However, the mixed method required more degrees of freedom for the same number of elements. On the other hand, the results for the stress concentration and stress singular problems were generally more accurate even using fewer elements (and total

number of degrees of freedom) than for the displacement models. Hence it seems fair to conclude that the mixed finite element method can produce more efficient solutions for problems involving stress concentrations or singularities.

# BIBLIOGRAPHY

1. Anderson, G.P., Ruggles, V.L., and Stibor, G., "Use of Finite Element Computer Programs in Fracture Mechanics", *International Journal of Fracture Mechanics*, Vol. 7, No. 1, 1971, pp. 63-76.
2. Bowie, O.L., "Rectangular Tensile Sheet with Symmetric Edge Cracks", *Journal of Applied Mechanics*, 31, 1964, pp. 208-212.
3. Bowie, O.L., and Neal, D.M., "A Note on the Central Crack in a Uniformly Stressed Strip", *Engineering Fracture Mechanics*, Vol. 2, 1970, pp. 181-182.
4. Cook, R.D., *Concepts and Applications of Finite Element Analysis*, John Wiley & Sons, Inc., New York, 1974.
5. Cowper, G.R., Lindberg, G.M., and Olson, M.D., "A Shallow Shell Finite Element of Triangular Shape", *International Journal of Solids Structures*, Vol. 4, 1970, pp. 1133-1156.
6. Dunham, R.S., and Pister, K.S., "A Finite Element Application of the Hellinger-Reissner Variational Theorem", *Proceedings of the Second Conference on Matrix Methods in Structural Mechanics*, Wright-Patterson Air Force Base, Ohio, AFFDL-TR68-150, 1968, pp. 471-487.
7. Finlayson, B.A., *The Method of Weighted Residuals and Variational Principles*, Academic Press, New York, 1972.
8. Finlayson, B.A., and Scriven, L.E., "The Method of Weighted Residuals--A Review", *Applied Mechanics Review*, 19, 1966, pp. 735-748.
9. Gallagher, R.H., *Finite Element Analysis*, Prentice-Hall, Englewood Cliffs, New Jersey, 1975.
10. Hellan, K., "Analysis of Elastic Plates in Flexure by a Simplified Finite Element Method", *Acta Polytechnica Scandinavica*, Civil Engineering Series No. 46, Trondheim, 1967.
11. Hellwig, G., *Differential Operators of Mathematical Physics*, Addison-Wesley Publishing Company, London, (transl.) 1967.
12. Herrmann, L.R., "A Bending Analysis of Plates", *Proceedings of the First Conference on Matrix Methods in Structural Mechanics*, Wright-Patterson Air Force Base, Ohio, AFFDL-TR66-80, 1966, pp. 577-604.
13. Herrmann, L.R., "Elasticity Equations for Incompressible and Nearly Incompressible Materials by a Variational Theorem", *American Institute of Aeronautics and Astronautics Journal*, Vol. 3, No. 10, 1965, pp. 1896-1900.
14. Huebner, K.H., *The Finite Element Method for Engineers*, John Wiley & Sons, New York, 1975.
15. Hutton, S.G., "Finite Element Method--A Galerkin Approach", Ph.D. Thesis, University of British Columbia, Canada, September 1971.

16. Hutton, S.G., and Anderson, D.L., "Finite Element Method: A Galerkin Approach", *American Society of Civil Engineers*, Engineering Mechanics Division, October, 1971, pp. 1503-1520.
17. Lorch, E.R., *Spectral Theory*, University Texts in the Mathematical Sciences, Oxford University Press, 1962.
18. Mikhlin, S.G., *Variational Methods in Mathematical Physics*, The Macmillan Company, New York, 1964.
19. Oden, J.T., *Finite Elements of Nonlinear Continua*, McGraw-Hill, New York, 1972.
20. Oden, J.T., "Generalized Conjugate Functions for Mixed Finite Element Approximations of Boundary-Value Problems", *The Mathematical Foundations of the Finite Element Method--with Applications to Partial Differential Equations*, A.K. Aziz edition, Academic Press, New York, 1972, pp. 629-669.
21. Oden, J.T., and Reddy, J.N., "On Dual Complementary Variational Principles in Mathematical Physics", *International Journal of Engineering Science*, Vol. 12, 1974, pp. 1-29.
22. Oden, J.T., "A General Theory of Finite Elements I Topological Considerations", *International Journal for Numerical Methods in Engineering*, Vol. 1, No. 3, 1969, pp. 205-221.
23. Oden, J.T., "A General Theory of Finite Elements II Applications", *International Journal for Numerical Methods in Engineering*, Vol. 1, No. 3, 1969, pp. 247-260.
24. Oliveira, E.R.A., "Theoretical Foundations of the Finite Element Method", *International Journal of Solids Structures*, Vol. 4, 1968, pp. 929-952.
25. Oliveira, E.R.A., "Completeness and Convergence in the Finite Element Method", *Proceedings of the Second Conference on Matrix Methods in Structural Mechanics*, Wright-Patterson Air Force Base, Ohio, AFFDL-TR68-150, 1968, pp. 1061-1090.
26. Olson, M.D., and Tuann, S.Y., "Primitive Variables versus Stream Function Finite Element Solutions for the Navier-Stoke's Equations", *International Centre for Computer Aided Design--Proceedings of the Second International Symposium on Finite Element Methods in Flow Problems*, S. Margherita Ligure (Italy), June 14-18, 1976.

Also see:

Tuann, S.Y., and Olson, M.D., "A Study of Various Finite Element Methods for the Navier Stoke's Equations", Structural Research Series, Report No. 14, Department of Civil Engineering, University of British Columbia, Vancouver, Canada, May 1976.

27. Parks, D.M., "A Stiffness Derivative Finite Element Technique for Determination of Crack Tip Stress Intensity Factor", *International Journal of Fracture*, Vol. 10, No. 4, December 1974, pp. 487-501.
28. Pian, T.H.H., and Tong, P., "Basis of Finite Element Methods for Solid Continua", *International Journal for Numerical Methods in Engineering*, Vol. 1, 1969, pp. 3-28.
29. Rice, J.R., "A Path Independent Integral and the Approximate Analysis of Strain Concentration by Notches and Cracks", *Journal of Applied Mechanics*, Vol. 35, 1968, pp. 379-386.
30. Reddy, J.N., and Oden, J.T., "Convergence of Mixed Finite Element Approximations of a Class of Linear Boundary-Value Problems", *Journal of Structural Mechanics*, Vol. 2, 1973, pp. 83-108.
31. Savin, G.N., *Stress Concentrations around Holes*, Pergamon Press, 1961.
32. Strang, G., *Linear Algebra and its Applications*, Academic Press, New York, 1976.
33. Strang, G., and Fix, G.F., *An Analysis of the Finite Element Method*, Prentice Hall, Englewood Cliffs, New Jersey, 1973.
34. Taylor, C., and Hood, P., "A Numerical Solution of the Navier Stoke's Equations using the Finite Element Technique", *Computer and Fluids*, Vol. 1, 1973, pp. 73.
35. Timoshenko, S.P., and Goodier, J.N., *Theory of Elasticity*, 3rd edition, McGraw Hill, New York, 1970.
36. Tong, P., "New Displacement Hybrid Finite Element Model for Continua", *International Journal for Numerical Methods in Engineering*, Vol. 2, 1970, pp. 73-83.
37. Tong, P., and Pian, T.H.H., "The Convergence of Finite Element Method in Solving Linear Elastic Problems", *International Journal of Solids Structures*, Vol. 3, 1967, pp. 865-879.
38. Tong, P., and Pian, T.H.H., "On the Convergence of the Finite Element Method for Problems with Singularity", *International Journal of Solids Structures*, Vol. 9, 1973, pp. 313-321.
39. Watwood, V.B., Jr., "The Finite Element for Prediction of Crack Behaviour", *Nuclear Engineering Design II*, 1969, pp. 323-332.
40. Wunderlich, W., "Discretisation of Structural Problems by a Generalized Variational Approach", *Proceedings of the International Association for Shell Structures, Pacific Symposium on Hydrodynamically Loaded Shells--Part I*, Honolulu, Hawaii, October 10-15, 1971.
41. Zienkiewicz, O.C., *The Finite Element Method in Engineering Science*, McGraw Hill, London, 1971.

42. Zienkiewicz, O.C., Cheung, Y.K., and Stagg, K.G., "Stresses in Anisotropic Media with Particular Reference to Problems of Rock Mechanics", *Journal of Strain Analysis*, Vol. 1, No. 2, 1966, pp. 172-182.
43. Balakrishnan, A.V., *Applied Functional Analysis*, Applications of Mathematics 3, Springer-Verlag, New York, 1976.

Interpolation u,v $\tau$ 's*		Degrees of Freedom			Sign of Eigen- values	No. of Eigen- values	Composition of Eigenvectors
		u,v	$\tau$ 's	Total			
Linear	Constant	6	3	9	(-)	3	$\tau$ 's constant; u,v linear.
					(0)	3†	$\tau$ 's= $u_x=v_y=u_y+v_x=0$ .†
					(+)	3	$\tau$ 's constant; u,v linear.
Linear	Linear	6	9	15	(-)	9	$\tau$ 's,u,v linear.
					(0)	3	$\tau$ 's= $u_x=v_y=u_y+v_x=0$ .
					(+)	3	$\tau$ 's,u,v linear.
Quadratic	Constant	12	3	15	(-)	3	$\tau$ 's constant; u,v quadratic.
					(0)	9**	$\tau$ 's=0; $\{u_x=v_y=u_y+v_x=0$ ; u,v quadratic}.
					(+)	3	$\tau$ 's constant; u,v quadratic.
Quadratic	Linear	12	9	21	(-)	9	$\tau$ 's linear; u,v quadratic
					(0)	3	$\tau$ 's= $u_x=v_y=u_y+v_x=0$ .
					(+)	9	$\tau$ 's linear; u,v quadratic.
Quadratic	Quadratic	12	18	30	(-)	18	$\tau$ 's,u,v quadratic.
					(0)	3	$\tau$ 's= $u_x=v_y=u_y+v_x=0$ .
					(+)	9	$\tau$ 's,u,v quadratic.

\* $\tau$ 's: All stresses  $\tau_{xx}$ ,  $\tau_{yy}$  and  $\tau_{xy}$  have the same type of interpolation.

\*\*Extra zero eigenvalues are associated with mechanisms which have the same u,v distributions as the approximating polynomials.

†Rigid body modes ( $u_x=0$ ;  $v_y=0$ ;  $u_y+v_x=0$ ).

TABLE I: Eigenvalues and eigenvectors of element matrix for triangular elements using different combinations of interpolations for u,v and  $\tau$ 's; linear elasticity plane stress.

Interpolation		Degrees of Freedom			Sign of Eigenvalues	No. of Eigenvalues	Composition of Eigenvectors
u,v	$\tau_{xx}, \tau_{yy}, \tau_{xy}$	u,v	$\tau$ 's	Total			
Bilinear	Constant	8	3	11	(-)	3	$\tau$ 's constant; u,v bilinear.
					(0)	5**	$\tau$ 's=0; $\{u_x=v_y=u_y+v_x=0; u,v \text{ bilinear.}\}$
					(+)	3	$\tau$ 's constant; u,v bilinear.
Bilinear	Bilinear	8	12	20	(-)	12	$\tau$ 's,u,v bilinear.
					(0)	3†	$\tau$ 's= $u_x=v_y=u_y+v_x=0$ .†
					(+)	5	$\tau$ 's,u,v bilinear.
Biquadratic*	Bilinear	16	12	28	(-)	12	$\tau$ 's bilinear; u,v biquadratic.
					(0)	4**	$\tau$ 's=0; $\{u_x=v_y=u_y+v_x=0; u,v \text{ biquadratic.}\}$
					(+)	12	$\tau$ 's bilinear; u,v biquadratic.
Biquadratic	Biquadratic	16	24	40	(-)	24	$\tau$ 's,u,v biquadratic.
					(0)	3	$\tau$ 's= $u_x=v_y=u_y+v_x=0$ .
					(+)	13	$\tau$ 's,u,v biquadratic.

\*Full quadratic in x and y plus  $x^2y$  and  $xy^2$ .

\*\*Extra zero eigenvalues are associated with mechanisms which have the same u,v distributions as the approximating polynomials.

†Rigid body modes ( $u_x=0; v_y=0; u_y+v_x=0$ ).

TABLE II: Eigenvalues and eigenvectors of element matrix for rectangular elements using different combinations of interpolations for u,v and  $\tau$ 's; linear elasticity plane stress.

Interpolations			Degrees of Freedom				Sign of Eigenvalues	No. of Eigenvalues	Composition of Eigenvectors
u,v	p	$\tau$ 's	u,v	p	$\tau$ 's	Total			
Linear	Linear	Linear	6	3	9	18	(-)	10	p const.; u,v, $\tau$ 's linear.
							(0)	$2^{\dagger}+3+0$	p linear; u=v= $\tau$ 's=0. $\{p=\tau$ 's=u, $x=v, y=u, y+v, x=0.\}$
							(+)	3	p const.; u,v, $\tau$ 's linear.
Quadratic	Linear	Linear	12	3	9	24	(-)	12	p, $\tau$ 's linear; u,v quadratic.
							(0)	$0+3*+0$	p= $\tau$ 's=u, $x=v, y=u, y+v, x=0.$
							(+)	9	p, $\tau$ 's linear; u,v quadratic.
Quadratic	Quadratic	Constant	12	6	3	21	(-)	6	$\tau$ 's const.; p,u,v quadratic.
							(0)	$3+3+6\#$	p quadratic; u=v= $\tau$ 's=0. $\{p=\tau$ 's=u, $x=v, y=u, y+v, x=0.\}$ p= $\tau$ 's=0; u,v quadratic.
							(+)	3	$\tau$ 's const.; p,u,v quadratic.
Quadratic	Linear	Quadratic	12	3	18	33	(-)	21	p linear; u,v, $\tau$ 's quadratic.
							(0)	3	p= $\tau$ 's=u, $x=v, y=u, y+v, x=0.$
							(+)	9	p linear; u,v, $\tau$ 's quadratic.
Quadratic	Quadratic	Quadratic	12	6	18	36	(-)	21	p, $\tau$ 's,u,v quadratic.
							(0)	$3+3+0$	p quadratic; u=v= $\tau$ 's=0. $\{p=\tau$ 's=u, $x=v, y=u, y+v, x=0.\}$
							(+)	9	p, $\tau$ 's,u,v quadratic.

$\dagger$ Self-equilibrating modes in pressure. \*Rigid body modes ( $u_x=0; v_y=0; u_y+v_x=0$ ). #Mechanisms.

Note: The number of zero eigenvalues appear in the order; self-equilibrating, rigid body and mechanisms respectively. Proper rigid body modes also have  $p=\tau$ 's=0.

TABLE III: Eigenvalues and eigenvectors of element matrix for triangular elements using different combinations of interpolations for u,v,p and  $\tau$ 's ( $\tau_{xx}, \tau_{yy}, \tau_{xy}$ ); two-dimensional, incompressible creeping flow (linear part of the Navier-Stokes equations).

Interpolations			Degrees of Freedom				Sign of Eigenvalues	No. of Eigenvalues	Composition of Eigenvectors
u,v	p	$\tau$ 's	u,v	p	$\tau$ 's	Total			
Bilinear	Bilinear	Bilinear	8	4	12	24	(-)	15	$p, \tau$ 's, u, v bilinear. $p$ bilinear; $\tau$ 's = u = v = 0. $\{p = \tau$ 's = u, $x = v, y = u, y + v, x = 0.\}$ $p, \tau$ 's, u, v bilinear.
							(0)	$1^{\dagger} + 3 + 0$	
							(+)	5	
Biquadratic	Bilinear	Bilinear	16	4	12	32	(-)	16	$p, \tau$ 's bilinear; u, v biquadratic. $p = \tau$ 's = u, $x = v, y = u, y + v, x = 0.$ $\{p = \tau$ 's = 0; u, v biquadratic. $p, \tau$ 's bilinear; u, v biquadratic.
							(0)	$0 + 3 + 1^{\#}$	
							(+)	12	
Biquadratic†	Bilinear	Biquadratic	16	4	24	44	(-)	28	$p$ bilinear, $\tau$ 's, u, v biquadratic. $p = \tau$ 's = u, $x = v, y = u, y + v, x = 0.$ $p$ bilinear; $\tau$ 's, u, v biquadratic.
							(0)	$0 + 3^* + 0$	
							(+)	13	
Biquadratic	Biquadratic	Biquadratic	16	8	24	48	(-)	26	$p, \tau$ 's, u, v biquadratic. $p$ biquadratic; $\tau$ 's = u = v = 0. $\{p = \tau$ 's = u, $x = v, y = u, y + v, x = 0.\}$ $p, \tau$ 's, u, v biquadratic.
							(0)	$2 + 3 + 0$	
							(+)	13	

†Self equilibrating modes in pressure. \*Rigid body modes ( $u, x = v, y = u, y + v, x = 0$ ). #Mechanisms.

Note: The number of zero eigenvalues appear in the order: self-equilibrating, rigid body and mechanisms, respectively. Proper rigid body modes also have  $p = \tau$ 's = 0.

TABLE IV: Eigenvalues and eigenvectors of element matrix for rectangular elements using different combinations of interpolations for u, v, p and  $\tau$ 's ( $\tau_{xx}, \tau_{yy}, \tau_{xy}$ ); two-dimensional incompressible creeping flow (linear part of the Navier-Stokes equations).

No. of Elem.	$\frac{10^2 \delta_M EI}{ql^4}$	$\frac{10^2 \theta_E EI}{ql^3}$	$\frac{10 V_E}{ql}$	$\frac{10^3 U_E EI}{q^2 l^5}$
2	1.041667	2.083333	2.500	2.604167
4	1.236979	3.515625	3.750	3.743489
6	1.273148	3.858025	4.167	3.975909
8	1.285807	3.987630	4.375	4.058838
10	1.291667	4.050000	4.500	4.097500
12	1.294850	4.084680	4.583	4.118575
14	1.296769	4.105928	4.643	4.131308
16	1.298014	4.119873	4.688	4.139582
18	1.298868	4.129515	4.722	4.145260
20	1.299479	4.136458	4.750	4.149333
EXACT	1.302083	4.166667	5.000	4.166667

TABLE V(a): Simply supported beam; moments at the nodes are exact.

No. of Elem.	$\frac{10^2 \theta_{LE} EI}{ql^3}$	$\frac{10^2 \delta_M EI}{ql^4}$	$\frac{10 \theta_M EI}{ql^3}$	$\frac{10 \delta_{RE} EI}{ql^4}$	$\frac{10 \theta_{RE} EI}{ql^3}$	$\frac{10^2 U_E EI}{q^2 l^5}$
2	--	4.687500	--	1.354167	1.770833	2.864583
4	5.33850	4.492190	1.601563	1.276042	1.705730	2.587891
6	3.74228	4.456020	1.554784	1.261574	1.685957	2.538795
8	2.88086	4.443360	1.531576	1.256510	1.678060	2.521770
10	2.34167	4.437500	1.517500	1.254167	1.674167	2.513917
12	1.97242	4.434320	1.508005	1.252894	1.671971	2.509659
14	1.70372	4.432400	1.501154	1.252126	1.670616	2.507093
16	1.49940	4.431150	1.495972	1.251628	1.669723	2.505430
18	1.33887	4.430300	1.491912	1.251286	1.669095	2.504290
20	1.20938	4.429690	1.488646	1.251042	1.668646	2.503474
EXACT	0.00000	4.427083	1.45833	1.250000	1.666667	2.500000

TABLE V(b): Cantilever; moments at the nodes are exact.

TABLES V: Numerical results for two second order beam equations; v-linear, M-linear. Rotations and shears are derived from v and M, respectively.

No. of Elem.	$\frac{10^3 \theta_E EI}{ql^3}$	$\frac{10^3 \delta_M EI}{ql^4}$	$\frac{10^2 M_M}{ql^2}$	$\frac{-10^2 M_E}{ql^2}$	$\frac{10^4 UEI}{q^2 l^5}$
2	--	2.60417	6.25000	6.250	6.510417
4	5.859	2.60417	4.68750	7.813	6.917320
6	4.822	2.60417	4.39815	8.102	6.939086
8	3.988	2.60417	4.29688	8.203	6.942750
10	3.375	2.60417	4.25000	8.250	6.943750
12	2.918	2.60417	4.22458	8.275	6.944111
14	2.566	2.60417	4.20918	8.291	6.944264
16	2.289	2.60417	4.19922	8.301	6.944338
18	2.065	2.60417	4.19239	8.308	6.944380
20	1.880	2.60417	4.18750	8.313	6.944401
EXACT	0.000	2.60417	4.16667	8.333	6.944444

TABLE V(c): Beam with both ends fixed, deflections at the nodes are exact.

No. of Elem.	$\frac{10^2 \theta_{LE} EI}{ql^3}$	$\frac{10^2 \delta_M EI}{ql^4}$	$\frac{10^2 \delta_{RE} EI}{ql^4}$	$\frac{10^2 \theta_{RE} EI}{ql^3}$	$\frac{-10 M_{LE}}{ql^2}$	$\frac{10 M_{RE}}{ql^2}$	$\frac{10^2 UEI}{q^2 l^5}$
2	--	2.34375	4.16667	--	3.12500	1.87500	1.1067708
4	3.1901	2.34375	4.16667	2.0182	3.28125	1.71875	1.1108398
6	2.3341	2.34375	4.16667	1.3696	3.31019	1.68982	1.1110575
8	1.8305	2.34375	4.16667	1.3467	3.32031	1.67969	1.1110942
10	1.5042	2.34375	4.16667	0.8292	3.32500	1.67500	1.1111042
12	1.2756	2.34375	4.16667	0.6920	3.32755	1.67245	1.1111078
14	1.1070	2.34375	4.16667	0.5937	3.32909	1.67092	1.1111093
16	0.9776	2.34375	4.16667	0.5198	3.33008	1.66992	1.1111101
18	0.8752	2.34375	4.16667	0.4623	3.33076	1.66924	1.1111104
20	0.7922	2.34375	4.16667	0.4162	3.33125	1.66875	1.1111107
EXACT	0.0000	2.34375	4.16667	0.0000	3.33333	1.66667	1.1111111

TABLE V(d): Beam with one end fixed and the other guided; deflections at the nodes are exact.

TABLES V: Numerical results for two second order beam equations; v-linear, M-linear. Rotations and shears are derived from v and M, respectively.

No. of Elem.	$\frac{10^2 \delta_M EI}{ql^4}$	$\frac{10^2 \theta_E EI}{ql^3}$	$\frac{10^3 \delta_Q EI}{ql^4}$	$\frac{10^3 UEI}{q^2 l^5}$
1	1.250000	5.000000	--	4.16667
2	1.302083	4.791667	9.244792	4.16667
3	1.301440	4.506173	--	4.16667
4	1.302083	4.375000	9.277344	4.16667
5	1.302000	4.306667	--	4.16667
6	1.302083	4.266975	9.276942	4.16667
7	1.302062	4.241983	--	4.16667
8	1.302083	4.225260	9.277344	4.16667
15	1.302082	4.184197	--	4.16667
16	1.302083	4.183129	9.277344	4.16667
EXACT	1.302083	4.166667	9.277344	4.16667

TABLE VI(a): Simply supported beam.

No. of Elem.	$\frac{10^2 \theta_{LE} EI}{ql^3}$	$\frac{10^2 \delta_M EI}{ql^4}$	$\frac{10 \theta_M EI}{ql^3}$	$\frac{10 \delta_{RE} EI}{ql^4}$	$\frac{10 \theta_{RE} EI}{ql^3}$	$\frac{10^2 UEI}{q^2 l^5}$
1	5.0000	4.375000	1.250000	1.25	2.000000	2.50
2	1.6667	4.427083	1.562500	1.25	1.708333	2.50
3	0.8025	4.426440	1.435185	1.25	1.679012	2.50
4	0.4688	4.427083	1.484375	1.25	1.671876	2.50
5	0.3067	4.427000	1.450000	1.25	1.669333	2.50
6	0.2161	4.427083	1.469907	1.25	1.668210	2.50
7	0.1604	4.427062	1.454082	1.25	1.667637	2.50
8	0.1237	4.427083	1.464844	1.25	1.667318	2.50
15	0.0360	4.427082	1.457407	1.25	1.666763	2.50
16	0.0317	4.427083	1.459961	1.25	1.666747	2.50
EXACT	0.0000	4.427083	1.458333	1.25	1.666667	2.50

TABLE VI(b): Cantilever

TABLES VI: Numerical results for two second order beam equations; v-quadratic, M-quadratic. Rotations and shears are derived. Moments and shears are exact in all cases.

No. of Elem.	$\frac{10^3 \theta_E EI}{ql^3}$	$\frac{10^3 \delta_Q EI}{ql^4}$	$\frac{10^3 \theta_Q EI}{ql^3}$	$\frac{10^3 \delta_M EI}{ql^4}$	$\frac{10^4 UEI}{q^2 l^5}$
1	8.333	--	--	2.083333	6.94444
2	6.250	1.432292	5.20833	2.604167	6.94444
3	3.395	--	--	2.597737	6.94444
4	2.083	1.464844	9.11458	2.604167	6.94444
5	1.400	--	--	2.603333	6.94444
6	1.003	1.464442	7.52315	2.604167	6.94444
7	0.753	--	--	2.603950	6.94444
8	0.586	1.464844	8.13802	2.604167	6.94444
15	0.175	--	--	2.604156	6.94444
16	0.155	1.464844	7.89388	2.604167	6.94444
EXACT	0.000	1.464844	7.81250	2.604167	6.94444

TABLE VI(c): Beam with both ends fixed.

No. of Elem.	$\frac{10^2 \theta_{LE} EI}{ql^3}$	$\frac{10^2 \delta_M EI}{ql^4}$	$\frac{10^2 \theta_M EI}{ql^3}$	$\frac{10^2 \delta_{RE} EI}{ql^4}$	$\frac{10^3 \theta_{RE} EI}{ql^3}$	$\frac{10^2 UEI}{q^2 l^5}$
1	5.0000	2.291670	4.16667	4.16667	33.3333	1.111111
2	1.6667	2.343750	7.29167	4.16667	04.1667	1.111111
3	0.8025	2.343107	6.01852	4.16667	01.2350	1.111111
4	0.4688	2.343750	6.51042	4.16667	00.5210	1.111111
5	0.3067	2.343667	6.16667	4.16667	00.2667	1.111111
6	0.2161	2.343750	6.36574	4.16667	00.1543	1.111111
7	0.1603	2.343728	6.20750	4.16667	00.0972	1.111111
8	0.1348	2.343750	6.27010	4.16667	00.0651	1.111111
15	0.0361	2.343749	6.24074	4.16667	00.0099	1.111111
16	0.0317	2.343750	6.26628	4.16667	00.0082	1.111111
EXACT	0.0000	2.343750	6.25000	4.16667	00.0000	1.111111

TABLE VI(d): Beam with one end fixed and the other guided.

TABLES VI: Numerical results for two second order beam equations; v-quadratic, M-quadratic. Rotations and shears are derived. Moments and shears are exact in all cases.

No. of Elem.	$\frac{10^2 \theta_E EI}{ql^3}$	$\frac{10^2 \delta_M EI}{ql^4}$	$\frac{10^3 UEI}{q^2 l^5}$
1	5.000000	--	4.166667
2	4.305556	1.307870	4.166667
3	4.209877	--	4.166667
4	4.185049	1.302594	4.166667
5	4.176092	--	4.166667
6	4.172123	1.302189	4.166667
EXACT	4.166667	1.302083	4.166667

TABLE VII(a): Simply supported beam.

No. of Elem.	$\frac{10^3 \theta_{LE} EI}{ql^3}$	$\frac{10^2 \delta_M EI}{ql^4}$	$\frac{10 \theta_M EI}{ql^3}$	$\frac{10 \delta_{RE} EI}{ql^4}$	$\frac{10 \theta_{RE} EI}{ql^3}$	$\frac{10^2 UEI}{q^2 l^5}$
1	8.3333	--	--	1.250	1.583333	2.50
2	1.3889	4.432870	1.458333	1.250	1.652778	2.50
3	0.4321	--	--	1.250	1.662346	2.50
4	0.1838	4.427594	1.458333	1.250	1.664828	2.50
5	0.0943	--	--	1.250	1.665724	2.50
6	0.0546	4.427189	1.458333	1.250	1.666121	2.50
EXACT	0.0000	4.427083	1.458333	1.250	1.666667	2.50

TABLE VII(b): Cantilever

TABLES VII: Numerical results for two second order beam equations, v-cubic, M-cubic. Moments and shears are exact in all cases.

No. of Elem.	$\frac{10^3 \theta_E EI}{ql^3}$	$\frac{10^3 \delta_M EI}{ql^4}$	$\frac{10^4 UEI}{q^2 l^5}$
1	8.3333	--	6.94444
2	1.3889	2.662037	6.94444
3	0.4321	--	6.94444
4	0.1838	2.609273	6.94444
5	0.0943	--	6.94444
6	0.0546	2.605228	6.94444
EXACT	0.0000	2.604167	6.94444

TABLE VII(c): Beam with both ends fixed.

No. of Elem.	$\frac{10^3 \theta_{LE} EI}{ql^3}$	$\frac{10^2 \delta_M EI}{ql^4}$	$\frac{10^2 \theta_M EI}{ql^3}$	$\frac{10^2 \delta_{RE} EI}{ql^4}$	$\frac{10^3 \theta_{RE} EI}{ql^3}$	$\frac{10^2 UEI}{q^2 l^5}$
1	8.3333	--	--	4.166667	-8.3333	1.111111
2	1.3889	2.349537	6.250	4.166667	-1.3889	1.111111
3	0.4321	--	--	4.166667	-0.4321	1.111111
4	0.1838	2.344261	6.250	4.166667	-0.1838	1.111111
5	0.0943	--	--	4.166667	-0.0943	1.111111
6	0.0546	2.343856	6.250	4.166667	-0.0546	1.111111
EXACT	0.0000	2.343750	6.250	4.166667	0.0000	1.111111

TABLE VII(d): Beam with one end fixed and the other guided.

TABLES VII: Numerical results for two second order beam equations, v-cubic, M-cubic. Moments and shears are exact in all cases.

No. of Elem.	$\frac{10^2 \delta_M EI}{ql^4}$	$\frac{10^2 \theta_E EI}{ql^3}$	$\frac{10^3 UEI}{q^2 l^5}$
1	--	--	--
2	1.852	5.5560	4.6300
3	--	4.5730	4.2337
4	1.360	4.5140	4.1956
5	--	4.3380	4.1766
6	1.338	4.3210	4.1723
EXACT	1.302	4.1667	4.1667

TABLE VIII(a): Simply supported beam; nodal moments and shears are exact.

No. of Elem.	$\frac{10\theta_{LE} EI}{ql^3}$	$\frac{10^2 \delta_M EI}{ql^4}$	$\frac{10\theta_M EI}{ql^3}$	$\frac{10\delta_{RE} EI}{ql^4}$	$\frac{10\theta_{RE} EI}{ql^3}$	$\frac{10^2 UEI}{q^2 l^5}$
1	1.6667	--	--	1.6667	1.6667	4.1667
2	0.5555	3.9350	1.2500	1.2500	1.9444	2.5463
3	0.2309	--	--	1.2551	1.5387	2.5324
4	0.1389	4.4840	1.5625	1.2500	1.7361	2.5029
5	0.0844	--	--	1.2507	1.6169	2.5043
6	0.0617	4.3470	1.4352	1.2500	1.6975	2.5006
EXACT	0.0000	4.4271	1.4583	1.2500	1.6667	2.5000

TABLE VIII(b): Cantilever; nodal moments and shears are exact.

TABLES VIII: Numerical results for four first order equations, forced boundary conditions on  $v$  and  $M$ ;  $v, \theta, M$  and  $V$  all linear.

No. of Elem.	$\frac{10^2 \theta_E EI}{ql^3}$	$\frac{10^3 \delta_M EI}{ql^4}$	$\frac{10^2 M_M}{ql^2}$	$\frac{10^2 M_E}{ql^2}$	$\frac{10^4 UEI}{q^2 l^5}$
1	--	--	--	--	--
2	1.3889	4.62960	8.3333	-8.3333	1.1574
3	0.9150	--	--	-8.2305	8.4675
4	0.3472	3.18290	4.1667	-8.3333	7.2338
5	0.3442	--	--	-8.3333	7.1547
6	0.1543	2.57210	4.6296	-8.3333	7.0016
EXACT	0.0000	2.60417	4.1667	-8.3333	6.9444

TABLE VIII(c): Beam with both ends fixed; shears are exact.

No. of Elem.	$\frac{10^2 \theta_{LE} EI}{ql^3}$	$\frac{10^2 \delta_M EI}{ql^4}$	$\frac{10^2 \delta_{RE} EI}{ql^4}$	$\frac{10^2 \theta_{RE} EI}{ql^3}$	$\frac{-10 M_{LE}}{ql^2}$	$\frac{10 M_{RE}}{ql^2}$	$\frac{10^2 UEI}{q^2 l^5}$
	$ql^3$	$ql^4$	$ql^4$	$ql^3$	$ql^2$	$ql^2$	$q^2 l^5$
1	4.1666	--	4.16667	4.1667	2.5000	2.50000	1.0466
2	5.5555	2.54629	4.16667	2.7778	3.3333	1.66667	1.1574
3	1.3775	--	4.16667	0.4515	3.3230	1.67695	1.1263
4	1.3888	2.40158	4.16667	0.6944	3.3333	1.66667	1.1141
5	0.5108	--	4.16667	0.1775	3.3320	1.66800	1.1132
6	0.6172	2.34050	4.16667	0.3086	3.3333	1.66667	1.1117
EXACT	0.0000	2.34375	4.16667	0.0000	3.3333	1.66667	1.1111

TABLE VIII(d): Beam with one end fixed and the other guided;  
shears are exact.

TABLES VIII: Numerical results for four first order equations,  
forced boundary conditions on  $v$  and  $M$ ;  $v, \theta, M$  and  $V$   
all linear.

No. of Elem.	(1) Simply Supp. $\frac{10^3 UEI}{q l^5}$	(2) Cantilever $\frac{10^2 UEI}{q l^5}$	(3) Fixed-fixed $\frac{10^4 UEI}{q l^5}$
1	---	---	---
2	3.472222	1.388884	---
3	4.034536	2.194787	---
4	4.123264	2.365451	6.510467
5	4.133495	2.440016	6.521569
6	4.158093	2.467577	6.858711
8	4.163954	2.488878	6.917318
10	4.165556	2.495289	6.933333
12	4.166131	2.497662	6.939086
16	4.166497	2.499243	6.942750
EXACT	4.166667	2.500000	6.944444

TABLE IX: Strain energy estimations for four first order beam equations with forced boundary conditions on  $v$  and  $\theta$ ;  $M, V, \theta$  and  $v$  all linear.

No. of Elem.	$\frac{10^2 \delta_M EI}{q l^4}$	$\frac{10^2 \theta_E EI}{q l^3}$	$\frac{10 M_M}{q l^2}$	$\frac{M_E}{q l^2}$	$\frac{10^3 UEI}{q l^5}$
1	---	---	---	---	---
2	2.43056	4.16667	0.83333	0.08333	6.076389
3	---	4.16816	---	0.00953	6.762226
4	2.17014	4.16667	1.45833	0.02083	6.727431
5	---	4.16793	---	0.00397	6.769543
6	2.13049	4.16667	1.20370	0.00926	6.762251
8	2.10504	4.16667	1.30208	0.00521	6.768121
10	2.10056	4.16667	1.23333	0.00333	6.769722
12	2.09298	4.16667	1.27315	0.00231	6.770298
16	2.08876	4.16667	1.26302	0.00130	6.770664
EXACT	2.08333	4.16667	1.25000	0.00000	6.770833

TABLE X(a): Simply supported beam, shears are exact.

TABLES X: Numerical results for four first order beam equations; forced boundary conditions on  $v$  and  $\theta$ ; shear strain energy included;  $M, V, \theta, v$  all linear.

No. of Elem.	$\frac{10^8 \delta_{RE} EI}{ql^4}$	$\frac{10^9 \theta_{RE} EI}{ql^3}$	$\frac{10^6 M_{LE}}{ql^2}$	$\frac{V_{LE}}{ql}$	$\frac{10^2 U_{EI}}{q^2 l^5}$
1	0.84821	1.07143	1.07143	1.35714	3.794643
2	1.43430	1.66667	3.39744	1.46154	3.151709
3	1.54113	1.63422	4.33756	1.17524	3.487009
4	1.55303	1.66667	4.56439	1.13636	3.513652
5	1.55948	1.66195	4.74883	1.07071	3.533663
6	1.56056	1.66667	4.80288	1.06272	3.535970
8	1.56188	1.66667	4.88839	1.03571	3.539845
10	1.56225	1.66667	4.92835	1.02299	3.540917
12	1.56238	1.66667	4.95016	1.01601	3.541304
16	1.56246	1.66667	4.97192	1.00904	3.541552
EXACT	1.56250	1.66667	5.00000	1.00000	3.541667

TABLE X(b): Cantilever.

No. of Elem.	$\frac{10^2 \delta_M EI}{ql^4}$	$\frac{10^2 M_M}{ql^2}$	$\frac{10^2 M_E}{ql^2}$	$\frac{10^3 U_{EI}}{q^2 l^5}$
1	--	--	--	--
2	1.04167	0.00000	0.00000	2.604167
3	--	--	6.51466	3.242249
4	1.12847	6.25000	6.25000	3.255208
5	--	--	7.58171	3.289003
6	1.05024	3.70370	7.40741	3.290038
8	1.06337	4.68750	7.81250	3.295898
10	1.04500	4.50000	8.00000	3.297500
12	1.05131	4.39815	8.10185	3.298075
16	1.04709	4.29688	8.20313	3.298442
EXACT	1.04167	4.16667	8.33333	3.298611

TABLE X(c): Beam with both ends fixed; shears are exact.

TABLES X: Numerical results for four first order beam equations; forced boundary conditions on  $v$  and  $\theta$ ; shear strain energy included;  $M, V, \theta, v$  all linear.

FINITE ELEMENT GRID	N	$\frac{10Et u_B}{(1-\nu^2)N_0L}$		$\frac{10^2Et u_C}{(1-\nu^2)N_0L}$		$\frac{10Et v_C}{(1-\nu^2)N_0L}$		$\frac{10Et v_D}{(1-\nu^2)N_0L}$		$\frac{-10N_{xxA}}{N_0}$	
		Elem. A*	Elem. B†	Elem. A	Elem. B	Elem. A	Elem. B	Elem. A	Elem. B	Elem. A	Elem. B
1×1	2	1.054258	1.507941	-1.1435	2.1934	2.99336	1.31824	4.332647	5.085466	0.00000	1.44190
2×2	4	1.443990	1.519821	-0.7670	1.8684	1.45335	1.28574	4.849820	5.073595	2.01236	1.40137
3×3	6	1.463880	1.519773	0.6555	1.8046	1.34960	1.27936	4.974455	5.073633	1.41893	1.40559
4×4	8	1.498170	1.519862	1.3373	1.7896	1.28864	1.27787	5.016690	5.073544	1.58424	1.40789
5×5	10	1.508706	1.519900	1.5268	1.7852	1.28480	1.27742	5.036405	5.073507	1.28638	1.40880
6×6	12	1.512260		1.6488		1.27514		5.047228		1.49870	
EXACT		1.519928	1.519928	1.7837	1.7837	1.27727	1.27727	5.073478	5.073478	1.40954	1.40954

	N	$\frac{10N_{yyA}}{N_0}$		$\frac{10N_{yyB}}{N_0}$		$\frac{10^2N_{xxB}}{N_0}$		$\frac{10N_{xxC}}{N_0}$		$\frac{10Et^2U}{(1-\nu^2)L^2N_0^2}$	
		Elem. A	Elem. B	Elem. A	Elem. B	Elem. A	Elem. B	Elem. A	Elem. B	Elem. A	Elem. B
	2	6.66667	8.55810	4.04167	4.70735	6.2500	3.9928	0.0000	0.3181	2.553610	2.787981
	4	9.16957	8.59863	3.54268	4.17500	0.9848	0.4235	0.7266	-0.0005	2.746331	2.793366
	6	7.75831	8.59441	4.31117	4.11902	4.8662	0.0848	-0.4544	-0.0299	2.782543	2.793540
	8	8.92269	8.59211	4.02879	4.10971	3.0654	0.0329	-0.3742	-0.0285	2.789962	2.793562
	10	8.39253	8.59120	4.05786	4.10767	1.9439	0.0166	-0.2945	-0.0233	2.792055	2.793567
	12	8.74161		4.13723		1.5472		-0.2530		2.792746	
EXACT		8.59046	8.59046	4.10670	4.10670	0.0000	0.0000	0.0000	0.0000	2.793570	2.793570

\*Mixed Finite Element; displacements and stresses linear.

†Displacement Finite Element; u and v full cubics [5].

TABLE XI: Numerical results for parabolically loaded plane stress problem.

No. of Elem. in Beam Depth N	Total No. of Elem.	Degrees of Freedom	Tip Deflec- tion $\delta_c =$ $v(L,0)$ . (in.)	$\tau_{xx}$ @ $x=12'', y=-6''$ ksi	Longitudinal Deflection @ $B=U_B$ . (in.)	Strain Energy $U(k-in.)$
2	32	131	0.336062	53.084	0.059717	6.731654
4	128	421	0.355121	60.501	0.064024	7.136889
6	288	871	0.355093	59.612	0.063980	7.140213
8	512	1481	0.355459	60.148	0.064038	7.145934
EXACT	(ELASTICITY)		0.355333	60.000	0.064000	7.146667

TABLE XII: Numerical results for the cantilever (plane stress) with boundary conditions B.C.1 (Figure 19). Mixed finite element; displacements and stresses linear.

No. of Elem. in Beam Depth N	Total No. of Elem.	Degrees of Freedom	Tip Deflec- tion $\delta_c =$ $v(L,0)$ . (in.)	$\tau_{xx}$ @ $x=12'', y=-6''$ ksi	Longitudinal Deflection @ $B=U_B$ . (in.)	Strain Energy $U(k-in.)$
1	8	46	0.245120	39.107	0.042410	4.902405
2	32	129	0.3359427	52.694	0.059602	6.718577
4	128	415	0.355464	60.469	0.064064	7.109509
6	288	861	0.355698	59.734	0.064087	7.114006
8	512	1467	0.355952	60.125	0.064146	7.119015
EXACT	(BEAM THEORY)		0.355833	60.000		7.116667

TABLE XIII: Numerical results for the cantilever (plane stress) with boundary conditions B.C.2 (Figure 19). Mixed finite element; displacements and stresses linear.

Element Type	Mesh	N	Number of Degrees of Freedom	Tip Deflection $\delta=v_C$ (in.)	$\tau_{xx}$ - Normal Stress @ $x=12"$ $y=-6"$ . (ksi)
C.S.T	A-1	2	48	0.19819	33.407
	A-2	4	160	0.30556	51.225
	A-3	8	576	0.34188	57.342
L.S.T	B-1	1	48	0.34872	
	B-2	2	160	0.35506	59.145
	B-3	4	576	0.35569	60.024
Q.S.T	C-1	1	68	0.35373*	58.973*
	C-2	2	214	0.35506	59.843
	C-3	4	268	0.35580	59.993
MIXED	M-1	1	46	0.24512*	39.108
DISPL.	M-2	2	129	0.33594	52.694
AND	M-4	4	415	0.35547	60.469
STRESSES	M-6	6	861	0.35570	59.734
LINEAR	M-8	8	1467	0.35595	60.125
BEAM THEORY				0.35583	60.000

\*Average of values at  $y=6"$  and  $y=-6"$ .

TABLE XIV: Comparison amongst C.S.T., L.S.T., Q.S.T., and mixed finite element. Cantilever with boundary conditions B.C.2 (Figure 19).

N	$\frac{Eu_A}{\tau_0 L}$	$\frac{Ev_A}{\tau_0 L}$	$\frac{Ev_C}{\tau_0 L}$	$\frac{Eu_D}{\tau_0 L}$	$\frac{\tau_{xxD}}{\tau_0}$	$\frac{\tau_{yyD}}{\tau_0}$	$\frac{\tau_{xxA}}{\tau_0}$	$\frac{EU^*}{\tau_0^2 L^2 t}$
2	0.4633	1.4778	1.1222	0.2440	0.7052	1.3835	0.6897	2.738912
4	0.4571	1.7771	1.1737	0.4271	1.4203	2.3751	-0.7849	3.122624
6	0.4507	1.7810	1.1771	0.4787	1.8202	3.0010	0.5045	3.166420
8	0.4739	1.8312	1.1849	0.5216	2.1230	3.4100	-0.2607	3.196404
10	0.4510	1.8186	1.1856	0.5364	2.4049	3.8175	0.0071	3.203674
12	0.4610	1.8272	1.1869	0.5546	2.6225	4.1357	0.0469	3.212178

TABLE XV(a):  $\tau_{yy}$  continuous at the crack tip D.

N	$\frac{Eu_A}{\tau_0 L}$	$\frac{Ev_A}{\tau_0 L}$	$\frac{Ev_C}{\tau_0 L}$	$\frac{Eu_D}{\tau_0 L}$	$\frac{\tau_{xxD}}{\tau_0}$	$\frac{\tau_{yyD}}{\tau_0}$	$\frac{\tau_{xxA}}{\tau_0}$	$\frac{EU^*}{\tau_0^2 L^2 t}$
2	0.0544	2.9301	2.8883	-0.7285	-0.1440	2.2921	-0.7936	1.704874
4	0.4568	1.7749	1.1719	0.4281	1.4257	3.0437	-0.7605	3.113852
6	0.4461	1.7709	1.1762	0.4817	1.8396	3.8743	0.4800	3.159226
8	0.4732	1.8273	1.1837	0.5252	2.1493	4.3664	-0.2376	3.191367
10	0.4996	1.8147	1.1848	0.5404	2.4361	4.8837	-0.0143	3.199594
12	0.4600	1.8241	1.1862	0.5585	2.6562	5.2798	0.0688	3.208874

TABLE XV(b):  $\tau_{yy}$  discontinuous at the crack tip D.

TABLES XV: Numerical results for the plane stress problem of square plate with symmetric edge cracks, Figure 29.

\*Exact value:  $U = 3.228 \frac{UE}{\tau_0^2 L^2 t}$ , Tong and Pian [38].

$\frac{r_{\Gamma_0}}{a}$	$-\frac{E\pi_M}{\tau_0^2 hbt}$	$-\frac{10^6 E \Delta \pi_M}{\tau_0^2 hbt}$	$-\frac{aE}{\tau_0^2 hbt} \frac{\Delta \pi_M}{\Delta a}$	$\frac{K_I}{\tau_0 \sqrt{a}}$	Error %
0.0	1.05942309	1.385584	0.274918	1.90402	10.98
0.1	1.05942339	1.680112	0.333358	2.09664	1.97
0.2	1.05942331	1.607250	0.318898	2.05067	4.12
0.5	1.05942333	1.626610	0.322740	2.06300	3.55
Initial Crack	1.05942171	EXACT $K_I$ ; ref. [2]		2.13884	

TABLE XVI: Stress intensity factors from the finite element analysis of the rectangular plate with symmetric edge cracks, Figure 33(a). (Mixed finite element; displacements and stresses linear).

$\frac{r_{\Gamma_0}}{a}$	$-\frac{E\pi_M}{\tau_0^2 hbt}$	$-\frac{10^6 E \Delta \pi_M}{\tau_0^2 hbt}$	$-\frac{aE}{\tau_0^2 hbt} \frac{\Delta \pi_M}{a}$	$\frac{K_I}{\tau_0 \sqrt{a}}$	Error %
0.0	1.04790510	1.408614	0.279486	1.91978	8.98
0.1	1.04790543	1.730814	0.343416	2.12804	0.89
0.2	1.04790535	1.645374	0.326464	2.07485	1.63
0.5	1.04790537	1.664358	0.330230	2.08679	1.06
Initial Crack	1.04790370	EXACT $K_I$ ; ref. [3]		2.10922	

TABLE XVII: Stress intensity factors from the finite element analysis of the rectangular plate with a central crack, Figure 33(b). (Mixed finite element; displacements and stresses linear).

Author(s)	Number of Elements	Degrees of Freedom	Accuracy of $K_I$ Error %	Type of Element
Watwood [38]	470	956	2.00	Triangular and rectangular
Anderson <i>et al.</i> [1]	1470	3000	0.14	Quadrilateral
Present result	174	505	1.97	Mixed triangles.* Symm. edge cracks
Present result	174	505	0.89	Mixed triangles. Central crack

TABLE XVIII: Comparison of stress intensity factors obtained from energy release rate using different elements and procedures.

\*Plane strain mixed finite element; displacements and stresses linear.

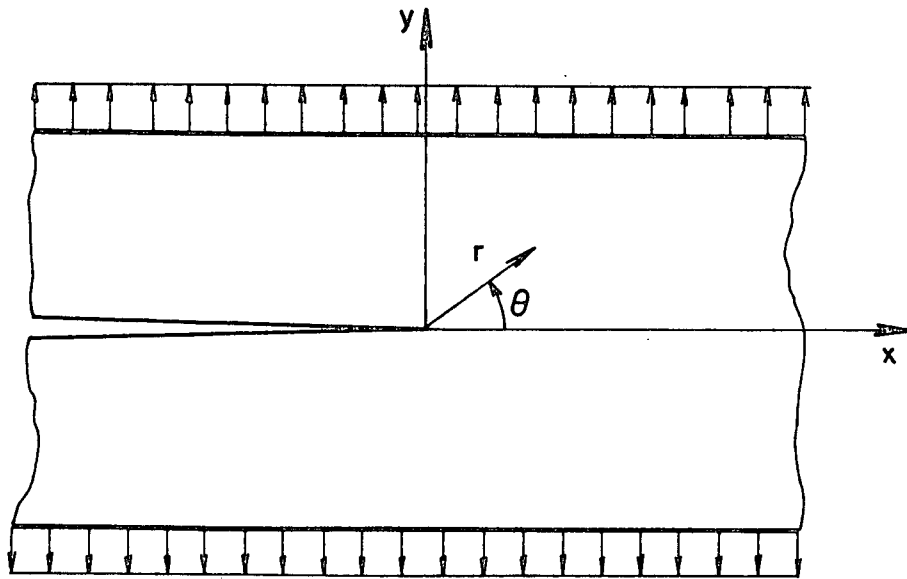


FIG.1: Mode I crack (opening mode).

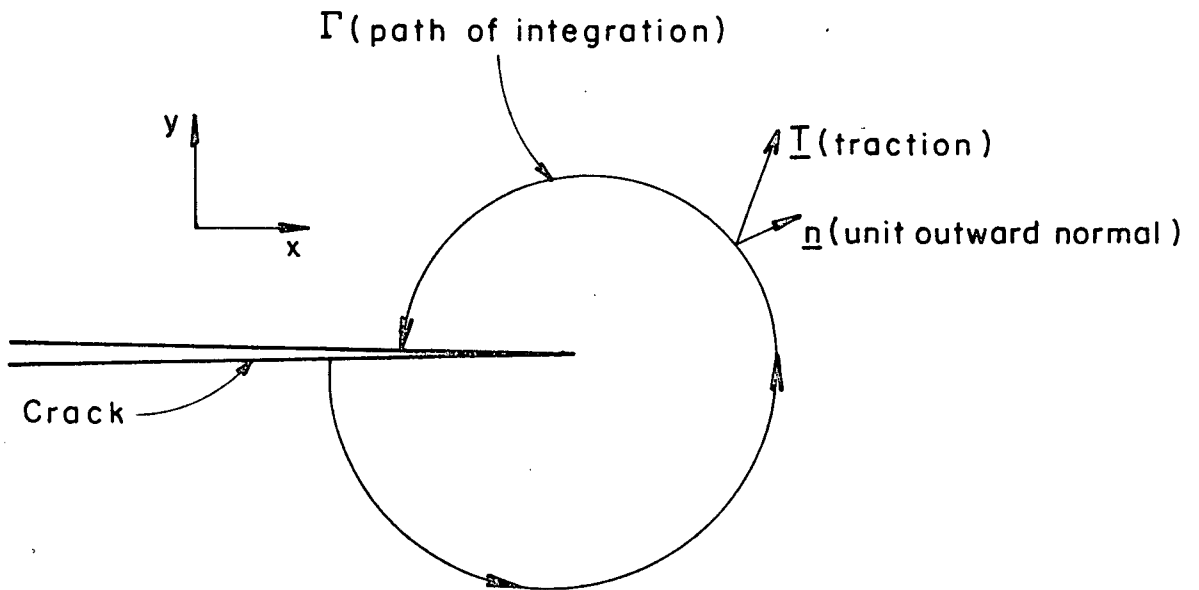


FIG.2: Typical contour for evaluation of  $J$ -integral.

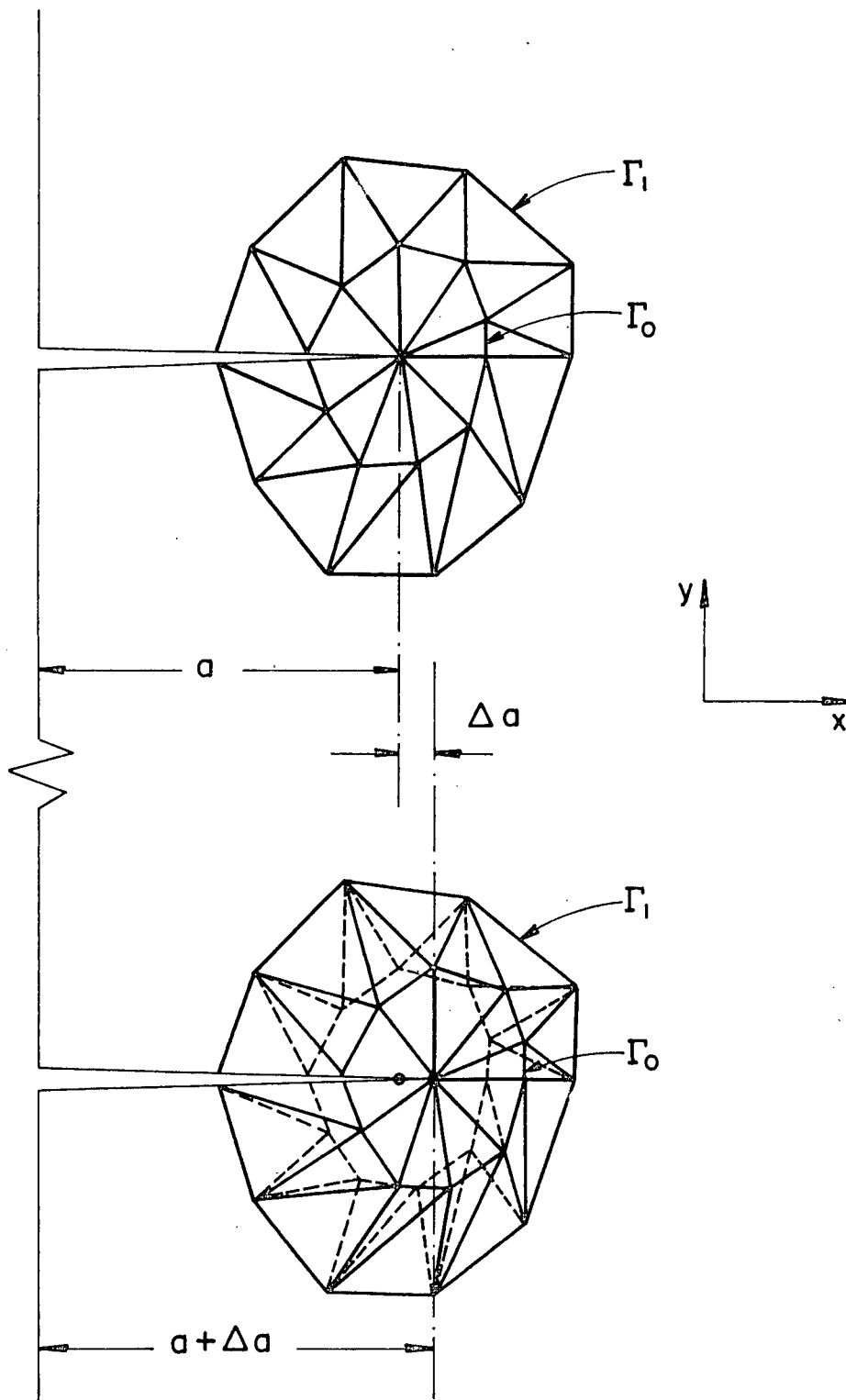


FIG.3: Accommodation of crack extension  $\Delta a$  by advancing nodes on the path  $\Gamma_0$ .

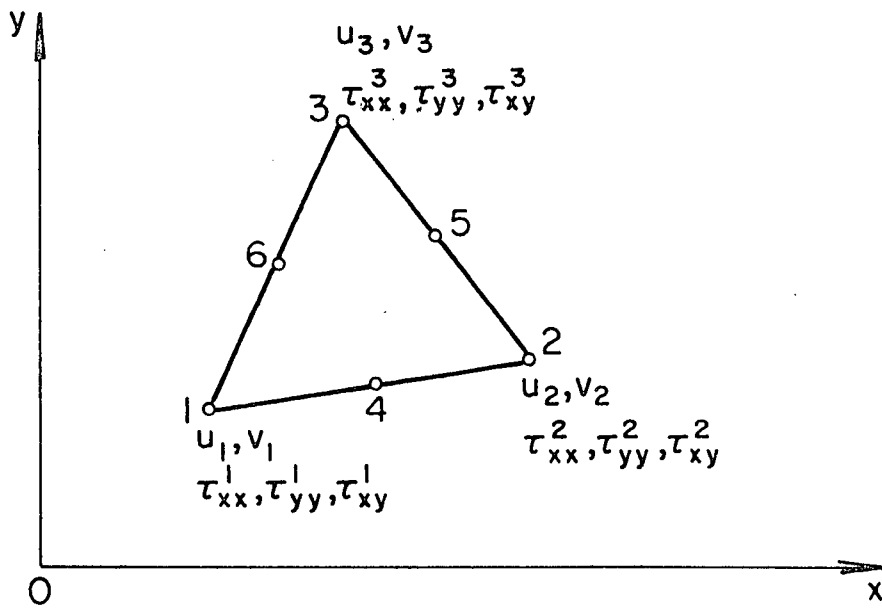


FIG.4: Node numbers and degrees of freedom for a triangular element.

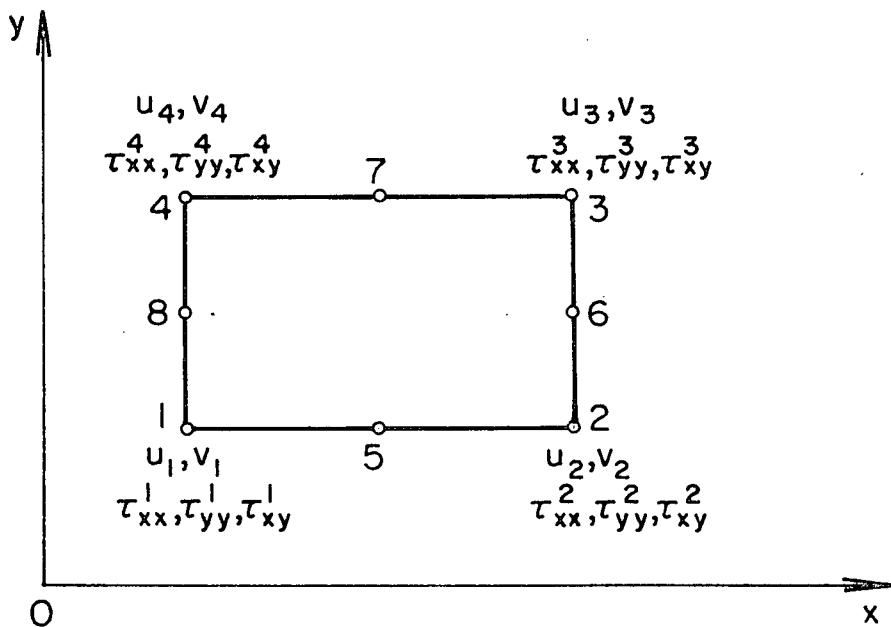


FIG.5: Node numbers and degrees of freedom for a rectangular element.

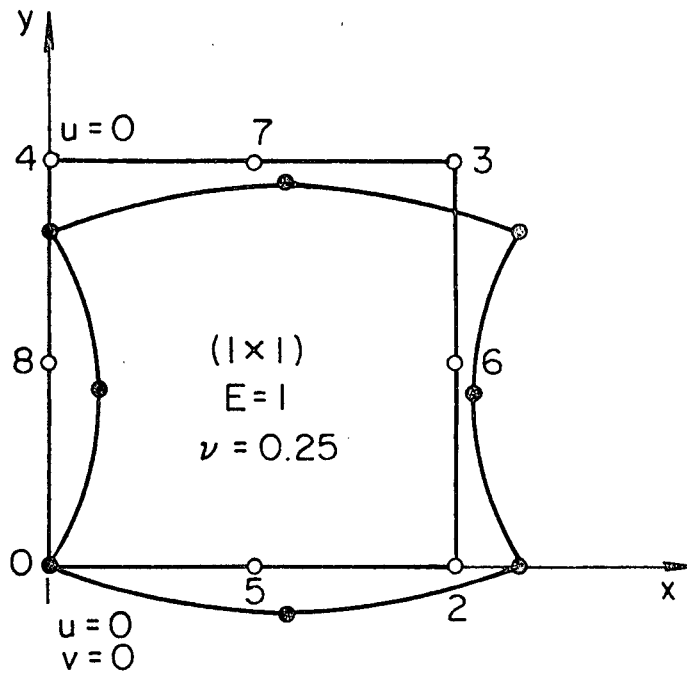


FIG.6: Mechanism for the fourth zero eigenvalue.

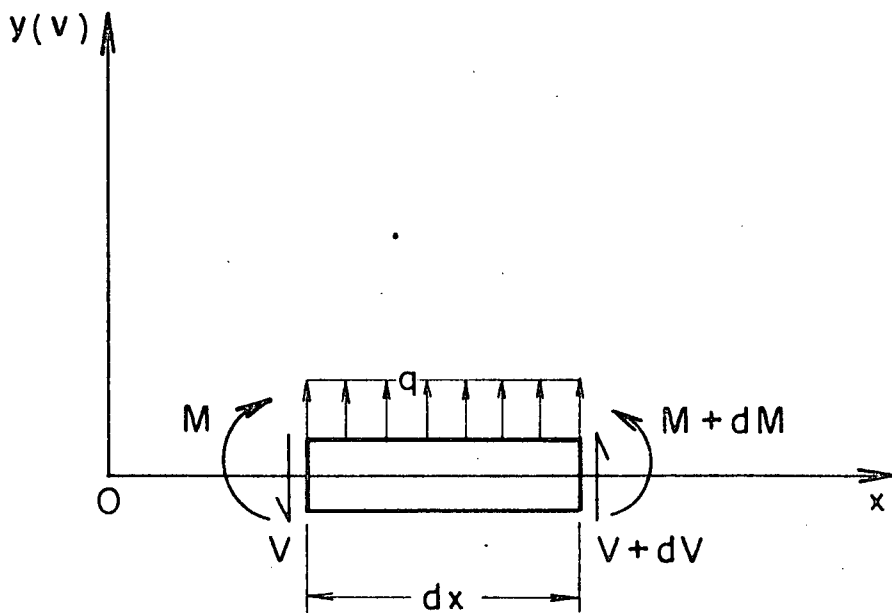


FIG.7: Forces acting on an infinitesimal beam element.

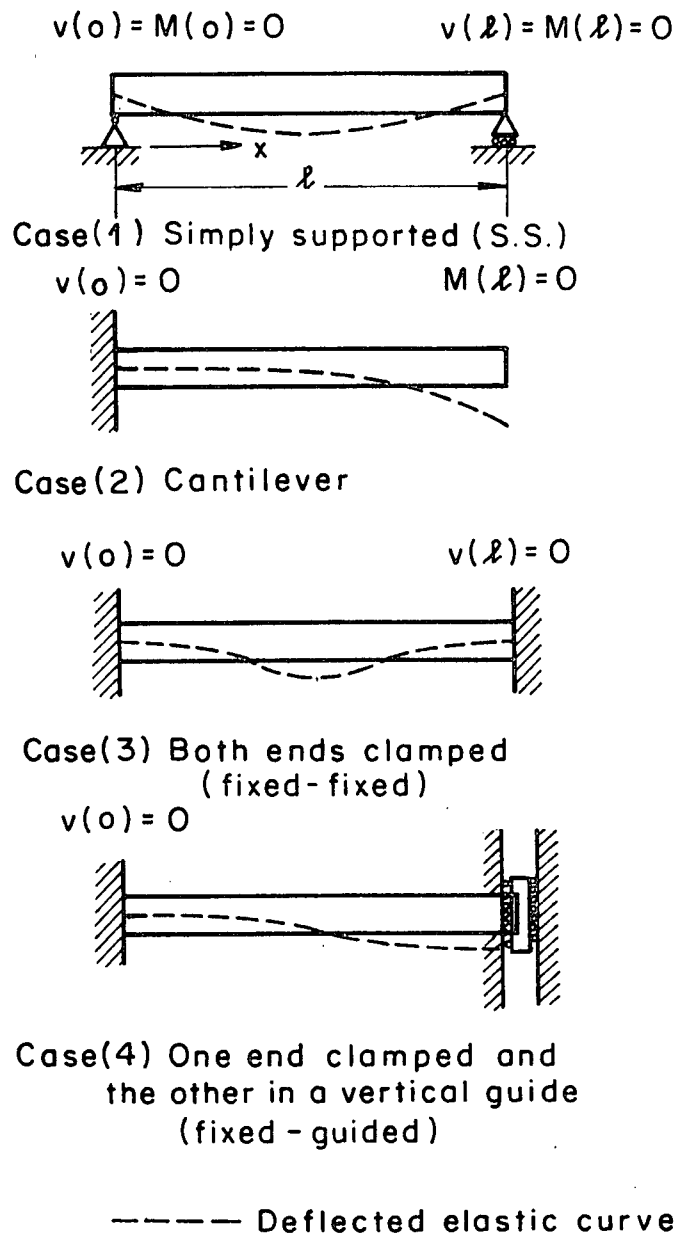


FIG.8: Forced boundary conditions on  $v$  and  $M$  for the beam problem.

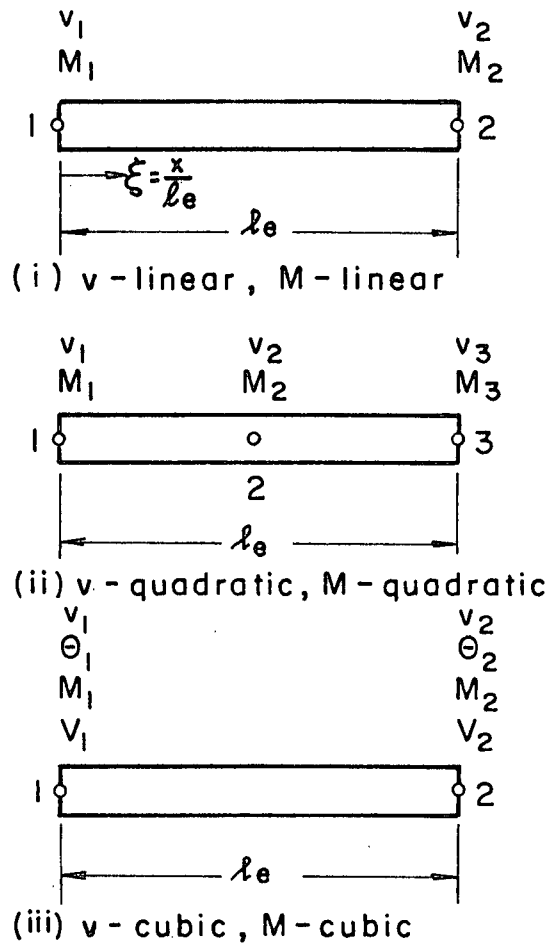


FIG.9: Degrees of freedom for the beam element - two second order equations.

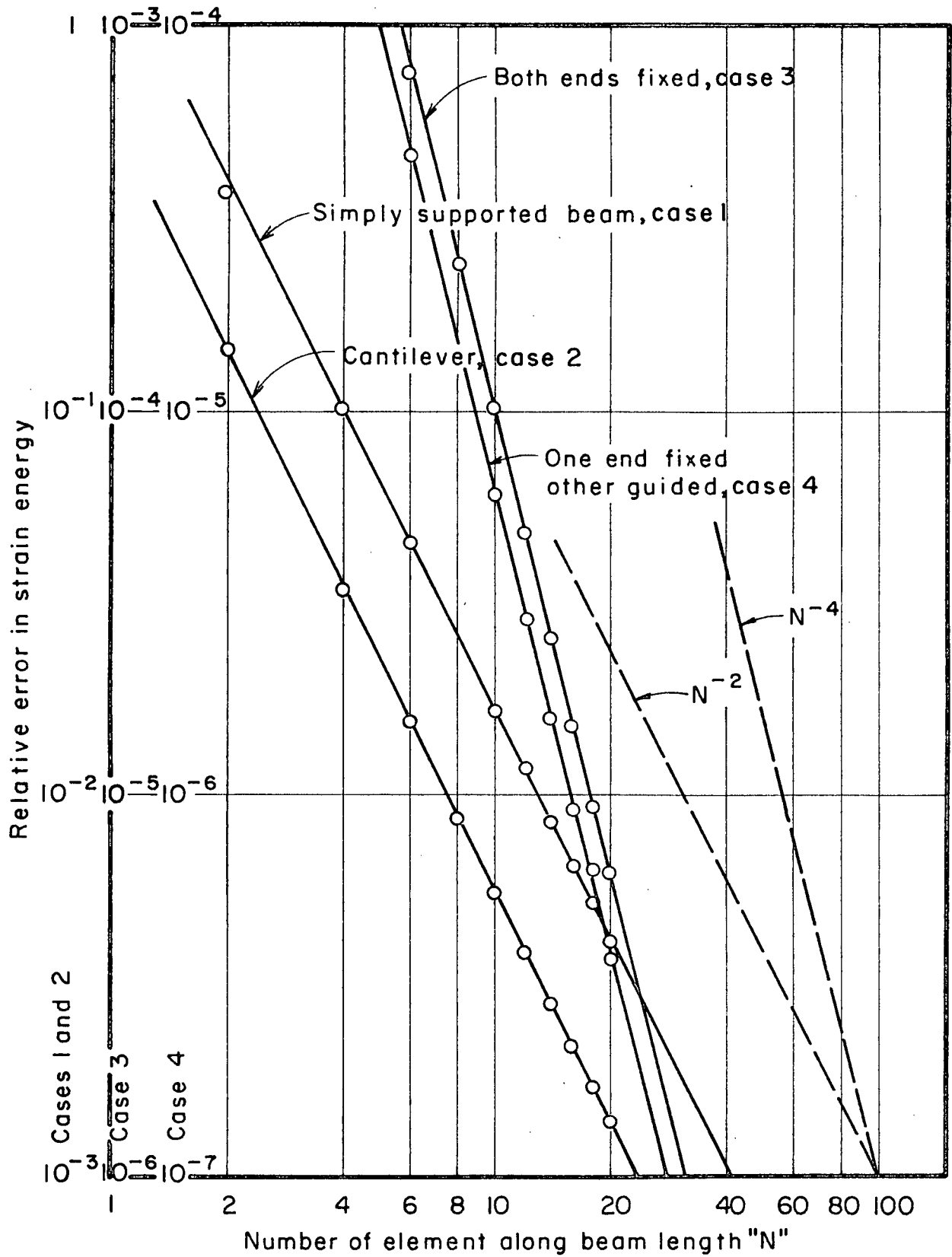


FIG. 10(a) Two second order beam equations ;  
displacement linear and moment linear.

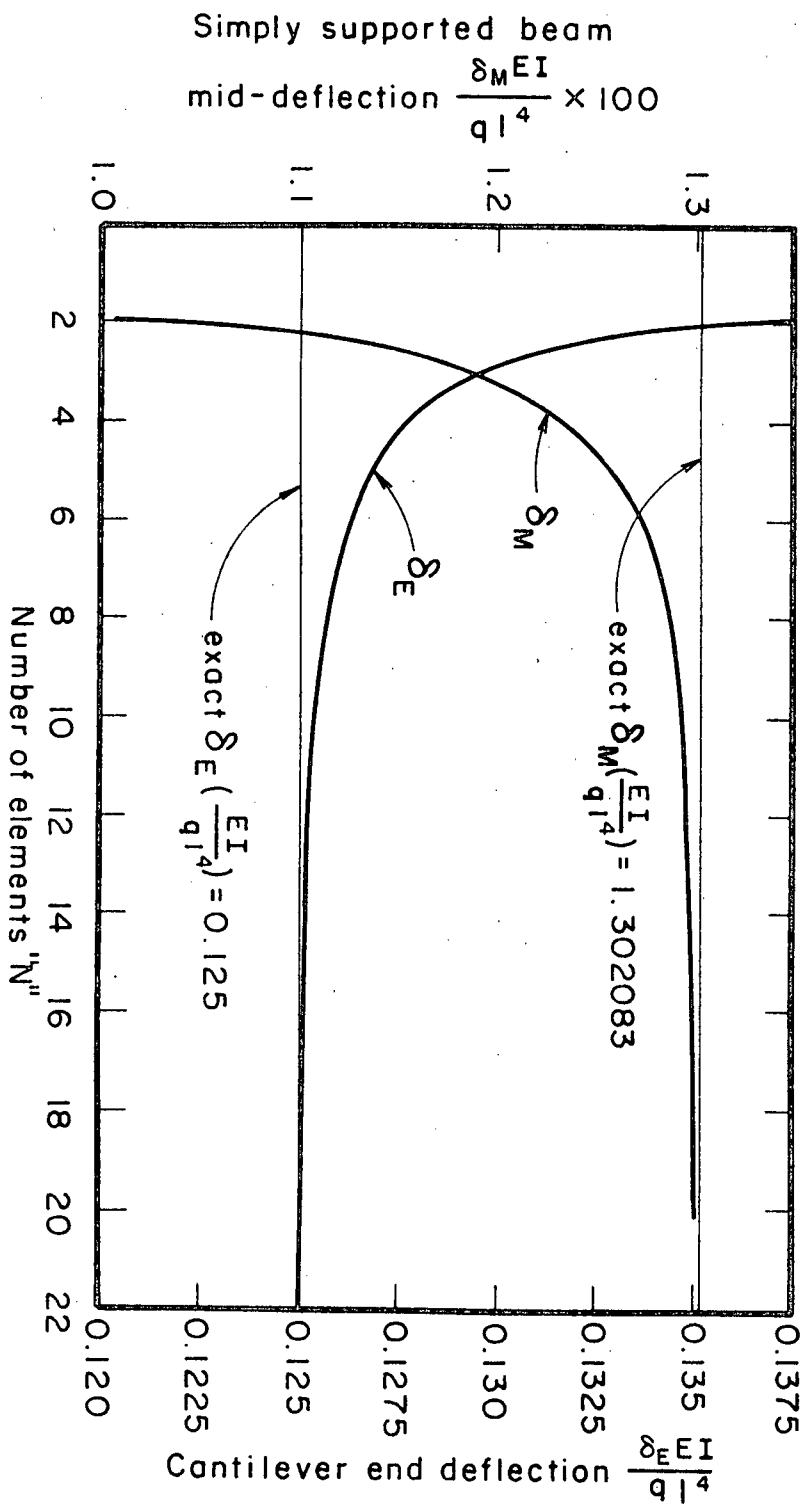


FIG.10(b): Two second order beam equations :  
displacement linear and moment linear.

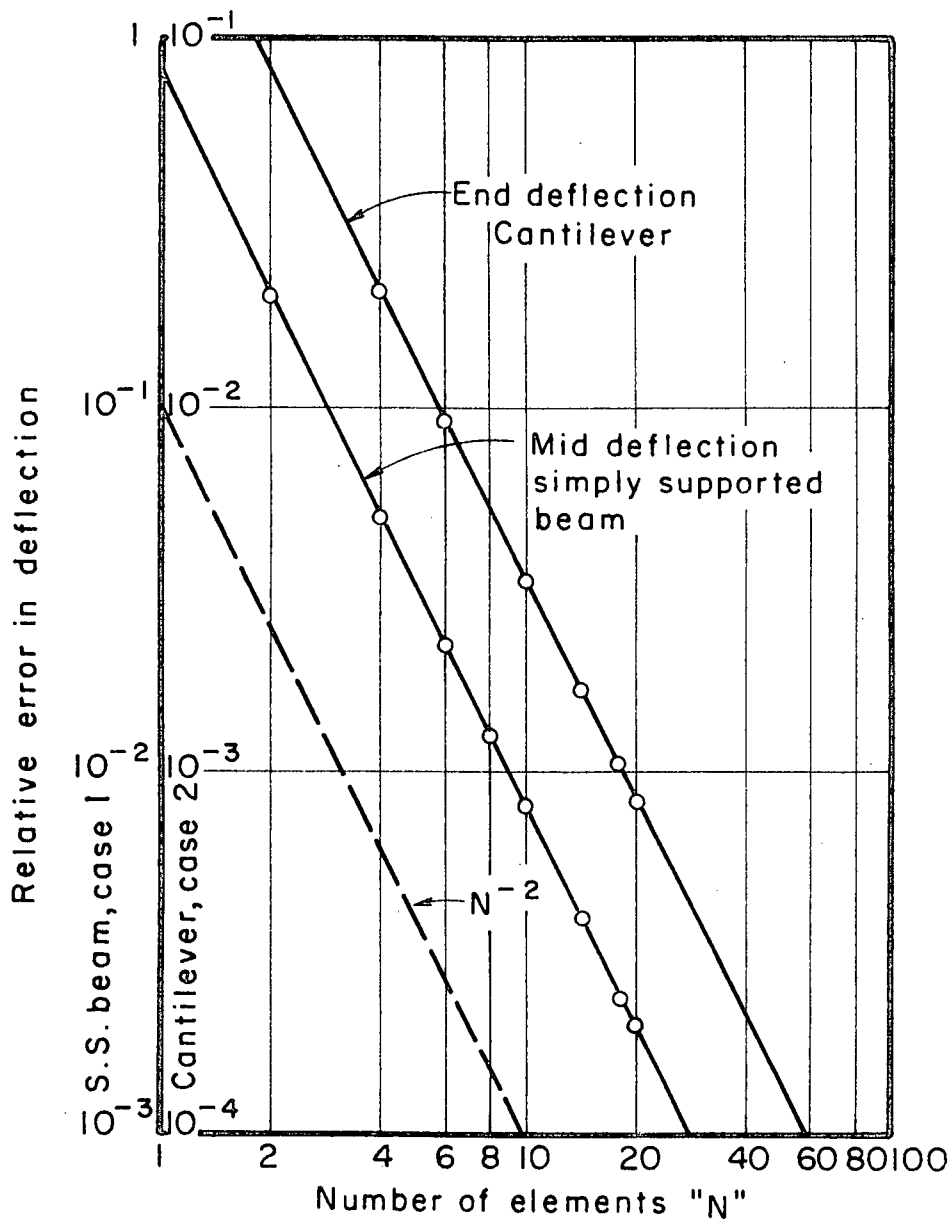


FIG.10(c): Two second order beam equations;  
displacement linear and moment linear.

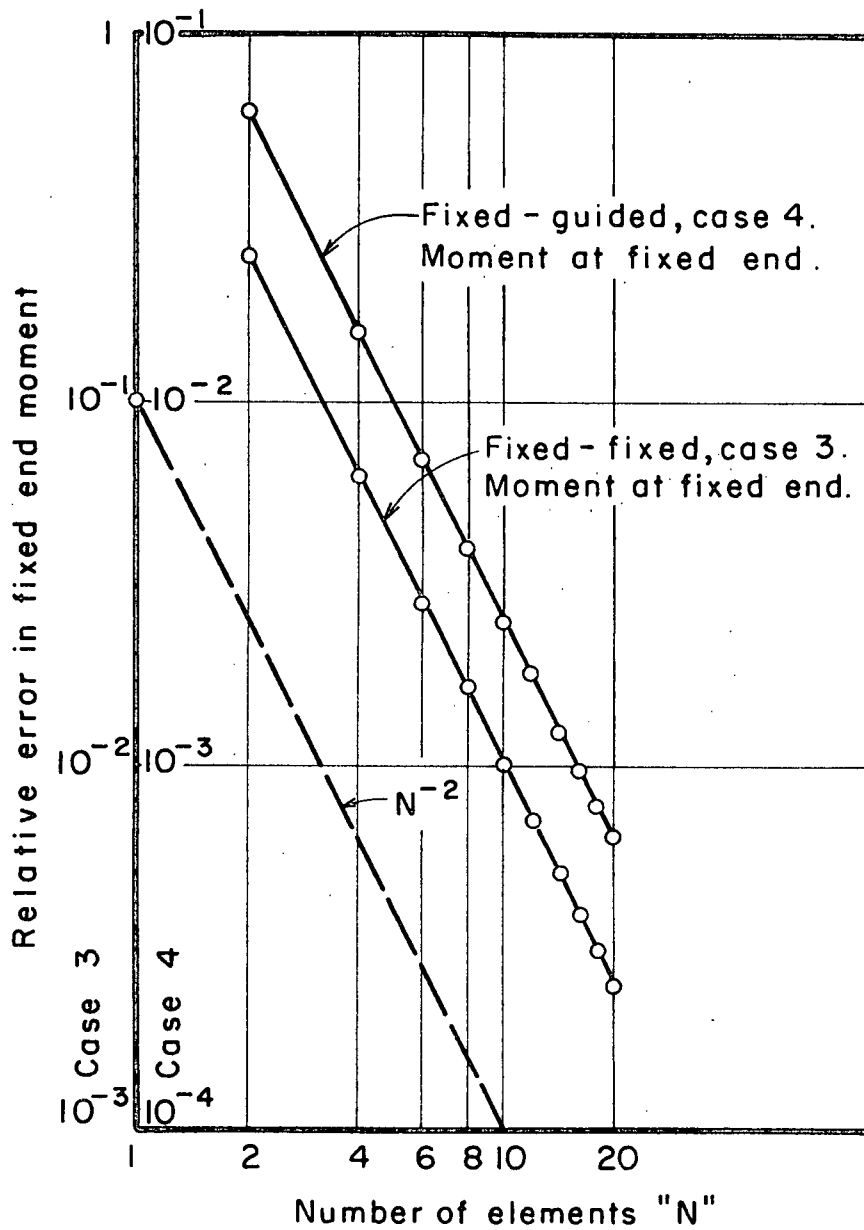


FIG. 10(d): Two second order beam equations;  
displacement linear and moment linear.

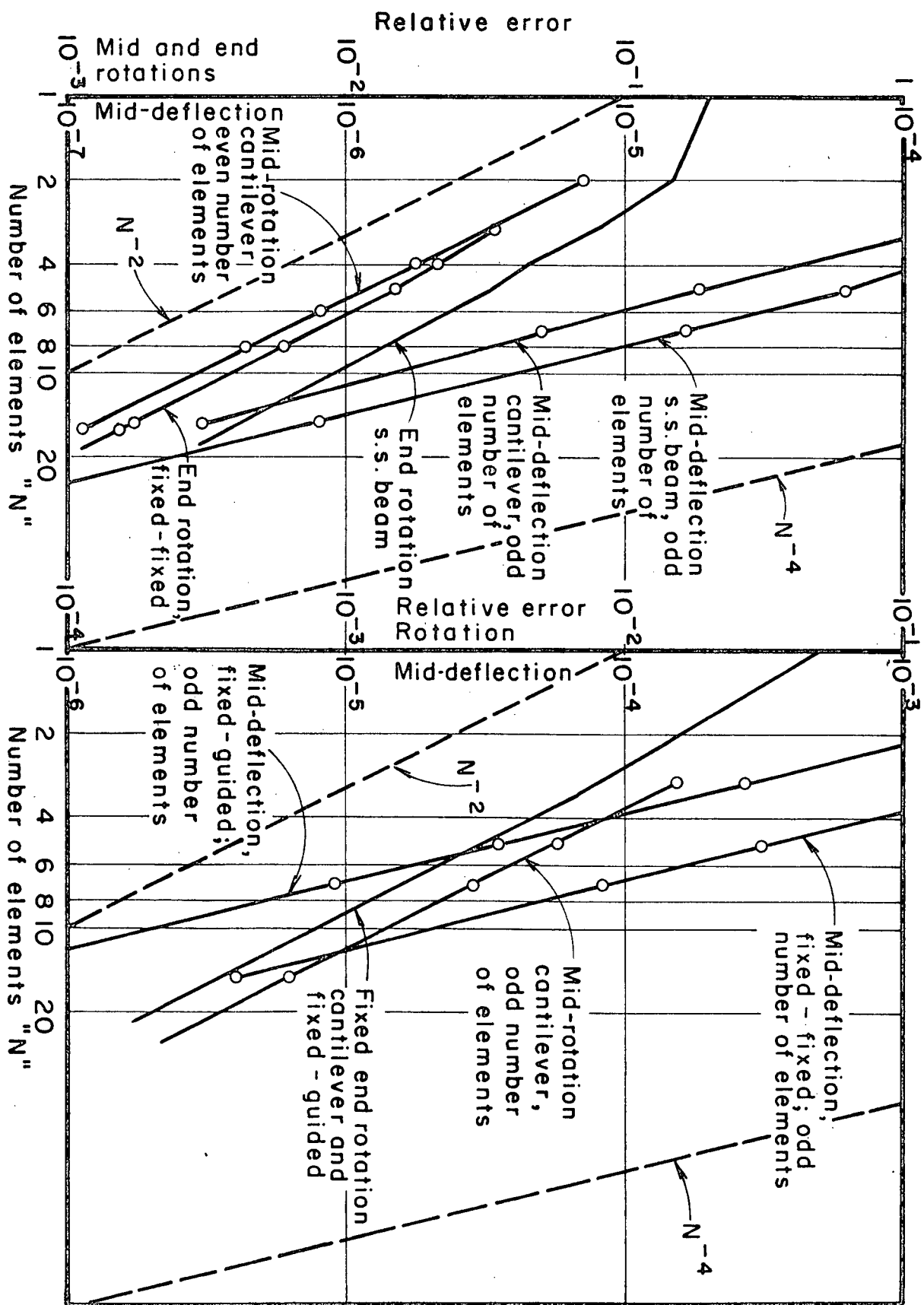


FIG.11: Two second order beam equations; displacement quadratic, moment quadratic.

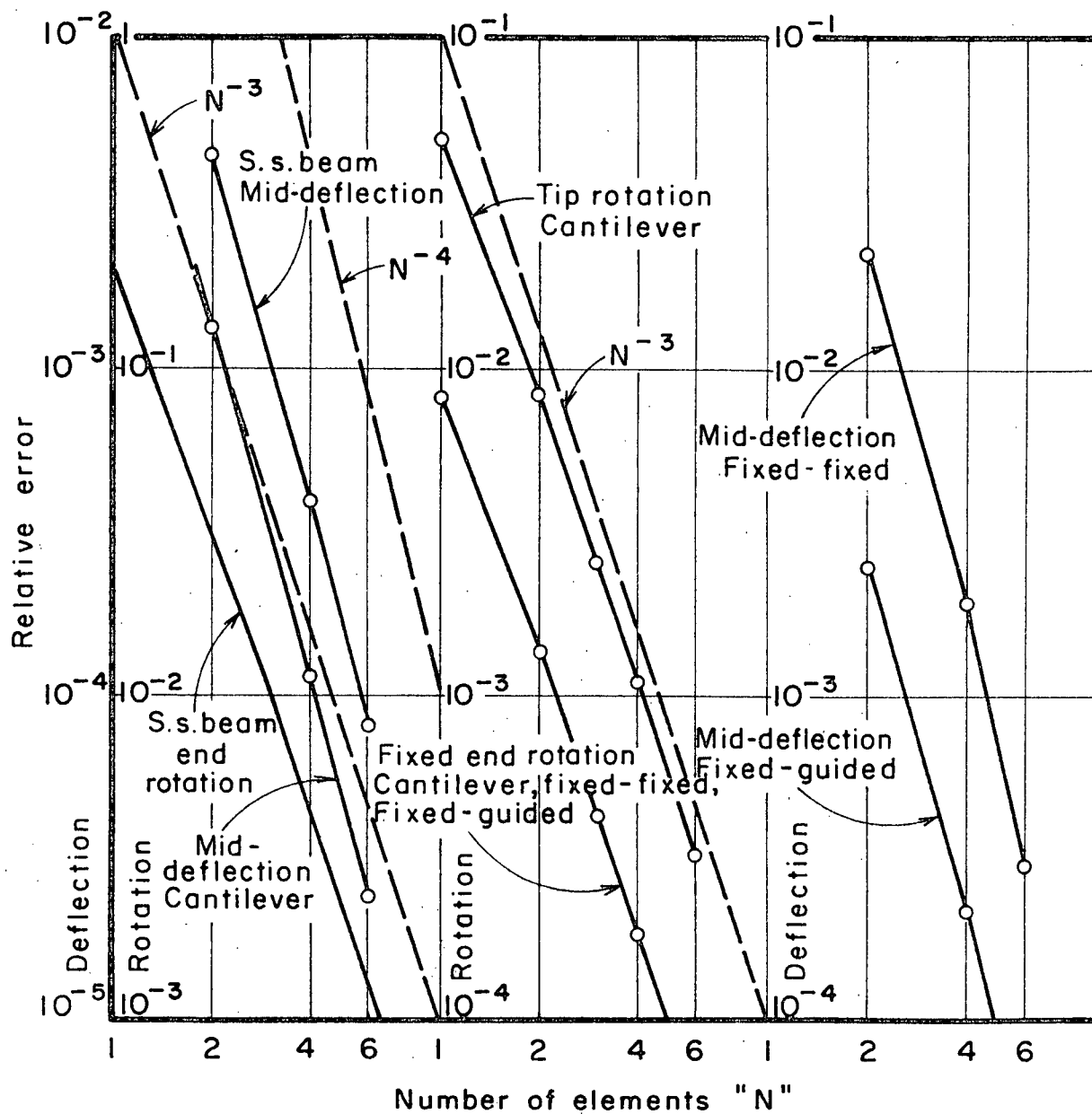


FIG.12: Two second order beam equations, displacement cubic and moment cubic.

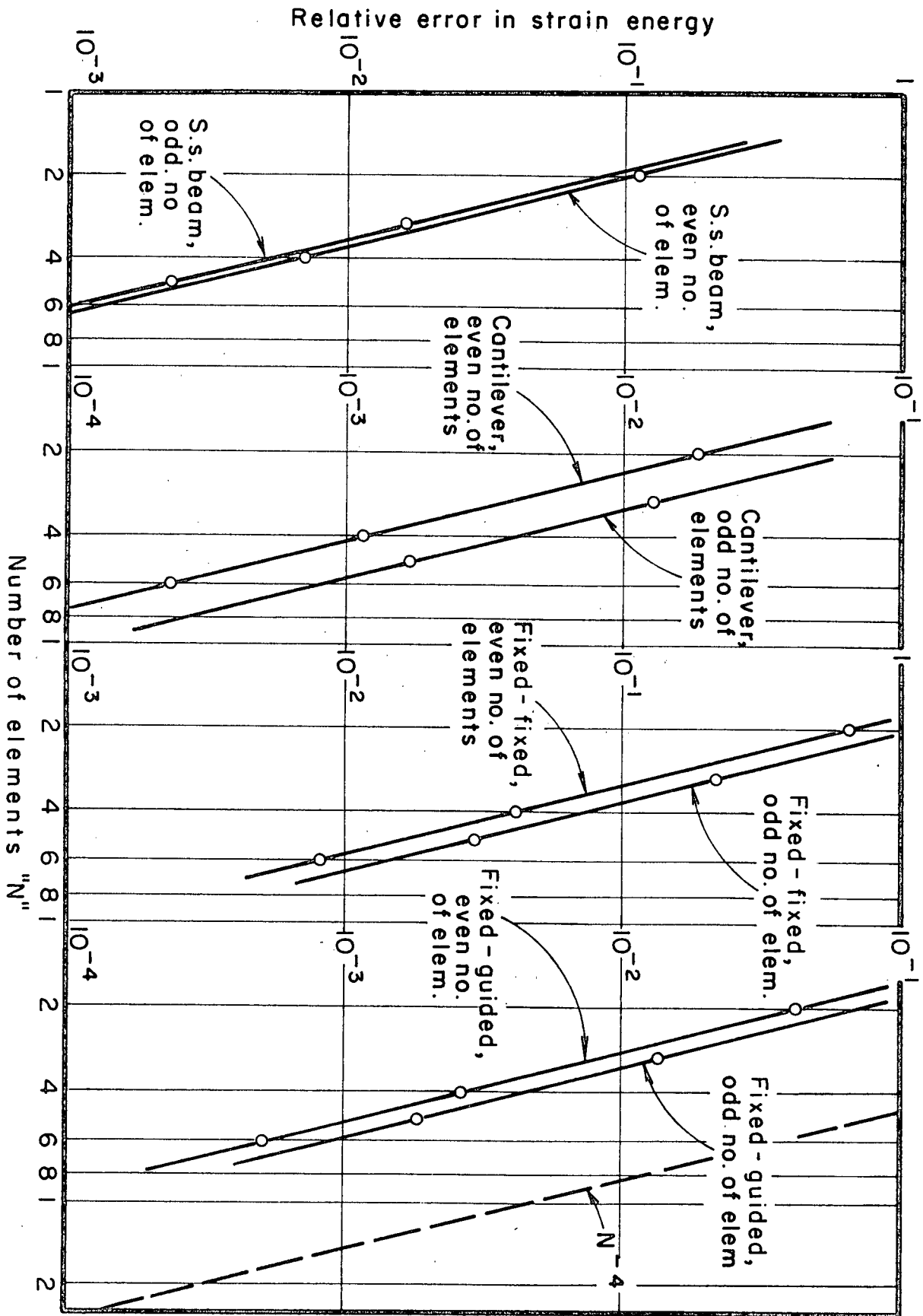


FIG. 13(a) Four first order beam equations, forced boundary conditions on  $v$  and  $M$ ;  $v, M, \Theta$  and  $V$  all linear.

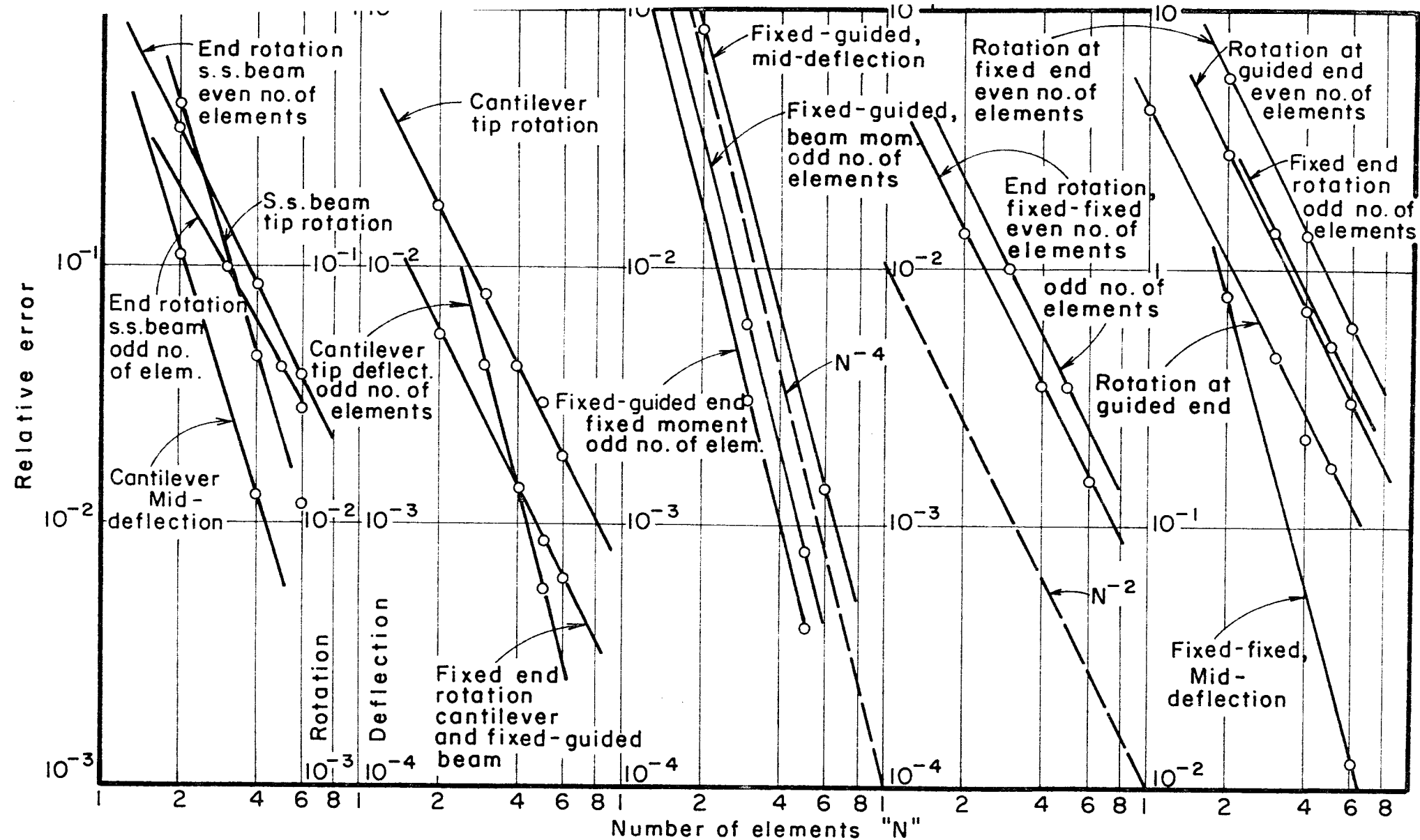


FIG.13(b): Four first order beam equations, forced boundary conditions on  $v$  and  $M$ ;  $v, M, \theta$  and  $V$  all linear.

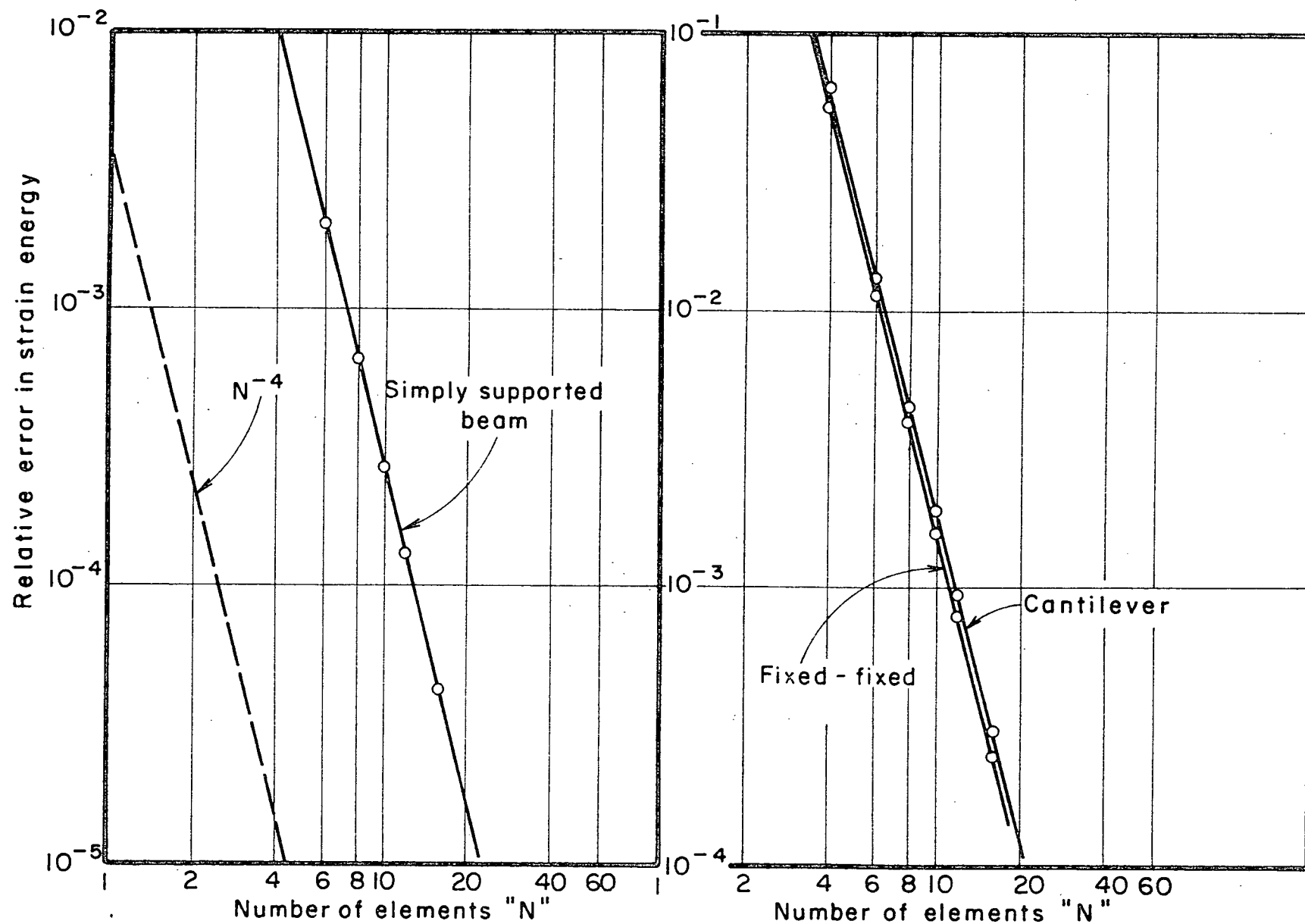


FIG.14: Four first order beam equations, forced boundary conditions on  $v$  and  $\theta$ ;  $v, \theta, M$  and  $V$  all linear.

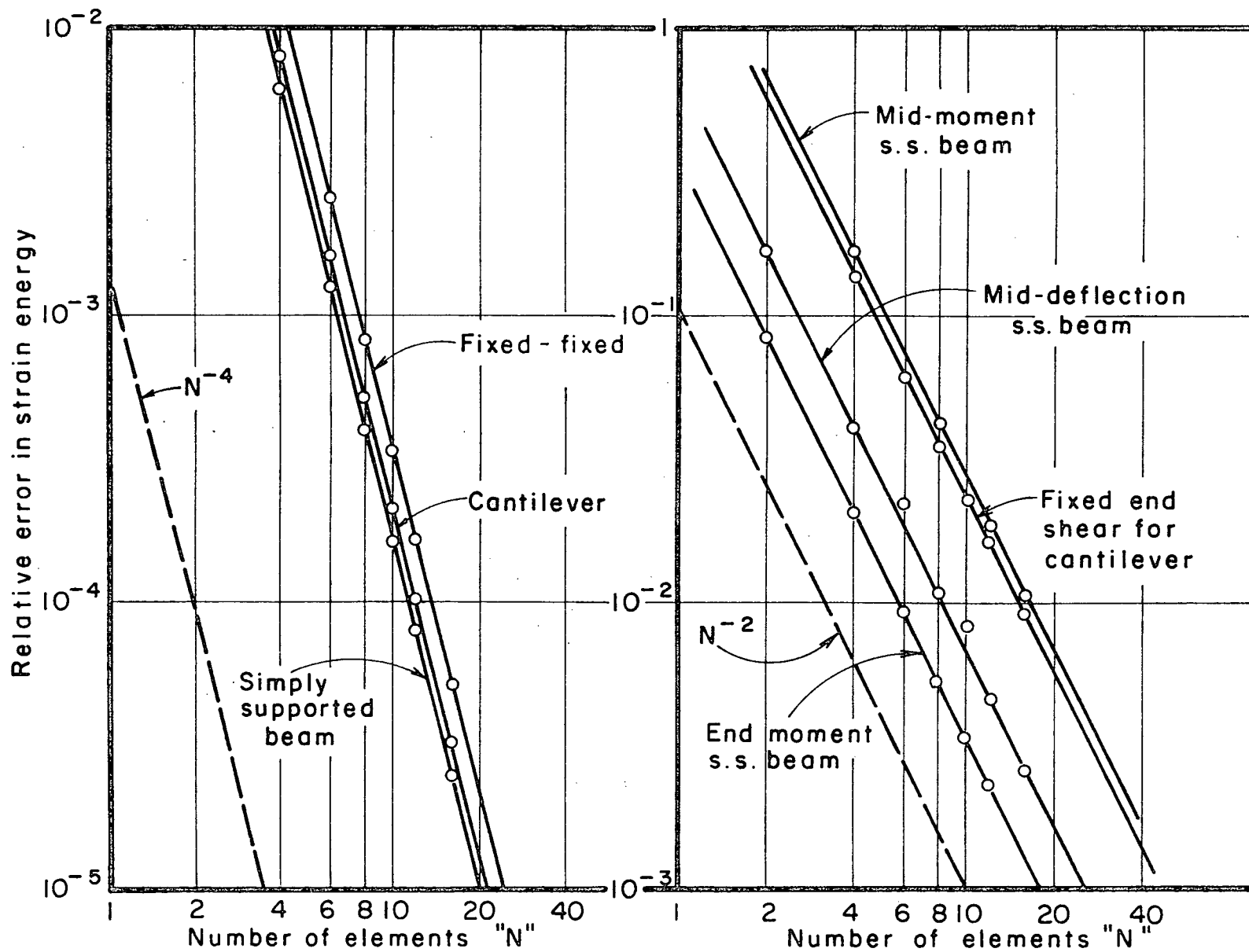


FIG.15(a) Four first order beam equations, forced boundary conditions on  $v$  and  $\Theta$ ; shear strain energy.

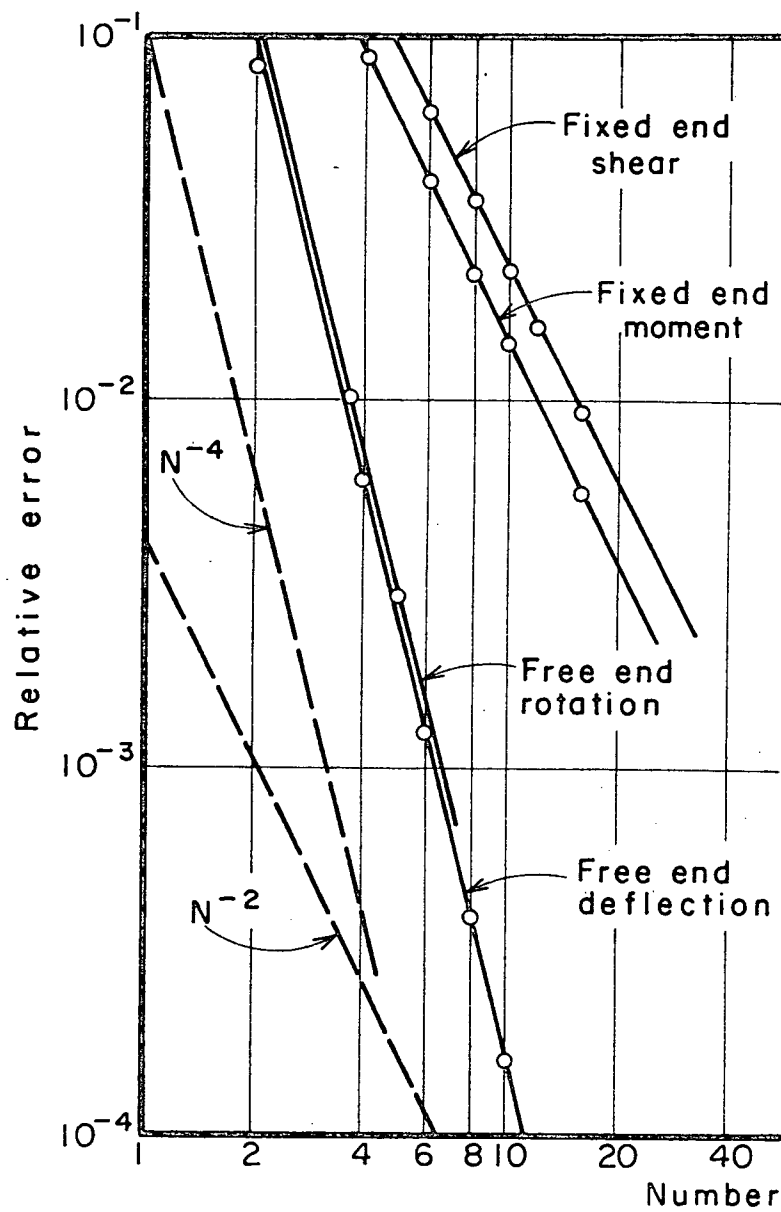


FIG.15(b) Cantilever

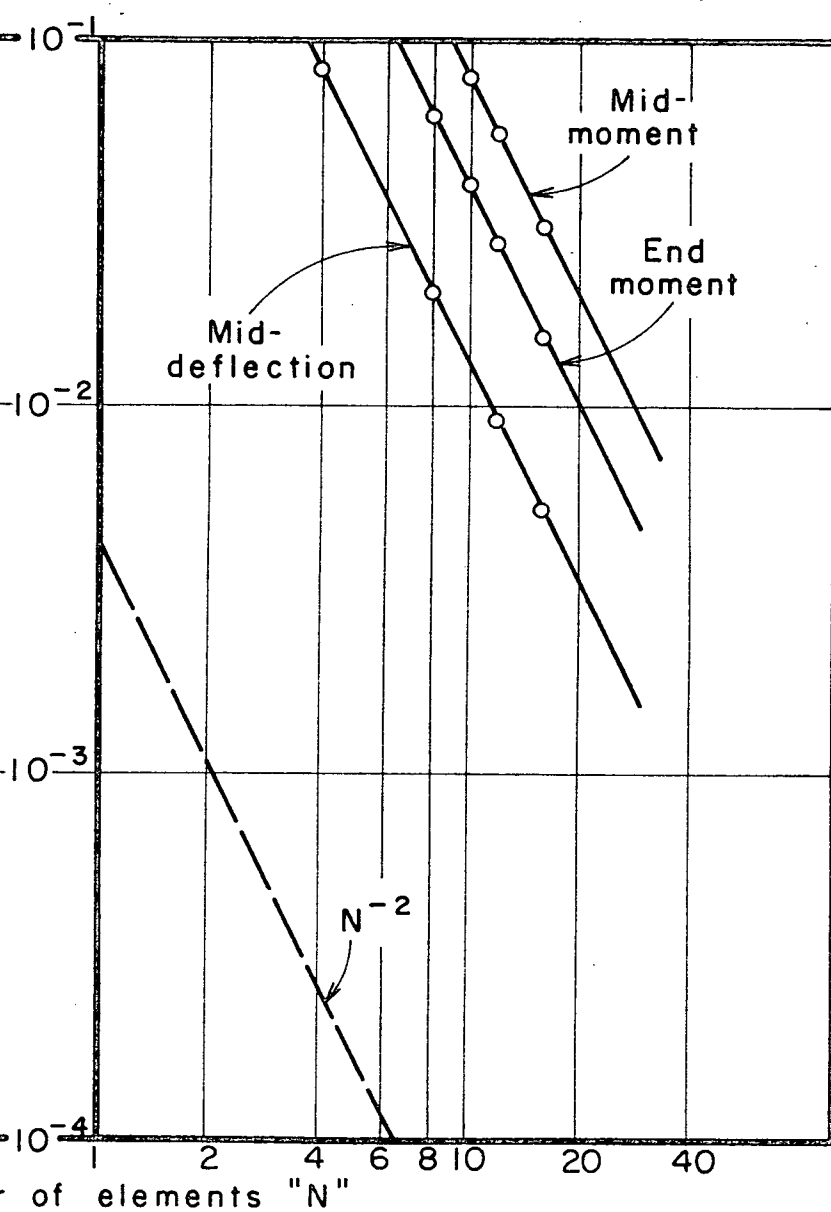


FIG.15(c) Beam clamped at both ends.

FIGS.15: Four first order beam equations, forced boundary conditions on  $v$  and  $\theta$ , shear strain energy included.

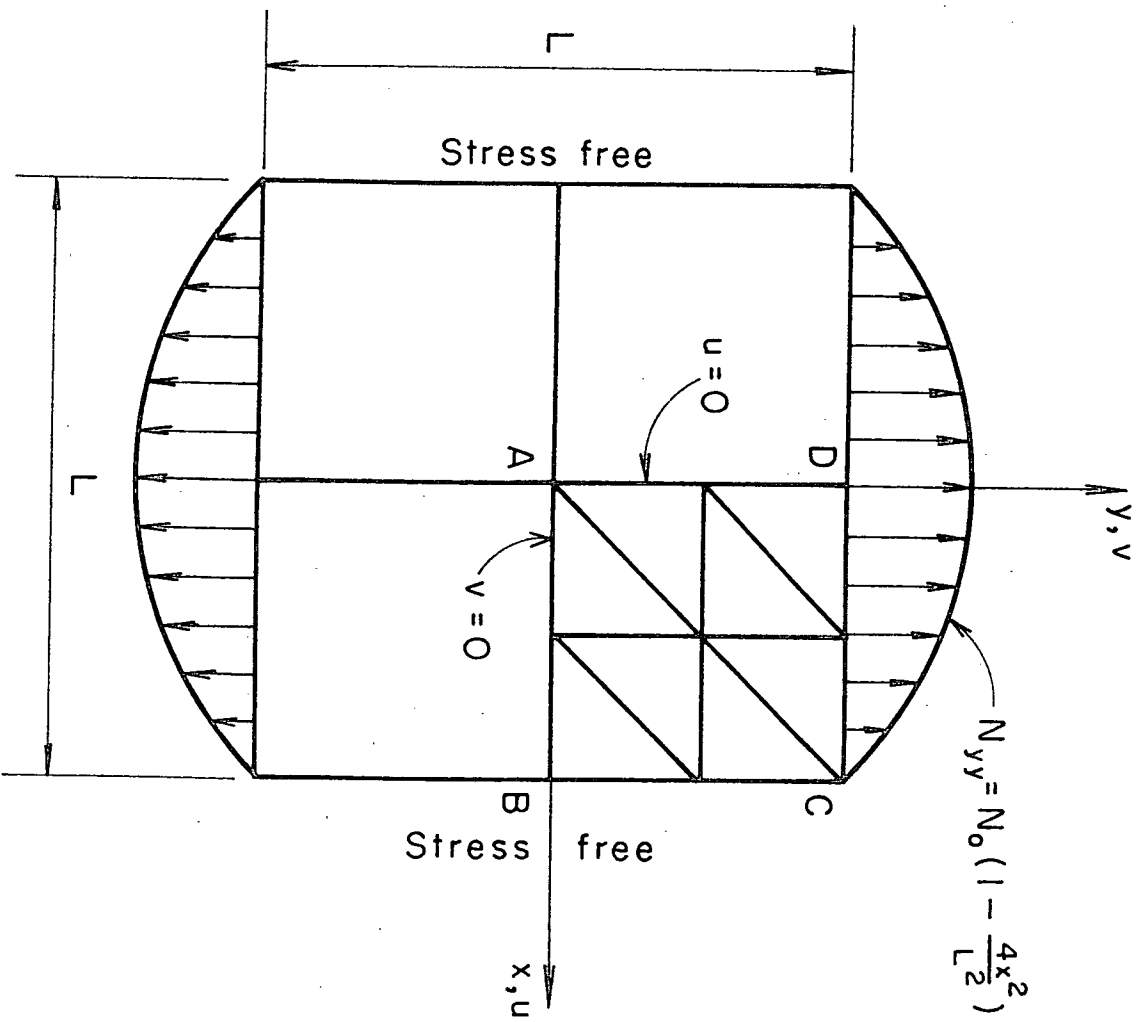
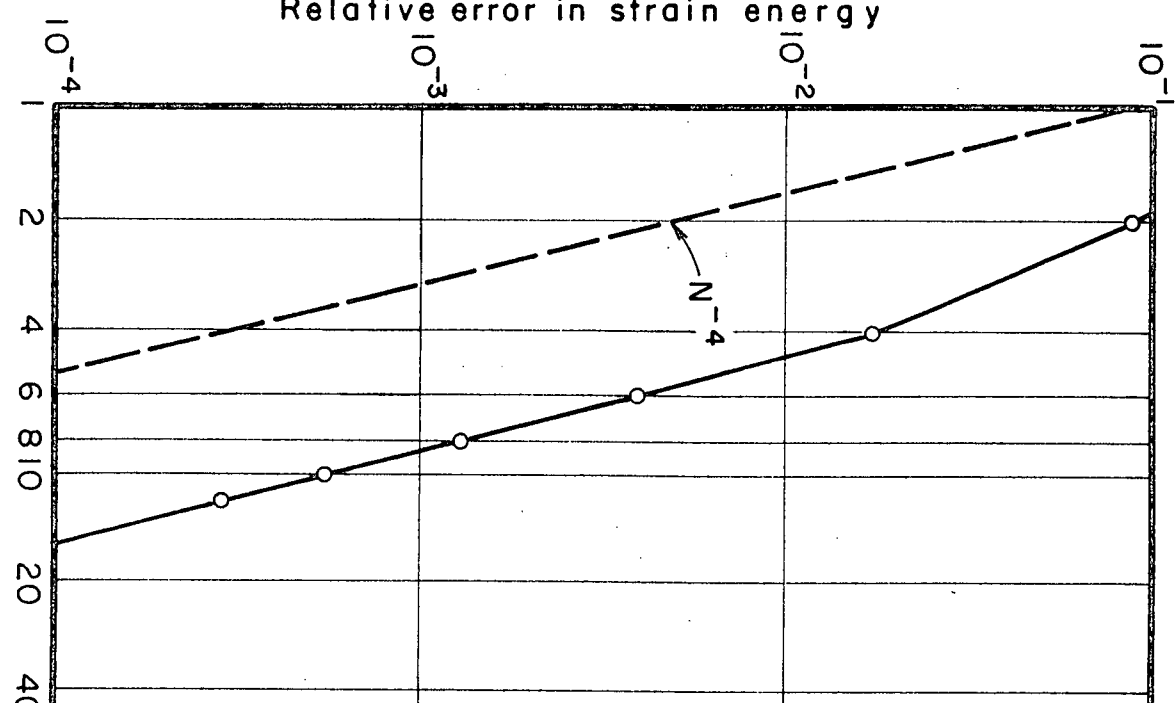


FIG. 16: Parabolically loaded plane stress problem ( $N=4$ ).

Relative error in strain energy



Relative error in displacement

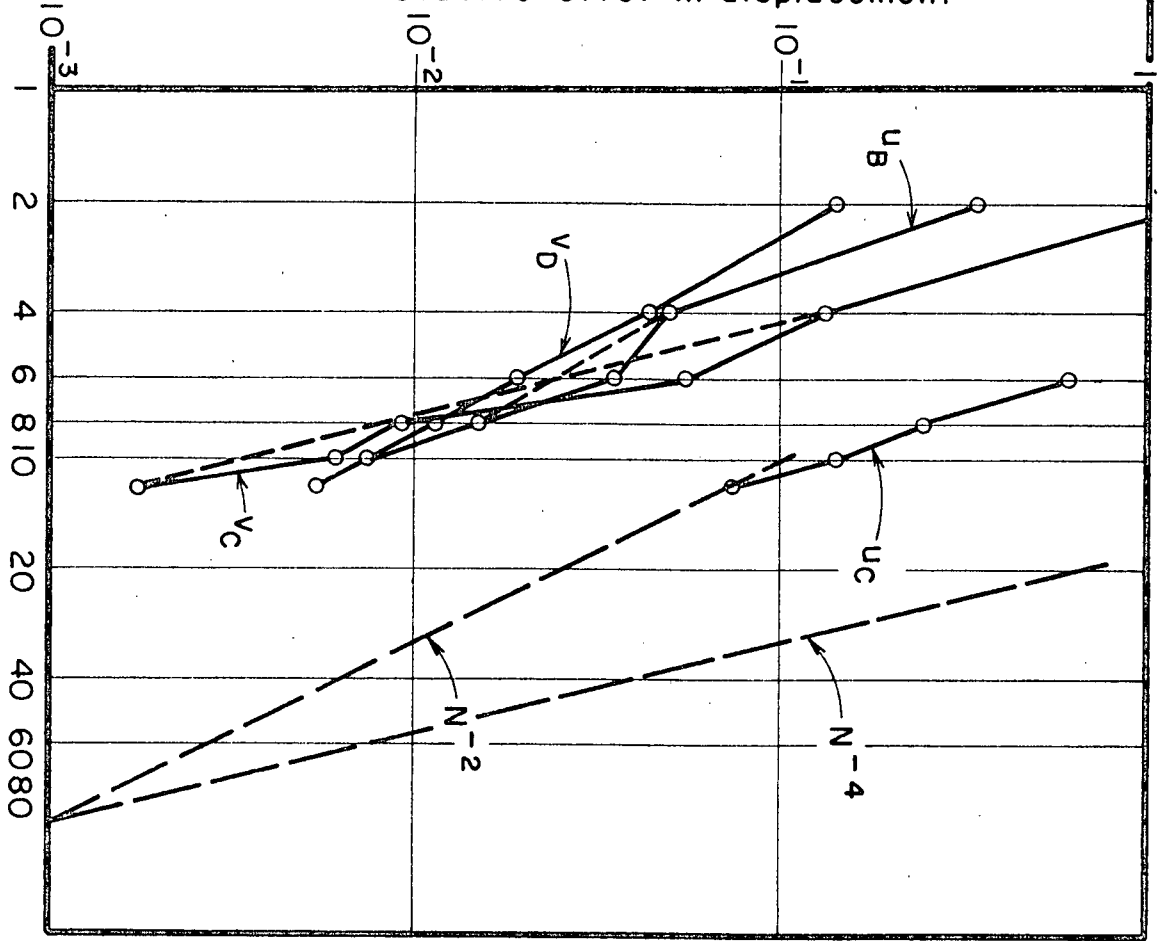


FIG.17(a): Strain energy convergence for parabolically loaded square plate; plane stress, mixed element. FIG.17(b): Displacement convergence for parabolically loaded square plate; plane stress, mixed element.

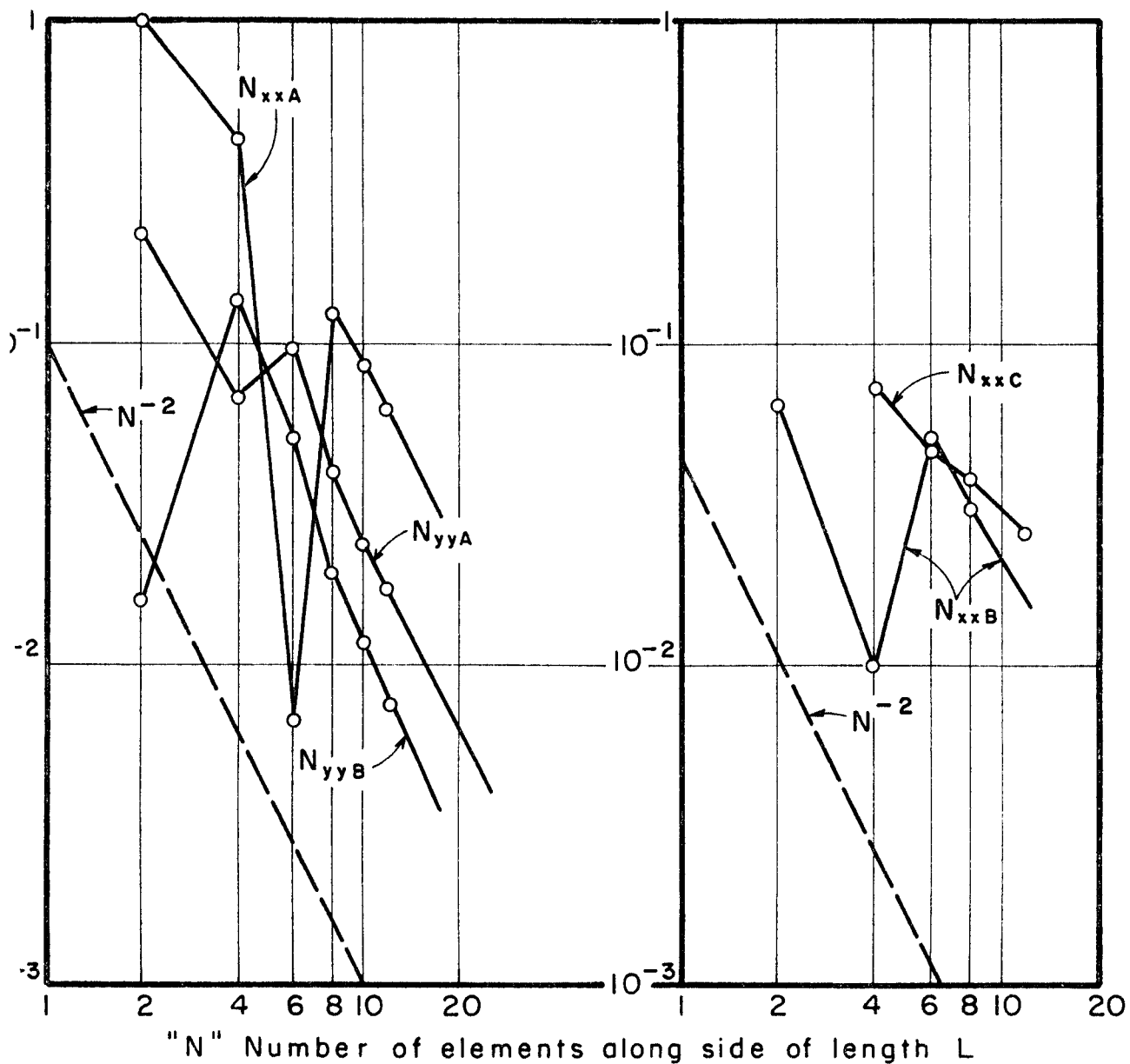


FIG.17(c): Stress convergence.

FIG.17 : Parabolically loaded plane stress problem using mixed element; displacements and stresses linear.

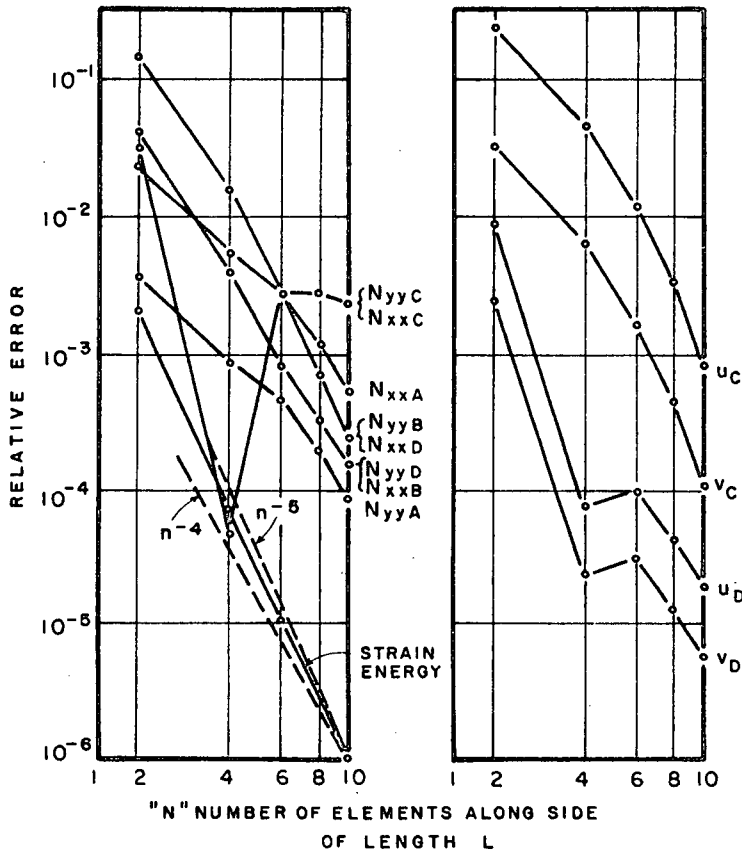


FIG.18: Parabolically loaded plane stress problem using displacement element (cubic displacements), Ref. [5].

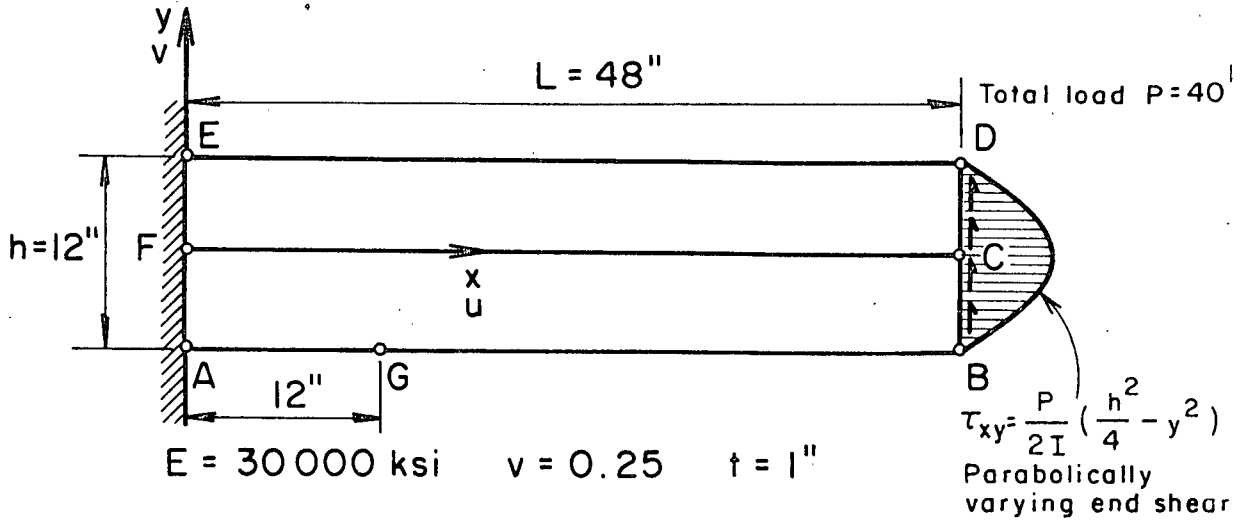


FIG.19(a) Cantilever beam and load system.

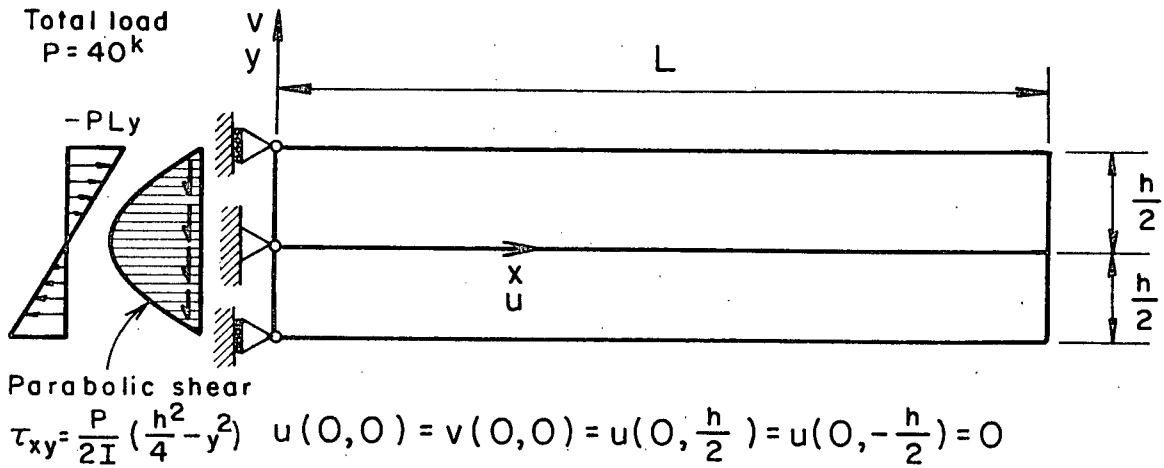


FIG.19(b) Fixed end boundary conditions B.C.1.

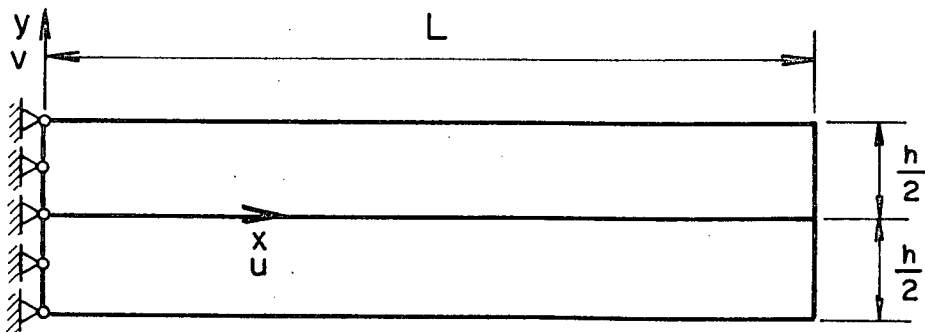


FIG.19(c) Fixed end boundary conditions B.C.2.

FIGS.19: Linear elasticity cantilever problem and forced boundary conditions used.

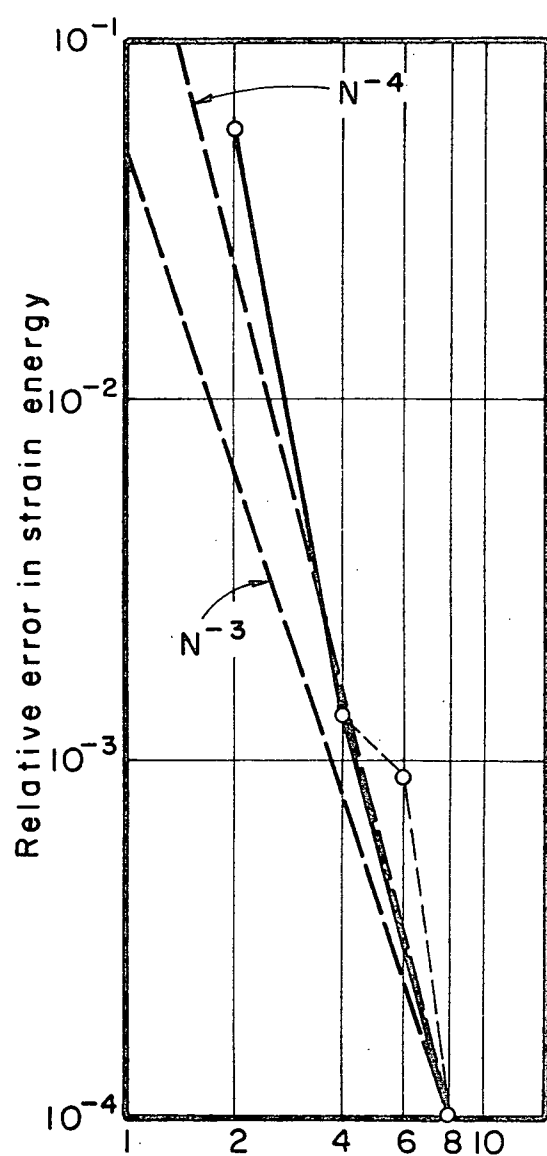


FIG.20(a)

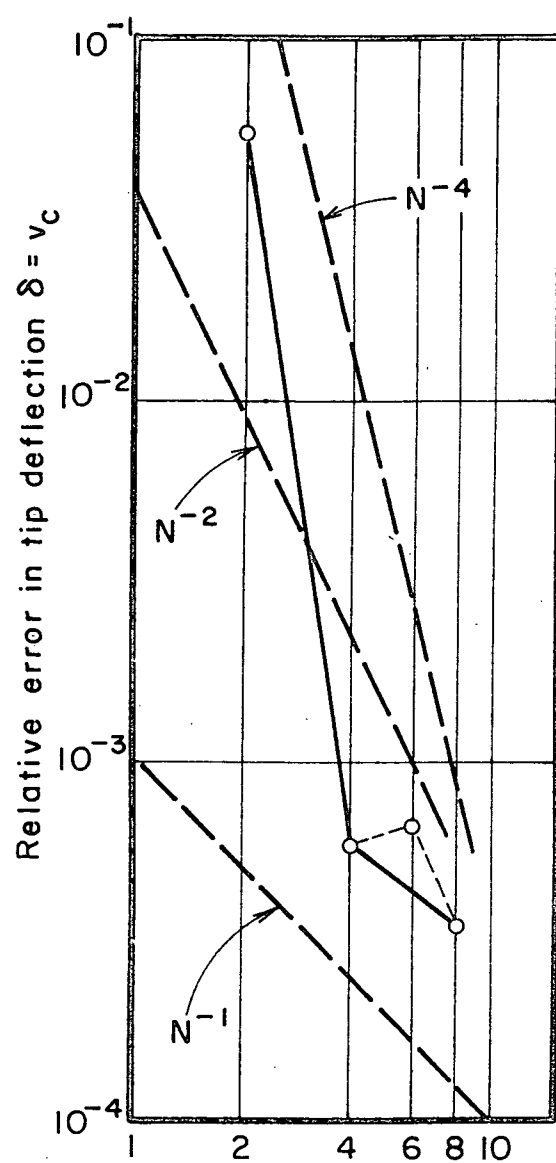


FIG.20(b)

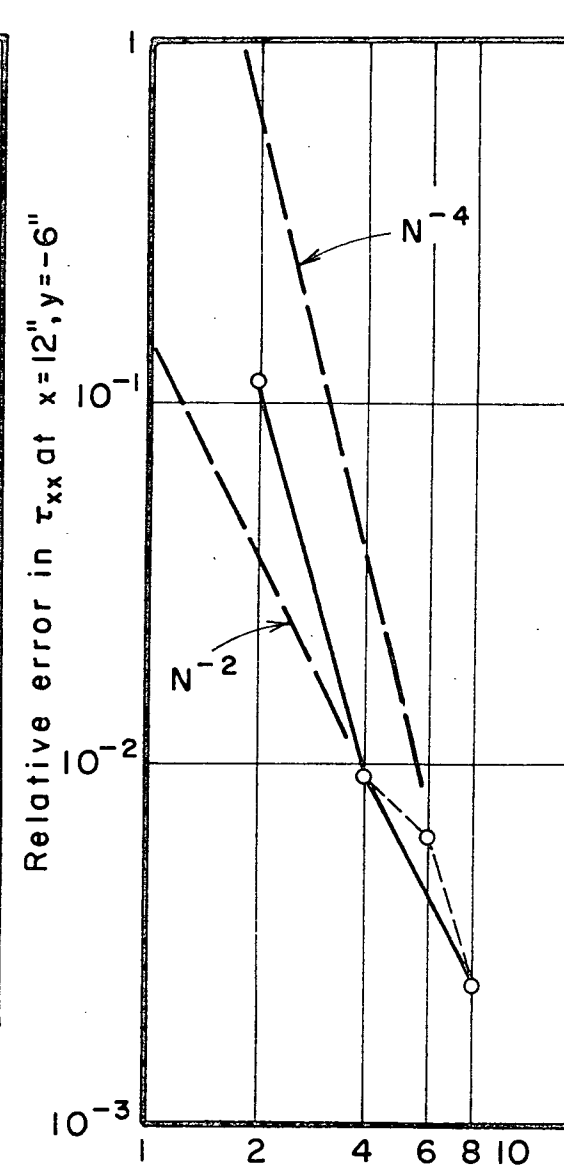
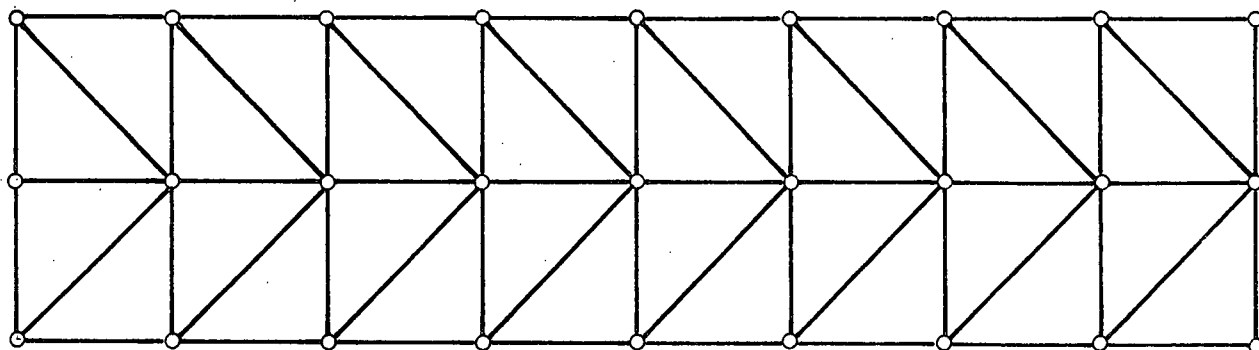
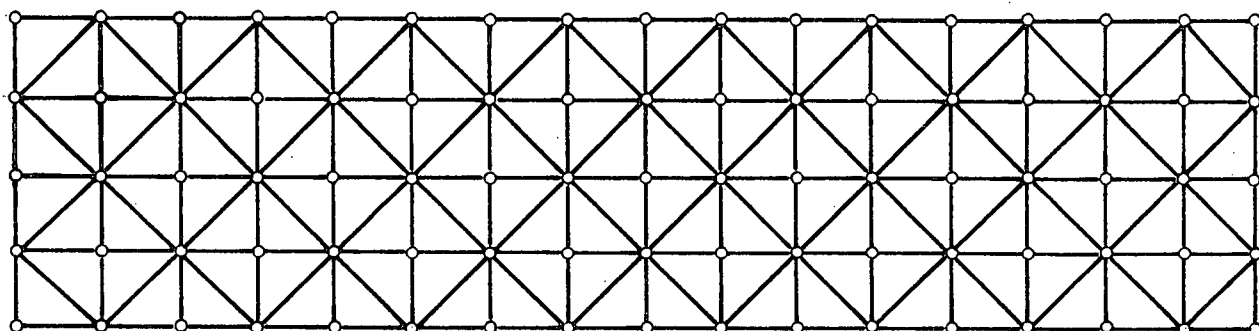


FIG.20(c)

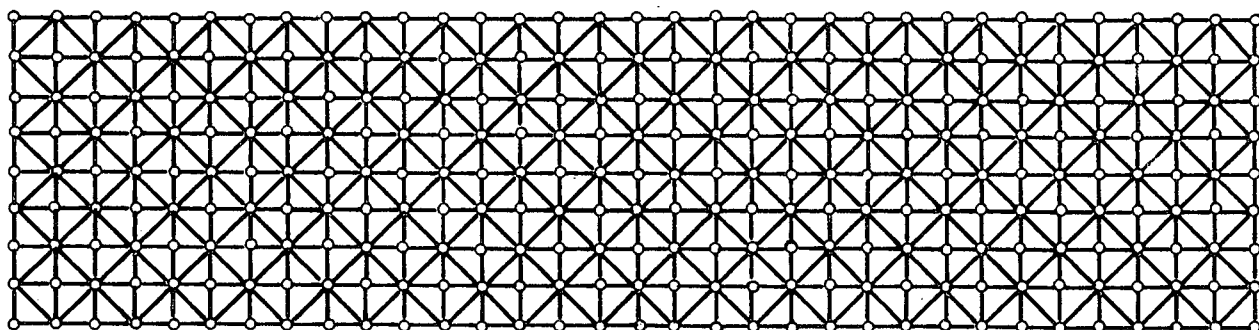
FIG.20: Convergence plots for the cantilever with boundary conditions B.C.1, using mixed finite elements; stresses and displacements all linear.



MESH A-1 - 32 C.S.T's  $N = 2$



MESH A-2 - 128 C.S.T's  $N = 4$



MESH A-3 - 512 C.S.T's  $N = 8$

FIG.21(a): Grids used for the constant stress triangular elements .

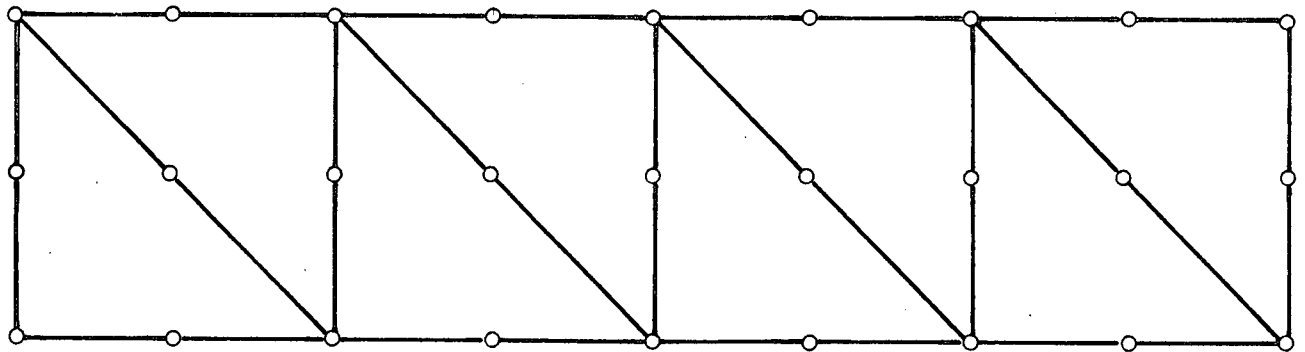
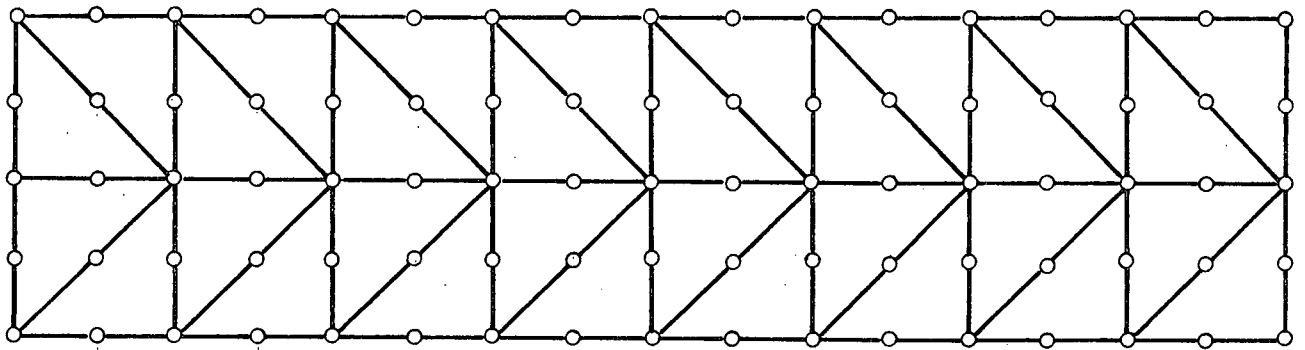
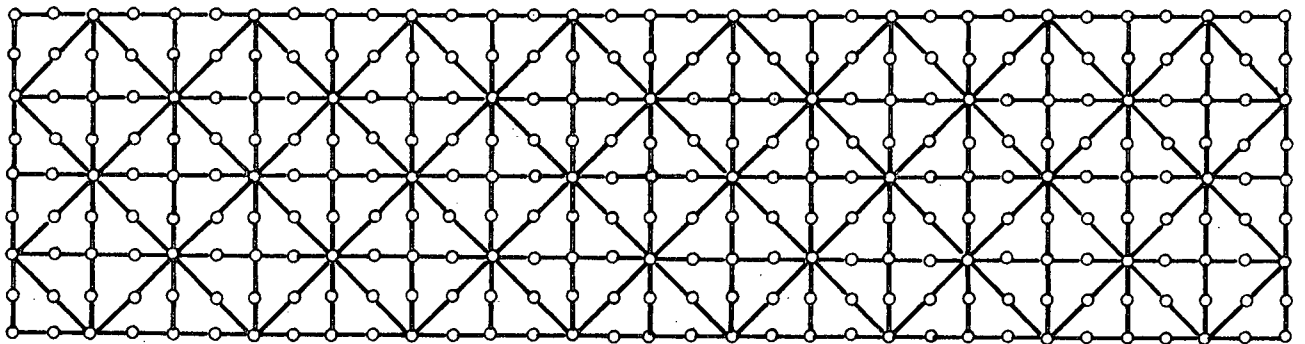
MESH B-1 - 8 L.S.T's  $N = 1$ MESH B-2 - 32 L.S.T's  $N = 2$ MESH B-3 - 128 LST's  $N = 4$ 

FIG.21(b): Grids used for the linear stress triangles.

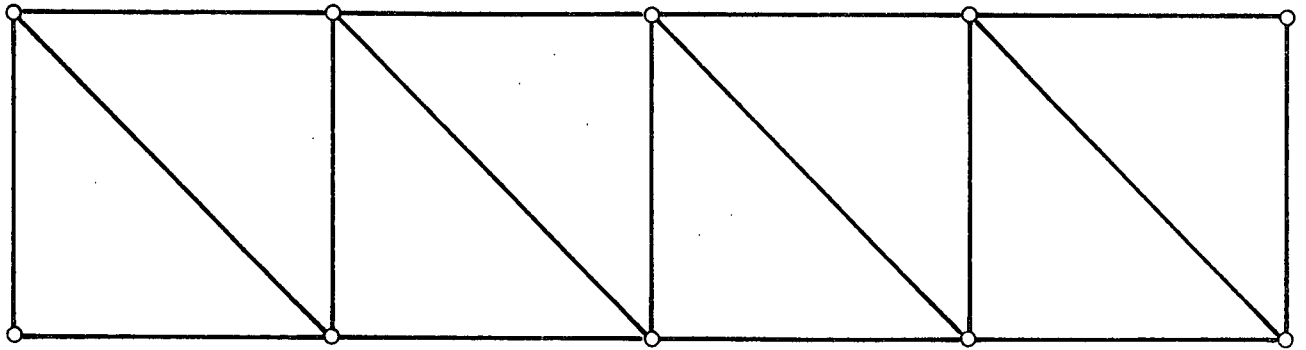
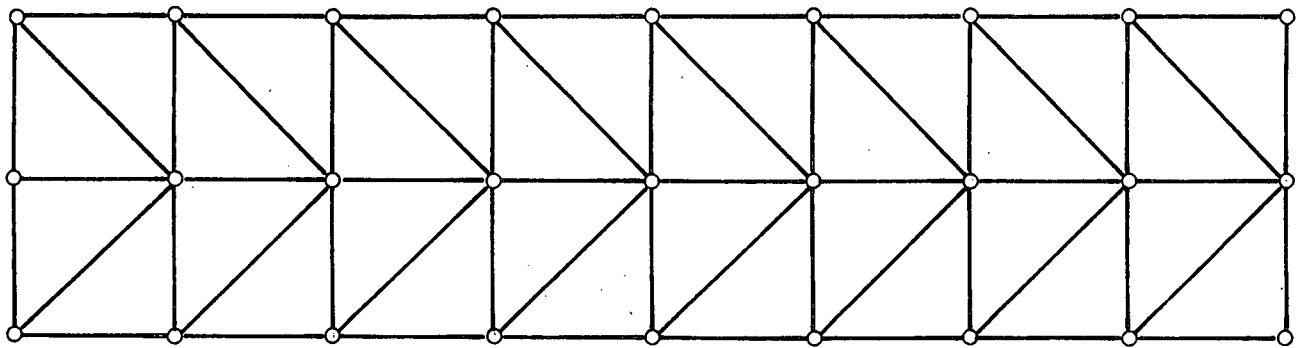
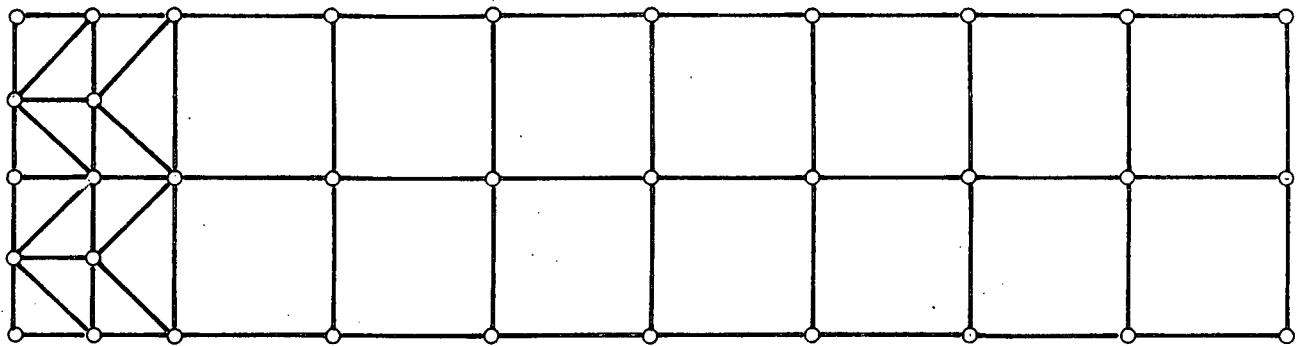
MESH C-1 - 8 Q.S.T's  $N = 1$ MESH C-2 - 32 Q.S.T's  $N = 2$ MESH C-3 - 42 Q.S.T's  $N = 4$ 

FIG.21(c): Grids used for the quadratic stress triangles.

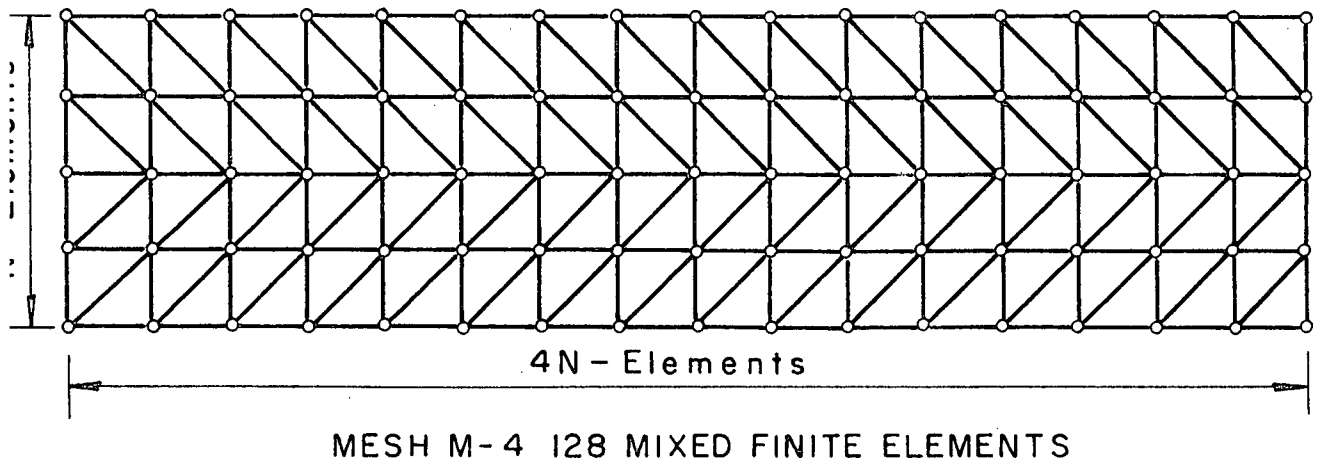
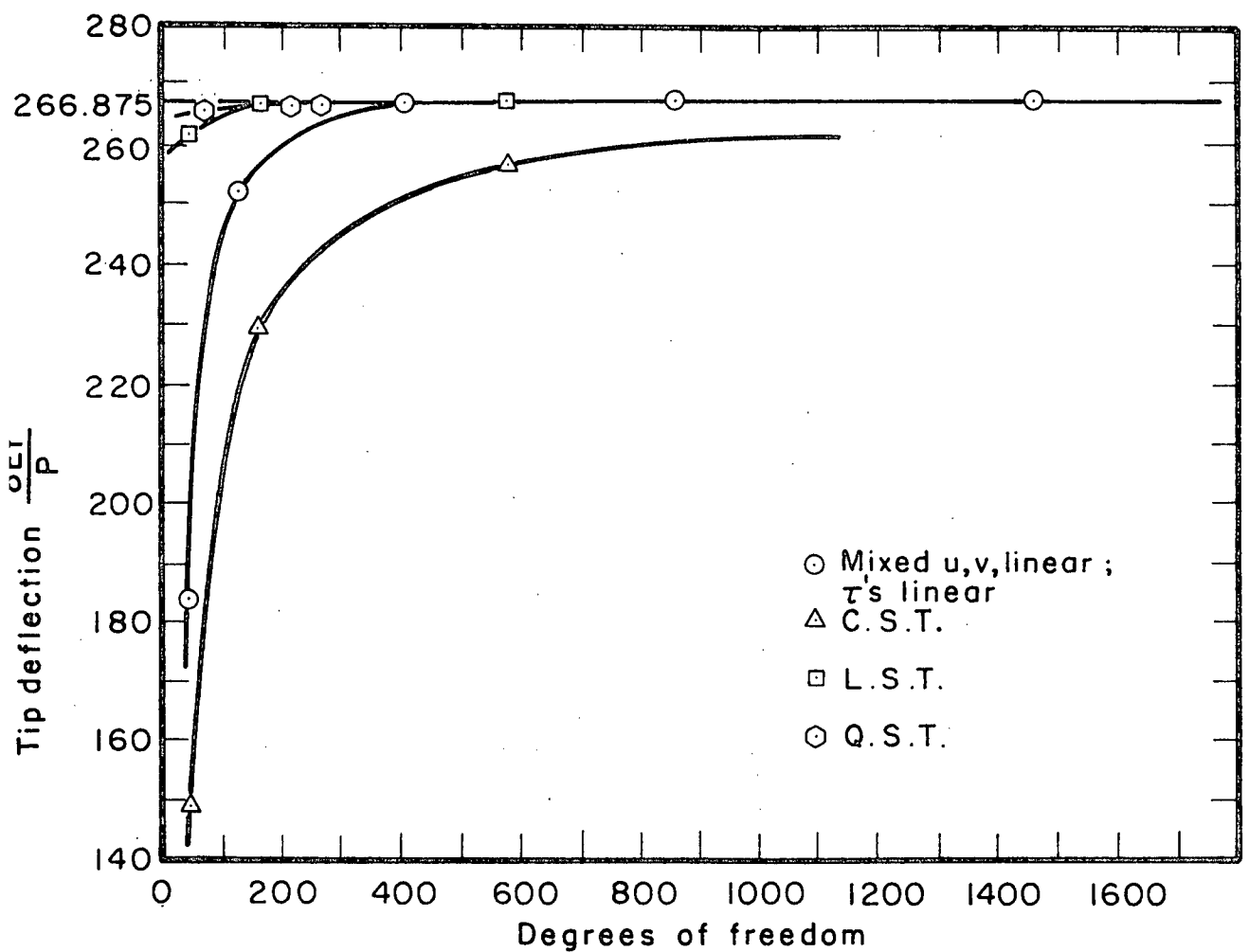
FIG.22: Typical mesh used for mixed finite element ( $N=4$ ).

FIG.23 (a): Plot of tip deflection vs. total degrees of freedom.

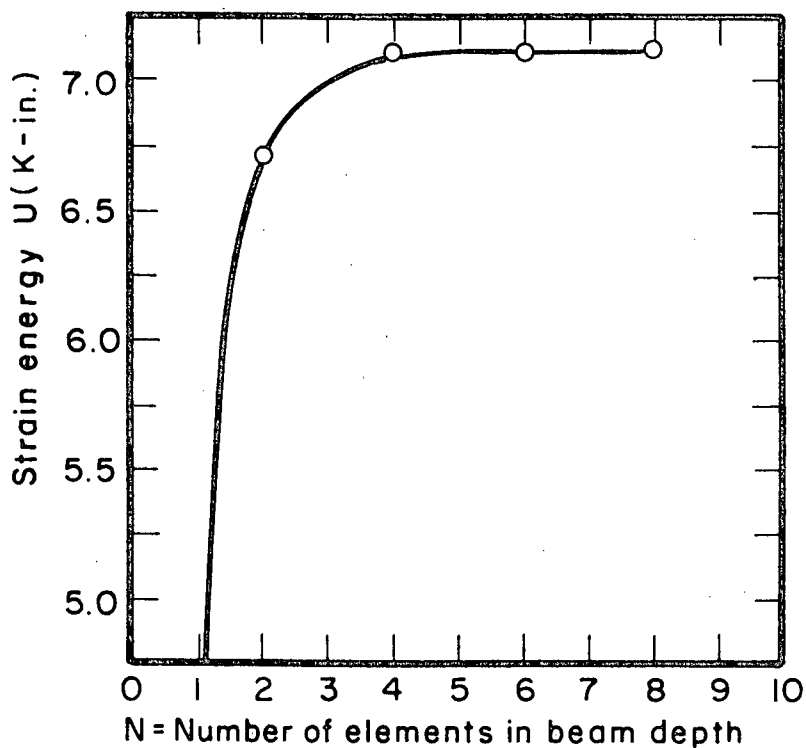


FIG. 23(b): Plot of strain energy versus number of elements in beam depth.

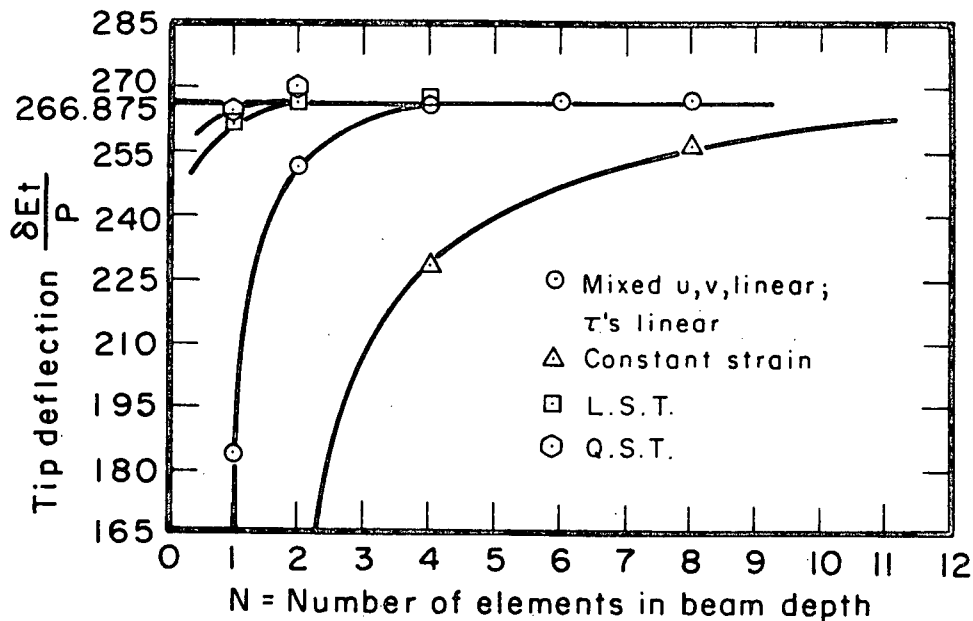


FIG. 23(c): Plot of tip deflection versus number of elements in beam depth.

FIGS. 23: Plots for the cantilever with boundary conditions B.C. 2, using mixed finite element; stresses and displacements all linear.

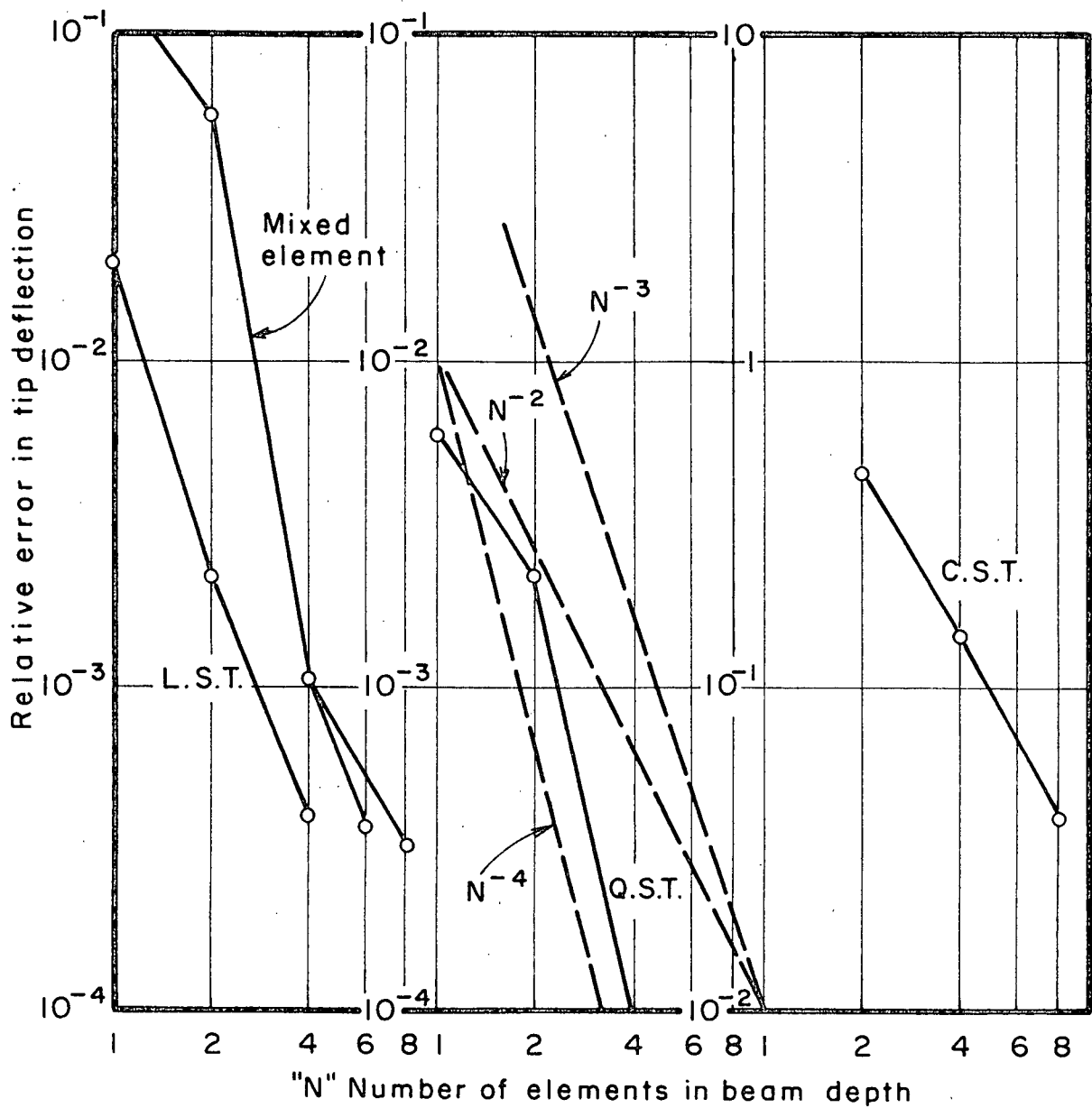


FIG. 24: Convergence of tip deflection for C.S.T., L.S.T., Q.S.T., and mixed finite element with stresses and displacements linear for boundary conditions B.C.2.

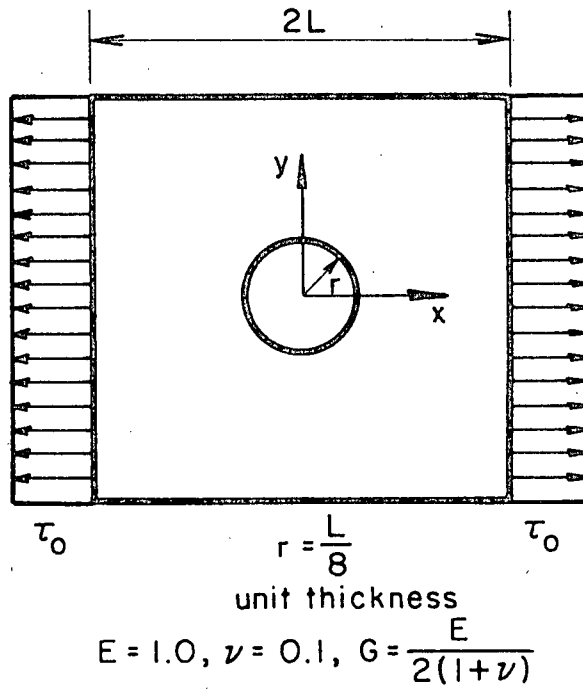


FIG.25(a): Isotropic case.

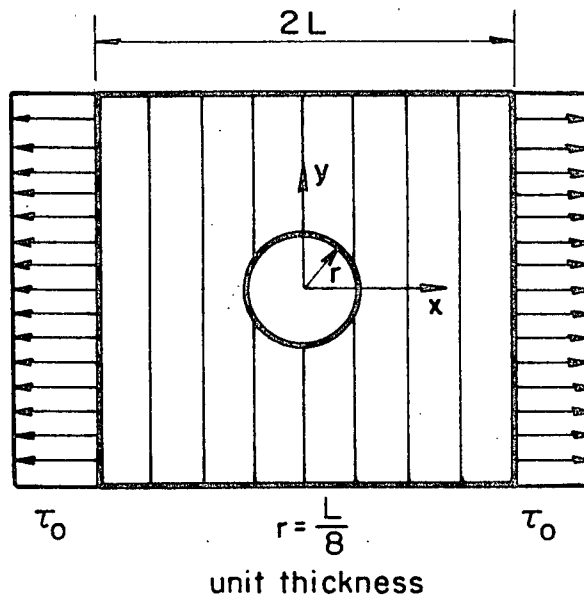


FIG.25(b): Orthotropic case.

FIGS.25: Model for infinite plate by a square plate with a circular hole at centre, isotropic and orthotropic.

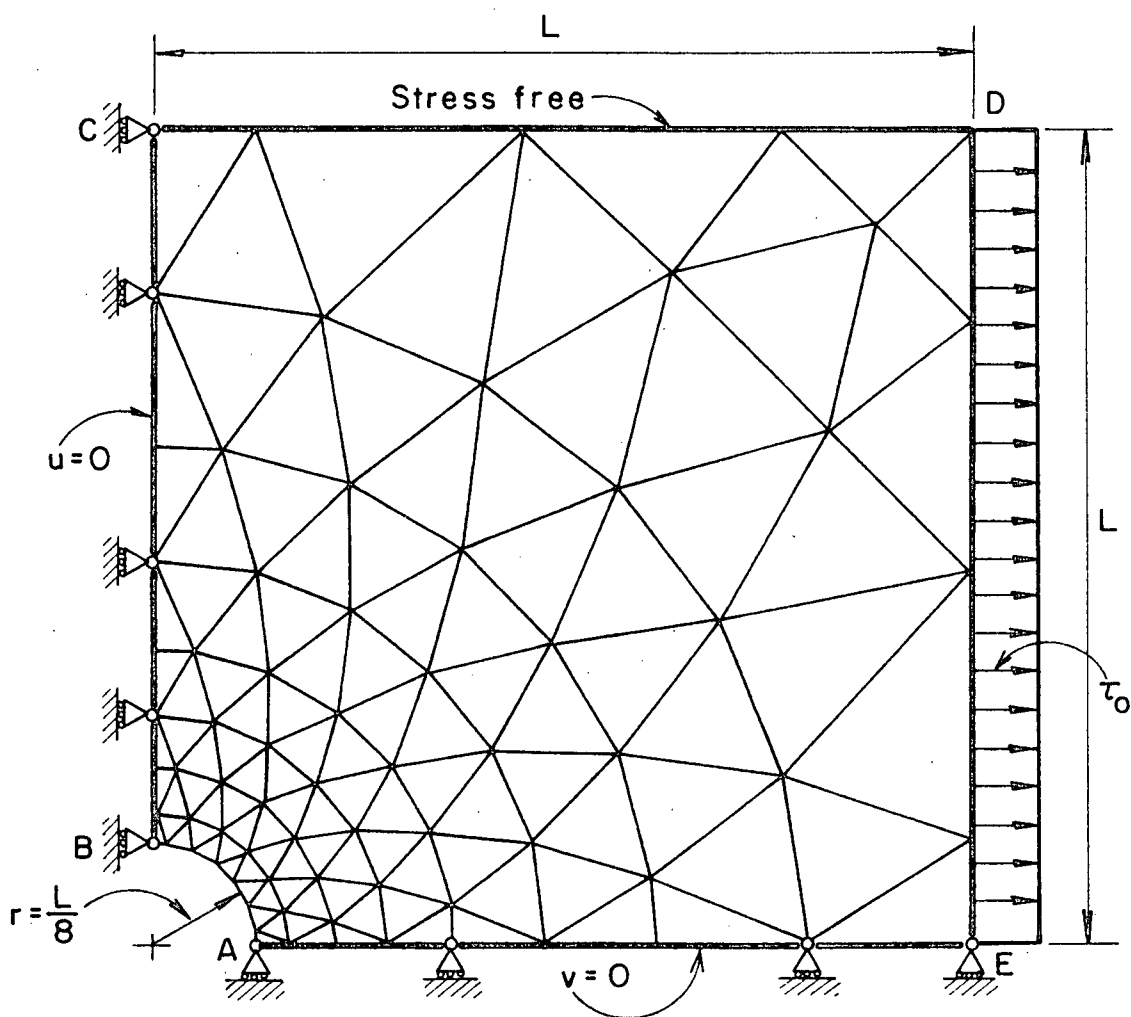


FIG.26: Finite element grid for the square plate with a circular hole in the middle.  
Isotropic and orthotropic cases.

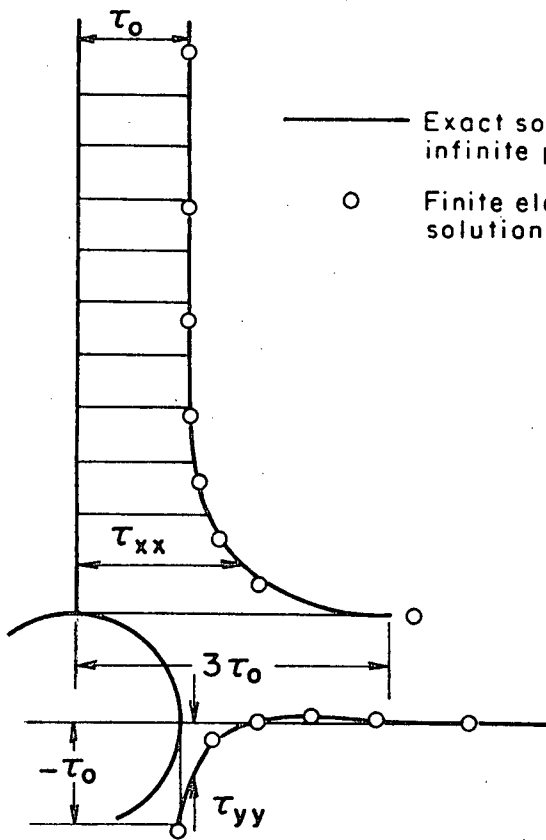


FIG. 27(a): Isotropic,  $E=1.0, \nu=0.1$   
and  $G = \frac{E}{2(1+\nu)}$

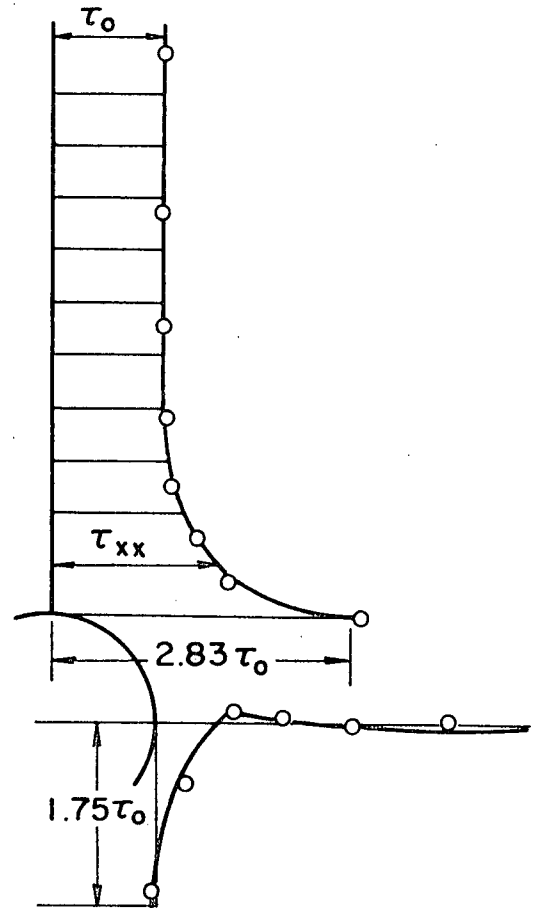


FIG. 27(b): Orthotropic,  $E_1=1.0, E_2=3.0$ ,  
 $\nu_1=0.1, \nu_2=0.0$  and  $G_{12}=0.42$

FIGS. 27: Comparison of theoretical and finite element (mixed) results for infinite plate with a circular hole in the middle.

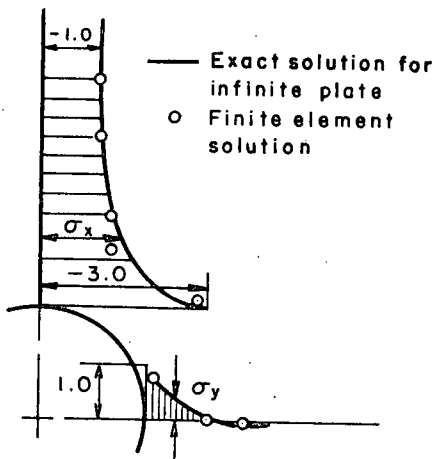


FIG. 28(a): Isotropic

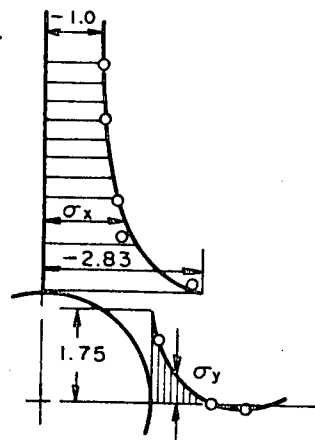


FIG. 28(b): Orthotropic

FIGS. 28: Comparison of theoretical and constant stress finite element, Zienkiewicz [42], results with the same material properties as used in the mixed method;  $\tau_0 = -1.0$ .

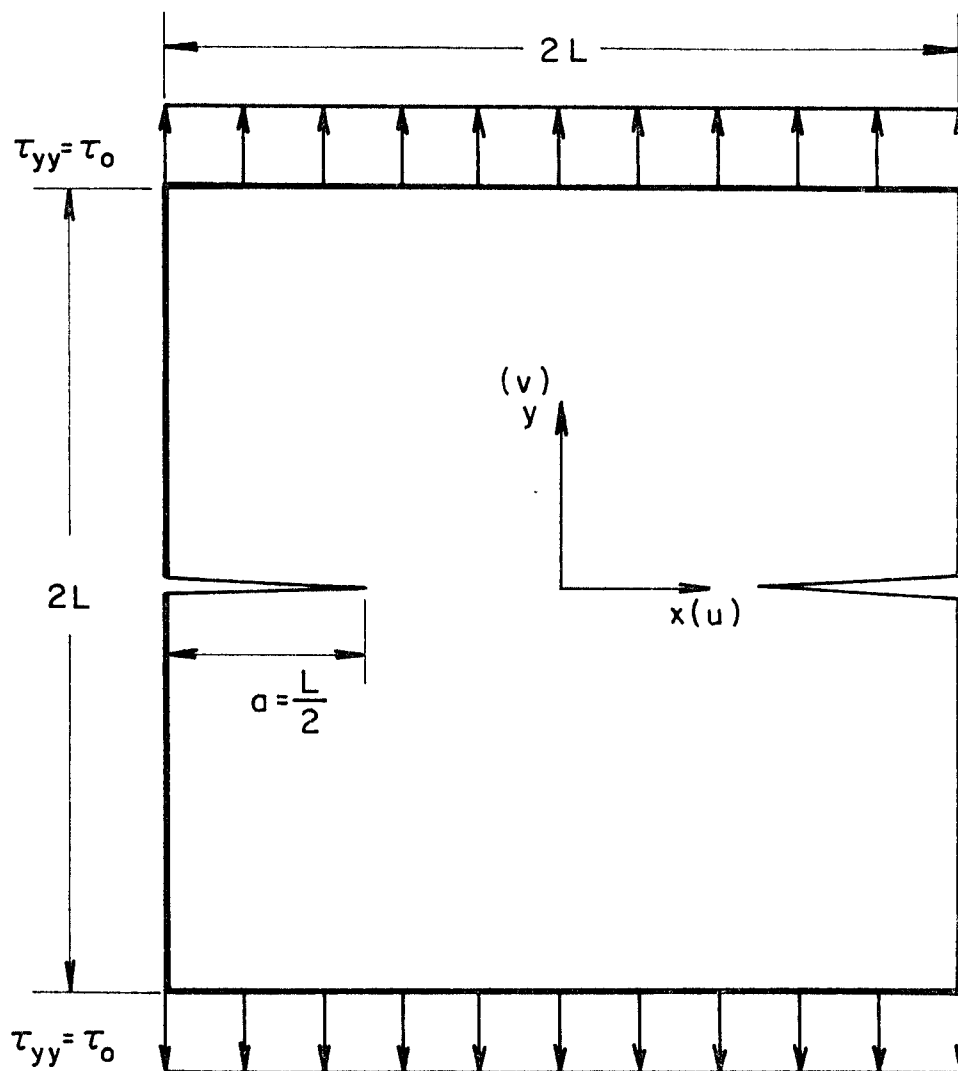


FIG. 29(a): Square plate with edge cracks under uniaxial tension,  $\nu = 0.3$ .

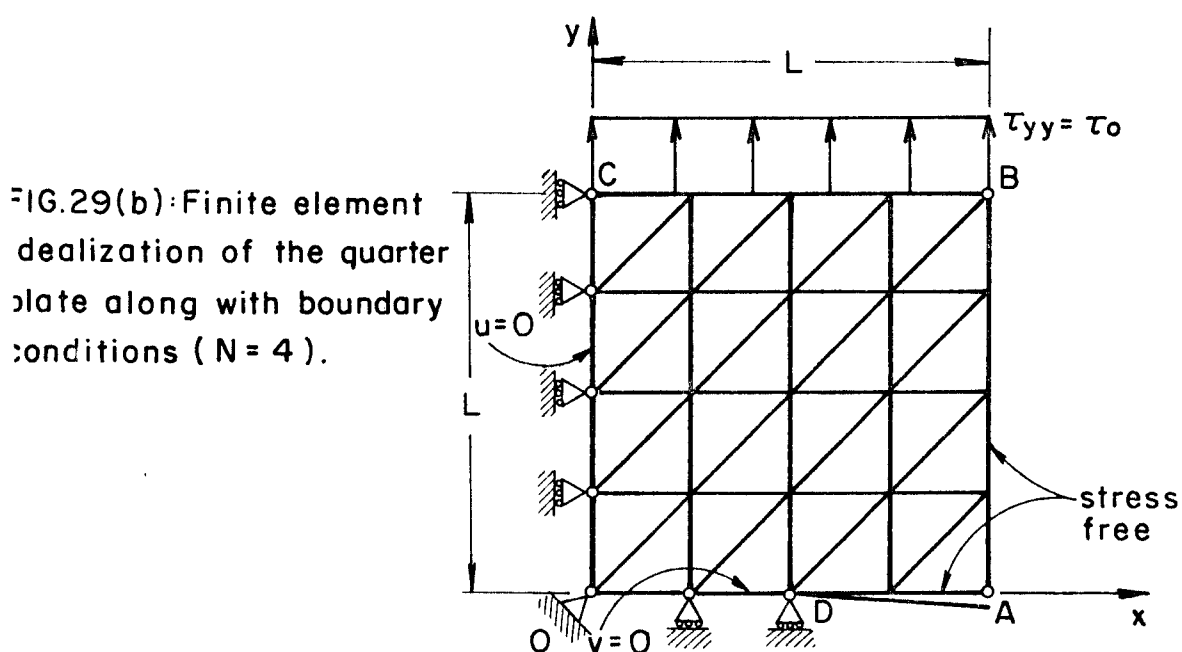


FIG. 29(b): Finite element idealization of the quarter plate along with boundary conditions ( $N = 4$ ).

FIGS. 29: Plane stress problem considered for investigation of energy convergence in the case of stress singularities.

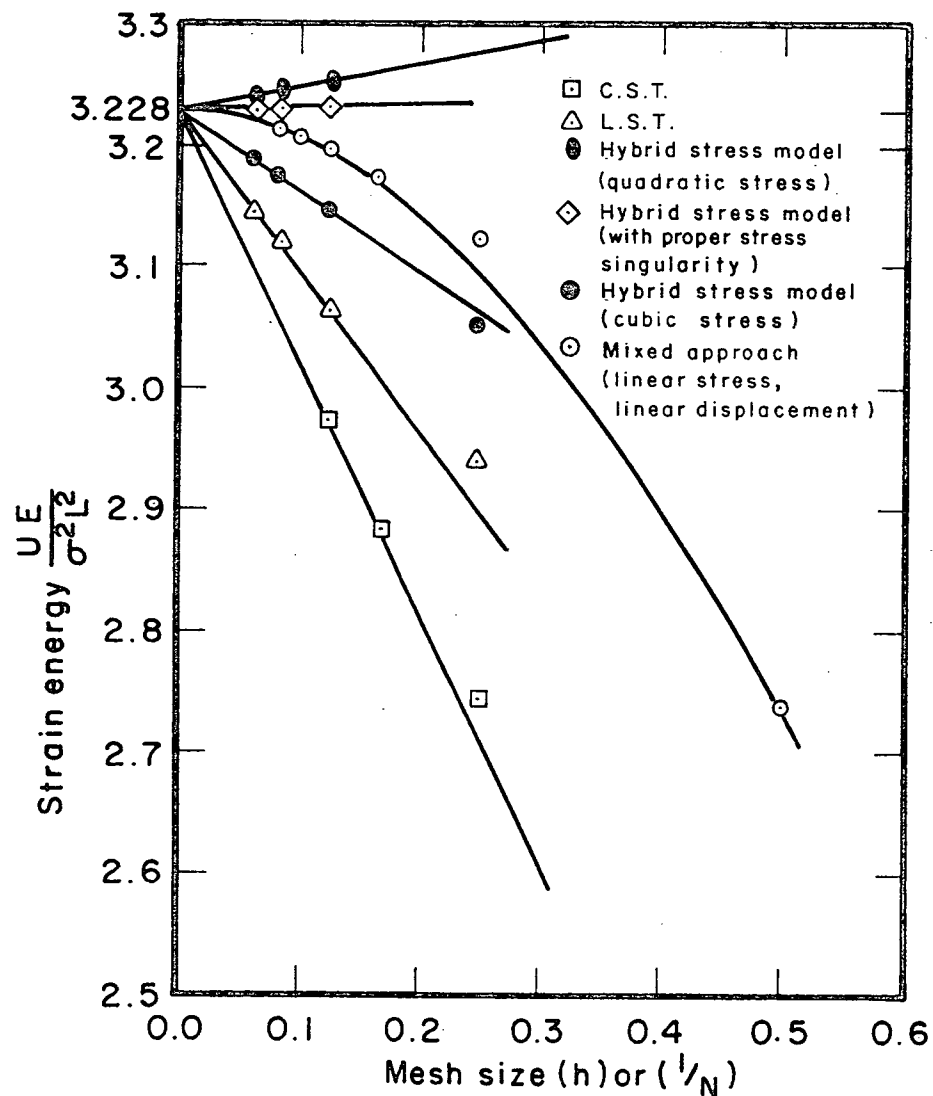


FIG.30(a):  $\tau_{yy}$  continuous at the crack tip D and comparison with results from other elements. ( Tong and Pian [38] ).

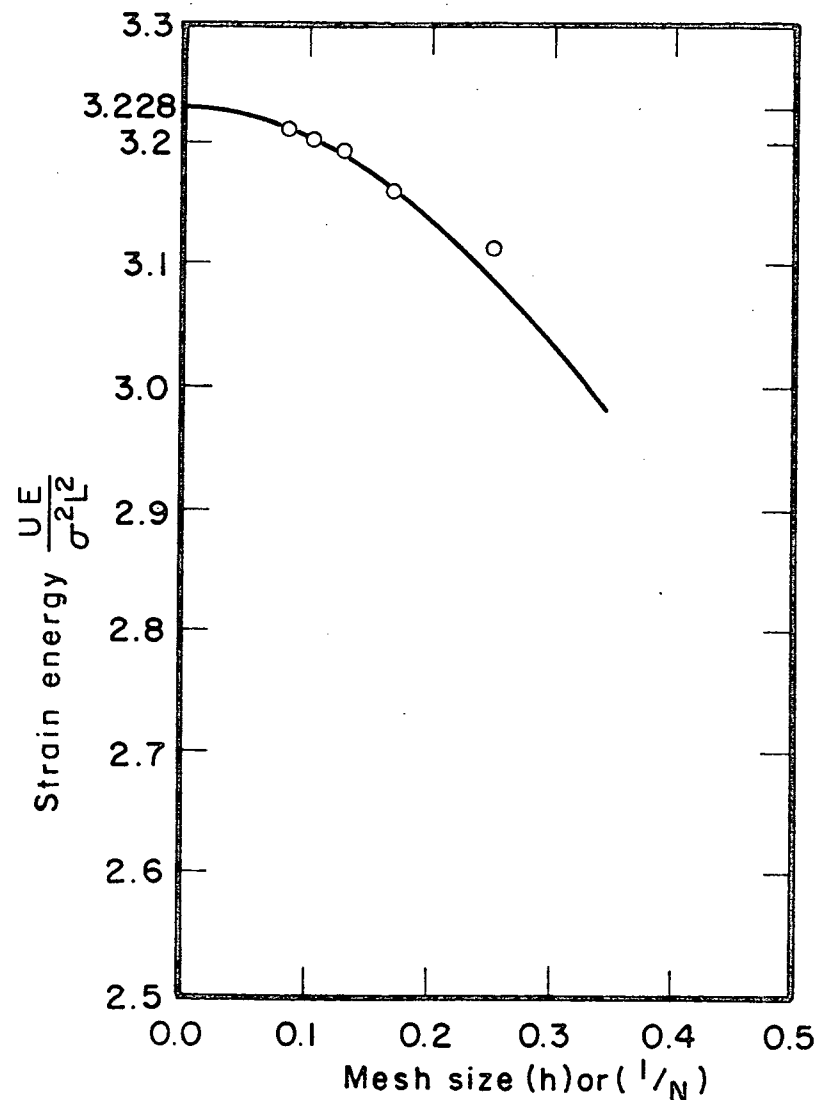


FIG.30(b):  $\tau_{yy}$  discontinuous at the crack tip D.

FIGS.30: Plots of strain energy versus the mesh size for the plane stress problem with symmetric edge cracks—Figure 29.

○  $\tau_{yy}$  stress continuous at the crack tip D.

△  $\tau_{yy}$  stress discontinuous at the crack tip D.

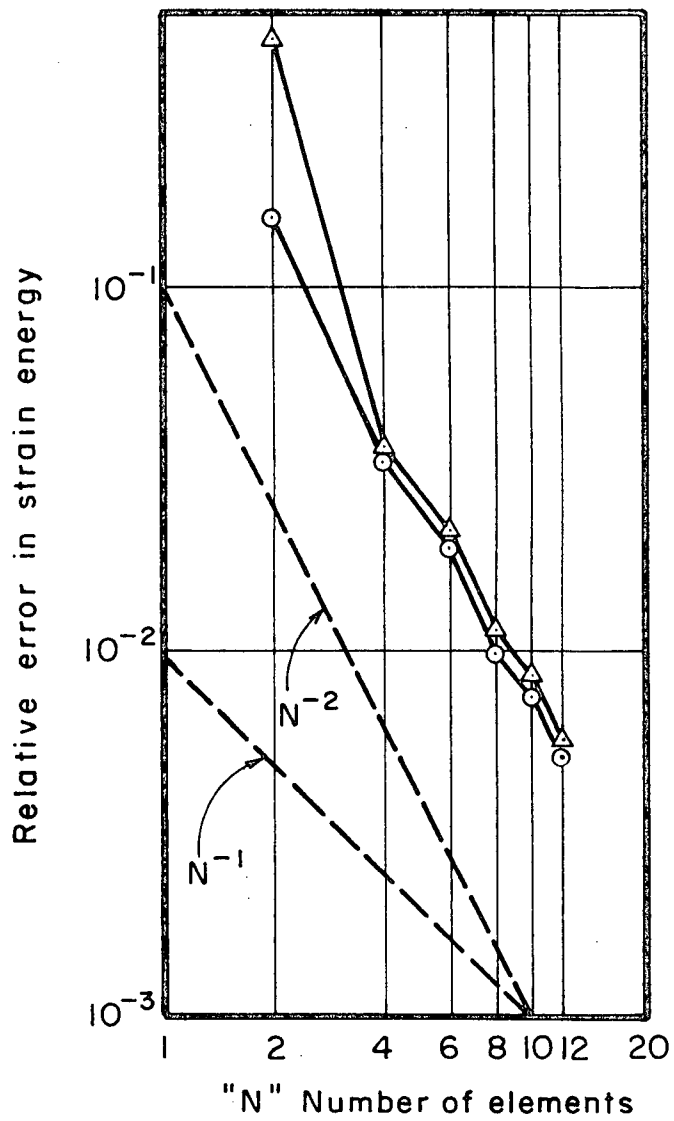


FIG.31 : Strain energy convergence for the plane stress problem square plate with symmetric edge cracks -Figure 29.

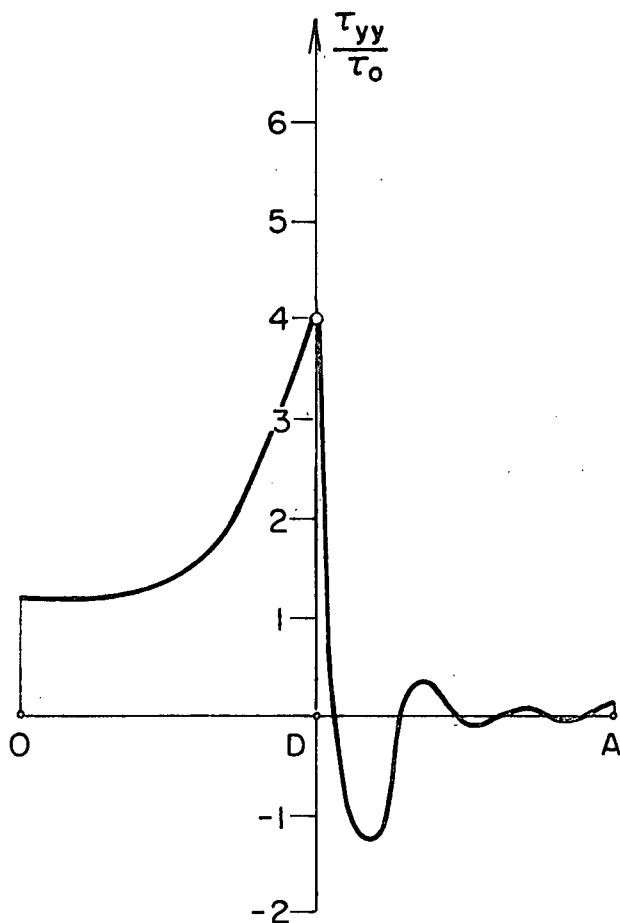


FIG.32(a):  $\tau_{yy}$  continuous at the crack tip D.

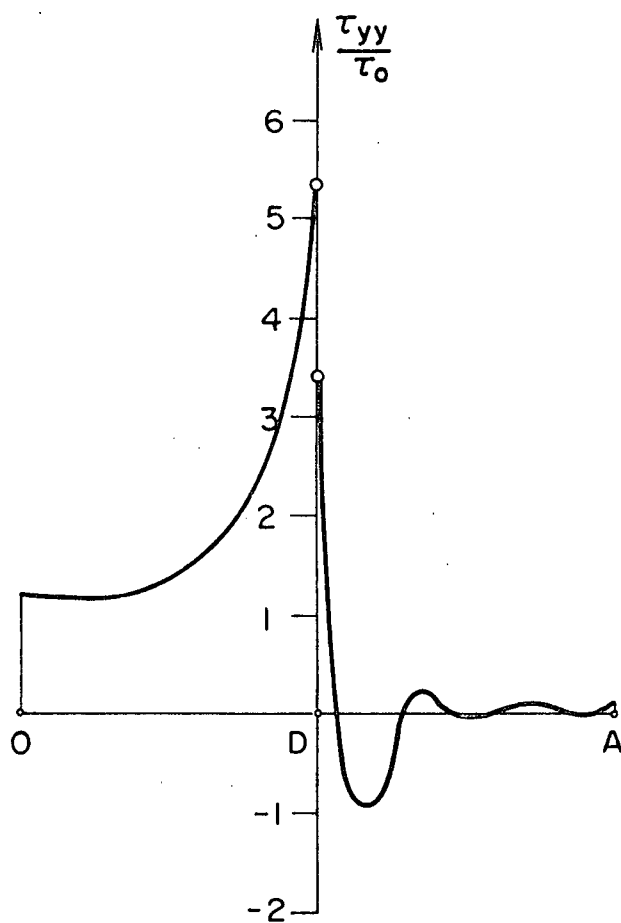


FIG.32(b):  $\tau_{yy}$  discontinuous at the crack tip D.

FIGS.32: Normal stress distribution along the middle of a square plate with symmetric edge cracks-Figure 29(b), ( $N = 12$ ).



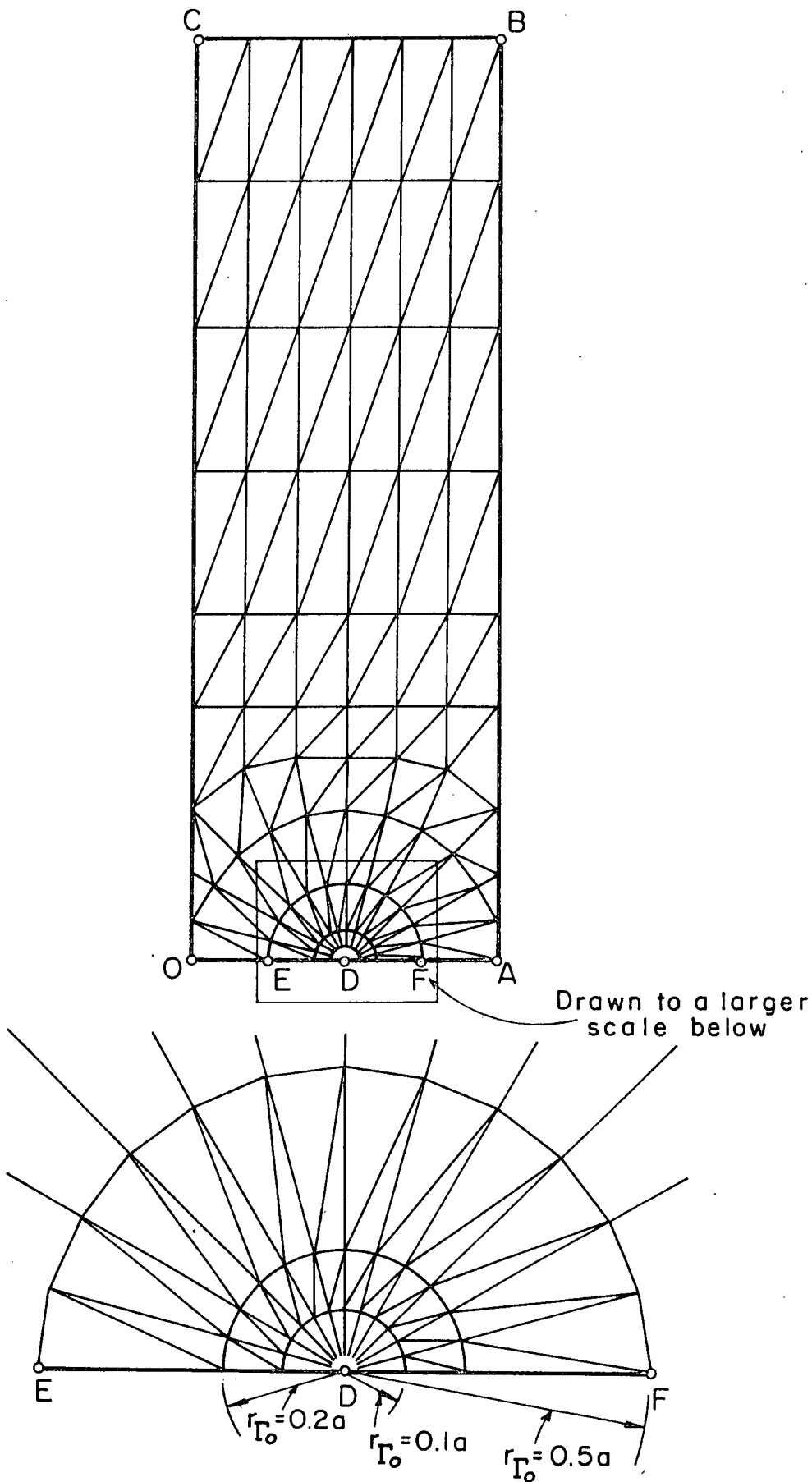


FIG.34: Finite element mesh used for determining the crack intensity factor  $K_I$ , used for both symmetric edge and central cracks.

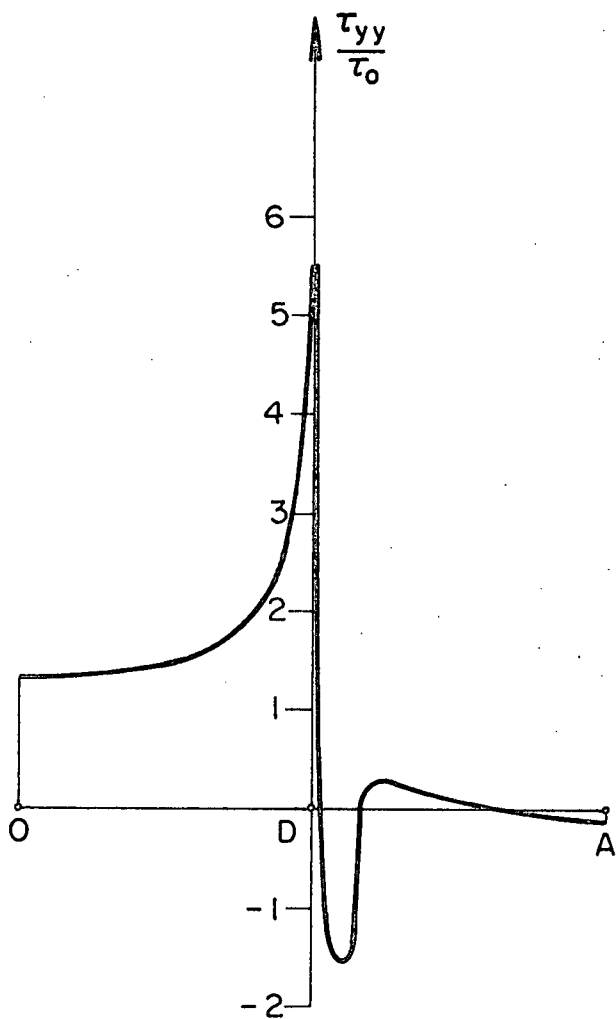


FIG. 35(a): Symmetric edge cracks.

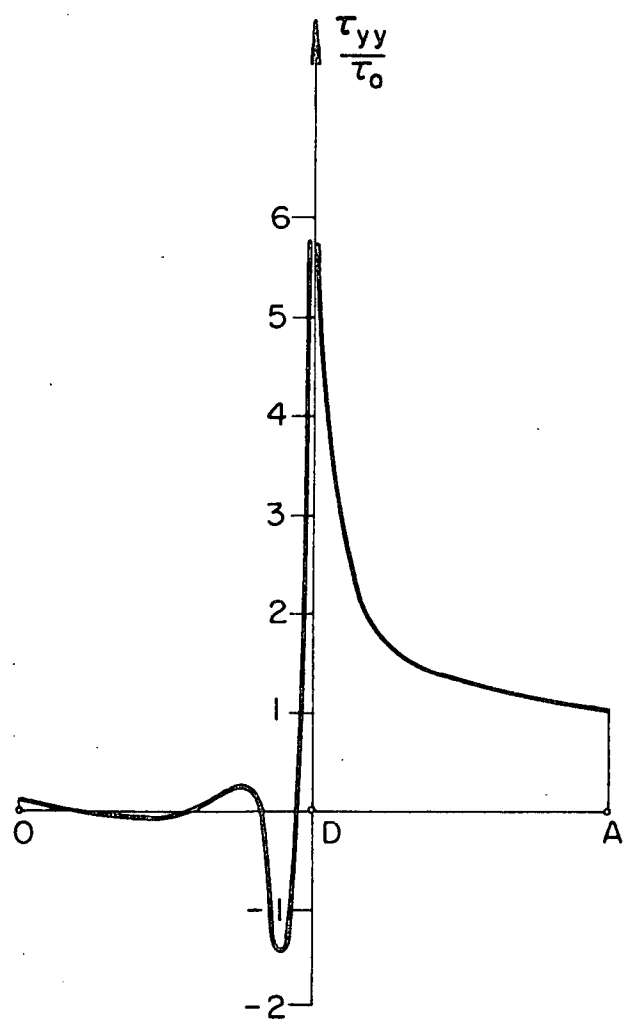


FIG. 35(b): Central Crack.

FIGS. 35: Normal stress distribution along the edge OA of the rectangular plates with cracks - Figure 33.

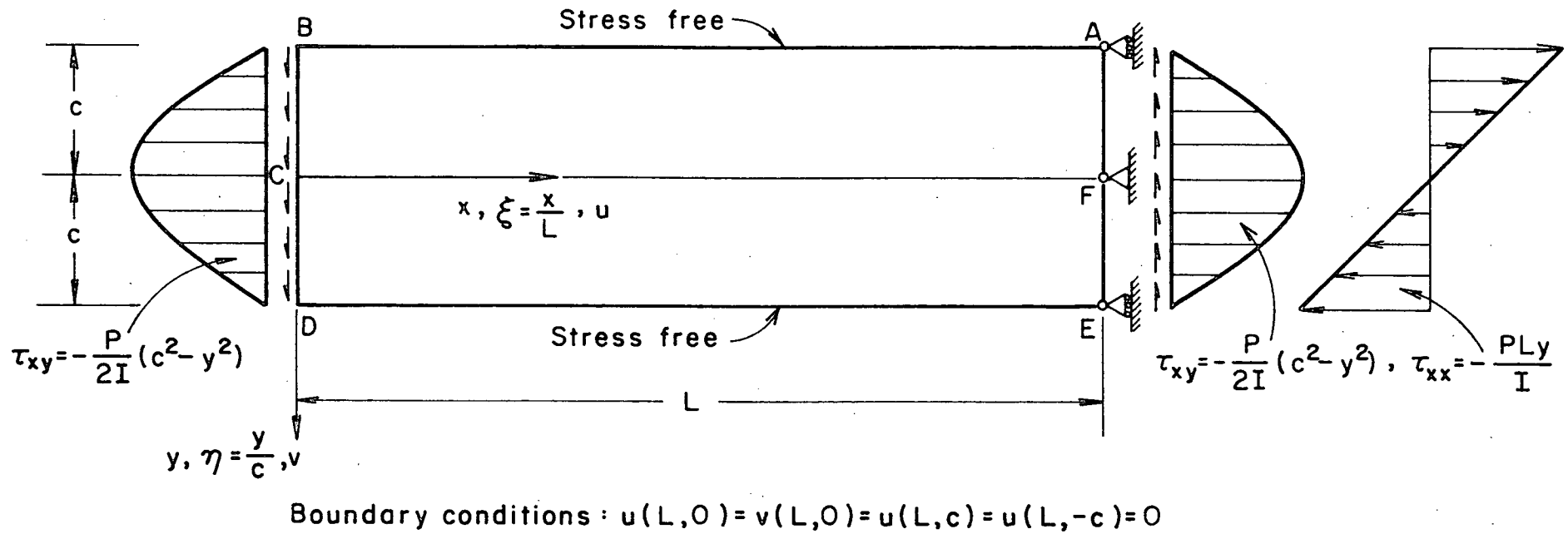


FIG.36: Boundary tractions and conditions for cantilever linear elasticity solution (Appendix D).

# APPENDIX A

## CALCULATION OF THE FINITE ELEMENT MATRIX; LINEAR DISPLACEMENTS AND STRESSES OVER A TRIANGULAR ELEMENT

The element matrix equation for plane stress linear elasticity is derived here for linear displacements and linear stresses in a triangular element using isotropic material. Also demonstrated are the modifications necessary to alter the element matrix for plane strain isotropic and orthotropic materials.

The element geometry is shown in Figure 4. Using area coordinates  $\rho_1, \rho_2, \rho_3$ , [41]; the linear approximations for  $u_i$  and  $\tau_{ij}$  can be written as

$$u_i = \langle \rho_1 \ \rho_2 \ \rho_3 \rangle \begin{Bmatrix} u_{i1} \\ u_{i2} \\ u_{i3} \end{Bmatrix}; \quad i=1,2. \quad (A.1)$$

$$\tau_{ij} = \langle \rho_1 \ \rho_2 \ \rho_3 \rangle \begin{Bmatrix} \tau_{ij}^1 \\ \tau_{ij}^2 \\ \tau_{ij}^3 \end{Bmatrix}; \quad i=j=1,2. \quad (A.2)$$

Note tensorial notation is implied. Comparing equations (A.1) and (A.2) with (4.1) gives

$$\phi_k = \psi_k = \rho_k; \quad k=1,2,3.$$

Consider the mixed variational principle for homogeneous boundary conditions in equation (5.13)

$$F(\underline{\Lambda}) = [\underline{\Lambda}, \underline{\Lambda}]_A - 2 \int_{\Omega} \underline{f}^T \underline{u} d\Omega = \int_{\Omega} [2 \underline{\tau}^T \underline{T} \underline{u} - \underline{\tau}^T \underline{C} \underline{\tau}] d\Omega - 2 \int_{\Omega} \underline{f}^T \underline{u} d\Omega \quad (A.3)$$

$$\text{where} \quad \underline{\tau} = \langle \tau_{xx} \ \tau_{yy} \ \tau_{xy} \rangle^T = \langle \tau_{11} \ \tau_{22} \ \tau_{12} \rangle^T; \quad (A.4)$$

$$\underline{u} = \langle u \ \ v \rangle^T = \langle u_1 \ \ u_2 \rangle^T; \quad (A.5)$$

$$\underline{f} = \langle f_x \ \ f_y \rangle^T; \quad (A.6)$$

$$T = \begin{bmatrix} \frac{\partial}{\partial x} & 0 \\ 0 & \frac{\partial}{\partial y} \\ \frac{\partial}{\partial y} & \frac{\partial}{\partial x} \end{bmatrix} \quad (A.7)$$

and

$$\underline{C} = \frac{1}{E} \begin{bmatrix} 1 & -\nu & 0 \\ -\nu & 1 & 0 \\ 0 & 0 & 2(1+\nu) \end{bmatrix}. \quad (A.8)$$

Substitution of (A.1) and (A.2) into (A.3) and integration over element domain

$\Omega$  yields

$$F(\underline{\Lambda}) = 2\underline{\tilde{\tau}}^T \begin{bmatrix} \underline{a} & 0 \\ 0 & \underline{b} \\ \underline{b} & \underline{a} \end{bmatrix} \underline{\tilde{u}} - \underline{\tilde{\tau}}^T \begin{bmatrix} \underline{c} & -\nu\underline{c} & 0 \\ -\nu\underline{c} & \underline{c} & 0 \\ 0 & 0 & 2(1+\nu)\underline{c} \end{bmatrix} \underline{\tilde{\tau}} - \begin{Bmatrix} \underline{d} \\ \underline{e} \end{Bmatrix} \underline{\tilde{u}}. \quad (A.9)$$

In (A.9) the submatrices  $\underline{a}, \underline{b}, \underline{c}, \underline{d}, \underline{e}, \underline{\tilde{\tau}}$  and  $\underline{\tilde{u}}$  are given by

$$a_{ij} = \int_{\Omega} \rho_i \rho_{j,x} d\Omega; \quad i=j=3. \quad (A.10)$$

$$b_{ij} = \int_{\Omega} \rho_i \rho_{j,y} d\Omega; \quad i=j=3. \quad (A.11)$$

$$c_{ij} = -\frac{1}{E} \int_{\Omega} \rho_i \rho_j d\Omega; \quad i=j=3. \quad (A.12)$$

$$d_i = \int_{\Omega} f_x \rho_i d\Omega; \quad i=1,2,3. \quad (A.13)$$

$$e_i = \int_{\Omega} f_y \rho_i d\Omega; \quad i=1,2,3. \quad (A.14)$$

$$\underline{\tilde{\tau}} = \langle \tau_{xx}^1 \tau_{xx}^2 \tau_{xx}^3 \tau_{yy}^1 \tau_{yy}^2 \tau_{yy}^3 \tau_{xy}^1 \tau_{xy}^2 \tau_{xy}^3 \rangle^T \quad (A.15)$$

$$\underline{\tilde{u}} = \langle u_1 u_2 u_3 v_1 v_2 v_3 \rangle^T. \quad (A.16)$$

Now for stationarity

$$\frac{\partial F(\underline{\Lambda})}{\partial \underline{\tilde{u}}} = 0 \quad (A.17)$$

$$\frac{\partial F(\tilde{\Delta})}{\partial \tilde{\tau}} = 0 \quad (\text{A.18})$$

which leads to the following matrix equation:

$$\begin{bmatrix} \underline{0} & \underline{0} & \underline{a}^T & \underline{0} & \underline{b}^T \\ \underline{0} & \underline{0} & \underline{0} & \underline{b}^T & \underline{a}^T \\ \underline{a} & \underline{0} & \underline{c} & -\nu \underline{c} & \underline{0} \\ \underline{0} & \underline{b} & -\nu \underline{c} & \underline{c} & \underline{0} \\ \underline{b} & \underline{a} & \underline{0} & \underline{0} & 2(1+\nu)\underline{c} \end{bmatrix} \begin{bmatrix} \underline{u} \\ \underline{\tau} \end{bmatrix} = \begin{bmatrix} \underline{d} \\ \underline{e} \\ \underline{0} \end{bmatrix} \quad (\text{A.19})$$

$$\text{or} \quad \underline{\tilde{E}} \tilde{\Delta} = \underline{p}. \quad (\text{A.20})$$

It is only a simple matter to evaluate the submatrices [a], [b] and [c].

If  $(x_i, y_i)$  are the coordinates of the  $i^{\text{th}}$  node of a triangular element

(Figure 4), then the matrices  $\underline{a}$  and  $\underline{b}$  in terms of nodal coordinates are

$$[\underline{a}]_{3 \times 3} = \frac{1}{6} \begin{bmatrix} y_2 - y_3 & y_3 - y_1 & y_1 - y_2 \\ y_2 - y_3 & y_3 - y_1 & y_1 - y_2 \\ y_2 - y_3 & y_3 - y_1 & y_1 - y_2 \end{bmatrix} \quad (\text{A.21})$$

$$[\underline{b}]_{3 \times 3} = \frac{1}{6} \begin{bmatrix} x_3 - x_2 & x_1 - x_3 & x_2 - x_1 \\ x_3 - x_2 & x_1 - x_3 & x_2 - x_1 \\ x_3 - x_2 & x_1 - x_3 & x_2 - x_1 \end{bmatrix} \quad (\text{A.22})$$

and the symmetric matrix  $\underline{c}$  in terms of the area A of the triangle and modulus of elasticity E is given by

$$[c]_{3 \times 3} = -\frac{A}{12E} \begin{vmatrix} 2 & 1 & 1 \\ 1 & 2 & 1 \\ 1 & 1 & 2 \end{vmatrix}. \quad (\text{A.23})$$

Since  $[c]$  is symmetric, the matrix of coefficients  $\underline{E}$  in equation (A.20) is also symmetric as expected.

Next the degrees of freedom  $\bar{\Delta}$  are so arranged by interchanging the corresponding rows and columns of  $\underline{E}$  such that

$$\bar{\Delta} = \langle u_1 \ v_1 \ \tau_{xx}^1 \ \tau_{yy}^1 \ \tau_{xy}^1 \ u_2 \ v_2 \ \tau_{xx}^2 \ \tau_{yy}^2 \ \tau_{xy}^2 \ u_3 \ v_3 \ \tau_{xx}^3 \ \tau_{yy}^3 \ \tau_{xy}^3 \rangle^T \quad (\text{A.24})$$

and the matrix  $\underline{E}$  becomes

$$\bar{\underline{E}}_{15 \times 15} = \begin{bmatrix} 0 & 0 & a_{11} & 0 & b_{11} & 0 & 0 & a_{21} & 0 & b_{21} & 0 & 0 & a_{31} & 0 & b_{31} \\ & 0 & 0 & b_{11} & a_{11} & 0 & 0 & 0 & b_{21} & a_{21} & 0 & 0 & 0 & b_{31} & a_{31} \\ & & c_{11} & f_{11} & 0 & a_{12} & 0 & c_{12} & f_{12} & 0 & a_{13} & 0 & c_{13} & f_{13} & 0 \\ & & & c_{11} & 0 & 0 & b_{12} & f_{12} & c_{12} & 0 & 0 & b_{13} & f_{13} & c_{13} & 0 \\ & & & & g_{11} & b_{12} & a_{12} & 0 & 0 & g_{12} & b_{13} & a_{13} & 0 & 0 & g_{13} \\ & & & & & 0 & 0 & a_{22} & 0 & b_{22} & 0 & 0 & a_{32} & 0 & b_{32} \\ & & & & & & 0 & 0 & b_{22} & a_{22} & 0 & 0 & 0 & b_{32} & a_{32} \\ & & & & & & & c_{22} & f_{22} & 0 & a_{23} & 0 & c_{23} & f_{23} & 0 \\ & & & & & & & & c_{22} & 0 & 0 & b_{23} & f_{23} & c_{23} & 0 \\ & & & & & & & & & g_{22} & b_{23} & a_{23} & 0 & 0 & g_{23} \\ & & & & & & & & & & 0 & 0 & a_{33} & 0 & b_{33} \\ & & & & & & & & & & & 0 & 0 & b_{33} & a_{33} \\ & & & & & & & & & & & & c_{33} & f_{33} & 0 \\ & & & & & & & & & & & & & c_{33} & 0 \\ & & & & & & & & & & & & & & g_{33} \end{bmatrix} \quad (\text{A.25})$$

Symmetric

where  $[f] = -v[c]$  and  $[g] = 2(1+v)[c]$ . The corresponding entries in the load vector  $\underline{p}$  are also interchanged and the modified load vector becomes

$$\{\bar{p}\} = \langle d_1 \ e_1 \ 0 \ 0 \ 0 \ d_2 \ e_2 \ 0 \ 0 \ 0 \ d_3 \ e_2 \ 0 \ 0 \ 0 \rangle^T. \quad (A.26)$$

The equation (A.20) alters to

$$\underline{\underline{E}} \underline{\underline{A}} = \underline{\underline{p}} \quad (A.27)$$

The boundary conditions associated with the plane elasticity problems considered in chapter 7 are of the type

$$\begin{aligned} u_i &= 0 & \text{on } S_u \\ \tau_{ij} n_j &= 0 & \text{on } S_\tau \\ \tau_{ij} n_j &= T_i^0 & \text{on } S_T \end{aligned} \quad (A.28)$$

when the body forces  $f_x$  and  $f_y$  are zero. Here  $S_u$  and  $S_\tau$  are the portions of the boundary  $S$  where the displacements and stresses are zero, respectively; and  $S_T$  the portion on which the tractions  $T_i$  are prescribed. The equations (A.28) are similar to equations (5.18) if  $u_i^0 = c_i^0 = \alpha = 0$  and  $S_M$  same as  $S_\tau$ . Thus equation (A.19) is similar to the equations (5.40) and (5.41) except that the former is expressed in the matrix form. Therefore the sub-load vectors  $\underline{d}$  and  $\underline{e}$  in the element matrix equation arise from the boundary integral  $\int_{S_T} T_i^0 \phi_i^k ds$  where the element boundary coincides with  $S_T$  and at present  $\phi_i^k = \rho_k$  since the same shape functions are used for  $u$  and  $v$ . Hence the derivation of the load vector  $\langle \underline{d}^T \ \underline{e}^T \rangle$  is identical to its generation in the displacement method.

The procedure for deriving the element matrix  $\underline{\underline{E}}$  in (A.25), outlined above, is quite general for plane elasticity. The only change that needs to be introduced in switching from isotropic plane stress to isotropic or orthotropic plane strain lies in the compliance matrix  $\underline{\underline{C}}$  of (A.8). For isotropic plane strain, the compliance matrix  $\underline{\underline{C}}$  is given by

$$\underline{\underline{C}} = \frac{1-\nu^2}{E} \begin{bmatrix} 1 & -\frac{\nu}{1-\nu} & 0 \\ -\frac{\nu}{1-\nu} & 1 & 0 \\ 0 & 0 & \frac{2}{1-\nu} \end{bmatrix} \quad (A.29)$$

and for orthotropic plane strain

$$\underline{C} = \frac{1}{E_1} \begin{bmatrix} (1-nv_1^2) & -v_1(1+v_2) & 0 \\ -v_1(1+v_2) & \frac{1}{n}(1-v_2^2) & 0 \\ 0 & 0 & \frac{1}{G_{12}} \end{bmatrix}$$

where  $n = \frac{E_2}{E_1}$ ; elastic constants  $E_1, v_1$  and  $G_{12}$  are associated with behaviour normal to the plane of strata; and the elastic constants  $E_2, v_2$  and  $G_{21}$  ( $G_{21}$  is independent here) with the plane of strata, as shown in Figure 25(b).

## APPENDIX B

### EIGENVALUE DISTRIBUTION FOR A REAL SYMMETRIC MATRIX

A quadratic form in  $n$ -variables,  $x_1, x_2, \dots, x_n$ , is an expression of the type

$$Q = \sum_{i=1}^n \sum_{j=1}^n a_{ij} x_i x_j = \underline{x}^T \underline{a} \underline{x} \quad (\text{B.1})$$

where  $\underline{a}$  is a symmetric matrix of constants. If the coefficients  $a_{ij}$  and the variables  $x_i$  are restricted to real values, then  $Q$  is real. Let  $v$  be the rank of matrix  $\underline{a}$ . Now there exists a nonsingular transformation

$$\underline{x} = \underline{t} \underline{y}, \quad (\text{B.2})$$

Strang [32], such that the coefficients  $t_{ij}$  can be chosen so that  $Q$  reduces to

$$Q = y_1^2 + y_2^2 + \dots + y_I^2 - y_{I+1}^2 - \dots - y_r^2. \quad (\text{B.3})$$

Equation (B.3) is called the canonical form of the quadratic form  $Q$ . The number of positive terms in (B.3), denoted by  $I$ , is called the index of the quadratic form. It is determined uniquely by the matrix  $\underline{a}$ .

The types of a quadratic form are determined by the rank  $r$  and the index  $I$ , as follows:

- (a)  $Q$  is positive definite if, and only if,  $I=r$ .
- (b)  $Q$  is positive semidefinite if, and only if,  $I=r < n$ .
- (c)  $Q$  is negative definite if, and only if,  $I=0$  and  $r=n$ .
- (d)  $Q$  is negative semidefinite if, and only if,  $I=0$  and  $r < n$ .
- (e)  $Q$  is indefinite if, and only if,  $0 < I < r$ .

These conditions are obvious from the canonical form in (B.3). Further the types of the matrix  $\underline{a}$  associated with the quadratic form  $Q$  in (B.1) correspond to the types of the quadratic form, i.e. the matrix  $\underline{a}$  associated with the positive definite quadratic form is also positive definite.

Since the matrix of coefficients (4.19) of the matrix equation (4.18) is symmetric indefinite, therefore attention shall be focussed on the quadratic form of type (e) above. The quadratic form associated with the matrix (4.19) is

$$Q = 2\underline{u}^T \underline{a} \underline{v} - \underline{v}^T \underline{b} \underline{v} = \begin{bmatrix} \underline{u}^T & \underline{v}^T \end{bmatrix} \begin{bmatrix} 0 & \underline{a} \\ \underline{a}^T & -\underline{b} \end{bmatrix} \begin{bmatrix} \underline{u} \\ \underline{v} \end{bmatrix} \quad (\text{B.4})$$

where  $\underline{b}_{n \times n}$  is a symmetric positive definite matrix, and  $\underline{a}_{m \times n}$  is a real rectangular matrix. Assuming that the rank  $r$  of the real symmetric matrix  $\begin{bmatrix} 0 & \underline{a} \\ \underline{a}^T & -\underline{b} \end{bmatrix}$  is  $m+n$ , then how many positive and negative real eigenvalues does this matrix possess? This necessitates determination of index  $I$  of the quadratic form (B.4).

Consider the negative of the quadratic form in (B.4)

$$Q_1 = -Q = \begin{bmatrix} \underline{v}^T & \underline{u}^T \end{bmatrix} \begin{bmatrix} \underline{b} & -\underline{a}^T \\ -\underline{a} & 0 \end{bmatrix} \begin{bmatrix} \underline{v} \\ \underline{u} \end{bmatrix}. \quad (\text{B.5})$$

The  $(m+n) \times (m+n)$  square matrix of equation (B.5) can be written as

$$\begin{bmatrix} b_{11} & b_{12} & \dots & b_{1n} & -a_{11} & -a_{21} & \dots & -a_{m1} \\ b_{21} & b_{22} & \dots & b_{2n} & -a_{12} & -a_{22} & \dots & -a_{m2} \\ \vdots & \vdots & \dots & \vdots & \vdots & \vdots & \dots & \vdots \\ b_{n1} & b_{n2} & \dots & b_{nn} & -a_{1n} & -a_{2n} & \dots & -a_{mn} \\ -a_{11} & -a_{12} & \dots & -a_{1n} & & & & \\ -a_{21} & -a_{22} & \dots & -a_{2n} & & & & \\ \vdots & \vdots & \dots & \vdots & & \underline{0} & & \\ \vdots & \vdots & \dots & \vdots & & \underline{M \times N} & & \\ -a_{m1} & -a_{m2} & \dots & -a_{mn} & & & & \end{bmatrix}. \quad (\text{B.6})$$

The principal minors for the matrix (B.6) can be written as

$$M_1 = |b_{11}|; \quad M_2 = \begin{vmatrix} b_{11} & b_{12} \\ b_{21} & b_{22} \end{vmatrix}; \quad M_3 = \begin{vmatrix} b_{11} & b_{12} & b_{13} \\ b_{21} & b_{22} & b_{23} \\ b_{31} & b_{32} & b_{33} \end{vmatrix}$$

etc. Since the submatrix  $\underline{b}$  is positive definite, therefore all principal minors up to  $M_n$  are positive. The  $M_{n+1}$  principal minor as determinant of the matrix

$$B_{-n+1} = \begin{bmatrix} b_{11} & b_{12} & \dots & b_{1n} & -a_{11} \\ b_{21} & b_{22} & \dots & b_{2n} & -a_{12} \\ \cdot & \cdot & \cdot & \cdot & \cdot \\ \cdot & \cdot & \cdot & \cdot & \cdot \\ b_{n1} & b_{n2} & \dots & b_{nn} & -a_{1n} \\ -a_{11} & -a_{12} & \dots & -a_{1n} & 0 \end{bmatrix} \quad (B.7)$$

which has a zero on the diagonal, cannot be positive. This holds because  $B_{-n+1}$  is not positive definite. Therefore  $M_{n+1}$  is either negative or zero. The latter cannot be true since if  $m=1$ , i.e. only one degree of freedom in  $u$ ; then the quadratic form is positive semidefinite which is not true.

Hence  $M_{n+1}$  is negative. As for the principal minors  $M_{n+2}$  to  $M_{n+m}$ , these can be either positive, zero or negative. However for rank  $r=m+n$  no two consecutive  $M_i$ 's can be zero; if  $M_k$  and  $M_{k+1}$  are zero then the rank of the matrix (B.6) is  $k$  or less. Further, any zero in an indicial sequence lies between adjacent terms with opposite signs.

Therefore the indicial sequence can be arranged as  $(1, M_1, M_2, \dots, M_n, M_{n+1}, \dots, M_{n+m})$ . The index  $I$  of the quadratic form equals the number of permanences of sign in any indicial sequence where any zero entry is given an arbitrary sign. Therefore the index  $I$  for  $Q$ , in (B.5) is  $n$  since the number of permanences in the indicial sequence above is  $n$ ; i.e. the signs of principal minors  $M_1$  to  $M_n$  are positive. Now the quadratic form  $Q$ , in (B.5) through nonsingular transformation of the type (B.2) can

be expressed in the form of (B.3) as

$$Q_1 = -Q = \tilde{v}_1^2 + \tilde{v}_2^2 + \dots + \tilde{v}_n^2 - \tilde{u}_1^2 - \tilde{u}_2^2 - \dots - \tilde{u}_m^2; \quad (\text{B.8})$$

or

$$Q = \tilde{u}_1^2 + \tilde{u}_2^2 + \dots + \tilde{u}_m^2 - \tilde{v}_1^2 - \tilde{v}_2^2 - \dots - \tilde{v}_n^2. \quad (\text{B.9})$$

Hence it can be deduced from (B.9) that the matrix (4.19) has  $m$  positive and  $n$  negative real eigenvalues.

Next, consider the finite element matrix equation (6.36) for the linear part of the Navier-Stokes equations. This is expressed in a slightly different form as follows:

$$\begin{bmatrix} \underline{0} & \underline{\alpha} & \underline{\beta} \\ \underline{\alpha}^T & \underline{0} & \underline{0} \\ \underline{\beta}^T & \underline{0} & -\underline{\gamma} \end{bmatrix} \begin{bmatrix} \underline{u} \\ \underline{p} \\ \underline{\tau} \end{bmatrix} = \underline{0} \quad (\text{B.10})$$

where  $\underline{\gamma}$  is a symmetric, positive definite  $(n \times n)$  matrix.

A rearrangement of (B.10) yields

$$\underline{S}\underline{\Lambda} = \begin{bmatrix} \underline{0} & \underline{\beta} & \underline{\alpha} \\ \underline{\beta}^T & -\underline{\gamma} & \underline{0} \\ \underline{\alpha}^T & \underline{0} & \underline{0} \end{bmatrix} \begin{bmatrix} \underline{u} \\ \underline{\tau} \\ \underline{p} \end{bmatrix} = \underline{0} \quad (\text{B.11})$$

where

$$\underline{\Lambda} = \langle \underline{u}^T \quad \underline{\tau}^T \quad \underline{p}^T \rangle; \quad (\text{B.12})$$

$$\begin{matrix} \underline{S} \\ (m+n+1) \times (m+n+1) \end{matrix} = \begin{bmatrix} \underline{0} & \underline{\beta} & \underline{\alpha} \\ \underline{\beta}^T & \underline{\gamma} & \underline{0} \\ \underline{\alpha}^T & \underline{0} & \underline{0} \end{bmatrix}; \quad (\text{B.13})$$

and  $\underline{\alpha}$  and  $\underline{\beta}$  are  $(m \times 1)$  and  $(m \times n)$  rectangular matrices, respectively. Let the rank  $r$  of the matrix  $\underline{S}$  be  $(m+n+1)$ . The matrix  $\underline{S}$  is symmetric and indefinite, therefore all its eigenvalues are real and it remains to be determined as to how many of these are positive or negative.

The quadratic form of the mixed variational principle associated with (B.11) is

$$Q = 2\underline{u}^T \underline{\beta} \underline{\tau} - \underline{\tau}^T \underline{\gamma} \underline{\tau} + 2\underline{u}^T \underline{\alpha} \underline{p}. \quad (\text{B.14})$$

The first two terms on the right hand side are identical to the quadratic form in (B.4). Further, it is possible to diagonalize the submatrix  $\begin{bmatrix} 0 & \underline{\beta} \\ \underline{\beta}^T & \underline{\gamma} \end{bmatrix}$  through a transformation of the type (B.2) as was done for (B.6).

Let such a nonsingular transformation be given by

$$\begin{bmatrix} \underline{u} \\ \underline{\tau} \end{bmatrix} = \begin{bmatrix} \underline{Q}_{11} & \underline{Q}_{12} \\ \underline{Q}_{21} & \underline{Q}_{22} \end{bmatrix} \begin{bmatrix} \underline{\tilde{u}} \\ \underline{\tilde{\tau}} \end{bmatrix}. \quad (\text{B.15})$$

and

$$\begin{bmatrix} \underline{u} \\ \underline{\tau} \\ \underline{p} \end{bmatrix} = \begin{bmatrix} \underline{Q}_{11} & \underline{Q}_{12} & \underline{0} \\ \underline{Q}_{21} & \underline{Q}_{22} & \underline{0} \\ \underline{0} & \underline{0} & \underline{I} \end{bmatrix} \begin{bmatrix} \underline{u} \\ \underline{\tau} \\ \underline{\tilde{p}} \end{bmatrix} \quad (\text{B.16})$$

to be complete, where  $\underline{I}$  is an  $(l \times l)$  identity matrix. The substitution of this transformation in the quadratic form  $Q$  in (B.14) (after some algebraic manipulations) yields;

$$Q = \begin{bmatrix} \underline{\tilde{u}}^T & \underline{\tilde{\tau}}^T & \underline{\tilde{p}}^T \end{bmatrix} \begin{bmatrix} \underline{\lambda}^m & \underline{0} & \underline{Q}_{11}^T \underline{\alpha} \\ \underline{0} & -\underline{\lambda}^n & \underline{Q}_{12}^T \underline{\alpha} \\ \underline{\alpha}^T \underline{Q}_{11} & \underline{\alpha}^T \underline{Q}_{12} & \underline{0} \end{bmatrix} \begin{bmatrix} \underline{\tilde{u}} \\ \underline{\tilde{\tau}} \\ \underline{\tilde{p}} \end{bmatrix} \quad (\text{B.17})$$

where  $\underline{\lambda}^m$  and  $\underline{\lambda}^n$  are  $(m \times m)$  and  $(n \times n)$  diagonal matrices with positive entries, respectively. The functional form in (B.14) for transformed variables then leads to the following matrix equation:

$$\underline{\tilde{\tilde{S}}} \underline{\tilde{\tilde{A}}} = \begin{bmatrix} \underline{\lambda}^m & \underline{0} & \underline{Q}_{11}^T \underline{\alpha} \\ \underline{0} & -\underline{\lambda}^n & \underline{Q}_{12}^T \underline{\alpha} \\ \underline{\alpha}^T \underline{Q}_{11} & \underline{\alpha}^T \underline{Q}_{12} & \underline{0} \end{bmatrix} \begin{bmatrix} \underline{\tilde{u}} \\ \underline{\tilde{\tau}} \\ \underline{\tilde{p}} \end{bmatrix} = 0. \quad (\text{B.18})$$



$-\lambda^n M_m$ . Therefore it is negative and the sign alternates thereafter up to  $(m+n)^{th}$ . Beyond  $(m+n)$ , the principal minors can be either positive, zero, or negative and for rank  $r=m+n+1$ , the zero entry would only appear between a positive and a negative entry in the indicial sequence  $\langle 1, M_1, M_2, \dots, M_m, M_{m+1}, \dots, M_{n+m}, M_{n+m+1}, \dots, M_{m+n+1} \rangle$ . Clearly the index  $I$  is  $m$  and hence only  $m$  eigenvalues of the matrix  $\tilde{S}$  are positive while  $(n+1)$  eigenvalues are negative, which also holds for matrix  $\underline{S}$  in (B.13).

# APPENDIX C

## EQUIVALENCE OF ENERGY PRODUCTS FOR FOUR FIRST ORDER BEAM EQUATIONS AND PLANE LINEAR ELASTICITY EQUATIONS

The energy products for the four first order beam equations (7.18) and the plane stress linear elasticity equations (5.19) after introducing the simple beam theory assumptions are shown to be the same when the shear energy contribution is dropped.

The four first order beam equations

$$\begin{bmatrix} 0 & 0 & 0 & -D \\ 0 & 0 & -D & -1 \\ 0 & D & -\frac{1}{EI} & 0 \\ D & -1 & 0 & 0 \end{bmatrix} \begin{bmatrix} v \\ \theta \\ M \\ V \end{bmatrix} = \begin{bmatrix} q \\ 0 \\ 0 \\ 0 \end{bmatrix} \quad (C.1)$$

where  $D = \frac{d}{dx}$  lead to the following energy product;

$$(\underline{A}_1 \underline{\Lambda}, \underline{\Lambda}) = \int_L \left[ -v \frac{dV}{dx} - \theta \frac{dM}{dx} - 2V\theta + M \frac{d\theta}{dx} - \frac{M^2}{EI} + v \frac{dv}{dx} \right] dx \quad (C.2)$$

From equation (5.11), the energy product for plane stress linear elasticity (unit thickness) is

$$(\underline{A}_2 \underline{\Lambda}, \underline{\Lambda}) = \int_{\Omega} [\underline{u}^T \underline{T}^* \underline{\tau} + \underline{\tau}^T \underline{u} - \underline{\tau}^T \underline{C} \underline{\tau}] d\Omega \quad (C.3)$$

for  $\underline{\Lambda} = \langle \underline{u}^T \quad \underline{\tau}^T \rangle$

and  $\underline{A} = \begin{bmatrix} \underline{0} & \underline{T}^* \\ \underline{T} & -\underline{C} \end{bmatrix}$

where

$$\underline{T}^* = -\underline{T}^T = \begin{bmatrix} \frac{\partial}{\partial x} & 0 & -\frac{\partial}{\partial y} \\ 0 & -\frac{\partial}{\partial y} & -\frac{\partial}{\partial x} \end{bmatrix}; \quad \underline{C} = \frac{1}{E} \begin{bmatrix} 1 & -\nu & 0 \\ -\nu & 1 & 0 \\ 0 & 0 & 2(1+\nu) \end{bmatrix}$$

and  $\underline{u} = \langle u \ v \rangle^T$ ;  $\underline{\tau} = \langle \tau_{xx} \ \tau_{yy} \ \tau_{xy} \rangle^T$ . When the basic assumptions of plane sections remain plane after bending and small deflections, following the nomenclature of Figure 7, the following quantities are obtained:

$$\tau_{yy} = 0 \quad (C.4a)$$

$$\tau_{xx} = -\frac{My}{I} \quad (C.4b)$$

$$\tau_{xy} = \frac{V}{2I} \left( \frac{h^2}{4} - y^2 \right) \quad (C.4c)$$

$$\text{and} \quad u = -y\theta. \quad (C.4d)$$

Here  $I$  is the moment of inertia about the  $z$ -axis;  $h$ , the height of the beam, and  $M, V, \theta$  and  $v$  are functions of  $x$  only. Since  $\tau_{yy} = 0$ ; the matrix operators  $\underline{T}^*$  and  $\underline{T}$  and the matrix  $\underline{C}$  reduce to

$$\underline{T}^* = -\underline{T}^T = \begin{bmatrix} -\frac{\partial}{\partial x} & -\frac{\partial}{\partial y} \\ 0 & -\frac{\partial}{\partial x} \end{bmatrix} \quad (C.4e)$$

$$\underline{C} = \frac{1}{E} \begin{bmatrix} 1 & 0 \\ 0 & 2(1+\nu) \end{bmatrix}. \quad (C.4f)$$

Now the substitution of equations (C.4) into (C.3) yields the following.

The first term on the right hand side of (C.3) becomes

$$\begin{aligned} \int_{\Omega} \underline{u}^T \underline{T}^* \underline{\tau} d\Omega &= \int_1 \int_{-\frac{h}{2}}^{\frac{h}{2}} \langle -y\theta \quad v \rangle \begin{bmatrix} -\frac{\partial}{\partial x} & -\frac{\partial}{\partial y} \\ 0 & -\frac{\partial}{\partial x} \end{bmatrix} \begin{Bmatrix} -\frac{My}{I} \\ \frac{V}{2I} \left( \frac{h^2}{4} - y^2 \right) \end{Bmatrix} dy dx \\ &= \int_1 \int_{-\frac{h}{2}}^{\frac{h}{2}} \left\{ -\frac{y^2}{I} \theta \frac{dM}{dx} - \frac{y^2}{I} \theta V - \frac{v}{2I} \frac{dV}{dx} \left( \frac{h^2}{4} - y^2 \right) \right\} dy dx. \end{aligned}$$

Since for unit thickness,  $\int_{-\frac{h}{2}}^{\frac{h}{2}} y^2 dy = I$ ; therefore integration on  $y$  yields;

$$\int_{\Omega} \underline{u}^T \underline{T}^* \underline{\tau} d\Omega = \int_1 (-\theta \frac{dM}{dx} - \theta V - v \frac{dV}{dx}) dx. \quad (C.5)$$

Now the second term on the right hand side of (C.3) takes the form

$$\begin{aligned} \int_{\Omega} \underline{\tau}^T \underline{T} u d\Omega &= \int_1 \int_{\frac{h}{2}}^{\frac{h}{2}} < \frac{My}{I} \quad \frac{V}{2I} (\frac{h^2}{4} - y^2) > \begin{bmatrix} \frac{\partial}{\partial x} & 0 \\ \frac{\partial}{\partial y} & \frac{\partial}{\partial x} \end{bmatrix} \begin{Bmatrix} -y\theta \\ v \end{Bmatrix} dy dx \\ &= \int_1 \int_{\frac{h}{2}}^{\frac{h}{2}} \{ \frac{y^2}{I} M \frac{d\theta}{dx} - \frac{\theta V}{2I} (\frac{h^2}{4} - y^2) + \frac{V}{2I} (\frac{h^2}{4} - y^2) \frac{dv}{dx} \} dy dx. \end{aligned}$$

Again integration on y gives

$$\int_{\Omega} \underline{\tau}^T \underline{T} u d\Omega = \int_1 (M \frac{d\theta}{dx} - \theta V + V \frac{dv}{dx}) dx. \quad (C.6)$$

Finally

$$\begin{aligned} \int_{\Omega} \underline{\tau}^T \underline{C} \underline{\tau} d\Omega &= \frac{1}{E} \int_1 \int_{\frac{h}{2}}^{\frac{h}{2}} < \frac{My}{I} \quad \frac{V}{2I} (\frac{h^2}{4} - y^2) > \begin{bmatrix} 1 & 0 \\ 0 & 2(1+\nu) \end{bmatrix} \begin{Bmatrix} -\frac{My}{I} \\ \frac{V}{2I} (\frac{h^2}{4} - y^2) \end{Bmatrix} dy dx \\ &= \frac{1}{E} \int_1 \int_{\frac{h}{2}}^{\frac{h}{2}} \{ \frac{y^2}{I^2} M^2 + \frac{h^2}{4I^2} (\frac{h^2}{4} - y^2)^2 \} dy dx. \end{aligned}$$

This, after integration on y, yields

$$\int_{\Omega} \underline{\tau}^T \underline{C} \underline{\tau} d\Omega = \int_1 (\frac{M^2}{EI} + \frac{(1+\nu)}{5EI} h^2 V^2) dx. \quad (C.7)$$

Adding the equations (C.5), (C.6) and (C.7) gives,

$$\int_{\Omega} [\underline{u}^T \underline{T}^* \underline{\tau} + \underline{\tau}^T \underline{T} u - \underline{\tau}^T \underline{C} \underline{\tau}] d\Omega = \int_1 \{ -v \frac{dV}{dx} - \theta \frac{dM}{dx} - 2V\theta + M \frac{d\theta}{dx} - \frac{M^2}{EI} + V \frac{dv}{dx} + \frac{(1+\nu)}{5EI} h^2 V^2 \} dx \quad (C.8)$$

where  $\int_1 \frac{(1+\nu)}{5EI} h^2 V^2 dx$  is the contribution to the energy product from the shear stress due to flexure. This is only significant for short beams and when it is dropped, the energy product in (C.3) becomes

$$(\underline{A_2\Lambda}, \underline{\Lambda}) = \int_I \left[ -v \frac{dV}{dx} - \theta \frac{dM}{dx} - 2V\theta + M \frac{d\theta}{dx} - \frac{M^2}{EI} + v \frac{dv}{dx} \right] dx. \quad (C.9)$$

This is exactly the same as in equation (C.2).

APPENDIX D

ELASTICITY SOLUTIONS FOR A CANTILEVER

An elasticity solution for the cantilever with the boundary tractions and the boundary conditions shown in Figure 36 is derived. It is also shown that the strain energy computed from the normal stress  $\tau_{xx}$  and the shear stress  $\tau_{xy}$  distributions is actually equal to half the total work done by the boundary tractions in moving through the displacements obtained from the elasticity solution on the boundaries.

The stress distributions are taken as

$$\tau_{xx} = - \frac{Pxy}{I} \quad (D.1a)$$

$$\tau_{yy} = 0 \quad (D.1b)$$

$$\tau_{xy} = - \frac{P}{2I}(c^2 - y^2) \quad (D.1c)$$

where  $P$  is the total load due to the shear stress at the ends. The equations (D.1) identically satisfy the equilibrium  $\nabla^4 \phi = 0$  for  $\tau_{xx} = \frac{\partial^2 \phi}{\partial y^2}$ ,  $\tau_{yy} = \frac{\partial^2 \phi}{\partial x^2}$  and  $\tau_{xy} = -\frac{\partial^2 \phi}{\partial x \partial y}$  everywhere inside the cantilever, as well as yield the same stresses on the boundary as applied tractions. The corresponding strains, by applying Hooke's law, are

$$\epsilon_{xx} = \frac{\partial u}{\partial x} = \frac{\tau_{xx}}{E} = - \frac{Pxy}{EI} \quad (D.2a)$$

$$\epsilon_{yy} = \frac{\partial v}{\partial y} = \frac{-\nu \tau_{xx}}{E} = \frac{\nu Pxy}{EI} \quad (D.2b)$$

$$\gamma_{xy} = \frac{\partial u}{\partial y} + \frac{\partial v}{\partial x} = \frac{\tau_{xy}}{G} = - \frac{P}{2IG} (c^2 - y^2) \quad (D.2c)$$

where  $G = \frac{E}{2(1+\nu)}$ . The strains derived in (D.2) also satisfy identically the

compatibility equation  $(\frac{\partial^2 \epsilon_{xx}}{\partial y^2} + \frac{\partial^2 \epsilon_{yy}}{\partial x^2} = \frac{\partial^2 \gamma_{xy}}{\partial x \partial y})$ .

By integration of (D.2a) and (D.2b),  $u$  and  $v$  are obtained as

$$u = -\frac{Px^2y}{2EI} + f_1(y); \quad v = \frac{vPy^2}{2EI} + f_2(x) \quad (D.3)$$

in which the functions  $f_1$  and  $f_2$  are as yet unknown functions of  $y$  and  $x$  only, respectively. Substitution of  $u$  and  $v$  above into equation (D.2c) yields

$$-\frac{Px^2}{2EI} + \frac{df_1(y)}{dy} + \frac{vPy^2}{2EI} + \frac{df_2(x)}{dx} = -\frac{P}{2IG} (c^2 - y^2). \quad (D.4)$$

In equation (D.4) some terms are functions of  $x$  only, some are functions of  $y$  only, and one is independent of both  $x$  and  $y$ . These can be grouped as

$$F(x) = -\frac{Px^2}{2EI} + \frac{df_2(x)}{dx}$$

$$G(y) = \frac{vPy^2}{2EI} + \frac{df_1(y)}{dy} - \frac{Py^2}{2IG}$$

$$K = -\frac{Pc^2}{2IG} \quad (\text{constant}).$$

Thus (D.3) becomes

$$F(x) + G(y) = K. \quad (D.5)$$

It can be concluded from (D.5) that  $F(x)$  and  $G(y)$  must be constants. Denoting these by  $d$  and  $e$ , respectively, therefore

$$d + e = k$$

and 
$$\frac{df_2(x)}{dx} = \frac{Px^2}{2EI} + d; \quad \frac{df_1(y)}{dy} = -\frac{vPy^2}{2EI} + \frac{Py^2}{2IG} + e.$$

Integrating these yields the functions  $f_1(y)$  and  $f_2(x)$ ;

$$f_1(y) = -\frac{vPy^3}{6EI} + \frac{Py^3}{6IG} + ey + g$$

$$f_2(x) = \frac{Px^3}{6EI} + dx + h.$$

Substitution in the expression for  $u$  and  $v$  in (D.3) gives

$$u = -\frac{Px^2y}{2EI} - \frac{vPy^3}{6EI} + \frac{Py^3}{6IG} + ey + g \quad (D.6)$$

$$v = \frac{vPxy^2}{2EI} + \frac{Px^3}{6EI} + dx + h. \quad (D.7)$$

The four constants  $d, e, g$  and  $h$  can now be determined from the four boundary conditions (Figure 36)

$$u(L,0) = v(L,0) = u(L,c) = u(L,-c) = 0 \quad (D.8)$$

and these are found to be

$$d = -\frac{PL^2}{6EI} \left[ 3 + (4+5v) \frac{c^2}{L^2} \right]$$

$$e = \frac{PL^2}{2EI} \left[ 1 - \frac{1}{3}(2+v) \frac{c^2}{L^2} \right]$$

$$g = 0$$

and

$$h = \frac{PL^3}{3EI} \left[ 1 + \frac{1}{2}(4+5v) \frac{c^2}{L^2} \right].$$

Finally the substitution for  $d, e, g$  and  $h$  in the equations (D.6) and (D.7)

and letting  $\xi = \frac{x}{L}$  and  $\eta = \frac{y}{c}$  gives

$$u(\xi, \eta) = \frac{PL^3}{2EI} \left[ \frac{c}{L} \eta (1-\xi^2) - \left( \frac{2+v}{3} \right) \frac{c^3}{L^3} \eta (1-\eta^2) \right] \quad (D.9)$$

$$v(\xi, \eta) = \frac{PL^3}{3EI} \left[ 1 - \frac{3}{2}\xi + \frac{1}{2}\xi^3 + \frac{1}{2} \frac{c^2}{L^2} \{ 3v\xi\eta^2 + (4+5v)(1-\xi) \} \right]. \quad (D.10)$$

Therefore the tip deflection  $\delta$  at C (Figure 36) is given by

$$\delta = v(0,0) = \frac{PL^3}{3EI} \left[ 1 + \frac{1}{2}(4+5v) \frac{c^2}{L^2} \right] \quad (D.11)$$

while the longitudinal deflection  $u$  at B, where  $\xi=0$  and  $\eta=-1$ , is obtained as

$$u_B = u(0,-1) = -\frac{PcL^2}{2EI}. \quad (D.12)$$

The strain energy in the cantilever can be computed by using the assumed stresses in (D.1) and the corresponding strains in (D.2) in the usual manner.

$$\begin{aligned}
 U &= \frac{1}{2} \int_0^L \int_{-c}^c [\tau_{xx} \epsilon_{xx} + \tau_{yy} \epsilon_{yy} + \tau_{xy} \gamma_{xy}] dy dx \\
 &= \frac{P^2}{2EI^2} \int_0^L \int_{-c}^c [x^2 y^2 + \left(\frac{1+\nu}{2}\right) (c^2 - y^2)^2 \frac{c^2}{L^2}] dy dx.
 \end{aligned}$$

After integration, the strain energy in the cantilever is

$$U = \frac{P^2 L^3}{6EI} \left[ 1 + \frac{12}{5}(1+\nu) \frac{c^2}{L^2} \right]. \quad (D.13)$$

The work done on the boundary can be computed from the following line integral

$$W = \int_{S_\tau} (\tau_{ij} n_j u_i) ds \quad (D.14)$$

where  $S_\tau$  is the portion of the boundary where the stresses are prescribed and  $n_j$ , the unit outward normal. For the cantilever in Figure 36, this integral takes the form

$$\begin{aligned}
 W &= \int_{-c}^c \tau_{xy}(0,y) v(0,y) dy + \int_{-c}^c \tau_{xy}(L,y) v(L,y) dy + \int_{-c}^c \tau_{xx}(L,y) u(L,y) dy \\
 &= W_1 + W_2 + W_3.
 \end{aligned} \quad (D.15)$$

Here

$$\begin{aligned}
 \tau_{xy}(0,y) &= -\frac{P}{2I} (c^2 - y^2) \\
 v(0,y) &= \frac{PL^3}{3EI} \left[ 1 + \frac{1}{2}(4+5\nu) \frac{c^2}{L^2} \right].
 \end{aligned}$$

Thus the first integral in the right hand side of (D.15) is given by

$$W_1 = \int_{-c}^c -\frac{P^2 L^3}{3EI^2} (c^2 - y^2) \left[ 1 + \frac{1}{2}(4+5\nu) \frac{c^2}{L^2} \right] dy$$

and after integration

$$W_1 = \frac{P^2 L^3}{3EI} \left[ 1 + \frac{1}{2}(4+5\nu) \frac{c^2}{L^2} \right]. \quad (D.16)$$

Next,  $\tau_{xy}(L,y)$  is the same as  $\tau_{xy}(0,y)$  and  $v(L,y)$  is given by

$$v(L,y) = \frac{\nu}{2} \frac{PL}{EI} y^2.$$

Then the second integral  $W_2$  is

$$W_2 = \int_{-c}^c -\frac{\nu}{4} \frac{P^2 L}{EI^2} y^2 (c^2 - y^2) dy$$

and leads to

$$W_2 = -\frac{\nu}{10} \frac{P^2 c^2 L}{EI}. \quad (D.17)$$

Finally to obtain  $W_3$

$$\tau_{xx}(L, y) = -\frac{PL}{I} y$$

and

$$u(L, y) = \frac{(2+\nu)}{6} \frac{Py}{EI} (y^2 - c^2).$$

Therefore

$$W_3 = \int_{-c}^c \frac{(2+\nu)}{6} \frac{P^2 L}{EI^2} y^2 (y^2 - c^2) dy$$

which gives

$$W_3 = \frac{(2+\nu)}{15} \frac{P^2 c^2 L}{EI}. \quad (D.18)$$

Adding (D.16), (D.17) and (D.18) yields

$$W = W_1 + W_2 + W_3 = \frac{PL^3}{3EI} \left[ 1 + \frac{12}{5} (1+\nu) \frac{c^2}{L^2} \right]. \quad (D.19)$$

Comparison of (D.19) with (D.13) gives

$$W = 2U. \quad (D.20)$$

Therefore the strain energy computed from the stress distributions in (D.1) is exactly half the work done by the boundary tractions in going through boundary displacements as obtained from the elasticity solutions (D.9) and (D.10).